Technical Report CERC-95-14
November 1995

US Army Corps of Engineers
Waterways Experiment Station

Effectiveness of Spur Jetties at Siuslaw River, Oregon

Report 1
Prototype Monitoring Study

by *Cheryl E. Pollock, David McGehee, Ronald W. Neihaus, Jr., WES*
Stephan A. Chesser, Portland District
Claire Livingston, DynTel

WES

Approved For Public Release; Distribution Is Unlimited

Prepared for Headquarters, U.S. Army Corps of Engineers

PRINTED ON RECYCLED PAPER

Technical Report CERC-95-14
November 1995

Effectiveness of Spur Jetties at Siuslaw River, Oregon

Report 1
Prototype Monitoring Study

by Cheryl E. Pollock, David McGehee, Ronald W. Neihaus, Jr.

U.S. Army Corps of Engineers
Waterways Experiment Station
3909 Halls Ferry Road
Vicksburg, MS 39180-6199

Stephan A. Chesser

U.S. Army Engineer District, Portland
333 SW First Avenue, Tenth Floor
Portland, OR 97208-2946

Claire Livingston

DynTel
3530 Manor Dr., Suite No. 4
Vicksburg, MS 39180

Report 1 of a series

Prepared for U.S. Army Corps of Engineers
Washington, DC 20314-1000

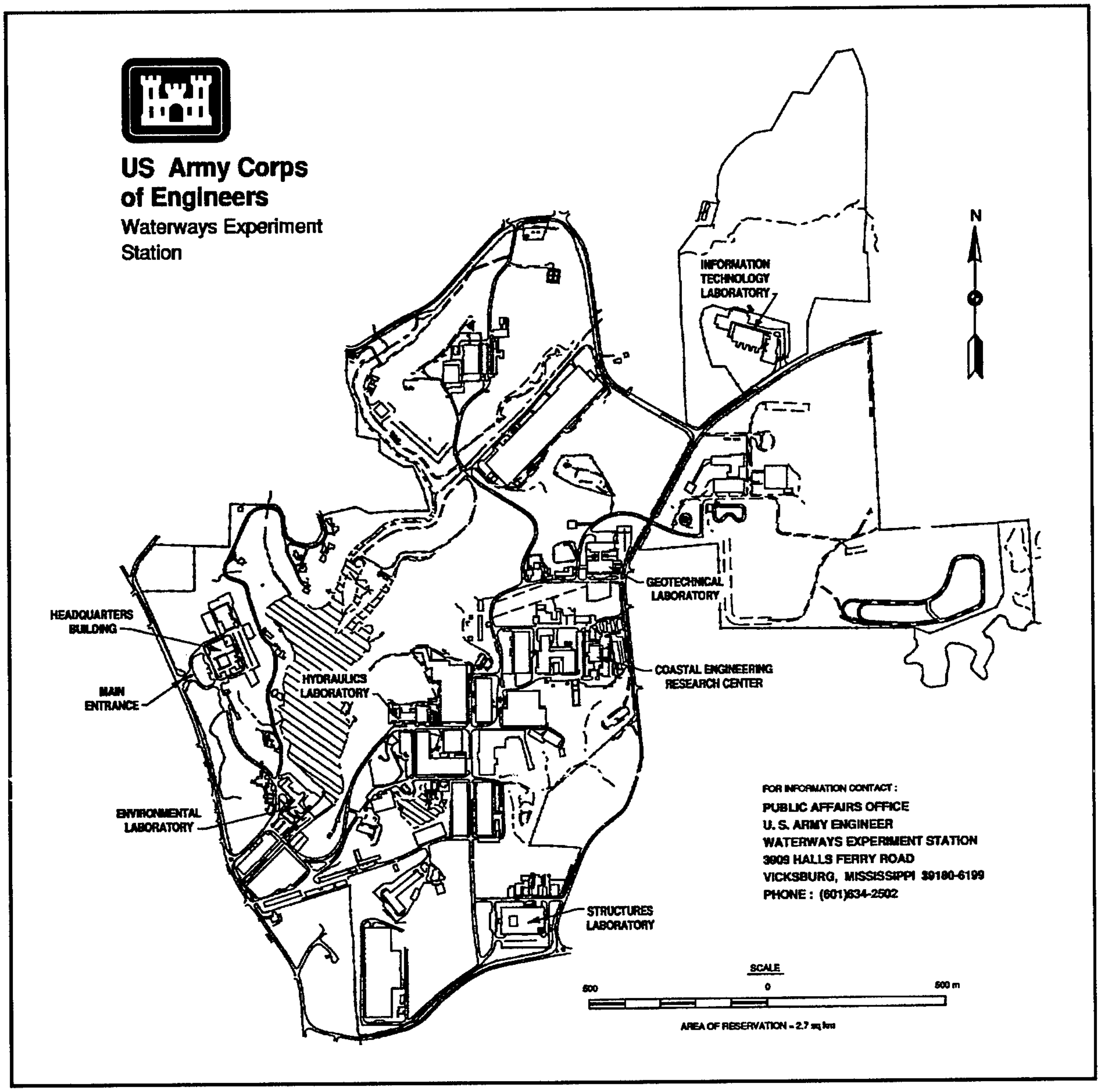

Waterways Experiment Station Cataloging-in-Publication Data

Effectiveness of spur jetties at Siuslaw River, Oregon. Report 1,
Prototype monitoring study / by Cheryl E. Pollock ... [et al.] ; prepared
for U.S. Army Corps of Engineers.
157 p. : ill. ; 28 cm. — (Technical report ; CERC-95-15 rept.1)
Includes bibliographic references.
Report 1 of a series.
1. Jetties — Oregon — Siuslaw River. 2. Siuslaw River (Or.)
3. Rivers — Oregon. 4. Coastal engineering — Oregon — Siuslaw
River. I. Pollock, Cheryl E. II. United States. Army. Corps of Engineers.
III. U.S. Army Engineer Waterways Experiment Station. IV. Coastal
Engineering Research Center (U.S. Army Engineer Waterways
Experiment Station) V. Series: Technical report (U.S. Army Engineer
Waterways Experiment Station) ; CERC-95-14 rept.1.
TA7 W34 no.CERC-95-14 rept.1

Contents

List of Figures

List of Tables

Preface

The study summarized in this report was conducted jointly by the U.S. Army Engineer Waterways Experiment Station's (WES's) Coastal Engineering Research Center (CERC) and the U.S. Army Engineer District, Portland (NPP). The effectiveness of spur jetties at the mouth of the Siuslaw River, OR, was selected for study by the CERC Monitoring Completed Coastal Projects (MCCP) Program. The MCCP Program Manager was Ms. Carolyn Holmes. This program was sponsored by Headquarters, U.S. Army Corps of Engineers (HQUSACE). The HQUSACE Technical Monitors were Messrs. John H. Lockhart, Jr., Charles Chesnutt, and Barry W. Holliday.

Work at CERC was performed under the general administrative supervision of Dr. Yen-hsi Chu, Chief, Engineering Applications Unit; Ms. Joan Pope, Chief, Coastal Structures and Evaluation Branch; Mr. Thomas W. Richardson, Chief, Engineering Development Division; Mr. Charles C. Calhoun, Jr., Assistant Director; and Dr. James R. Houston, Director, CERC.

This report was prepared by Ms. Cheryl E. Pollock, CERC; Messrs. Stephen Chesser, NPP; David McGehee and Ronald W. Neihaus, Jr., CERC; and Ms. Claire Livingston, Dyntel. Field tests, directed by Ms. Pollock and Mr. Chesser, were conducted jointly by CERC and NPP. Assistance in planning this study was also provided by Ms. Holmes, and Messrs. Thomas W. Richardson and David McGehee (CERC), and Mr. Mike Hemsley, National Oceanic and Atmospheric Administration. Figures were prepared by Ms. Mary Allison and Mr. Robert Chain (both of CERC). Ms. Janie Daughtry (CERC) assisted with final report preparation.

Director of WES during publication of this report was Dr. Robert W. Whalin. Commander was COL Bruce K. Howard, EN.

Conversion Factors, Non-SI to SI Units of Measurement

Non-SI units of measurement used in this report can be converted to SI units as follows:

Multiply	By	To Obtain
acre-feet	1,233.489	cubic meters
cubic feet per second	0.02831685	cubic meters
cubic yards	0.7645549	cubic meters
feet	0.3048	meters
inches per second	2.54	centimeters per second
miles (U.S. nautical)	1.852	kilometers
miles (U.S. statute)	1.609347	kilometers
pounds (mass)	0.4535924	kilograms

1 Introduction

Study Overview

In 1985, the rubble-mound jetties at the entrance to the Siuslaw River, Florence, OR, were extended offshore. The north jetty extension was 580 m (1,900 ft), and the south extension was 670 m (2,198 ft).[1] In addition, on the ocean side of each jetty, one 122-m-(400-ft-) long spur oriented 45 deg to the main structure was constructed 275 m (902 ft) shoreward of the seaward end of each of the twin jetties. The heads of the jetties were constructed to depths of 7 m (23 ft). Depending upon the wave conditions, the breaker zone may occur inside the spurs or may extend well seaward of the jetty tips. Figures 1 and 2 show the jetties prior to and after the extension, respectively. The spur system was investigated as a cost-reducing alternative to significant linear jetty length extension, which would reduce sediment shoaling and dredging requirements in the channel and improve navigability. Cost reductions were expected in reduced maintenance dredging and in actual construction and material cost.

Monitoring and evaluation of the jetty system were conducted through the U.S. Army Corps of Engineers (USACE), Monitoring of Completed Coastal Projects (MCCP) Program by the U.S. Army Engineer (USAE) Waterways Experiment Station (WES), Coastal Engineering Research Center (CERC) in coordination with the USAE District, Portland (NPP). Data collected during field monitoring of the area were related to incident wave conditions and analyzed to evaluate structure performance. The favorable results of this MCCP study substantiate physical model test findings and indicate potential application of spur jetties at other sites. The Corps Coastal Program is sponsoring a follow-up study to develop design guidance for spur jetties.

The innovative concept of the spur jetties arose as a result of physical model studies conducted at CERC for the Rogue River project on the southern Oregon coast (Bottin 1983). Model results with spur jetties indicated that sediment in the nearshore zone moved toward the jetties and into an eddy which tended to deflect material away from the structure. Sediment would flow back toward shore where it is either reintroduced into the littoral

[1] A table of factors for converting non-SI units of measurement to SI units is presented on page ix.

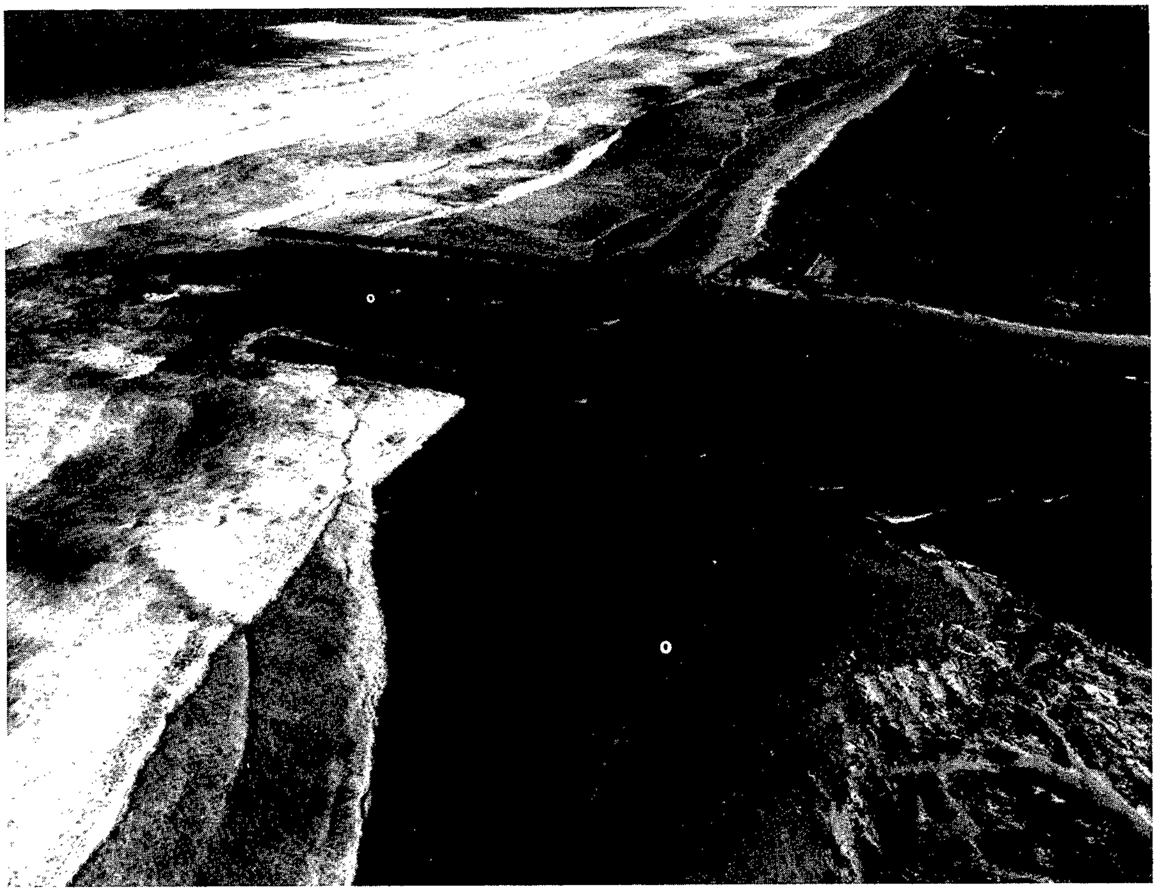

Figure 1. Siuslaw jetties prior to 1985 extension

transport system or carried by a jet of water away from the jetty parallel to the spur. Under certain conditions, some material was carried around the end of the spurs and into the "V" formed by the spurs and the jetty trunk, and some material continued around the jetty head and into the entrance. Qualitative evaluations of the Siuslaw River jetty extensions were made using the Rogue River physical model (Bottin 1983). Overall, the model study indicated the spurs alter the circulation pattern and potentially cause significant reduction of sediment shoaling in the navigation channel.

Original construction design for the Siuslaw jetties called for a 609.6-m (2,000-ft) north extension and a 762-m (2,500-ft) south jetty extension with both jetties terminating at a depth of -9.1 m (-30 ft) mean lower low water (mllw). The cost estimate made by NPP was $17 million based on 1975 price levels. Since the actual jetty construction was done in 1985, the Engineering News Record Construction Cost Index was used to update this estimate to 1985 price levels. The indexed estimate for 1985 for the original design is $32.2 million.

The new jetty design, based on 1981 physical model studies, called for a 580-m (1,900-ft) north jetty extension with a 122-m (400-ft) spur and a 701-m

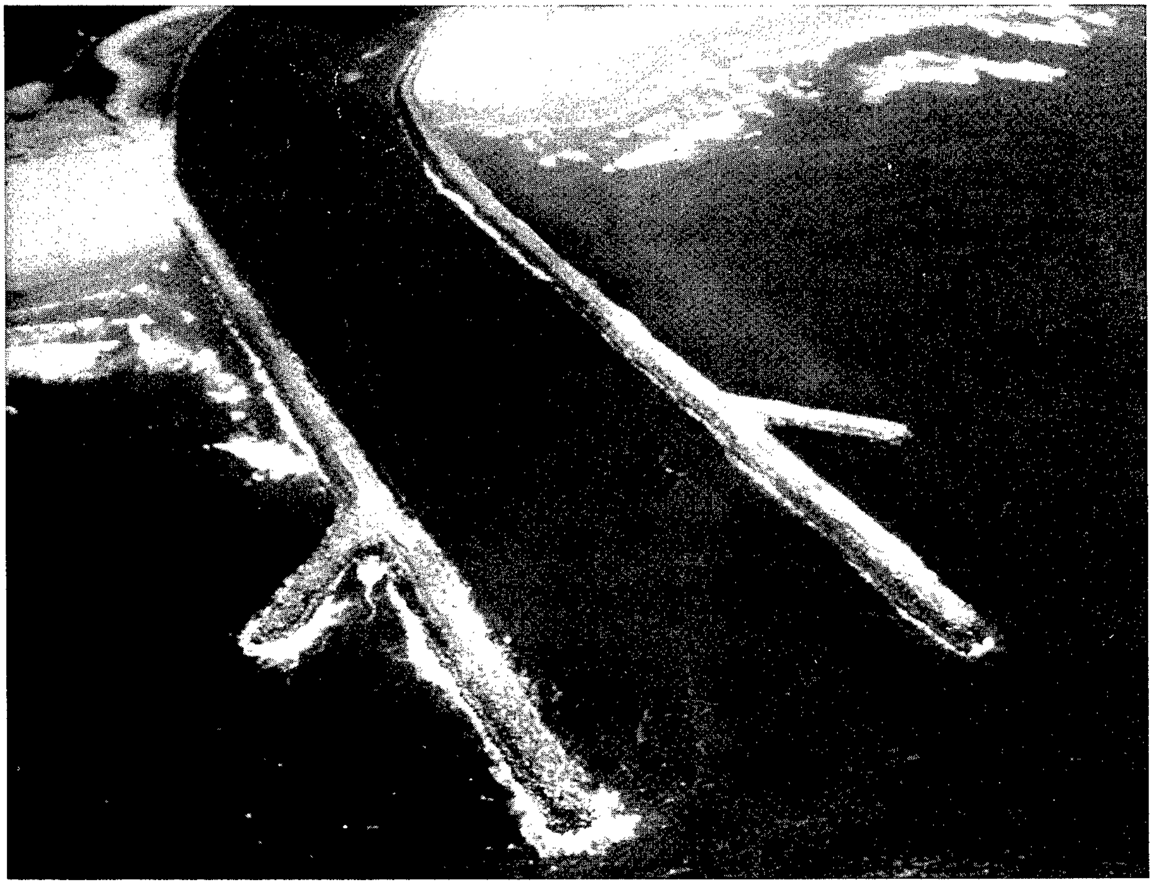

Figure 2. Jetties at Siuslaw River after 1985 extension

(2,300-ft) south jetty extension with a 122-m (400-ft) spur with both jetties terminating at a depth of -7.6 m (-25 ft) mllw. The actual construction varied slightly from the plan as described above but the actual cost in 1985 was $27.7 million.

Study Objectives and Monitoring

The objectives of the study were to determine if the spurs effectively deflect sediment; to identify shoaling patterns near the jetties; to compare existing prototype conditions to those predicted by the physical model study; to evaluate the effectiveness of the system in reducing the requirements for maintenance dredging; and to evaluate the impact of the jetties on the surrounding beaches. The last objective is chiefly addressed in a companion study, "Siuslaw Shoreline Surveillance 1981-1990" conducted by the NPP (Chesser 1992).

Monitoring for this study has included waves, currents, and bathymetric changes. Beginning in 1981 and ending in 1990 on a biyearly basis, NPP has collected beach profiles adjacent to the jetties using a helicopter-supported lead line system that allowed collection of a continuous transect across the beach through the surf zone and into deep water. Profiling has been done on 305-m (1,000-ft) intervals for a distance 8 km (5 miles) north of the jetties and 9.7 km (6 miles) south. Profiling intervals were 152.4 m (500 ft) for the first mile in both directions. In addition, bathymetry soundings have been taken in the navigation channel. After the construction of the jetty extensions, bathymetry measurements in a close grid have been taken around the spurs. These data are investigated to estimate annual dredging requirements and to identify shoaling patterns within the channel and exterior to the channel, as well as to evaluate the impacts of the 1985 jetty improvements on the surrounding beaches. An accuracy test of the helicopter bathymetry measurement technique used since 1960 along the north Pacific coast was conducted as part of this study.

To aid in the design, construction, and evaluation of nearshore structures, site-specific hydrographic climatology is necessary. Long-term directional wave records for localized regions rarely exist and are often expensive and difficult to obtain. Short-term, site-specific wave records may be correlated with adjacent longer-term directional wave records to determine their equivalence. Longer term records may then be translated and applied to nearby sites, providing useful cost-effective data sources for previously undocumented regions.

To evaluate incident wave activity at Siuslaw River a wave gauge was deployed offshore of the entrance for approximately 1 year, and the measurements correlated with other longer term sources of data. Under the Coastal Field Data Collection Program, wave information was collected from a Wave Rider buoy located offshore of the Coquille River approximately 97 km (60.3 miles) south of the Siuslaw River in 10 m (32.8 ft) of water. This document compares wave elevation and period at the Coquille buoy to that at the buoy located directly offshore of the Siuslaw River entrance. Measured differences were found to be within the uncertainty of the individual measurements; therefore, wave climatology at both locations can be considered equivalent. Data from the Coquille buoy are related to current and shoaling patterns near the Siuslaw River jetties to evaluate system response.

Bottom trailing drogues, dye studies, and aerial photographs were conducted to define current patterns in the area, but these efforts were found inadequate to delineate bottom currents in the area. The drogues only provided release and recovery locations and were relatively inconclusive for identifying any circulation patterns. The dye studies and aerial photos exhibited the circulation patterns of the surface currents but did not establish that the bottom currents were similar to the surface currents in this dynamic area which included the breaker zone and regions seaward of the breaker zone. To address this shortcoming, a helicopter current measurement system was developed and employed on two separate occasions to measure bottom currents and to establish bottom current patterns in the area. Localized current patterns induced by the spur jetties were identified, related to longshore current strengths, and correlated with physical model studies instrumental in the design of the jetty structures.

Site Description and Location

The Siuslaw River is approximately 173.8 km (108 miles) long and enters the Pacific Ocean near the City of Florence, OR, approximately 240 km (154 miles) south of the northern state border defined by the Columbia River (Figure 3). The city of Florence is located on the north bank at about river mile 5. South from Florence stretches the Dunes National Recreation Area (NRA), an area of active and partially stabilized sand dunes. These form the south bank of the Siuslaw River, which is the northern boundary of the NRA. North of Florence is an older, stable dune region, much of which is developed for home sites. Normal mean flows at the mouth of the Siuslaw River have been estimated as 89.2 cu m/sec (3,150 cfs) from precipitation records covering a period of about 27 years. The lower 42 km (26.1 miles) of the river are subject to tidal influences. The diurnal range of tide at the entrance is 2.0 m (6.6 ft) and the estimated extreme high water is 3.4 m (11.2 ft) above mllw. The tidal prism of the Siuslaw estuary covers approximately 9.1 km^2 (8,400 acre-ft) for the diurnal range.

The Siuslaw River entrance is located on the central Oregon coast near the northern end of what has been identified as the largest littoral cell within the state (Figure 3). The cell extends over about 90.8 km (49 n.m.) between Cape Arago to the south and Heceta Head 14.8 km (8 n.m.) to the north. There are two other jettied river entrances within the cell; both lie to the south of Siuslaw River. They are the Umpqua River, about 38.9 km (21 n.m.) south, and Coos Bay, approximately 74.1 km (40 n.m.) south. The Umpqua River system is the major contributor of sediments to the littoral cell. The Siuslaw River does supply some sediment but not on an annual basis.

Improvements of the Siuslaw River for navigation began before the turn of the century with the start of a jetty system. Federal participation in the project began in about 1910 and consists of two entrance jetties, an entrance channel 5.5 m (18 ft) deep, a navigation channel from the mouth to Florence 4.9 m (16 ft) deep and a 3.7-m- (12-ft-) deep channel to river mile 16. The north jetty is about 2,957 m (9,700 ft) long and the south jetty is 1981 m (6,500 ft) long. Both jetties were completed in 1917. Since that time, other improvements were authorized, the latest of which provided for extending the jetties to about the -6.1-m (-20-ft) depth. Prior to stabilization by the jetty system, the entrance of the river migrated back and forth over a distance of about 3.2 km (2 miles) north and south.

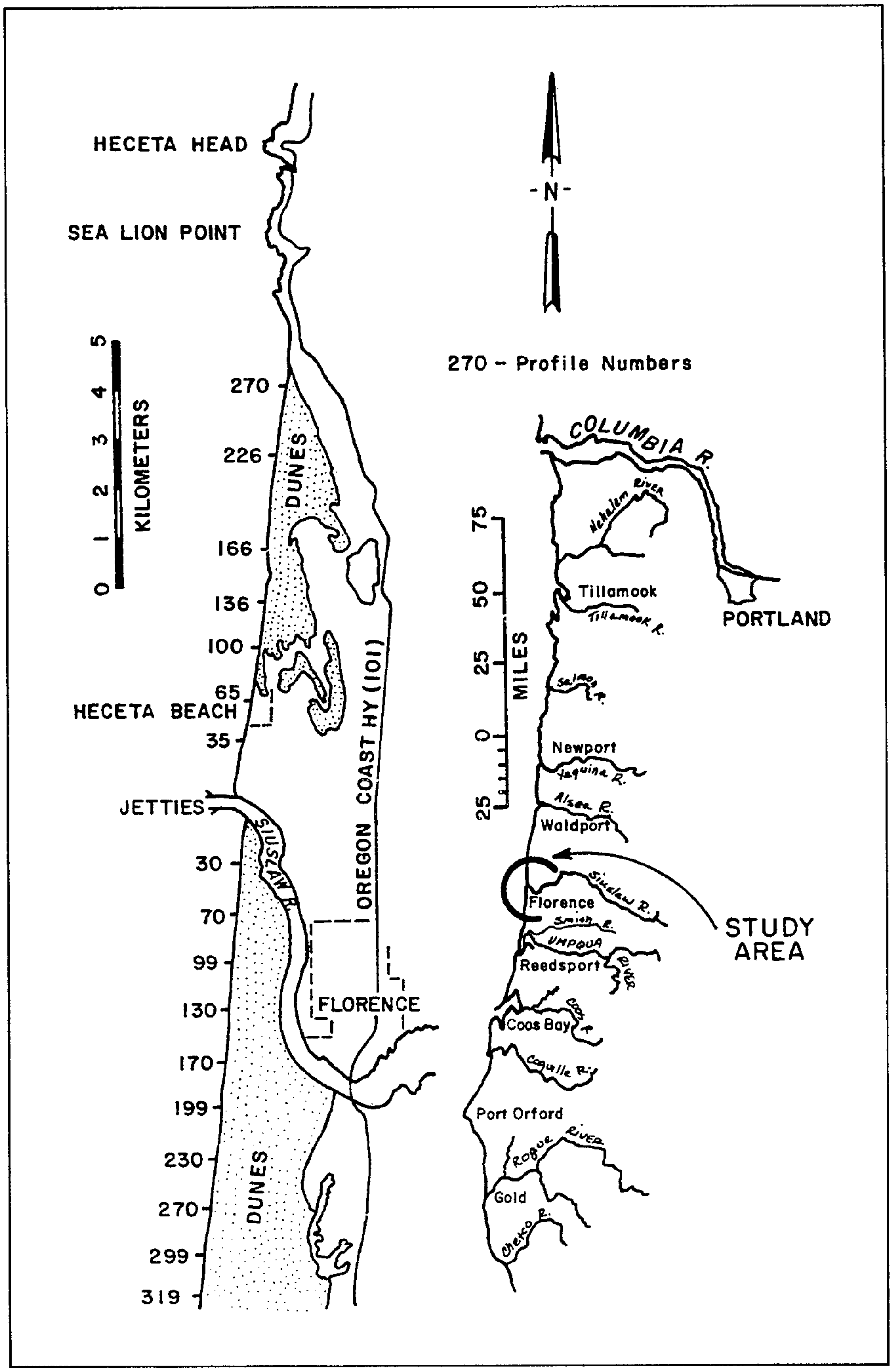

Figure 3. Location map of the Oregon Coast

Previous Studies

Prior to the last authorized improvement, a 183-m (600-ft) extension to the north jetty was authorized, but not constructed. When consideration was given to completing that extension, a contract was awarded to Oregon State University to study the potential impacts of jetty extension on the adjacent shorelines and the local littoral system (Komar 1975). The study concluded that construction of the original jetties at Siuslaw River would produce a rapid readjustment of the shoreline with accretion near the structures and erosion of the beaches. The study found that there had been relatively little overall change in the shoreline for the last 40 to 50 years and that further extension should cause no further overall realignment. The study did cite the possibility of some localized readjustment resulting in accretion next to the structures and related minor erosion over some distance to the north and south. Historical evidence was found of instances of shoreline erosion near Heceta Beach, about 3.2 km (2 miles) to the north of the entrance (Figure 4), which indicated the potential for localized shoreline problems with or without the jetty extensions. The beach area from Siuslaw River south to the entrance to Coos Bay (except for a small parcel south of the Umpqua River entrance) is within the boundaries of the Oregon Dunes National Recreational Area and there is very minimal development. The Heceta Beach area to the north is the site of a motel-restaurant complex and numerous homes; both summer and full-time residences. Any adverse shoreline changes would have much greater impacts if they occurred on the north side as opposed to the relatively undeveloped south side.

A physical model study of jetty designs for the proposed extensions at the Siuslaw River entrance was conducted at WES in 1981. The focus of the study was on the optimum length and design of the extensions to minimize longshore sediment transport around the ends of the jetties. Tracer material was used in the model to evaluate sediment movement for a number of test conditions. The most promising results were obtained with spur jetties at 45 deg to the main jetty. The spurs were 122 m (400 ft) long on the ocean side of each main jetty and 274 m (900 ft) shoreward of the outer end. This led to the least transport around the jetty ends. It was noted that as the shoreline near the jetties builds seaward, the spurs may lose effectiveness (Bottin 1981, 1983).

Studies related to ocean disposal at Siuslaw were conducted between 1984 and 1988. In 1984, a side-scan and seismic survey was done throughout the area within 2.4 km (1.5 miles) of the entrance. Prominent sand waves with north-south crests were found inshore of about the -12.2-m (-40-ft) depth contour. Wave and current data were recorded at -15.2-m (-50-ft) depths for 3 weeks in spring and 2 weeks in summer 1985. In both cases the predominant bottom currents were toward the north, although there were southward currents in summer. Offshore sediment samples collected in 1984, 1985, and 1988 show a well-sorted, fine sand throughout the offshore. Seabed drifters were used to monitor bottom currents near the ocean disposal site in the

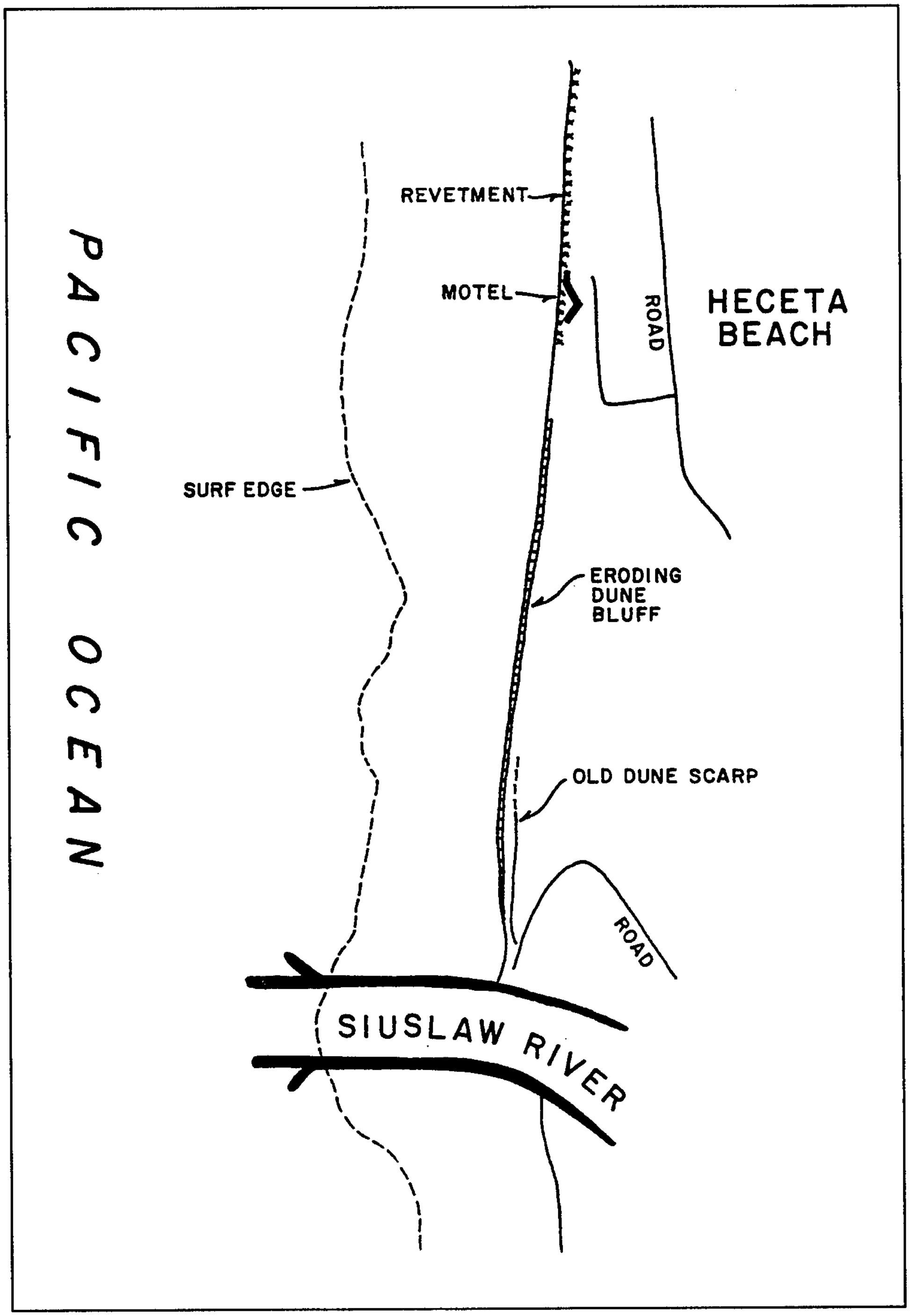

Figure 4. Heceta Beach location map

summers of 1986 and 1987. Drifter recoveries indicated predominant southward currents during the release periods (Hicks and Babcock 1988).

Background

Physical changes in the beach and nearshore at Siuslaw are due to sediment movement by waves and currents. Waves are constantly moving sediment out to depths of at least -9.1 m (-30 ft) year round, and probably to over -30.5 m (-100 ft) during winter storms. Waves generated by local winds are called seas and generally are steeper with shorter periods than longer period waves generated by distant storms called swells. Seasonal wave directions along the Oregon coast are from the north in summer and from the south in winter, with mixed directions in spring and fall. Large-scale storm systems affect the coast throughout the winter, most often resulting in large swells from the south.

Coastal winds generate direct currents as well as local waves. These are very important in longshore movement of sand. Figure 5 shows the relationship of winds and longshore current directions in a study at Newport, OR (Fox and Davis 1974). During their study period, two low-pressure systems caused winds towards the north on 6-9 and 17-22 July 1973. After a 2- to 3-day lag, longshore currents shifted from south to north in response. The currents again lagged several days when high pressure returned before resuming their southerly direction. For sediments already in motion due to wave action, such currents can result in a net transport in the direction of the current even if the longshore current is not strong enough to transport sediment by itself.

Onshore/offshore movement of sands is also seasonal and consists of general buildup of the beach during the summer months, followed by erosion and offshore deposition during the winter. Even during mild winters with little beach erosion, the beach face steepens. During severe winter storms, the beach and dune areas may suffer significant erosion. In some cases the beach material forms an offshore bar which "stores" the material for return to the beach. If the material moves too far offshore, it may take more than one season to return, or it may be lost to the littoral system. This may have been the case during the El Niño winter storms of 1982-1983.

Figure 6 is a cartoon illustrating the seasonal beach erosion/accretion cycle along the Oregon coast. During summer, local winds are predominantly from the north, ocean swell is from the northwest, and the beach is wide with no prominent offshore bars. During winter, the winds are strongest from the south, and ocean swell is from the southwest. Larger waves erode the beach, reducing its width and creating offshore bars.

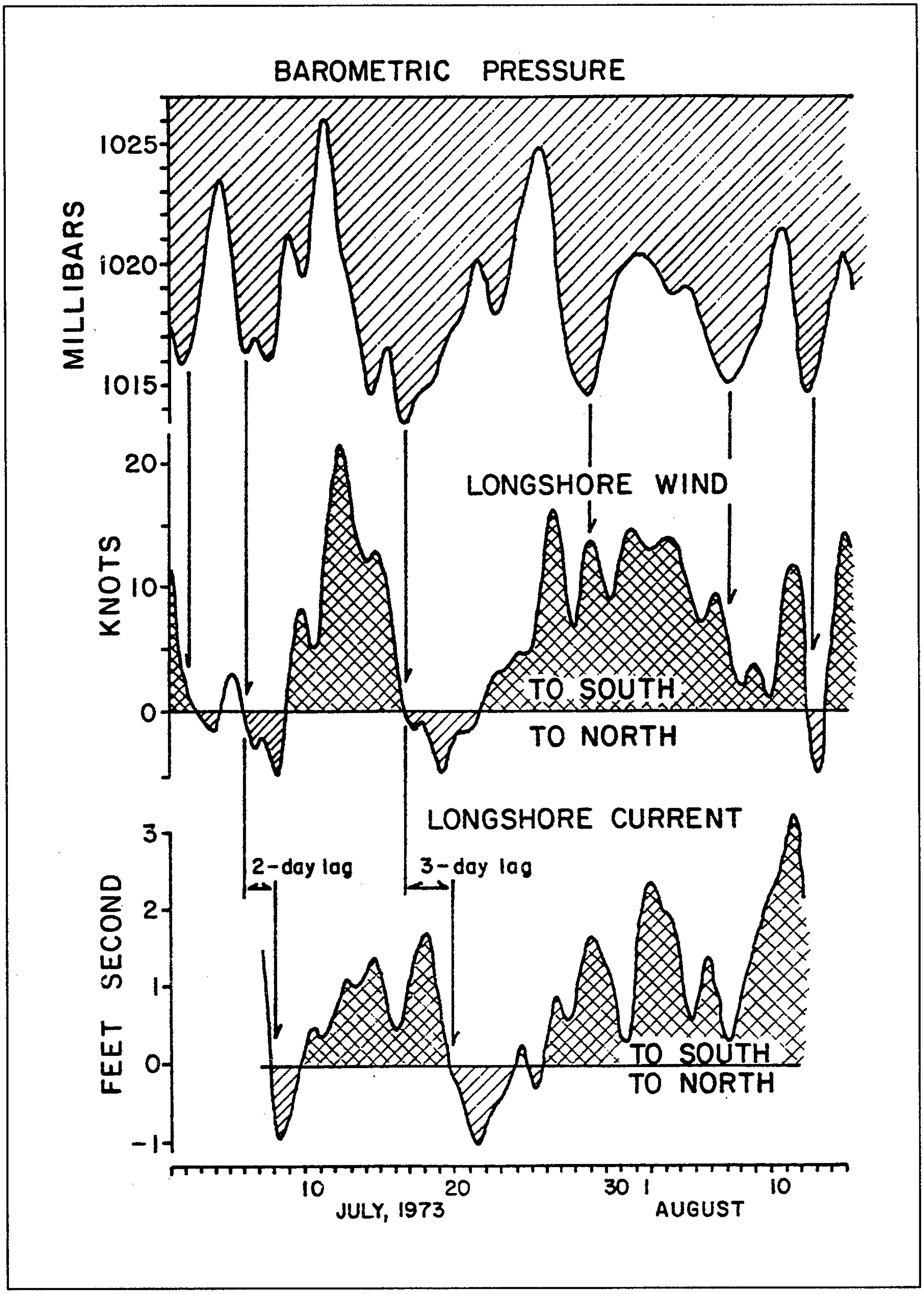

Figure 5. Winds and longshore current direction relationship

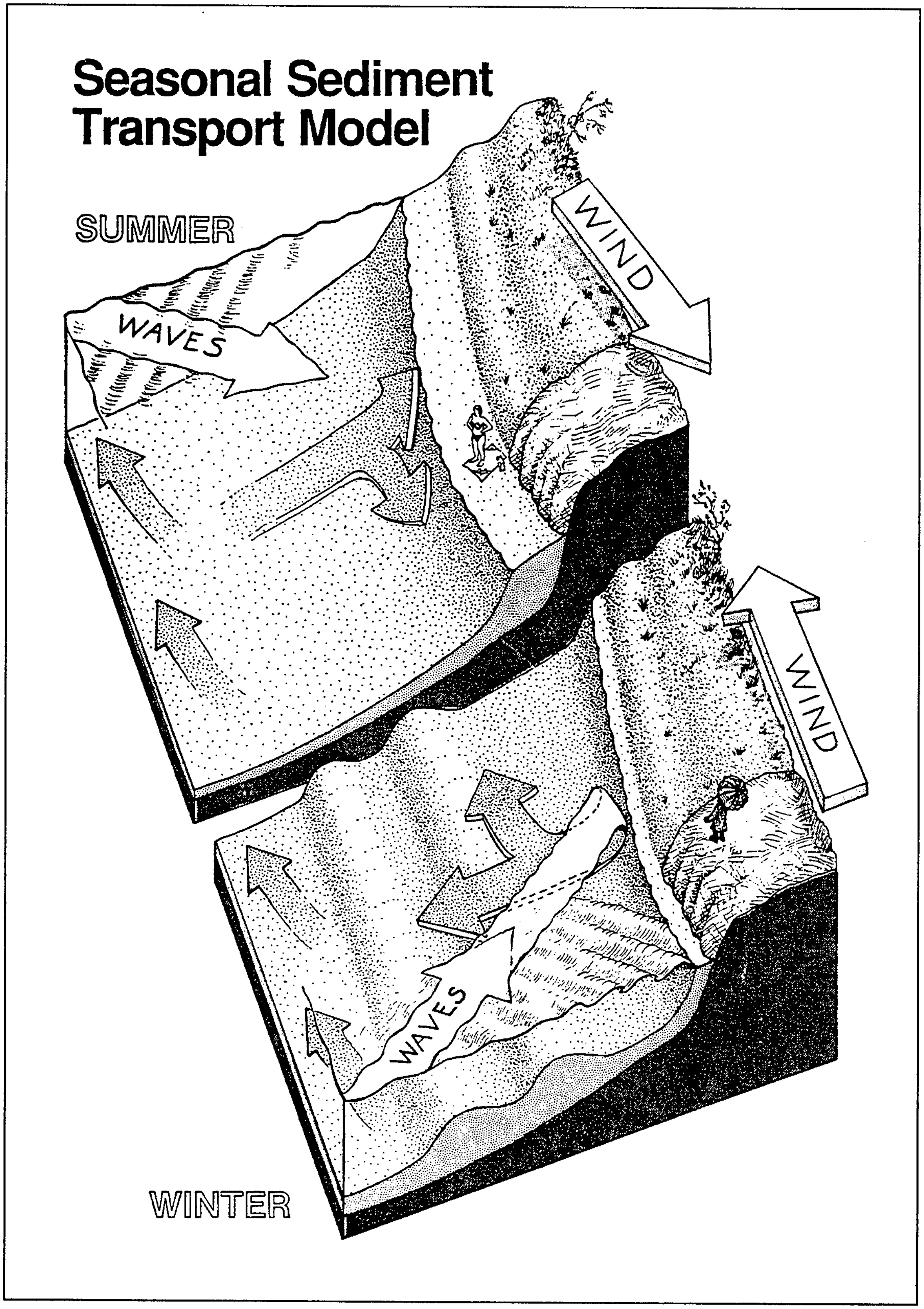

Figure 6. Seasonal beach erosion/accretion cycle

2 Incident Wave Conditions

Wave data were required to define the wave climate at the Siuslaw River, OR, study site for evaluating potential application of the spur jetty concept to other sites, and to relate occurrence of any observed response of the system (i.e., shoreline change or jetty damage) to incident conditions. Since the study encompassed neither the time nor the funds to operate a wave gauge at the site for a sufficient period to obtain climatic statistics directly, a gauge was deployed for approximately 1 year near the entrance to the Siuslaw River, and the measurements compared to other, longer term sources of data at adjacent locations. The comparison is made to determine the applicability of the longer term data source to the study site. The first section of this chapter validates this assumption. The second section of the chapter presents a summary of the long-term wave record paralleling the MCCP study period. The third section of the chapter discusses the climatic event "El Niño."

Wave Analyses: Comparison of Adjacent Gauges

Background

The nearest long-term wave gauge is located about 93 km (50 n.m.) southward, near the entrance to the Coquille River in Oregon (Figure 7). The Coquille gauge has been operating intermittently since 1983 at latitude 43.1 °N, longitude 124.5 °W in 65 m (213 ft) of water. It is a part of the Coastal Data Information Program (CDIP), a network of wave gauges jointly managed by the Corps of Engineers' Field Wave Gaging Program and the State of California Department of Boating and Waterways, and operated by the Scripps Institution of Oceanography (SIO). The Siuslaw wave gauge funded by the MCCP study became part of the CDIP when it was deployed at latitude 44°01'N and longitude 124°15'W in 66 m (217 ft) of water, or about 9.3 km (5 n.m.) west of the Siuslaw River entrance (Figure 7). The gauge was operated between 15 September 1988 and 11 January 1990.

The gauges at Coquille River and Siuslaw were Waverider brand non-directional, surface-following buoys that measure vertical acceleration. Double integration of the acceleration signal is performed in the gauge to provide a

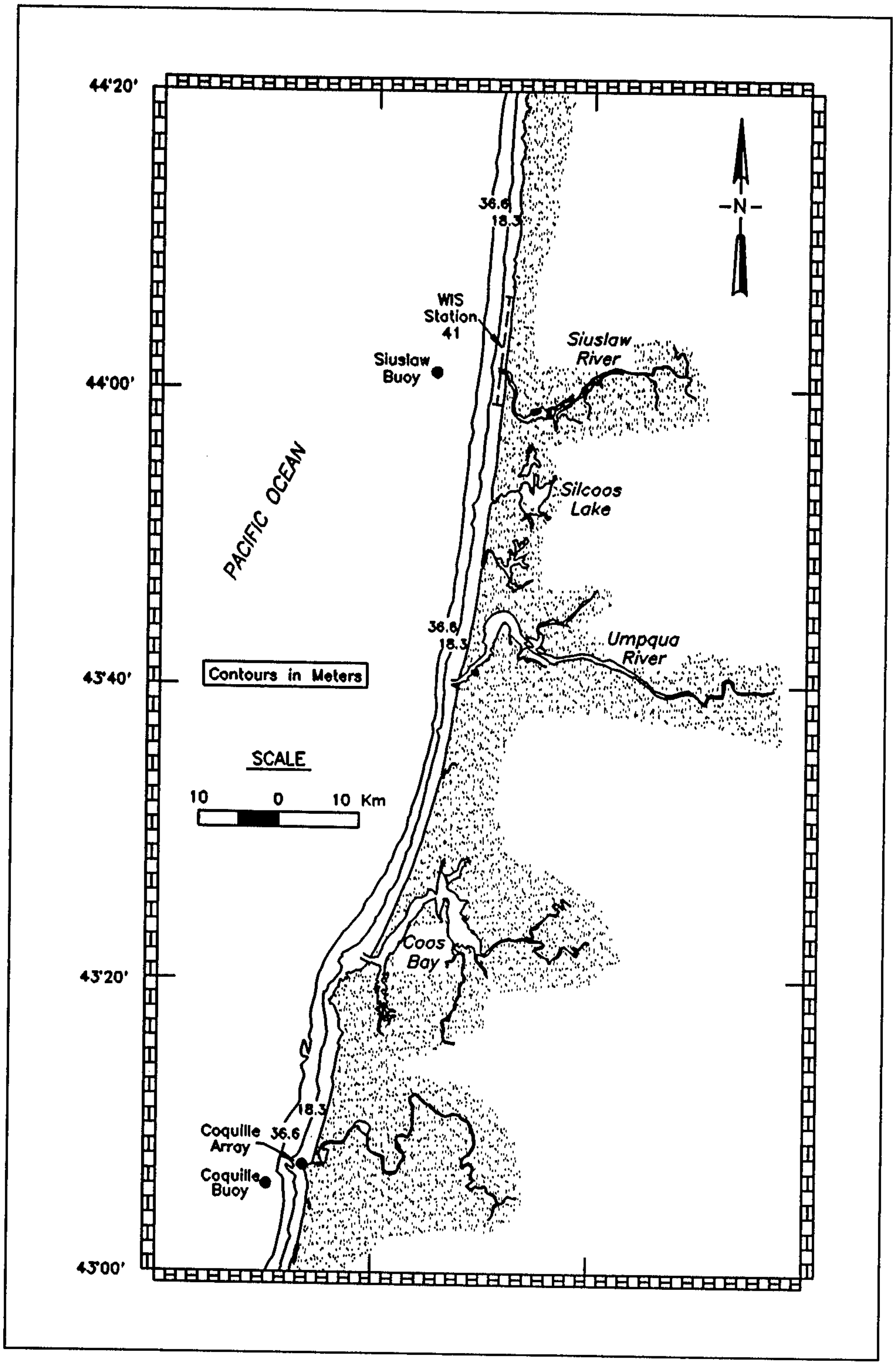

Figure 7. Locations of wave buoys

time series of the sea surface elevation. The time-series signal from the gauge was transmitted to a receiving station on shore and stored in a memory buffer. The shore station was polled over land telephone lines every 3 hr by a central computer at SIO for downloading the data. Each recovered time series contained 2,000 measurements sampled at 1 Hz. Each sea surface time series was spectrally analyzed to produce a one-dimensional power spectrum. The significant wave height, calculated from the zeroth moment of the power spectrum, and the peak period, defined as the center of the frequency band at which the maximum of the power spectrum occurs, are the two wave parameters that will be utilized in the following discussion. The Waverider buoy does not measure wave direction.

The CDIP produces a standard monthly summary that provides a table containing the significant wave height, the total energy, and a coarse resolution energy spectrum with eight 2-sec period bands between 4 and 22 sec, plus the remaining energy in periods greater than 22 sec, for each measurement interval (Scripps Institution of Oceanography 1990). In general, the vertical response of accelerometer-type wave gauges decreases for longer period (over 22 sec) waves. The summary also provides a stacked plot of the energy spectrum for the month, and a persistence table (the number of days the wave height exceeds a range of values). Figure 8 is an example of the spectral plot, and Table 1 is a portion of the spectral table, for the Siuslaw gauge for the month of December, 1989.

Up until 1990, the CDIP also produced an annual report that contains statistical summaries of the wave parameters for the entire year. In 1990, the annual report was changed to a cumulative report that contains updated statistics for the entire data set for each gauge in the network (Seymour et al. 1992). It provides cumulative probabilities of exceedence for height and period, seasonal probabilities of height exceedence, and joint distribution of height and period (number of occurrences).

The other source of wave data available for describing the conditions near the Siuslaw River entrance is the Wave Information Study (WIS), a 20-year (1956-1975) numerical hindcast of wave conditions managed by the Corps' Coastal Field Data Collection Program (Brooks and Brandon 1995). The hindcast is produced from hourly atmospheric pressure readings over the north Pacific provided by the National Weather Service. The pressure field is used to generate a deep-ocean wave field using a numerical spectral wave generation model. The size of the deep-ocean grid precludes representation of smaller atmospheric events, such as hurricanes. The deep-ocean wave field is transformed into coastal "stations" using a wave propagation model. Nearshore stations are representative of a stretch of coastline approximately 11 km (6 n.m.) long at the 10-m (33-ft) depth contour. The result is hourly directional spectral wave conditions for each station in the hindcast. Because the numerical grid does not include the Southern Pacific, long-period swell generated in the Southern Hemisphere is not represented in the hindcast.

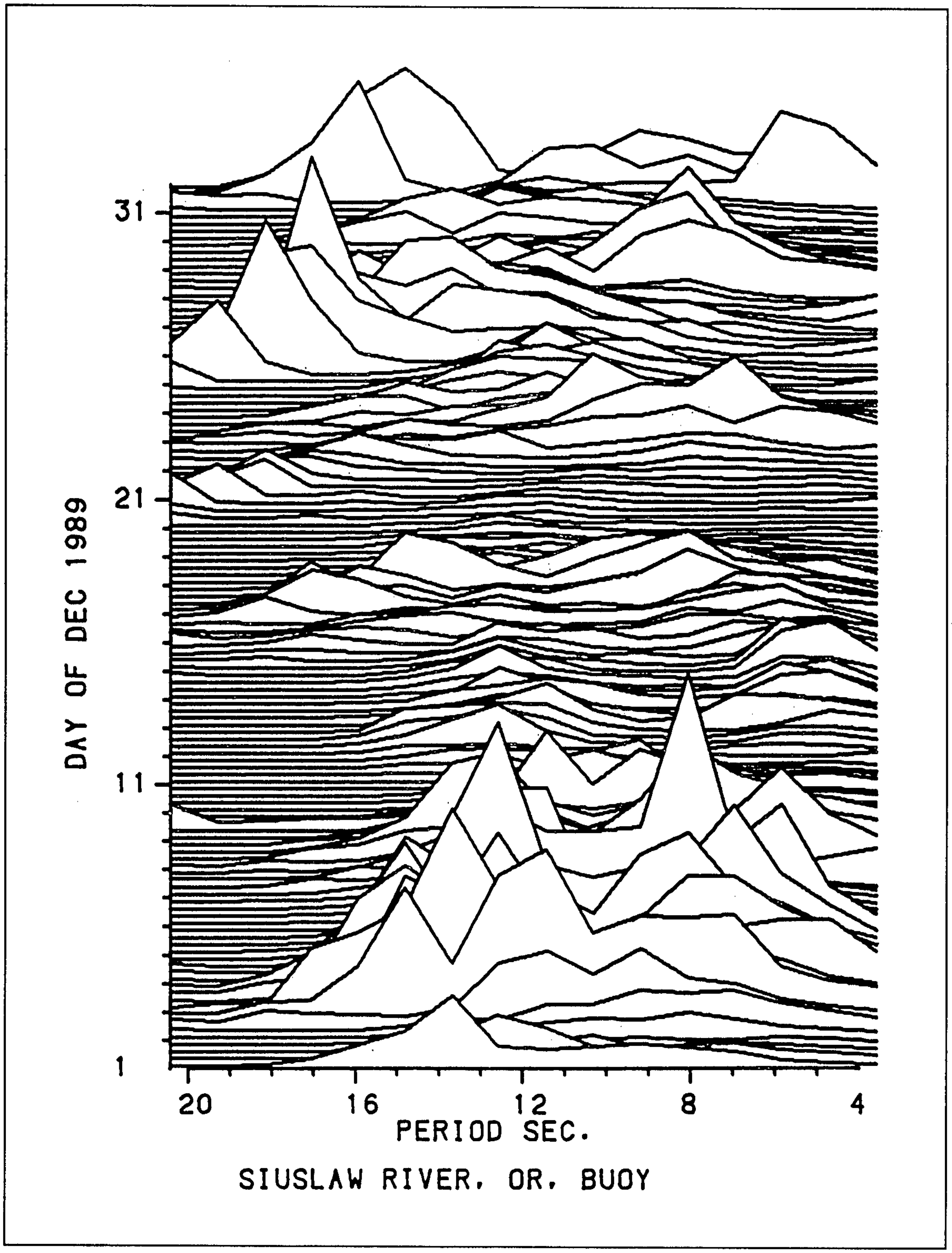

Figure 8. Sample time series of energy density spectra from CDIP, December 1989

Table 1
Sample Tabular Listing from CDIP Monthly Summary[1]

PST		Significant Height, cm	Total Energy cm sq	Percent Energy in Band (Total Energy Includes Range 2048-4 secs) Band Period Limits, secs								
Day	Time			22+	22-18	18-16	16-14	14-12	12-10	10-8	8-6	6-4
1	0240	210.0	2,757.1	0.1	0.2	3.2	21.8	34.7	14.2	16.3	7.7	2.2
1	0838	180.8	2,043.8	0.1	0.1	0.7	13.4	35.6	22.7	10.8	12.7	4.4
1	1435	124.1	962.3	0.1	0.2	0.7	13.0	14.9	32.7	11.4	19.7	7.9
1	2038	98.7	608.8	0.1	0.2	0.6	5.0	19.3	13.4	22.6	22.0	17.3
2	0235	156.7	1,533.9	0.1	0.2	0.2	2.8	8.5	25.1	31.1	22.4	10.1
2	0835	209.5	2,742.4	0.2	0.9	0.3	2.0	9.0	20.1	29.3	26.1	12.5
2	1434	277.7	4,821.2	0.3	1.3	5.2	3.4	16.6	26.6	26.1	14.1	6.7
2	2035	419.6	11,003.3	0.2	0.5	2.9	16.8	17.9	23.2	18.4	14.2	6.3
3	0237	397.6	9,880.9	0.1	0.8	7.1	18.9	34.0	11.0	10.8	11.5	6.2
3	0834	327.3	6,696.4	0.1	0.4	2.3	23.9	28.1	17.4	16.4	6.8	5.1
3	1435	421.9	11,122.3	0.2	0.6	2.8	21.3	24.1	12.6	14.3	13.4	11.1
3	2034	417.7	10,905.0	0.2	0.3	4.5	21.0	15.3	13.9	17.1	18.3	9.8

[1] From CDIP monthly report, December 1989.

The WIS model calculates reduced parameters—significant wave height, peak period, and peak direction—for climatic analysis. The WIS publishes a statistical summary of the hindcast results (Jensen, Hubertz, and Payne 1989) that provides joint distribution of height and period in seven directional bands, plus for all directions combined; the mean and highest wave heights by month and year; and mean and extreme values for the entire record. The WIS station that brackets the Siuslaw River entrance is station 41, extending from latitude 43°59'N, longitude 124°09'W to latitude 44°06'N, longitude 124°08'W in the 10-m water depth. Figure 7 shows the location of the gauges as well as the hindcast station.

Time Domain Comparisons

The complete data set of concurrent wave measurements (within 10 min) from the Siuslaw and Coquille gauges contains 2,930 records. Figure 9 illustrates the calculated correlation coefficient for both significant wave height and peak period for the two sites, seasonally as well as annually (Jan - Mar = winter, April - June = spring, etc.). The correlation is quite high for the heights, 0.96 for the entire year, with a low of 0.91 for the summer. Maximum wave period correlation is 0.75 for the entire year. The lower correlation

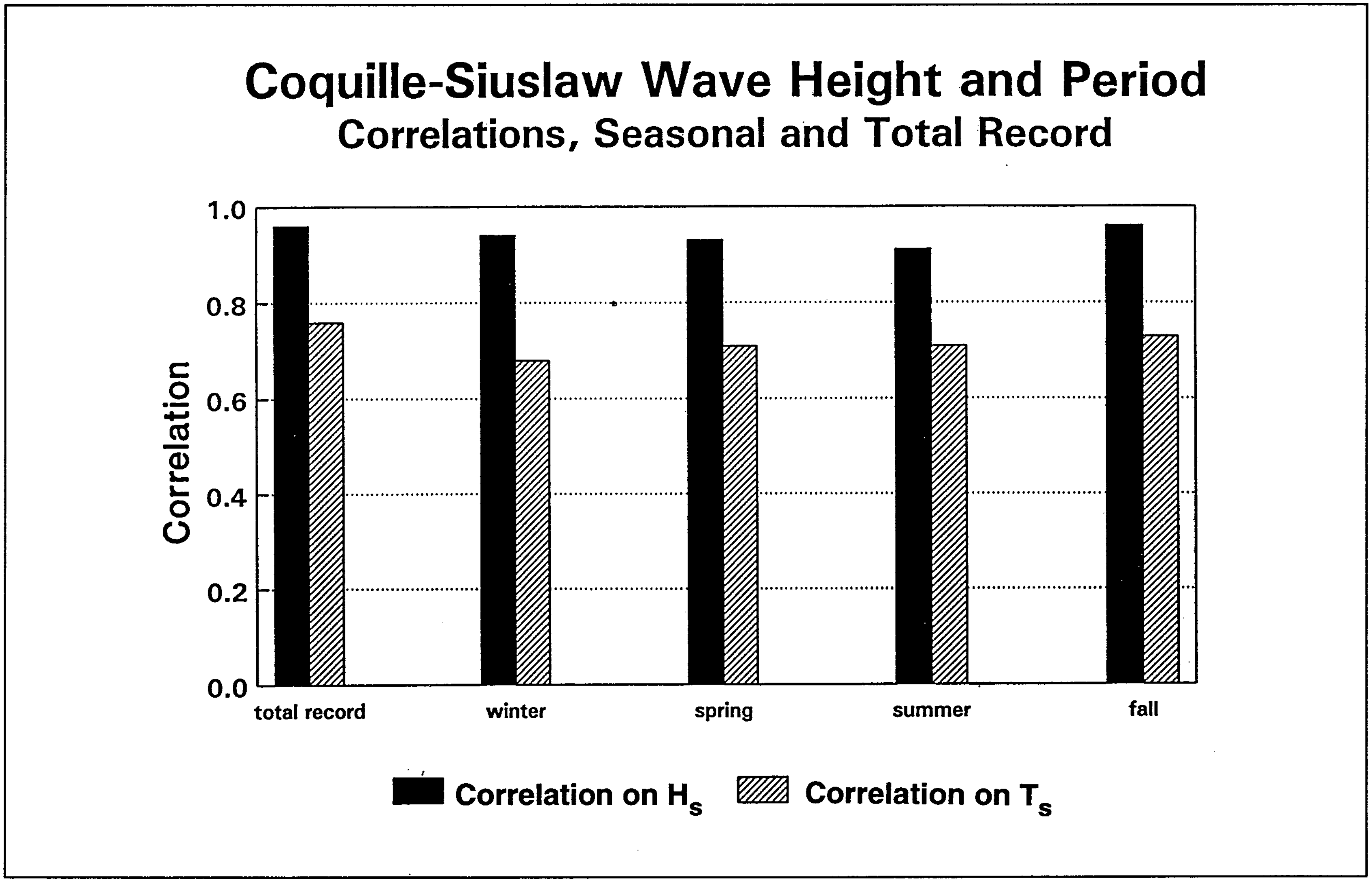

Figure 9. Wave height and period correlations for Siuslaw and Coquille

for the peak periods is partially due to the coarse resolution of the period spectra. For example, reducing the wave heights to only nine bins reduces the correlation from 0.96 to 0.85. Variance in peak period is also explained by the character of the parameter. A complex spectrum may have two (or more) peaks of nearly equal energy density at two widely different frequencies. Slight differences in energy level of the multiple peaks between two sites, or between successive measurements at one site, can result in the large jumps in the period designated as the peak.

Figure 10 plots the percent occurrence of the ratio of wave heights at Siuslaw to Coquille, H_1/H_2, again by season and annually. The annual curve illustrates that nearly 30 percent of the time, the ratio was 1.055. Taking the seasonal variation into account, the ratio for most cases varies from 1.022 for the spring to 1.116 for the winter. Seasonal differences in the ratio are assumed to be principally influenced by variations in typical wave direction. Without directional information to better define this relation, the seasonal differences from the annual ratio (on the order of 5 percent of the wave height) will be ignored.

Figure 11 places confidence limits on the uncertainty associated with using the predictive value of 1.055 for the entire data set. The estimator, $H_1 = 1.055\ H_2$, will be correct to within 5 percent 33 percent of the time, to within 10 percent 58 percent of the time, and to within less than 22 percent of the actual value 90 percent of the time. Another indicator of the uncertainty is the absolute mean error e where

$$e = H_1 - 1.055\ H_2 = 22\ \text{cm} \tag{1}$$

The standard deviation of e is 31 cm.

There are inherent uncertainties in the reduced parameters (which are themselves a statistical property) for any single wave record. A rigorous uncertainty analysis for wave parameters is beyond the scope of this report, but the order of the uncertainty makes both the seasonal variation and the difference from unity in the wave ratio negligible.

Climatic Statistical Comparisons

Figure 12 compares the seasonal probability of exceeding selected wave heights for the single year of data at Siuslaw to the multi-year record at Coquille. Most of the probabilities for the two gauges are within a few percent. The largest difference is an 8-percent higher probability of 2-m (6.6-ft) waves occurring at Coquille than Siuslaw in the spring. The slightly higher (5.5 percent) wave heights at Siuslaw in the time domain are partially offset by the longer record at Coquille.

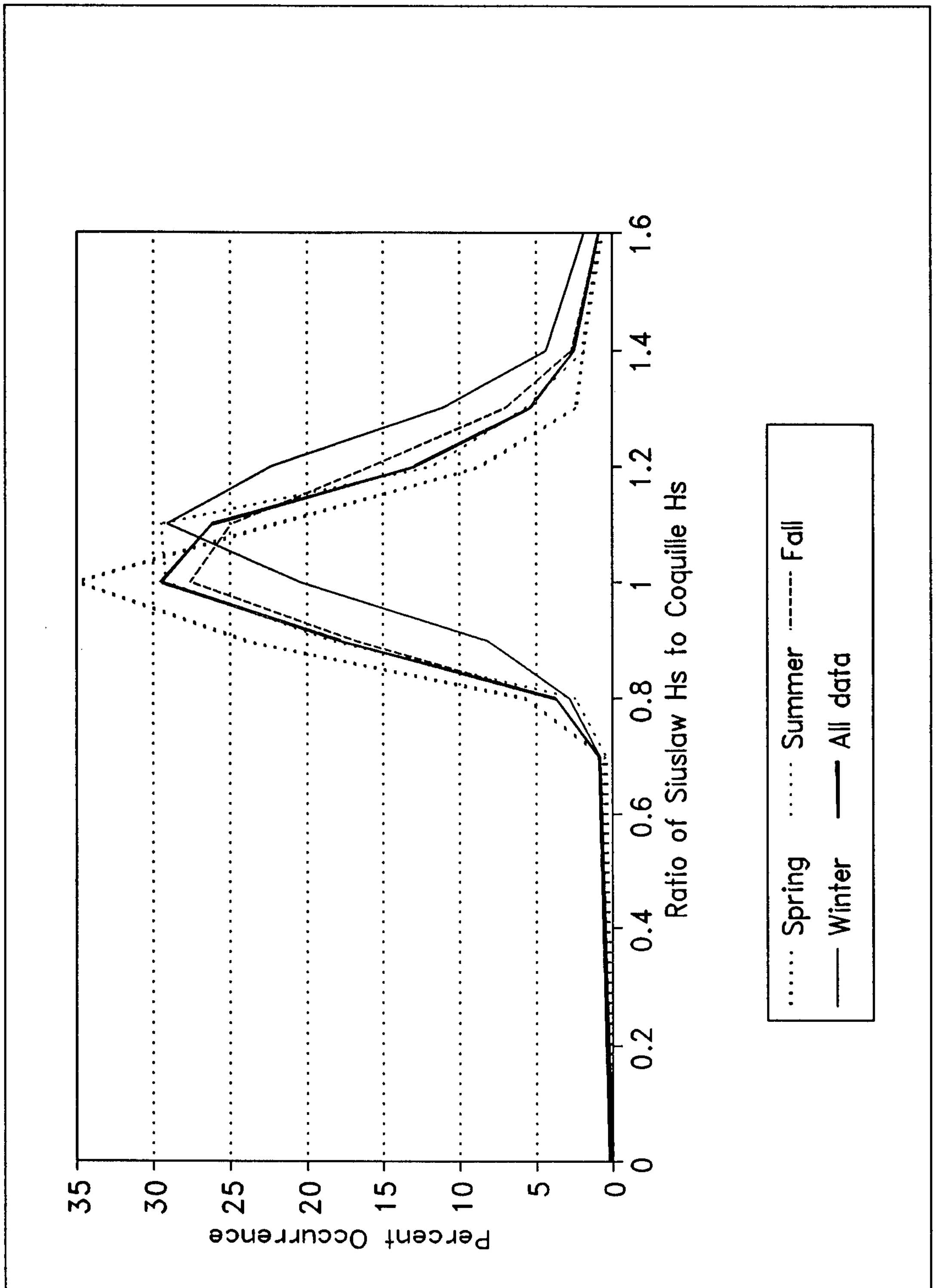

Figure 10. Seasonal and total probability distribution of wave height ratios for Siuslaw and Coquille

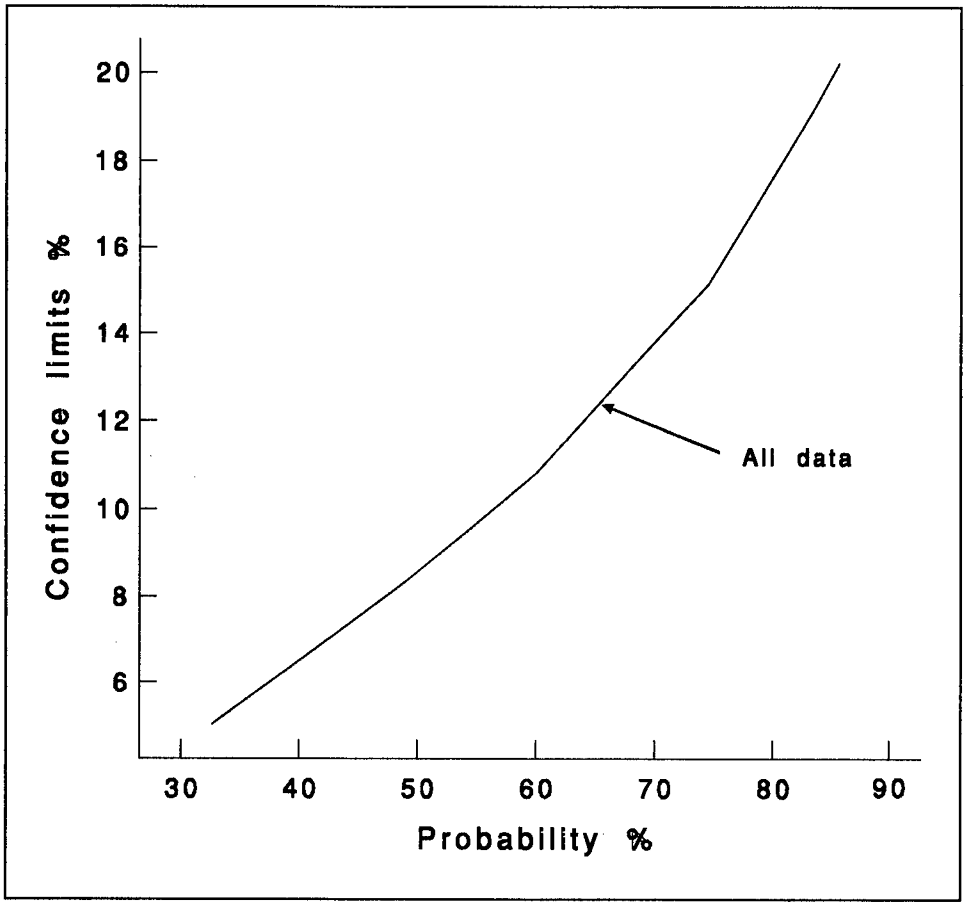

Figure 11. Seasonal and total confidence limit probability distributions for wave height ratio of 1.055 for Siuslaw and Coquille

Because of the uncertainties in peak period described above, a joint correlation of height and period will only be presented graphically. Figure 13 shows the shape and percent occurrence at the two sites to be quite similar. The most common condition at both sites is waves between 1 and 1.5 m (3.3 and 4.9 ft) at about 7 sec. Use of the Coquille statistics to describe the climate at Siuslaw is justified by the longer, more reliable record and will not result in significant errors in assigning probabilities of occurrence of future events. Cumulative height probabilities for Coquille are shown in Table 2.

Figure 14 is a plot of the cumulative height probabilities of exceedence for WIS station 41, the Siuslaw gauge and the Coquille gauge; Figure 15 is a similar plot for peak periods. Wave height probabilities at Siuslaw are slightly skewed upward relative to Coquille, as expected. Period plots for the two gauges are essentially identical. The smoother shape of the Coquille plot is evidence of the longer, more stable record.

Ideally, the 20-year hindcast at a site near Siuslaw would provide an even more reliable climate than shorter-duration measurements. There are some differences in the format between the two data sources, but they should not

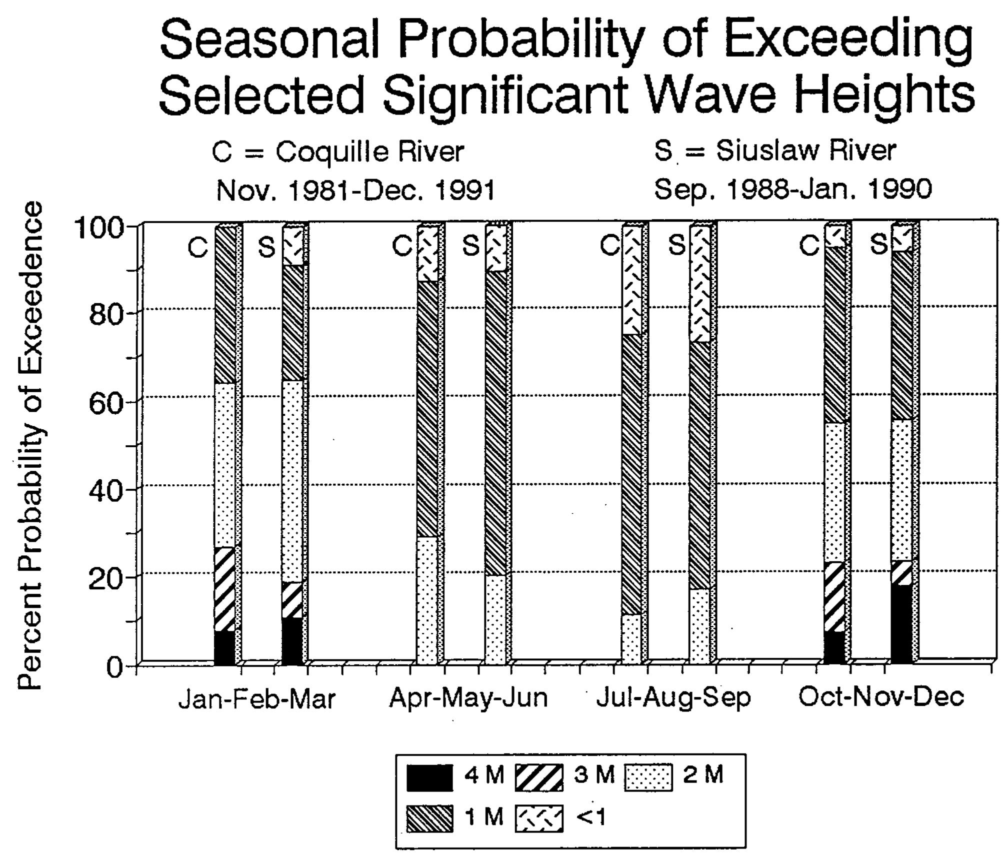

Figure 12. Seasonal probability of exceeding selected significant wave heights for Coquille and Siuslaw Rivers (Seymour et al. 1992)

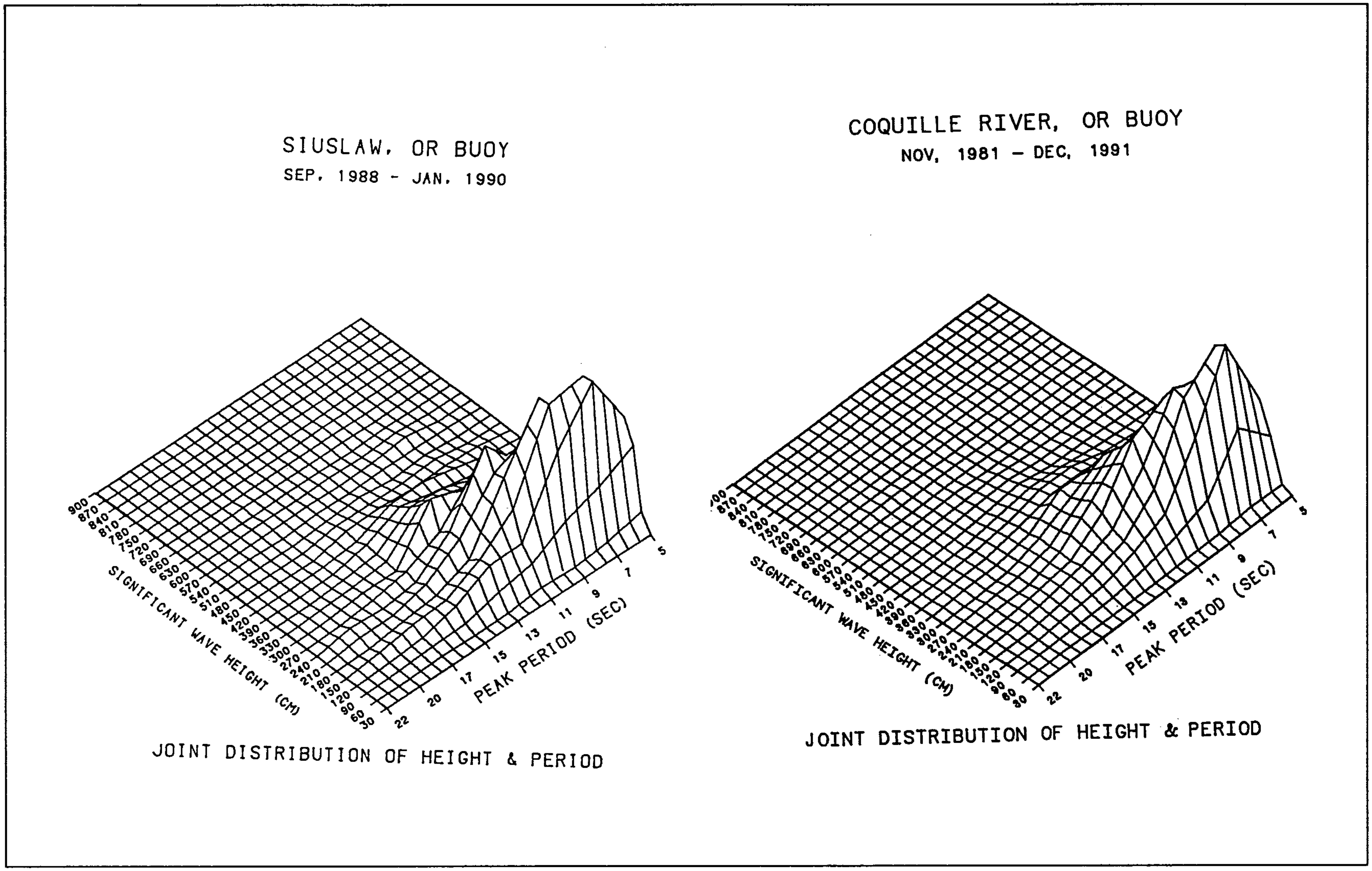

Figure 13. Joint distribution of height and period measurements for Siuslaw and Coquille Rivers (Seymour et al. 1992)

Table 2
Coquille River, OR, Buoy (November 1981 - December 1991)

Cumulative Height Probabilities			Cumulative Peak Period Probabilities		
Height, cm	Probability	Occurrence, hr	Period, sec	Probability	Occurrence, hr
900	0.0000	<12	22+	0.0005	36
870	0.0000	<12	20	0.0087	616
840	0.0000	<12	17	0.0306	2,169
810	0.0001	<12	15	0.0848	6,007
780	0.0001	<12	13	0.2091	14,806
750	0.0003	20	11	0.4099	29,027
720	0.0005	36	9	0.6613	46,826
690	0.0010	72	7	0.9046	64,056
660	0.0019	134	5	1.0000	70,810
630	0.0036	253			
600	0.0050	352			
570	0.0065	460			
540	0.0097	683			
510	0.0149	1,056			
480	0.0222	1,569			
450	0.0316	2,237			
420	0.0459	3,252			
390	0.0683	4,837			
360	0.0948	6,711			
330	0.1341	9,497			
300	0.1874	13,268			
270	0.2578	18,255			
240	0.3562	25,226			
210	0.4836	34,242			
180	0.6243	44,206			
150	0.7820	55,371			
120	0.9250	65,501			
90	0.9945	70,421			
60	0.9998	70,794			
30	1.0000	70,810			

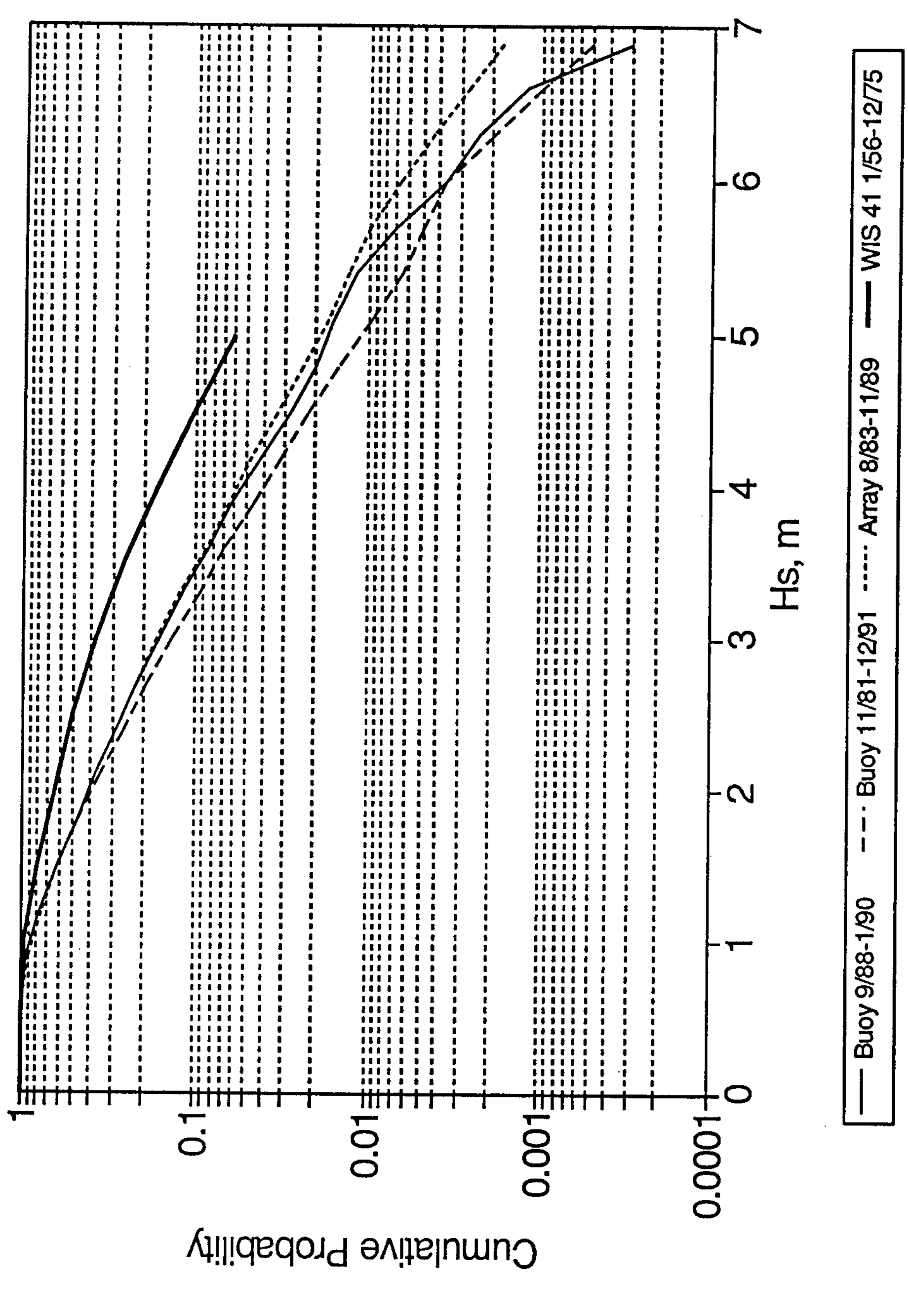

Figure 14. Cumulative wave height probabilities of exceedence (Seymour et al. 1992; Jensen, Hubertz, and Payne 1989)

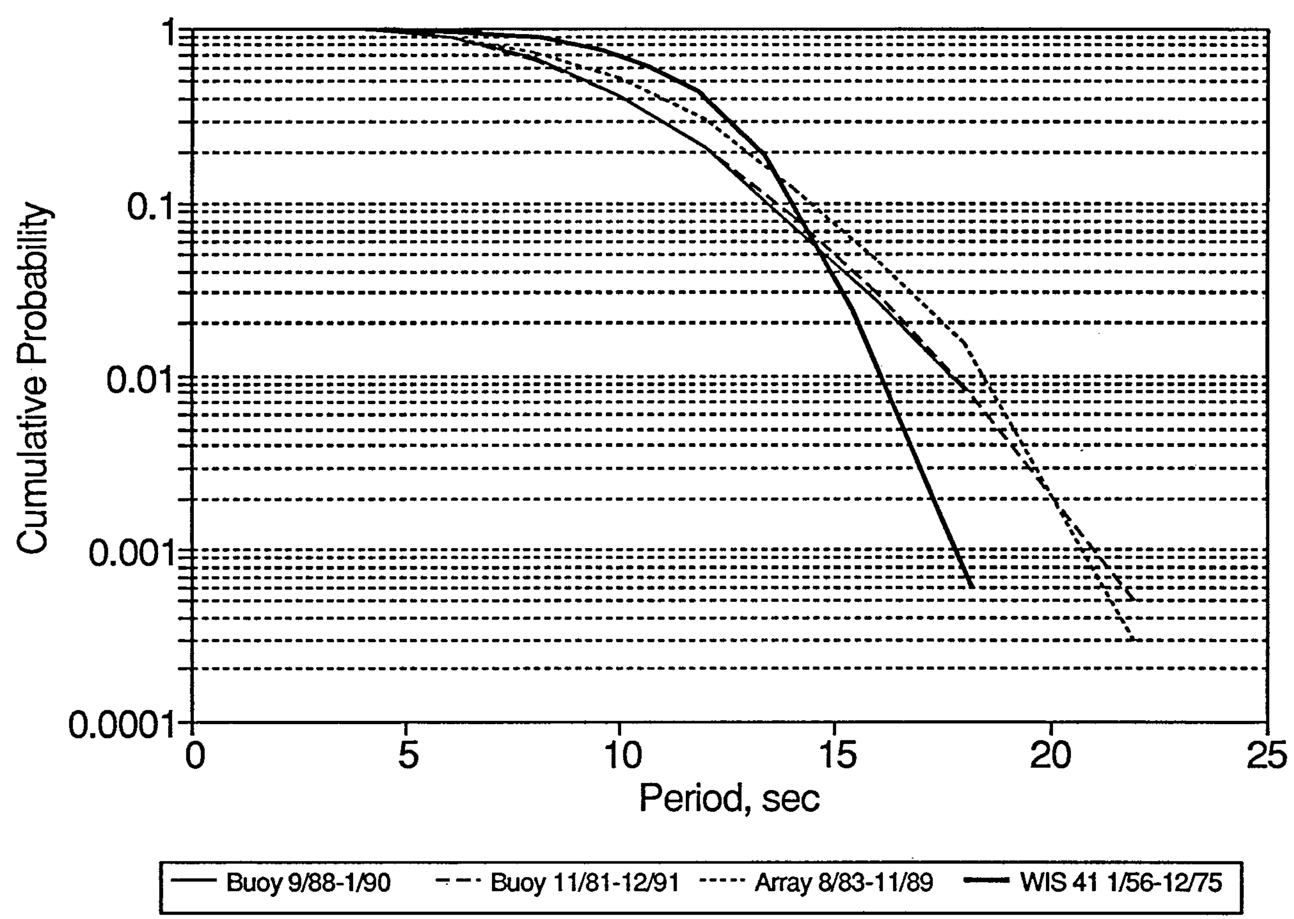

Figure 15. Cumulative peak period probabilities of exceedence (Seymour et al. 1992; Jensen, Hubertz, and Payne 1989)

affect the plotted results. The WIS statistics are provided in height and period bins similar, though not identical, to the CDIP data, and standard WIS output does not provide detail for waves over 5 m (16.4 ft), as is done for the CDIP data.

The WIS data show significant overprediction of the occurrence of wave heights below 5 m (16.4 ft). This could be partially due to shoaling processes between the 65- and 66-m (213- and 217-ft) depth of the gauges and the 10-m (32.8-ft) depth of the hindcast station. Data from another CDIP shallow-water, 10-m (32.8-ft) gauge at Coquille, a pressure array located shoreward of the Coquille buoy (see Figure 7), are also plotted in Figures 14 and 15. The plots show that statistically, some shifting of the spectra has occurred in shallower water, towards higher waves which tend to be longer in period. Again, the coarse resolution of the spectrum causes a significant jump when the peak period moves just one band. Shoaling effects at Siuslaw, which has a more regular bottom slope from the 60-m (197-ft) to 10-m (32.8-ft) contours than does Coquille, are not expected to be any more pronounced.

The WIS data overpredict wave periods below 15 sec, then underpredict the occurrence of swell waves longer than 15 sec by approximately an order of magnitude. Shoaling processes do not generally result in a significant shift in spectral peak. The actual data are more broadly distributed in period than predicted.

Conclusions

For estimation of historical wave conditions (i.e., conditions at a particular time) at Siuslaw before 1983, when the Coquille gauge was established, the WIS database is the best available source. For estimation of conditions at Siuslaw after 1983, when the Siuslaw gauge was not in place, the Coquille data should be adequate for most engineering applications. Adjusting the wave heights upward by 5 percent will improve the statistical confidence slightly. Obviously, the measured data at Siuslaw are the best source when available. Probabilities of exceedence for wave periods at Siuslaw are represented well by the Coquille data. Probabilities of exceedence for wave heights at Siuslaw are represented less confidently by the Coquille data, but agreement between the gauges is significantly better than agreement with the hindcast. Shoaling effects will occur between the offshore buoy location and any position shoreward, such as the 10-m (32.8-ft) depth of the WIS station, but are probably not as pronounced as indicated by the hindcast.

Local Wave History

Historical wave information sources were evaluated in the previous section for application to the Siuslaw River region. The wave information data set collected by the CDIP gauge located near Coquille River, OR (Figure 7) was determined to be the best long-term indicator of incident wave conditions at Siuslaw River for the time frame of this MCCP study and is adequate for engineering applications. Information regarding the wave gauge, collection processes, and confidence limits are described previously in this chapter. Presented in the following section are the historic wave record and a review of monthly, annual, and seasonal averages and variances.

Wave data information from the CDIP Coquille River, OR, gauge was provided by SIO. The gauge was located in approximately 65 m (213 ft) of water and sampled on 6-hr intervals. Data records were compiled into monthly averages for each individual year. Tables 3 and 4 display the monthly averages of wave heights H_o and wave periods T, respectively, for each of the years 1981 through 1992. Unfortunately, sampling was intermittent; not all 12 months were measured for each year, and every day was not gauged for each month. Omitted entries indicate periods when the gauge was inoperable for a significant portion of a month. Additionally, Tables 3 and 4, respectively, provide the average annual wave height and wave period determined by taking the average of all months of the given year. Displayed in the final columns of Tables 3 and 4 are the overall average of all the monthly averages (AMA) for the study period. Although the record is not complete or long enough to provide a statistical average, the AMA value associated with each month is used as a comparison value to indicate whether a specific month in a given year was significantly higher or lower in wave activity than the average norm of the study period.

Figure 16 graphs the AMA wave height for the time period 1981 through 1992 superimposed over the AMA wave period of the same time (note the "Y" axis is different for the two curves). The curves exhibit seasonality by showing parallel periods of high and low wave heights versus long- and short-period waves. Shorter wave periods and lower wave heights occur in the summer months and longer period waves and higher wave heights occur in the winter months.

Events of extreme high and low wave height or wave period were detected by comparing successive years of the monthly average wave heights and wave periods to a repeating annual cycle of the respective AMAs (Figures 17 and 18).

Wave height

The years with greatest fluctuation above and below the AMA values of monthly wave height averages are 1982, 1985, 1988, and 1990. During the winter of 1981 and year 1982, the most dramatic fluctuations in wave heights above and below the AMA occurred. The gauge was nonoperational during most of 1983 but, the climatic event El Niño, which began in 1982, continued and the wide variance in wave activity, as indicated from the AMA, most likely persisted. The three highest exceedences of the AMA wave height for the study period occurred in December 1982, November 1981, and March

Table 3
Monthly Buoy Wave Height (H_O) Averages in Meters for Coquille River, OR

Month	1981	1982	1983	1984	1985	1986	1987	1988	1989	1990	1991	1992	Monthly 1981-1992 Avg. (AMA)
Jan		3.1			2.1	2.9		2.5	2.6	3.3	2.0	3.0	2.7
Feb		2.5			2.3	2.7	2.4	2.3	2.2	3.0	2.2	2.4	2.4
Mar		2.8			3.1	2.3	2.1	2.9	2.3	2.1	2.5	1.7	2.4
Apr		2.6			1.9	2.3	1.9		1.7	1.7	2.1	1.6	2.0
May		1.8			1.5	1.8	1.6		1.6	1.7	1.8	1.2	1.6
Jun		1.1			1.6	1.5	1.5	1.0	1.7	1.5	1.4	1.1	1.4
Jul		0.8			1.2	1.4		1.2	1.2	1.4	1.2	1.2	1.2
Aug		1.3	1.1	1.7	1.4	1.3		1.4	1.2	1.2	1.4	1.2	1.3
Sep		1.7	1.6	1.4	1.7	1.5	1.2	1.6	1.5	1.4	1.6	1.3	1.5
Oct		2.2		1.8	1.9	1.7	1.3	1.5	1.8	2.2	1.7	1.6	1.8
Nov	3.5	2.7		2.9	1.7		1.7	3.1	2.2	2.4	2.6	1.8	2.5
Dec	3.2	3.8		2.4	2.2			3.0	1.9	2.5	2.7	2.4	2.7
Annual Avg.	3.3	2.2	1.3	2.1	1.9	1.9	1.7	2.0	1.8	2.0	1.9	1.7	

Table 4
Monthly Buoy Wave Period (T) Averages in Seconds for Coquille River, OR

Month	1981	1982	1983	1984	1985	1986	1987	1988	1989	1990	1991	1992	Monthly 1981-1992 Avg. (AMA)
Jan		10.7			11.5	11.3			11.3	11.9	11.5	12.3	11.5
Feb		10.4			9.9	11.7	11.6	12.7	9.1	11.2	11.3	10.8	11.0
Mar		11.5			11.4	10.5	10.2	11.9	10.0	10.4	10.7	11.1	10.8
Apr		9.2			9.6	10.3	11.0		9.2	9.2	10.9	9.7	9.9
May		8.1			8.4	9.2	8.8		9.0	8.4	9.2	8.2	8.6
Jun		7.0			8.4	8.6	8.0	6.7	8.4	8.2	8.6	7.7	7.9
Jul		7.0			7.4	7.7		6.8	7.3	7.6	7.3	8.0	7.4
Aug		8.3	8.3	9.7	8.4	7.5		7.3	6.8	7.6	7.4	8.3	8.0
Sep		8.3	7.7	8.6	8.8	7.4	11.0	8.3	9.0	8.7	9.6	8.8	8.7
Oct		10.1		8.6	9.9	9.7	11.3	8.9	9.2	10.3	9.5	10.5	9.8
Nov	11.4	10.6		10.4	9.4			11.1	12.0	10.5	11.7	11.2	10.9
Dec	10.5	10.9		10.4	12.8			11.3	10.7	10.7	12.7	11.1	11.9
Annual Avg.	11.0	9.3	8.0	9.6	9.7	9.4	9.0	8.5	9.3	9.5	10.0	9.8	

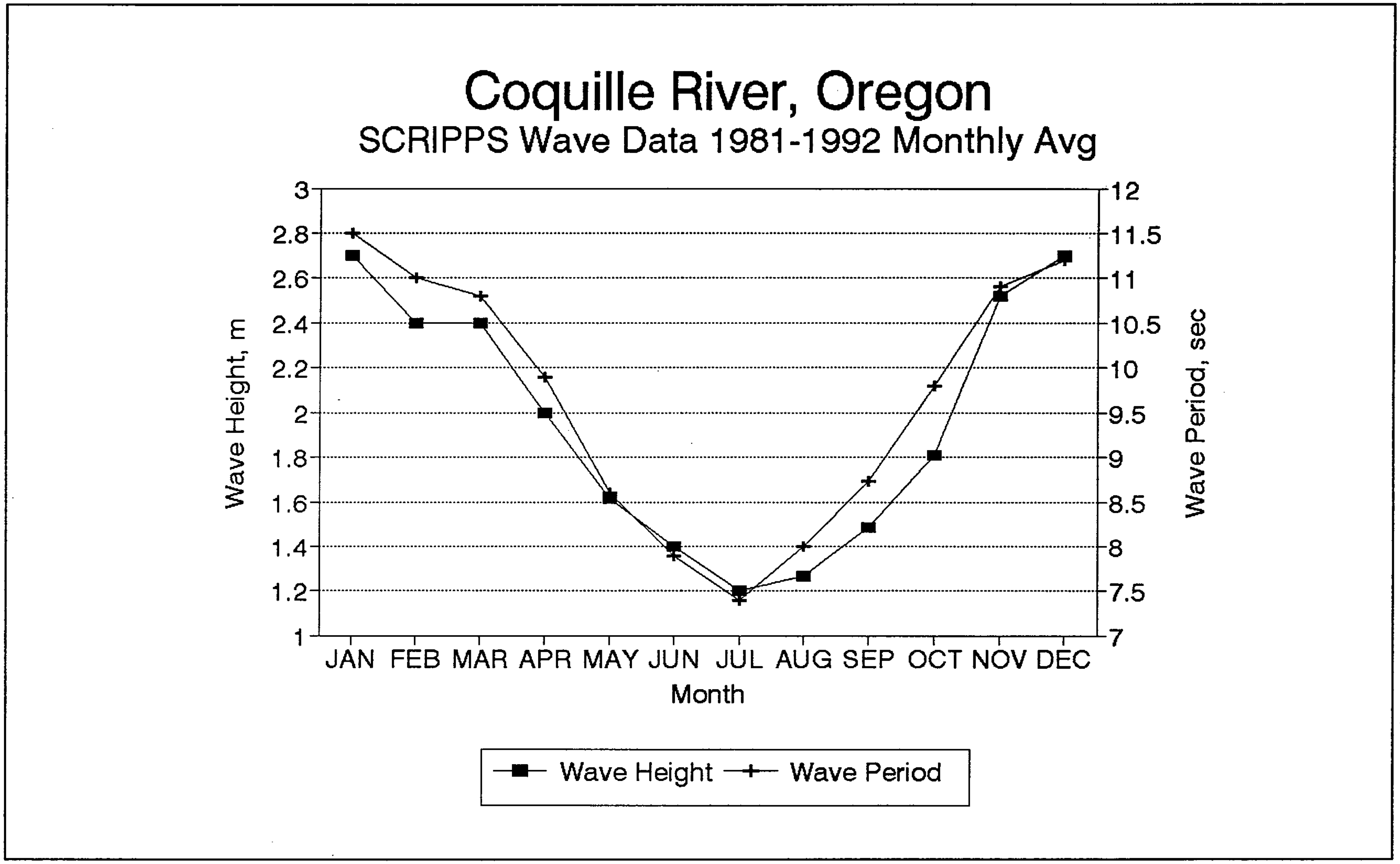

Figure 16. Average monthly averages (AMA) of wave height and wave period from Coquille River, OR, wave buoy data for the 1981-1992 study period

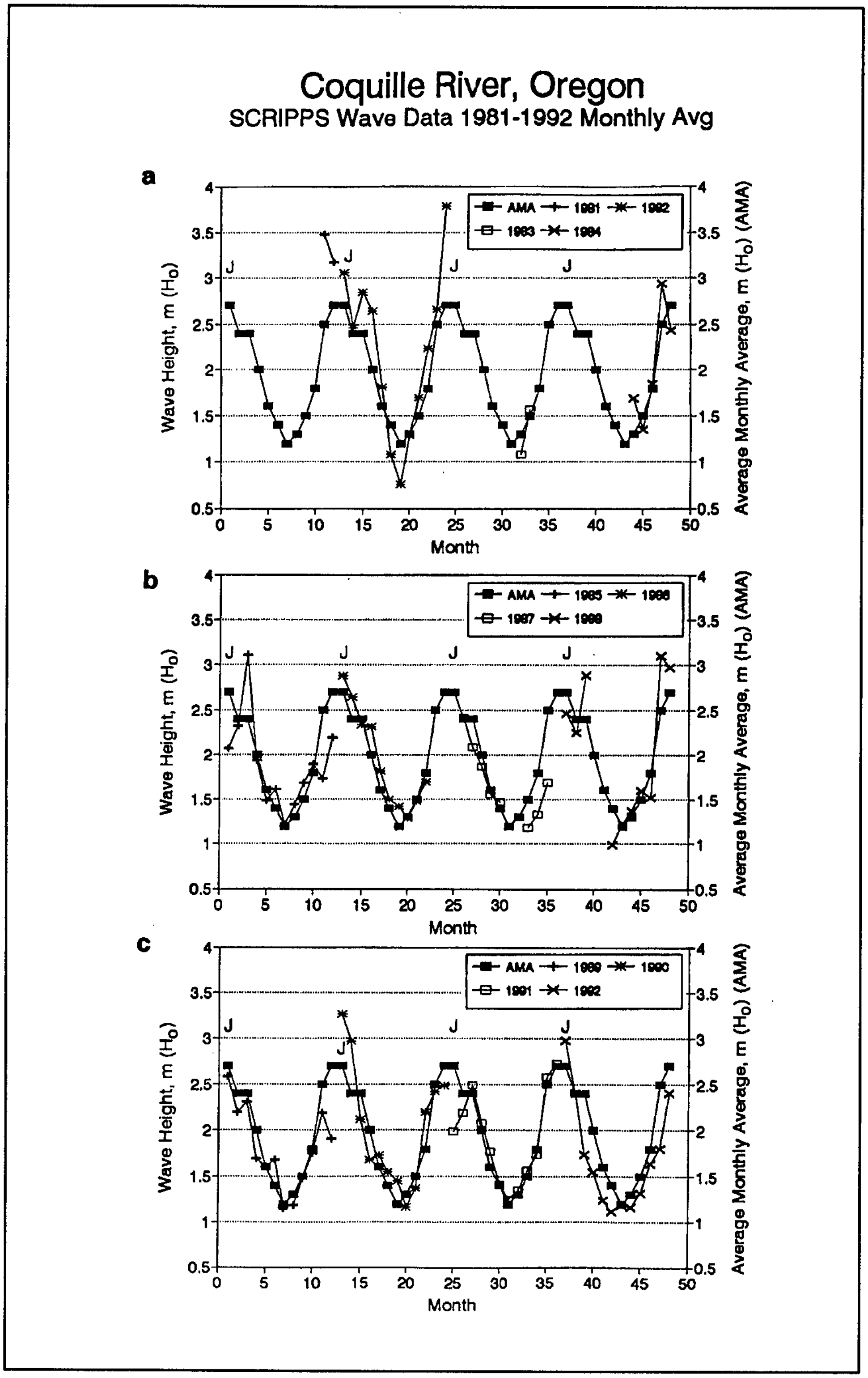

Figure 17. Wave height monthly averages as compared to wave height average monthly averages (AMA) from Coquille River, OR, wave buoy data for 1981-1992. X-axis depicts months from January 1981 to December 1992 as consecutive numbers beginning with 1

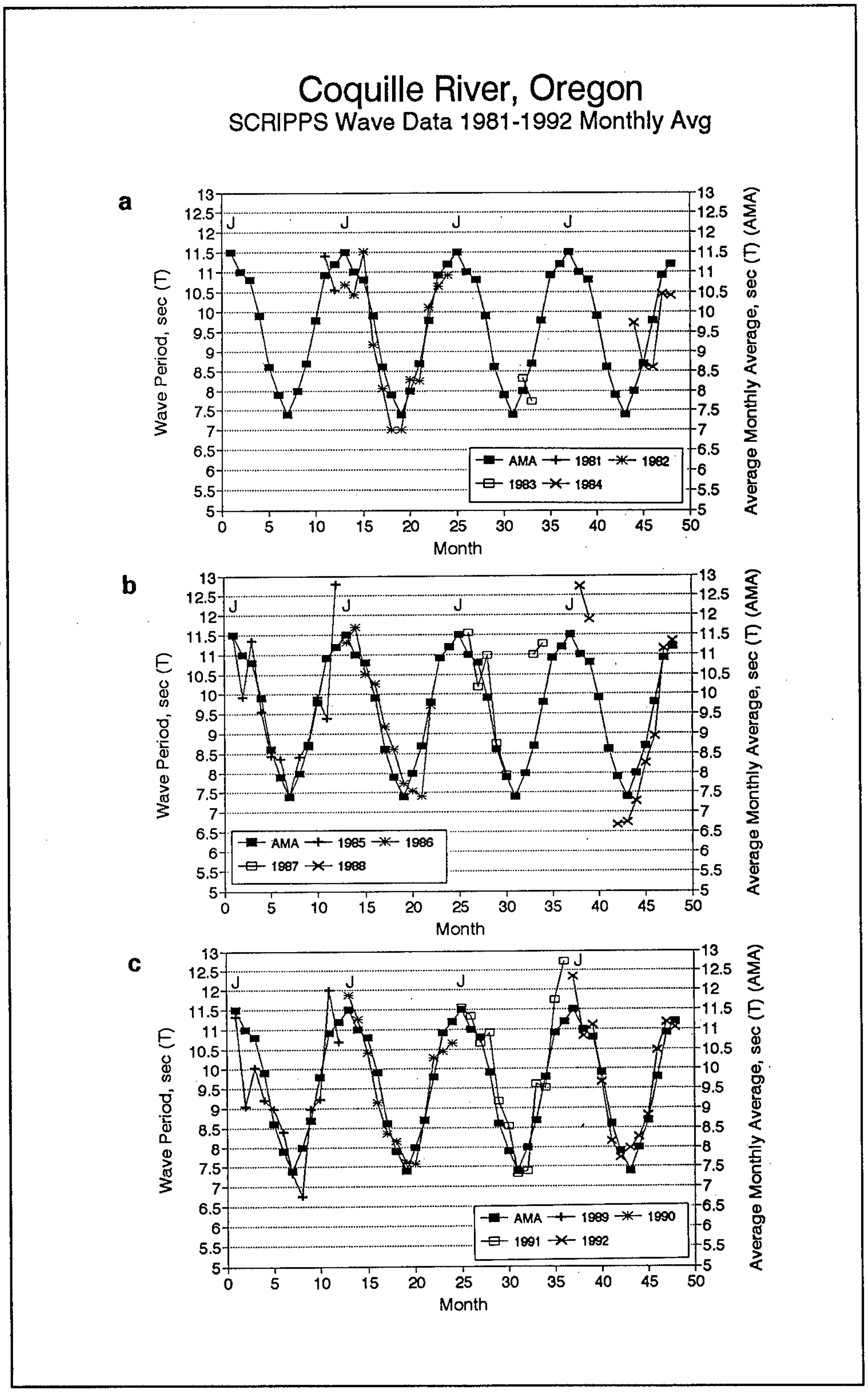

Figure 18. Wave period monthly averages as compared to wave period average monthly averages (AMA) from Coquille River, OR, wave buoy data for 1981-1992. X-axis depicts months from January 1981 to December 1992 numbered consecutively beginning with 1

1985, exceeding the AMA by 1.1 m, 1.0 m, and 0.7 m, respectively. Summer and winter of 1988 monthly averages showed extreme values in excess of the respective AMA both high and low. January 1990 and 1992, and February of 1990 also showed higher monthly averages than the AMA.

Full analysis of the years 1981, 1983, and to some extent, 1984, was not possible due to the lack of available CDIP wave data. The following tabulation lists years that experienced monthly wave height values in excess of ±0.6 m (1.97 ft):

Year	Month	Deviation in excess of ±0.6 m
1981	November	+1.0
1982	April	+0.6
	December	+1.1
1985	January	-0.6
	March	+0.7
	November	-0.8
1987	November	-0.8
1988	November	+0.6
1989	December	-0.8
1990	January	+0.6
	February	+0.6
1991	January	-0.7
1992	March	-0.7
	November	-0.7

Wave period

The values used in the analysis of the wave period are the peak periods. These values may not always be meaningful if the spectrum peak is not well-defined, as in the case of a bimodal spectrum or a broad-peaked spectrum. Overall, the monthly wave period averages of most years in the study time period paralleled the wave period AMA values, while some years (1984, 1985, 1987, 1988, 1989) and the winter of 1991-1992 demonstrated several values of dramatic deviations.

The following tabulation lists years experiencing monthly wave period average values in excess of ±1.00 sec:

Year	Month	Deviation in excess of ±1.0 sec
1984	August	+1.73
	October	-1.21
1985	February	-1.08
	November	-1.51
	December	+1.59
1986	September	-1.32
1987	April	+1.07
	September	+2.27
	October	+1.47
1988	February	+1.73
	March	+1.08
	June	-1.22
1989	February	-1.94
	August	-1.23
	November	+1.10
1991	April	+1.01
	December	+1.52

Erosion/accretion criteria

Various predictive criteria to determine whether a beach will be eroded by waves of specific height and period for several different locations are discussed in Larson and Kraus (1989). Two of these criteria were applied to the Coquille River wave data and found to predict excessive erosion conditions for the region based on net zero loss of sediment volume to the region during the 1981-1992 study period. In contradiction with the predictions, subsequent chapters identify measured accretion in the volume of material present in the region during the study period.

Beach erosion was predicted from the monthly wave height and wave period for the Coquille River site using the formula $H_o/wT > 3.2$ (Larson and Kraus 1989, Kraus 1990) where w is the sand fall speed in quiet water. The fall speed used for 0.25-mm sand (estimated median grain size of Siuslaw River, OR) at 10 °C water temperature is 0.029 m/sec (0.095 ft) (McLellan, Kraus, and Burke 1990). The beach grain size of Siuslaw River study site ranges from 0.15 mm to 0.3 mm. The smaller the grain size, the more probability of erosion. The equation $H_o/wT > 3.2$ denotes erosion is probable, $H_o/wT > 4.0$ suggests erosion is highly probable, $H_o/wT < 3.2$ indicates accretion is probable, and $H_o/wT < 2.4$ implies accretion is highly probable.

The criterion values of 4.0 and 2.4 are "...error estimates formed by decreasing and increasing the empirical coefficient by 25 percent..." to be used in the field (Kraus 1990).

According to Kraus' (1990) 25-percent error criteria value of 4.0, only 2 months showed conditions in which accretion would be expected on the shoreline, July of 1982 and September of 1987. For all the remaining months of the 1981 to 1992 study time period, conditions are favorable for erosion (Figure 19).

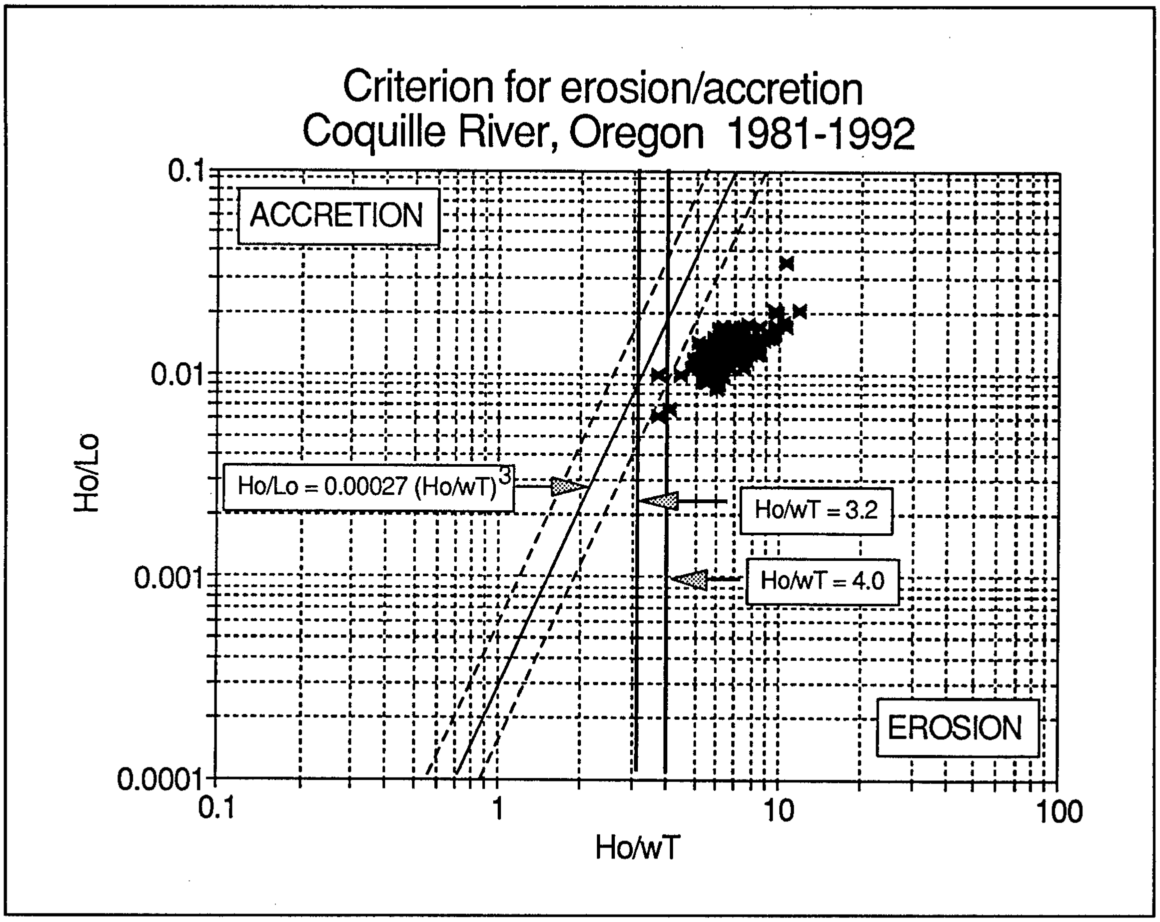

Figure 19. Erosion and accretion predictions for Coquille River, OR, using several criteria. 10 °C water temperature was used for calculations

Another criterion (Larson and Kraus 1989) for probable erosion is described by the formula $H_0/L_0 = M\ (H_0/wT)^3$, where *M (empirical factor) = 0.00027* for significant wave height (Kraus 1990). According to this criterion all wave conditions are shown to be erosional events (Figure 19). The dashed lines represent predictions obtained with one-half and double the value of the empirical coefficient and provide a measure of reliability of the prediction (Kraus 1990).

El Niño

Definition

El Niños are atmospheric and oceanic phenomena which usually develop during the Christmas season. The main impact of an El Niño is felt in the Pacific Ocean off of the Peruvian coast. The Peruvian coastal waters become warm and non-nutrient rich, causing sea life such as fish and marine mammals and birds to die in massive numbers. El Niños are now thought to be triggered by "...the breakdown of equatorial trade winds in the central and western Pacific..." (Komar and Good 1989). When the trade winds cease, or are reduced, the potential energy of the west-to-east surface-sloping water in the western equatorial Pacific, formed by normal periods of strong southeast trade winds, is released. A bulge of eastward-flowing warm surface water along the equator is produced, causing an El Niño (as cited by Komar and Good (1989)). The eastward moving sea-level bulge is confined to the equator by the Coriolis force constantly turning the bulge towards the equator. Once the bulge reaches the South American coast, it splits and travels north and south. The northward moving sea level wave travels along the coast and does not dissipate due to the combined effects of wave refraction over the continental shelf and slope and the Coriolis force. In fact, because of these forces, the wave's height is maintained or even increased as it travels along the coast (Komar 1986). Changes in sea level due to these shelf-trapped surface waves are important contributors to the erosion of the Oregon coast during an El Niño (Komar and Good 1989).

Seasonal wave climate along the Oregon coast

The Oregon coast has two oceanographic seasons influenced by regional weather patterns in the northeast Pacific. Beginning by October, a series of intense low-pressure systems move eastward onto the coastline, producing large ocean swell and acute local seas from the southwest. Significant wave heights up to 6 m (19.7 ft) occur annually. In between these storm events there is a prevalence of onshore winds and local seas from the northwest with waves under 3 m (9.8 ft). Beginning in April, a fairly stable northeast Pacific high-pressure system becomes established, resulting in a predominance of ocean swell and winds from the northwest with wave heights from 1-3 m (3.3-9.8 ft). Intense storms of 2-3 days duration can occur between April and October with resulting increased wave heights. This is well-documented in wave records from the CDIP (Seymour et al. 1992).

Littoral response

Sediment transport in the littoral system is also seasonal and consists of a general buildup of the beach in the summer with erosion taking place in the winter. During winter storms, material eroded from the beach is moved offshore, forming bars at depths up to -16 m (-53 ft). During summer-like wave conditions, this offshore material is carried back onto the beach. If excess material is moved too far offshore by winter storms, it may take more than one summer season to restore the shoreline. Particularly severe winter conditions may result in long-term "loss" of material from the littoral system due to headland bypassing or deep deposition (Komar 1975).

Shoreline changes due to original jetty construction disregarding El Niños

Large changes can occur, however, in shorelines of areas with zero net littoral sand drift as a result of jetty construction (Komar, Lizarraga-Arciniega, and Terich 1976). Due to the construction of the original Siuslaw River jetties (1891-1915), the shoreline progressively accreted north and south of the jetties with time (more accretion to the north) until about 1939, when the shorelines stabilized (Komar 1975). Komar explained the larger accretion to the north as having resulted "from the jetty construction leaving a larger area to be filled before the shoreline was straightened into an equilibrium configuration where the net transport is again nearly zero over the longterm." Thus all of the pronounced shoreline changes occur within a few years after jetty construction.

1982-83 El Niño effects of the Oregon coast

The 1982-83 El Niño caused a substantial amount of erosion along the Oregon Coast. High sea levels (Figure 20 (Komar (1986), from data of Huyer, Gilbert, and Pittock (1983))), southward displacement of storms causing high-intensity waves (Figure 21 (Peterson et al. 1990)), and northward movement of sands, were the main contributors for the erosion along the Oregon Coast (Komar 1986). Peak sea level for Newport, OR, for the 1982-83 El Niño was about 68 cm (27 in.) in February 1983, which is about 35 cm (14 in.) above normal winter level (Komar 1986). Three large storms, due to the 1982-83 El Niño, with waves achieving breaker heights of about 7 m (23 ft), occurred at Newport, OR, in mid-December 1982, late January 1983, and mid-February 1983. Usually, conditions to create breaker height waves of this magnitude occur only once every 2 years on the Oregon coast (Komar 1986). Because of these southward displaced high-intensity storms, the Oregon coast received waves approaching more from the southwest than usual (Peterson et al. 1990), which in turn caused the movement of sand more northward than usual. The simultaneous occurrence of three important factors (large storms, sea level approaching a maximum, and high spring tide levels), resulted in the substantial erosion that was experienced (Komar 1986). Erosion on the Oregon coast continued, mostly due to high water levels and storm-generated high wave heights, long after the initial El Niño processes ceased. The Oregon beaches' equilibria was disturbed by the unusual northward transport of sand. It is because of this northward transport of sediment that some places along Oregon's coast experienced erosion for up to 6 years after the 1982-83 El Niño (Komar and Good 1989).

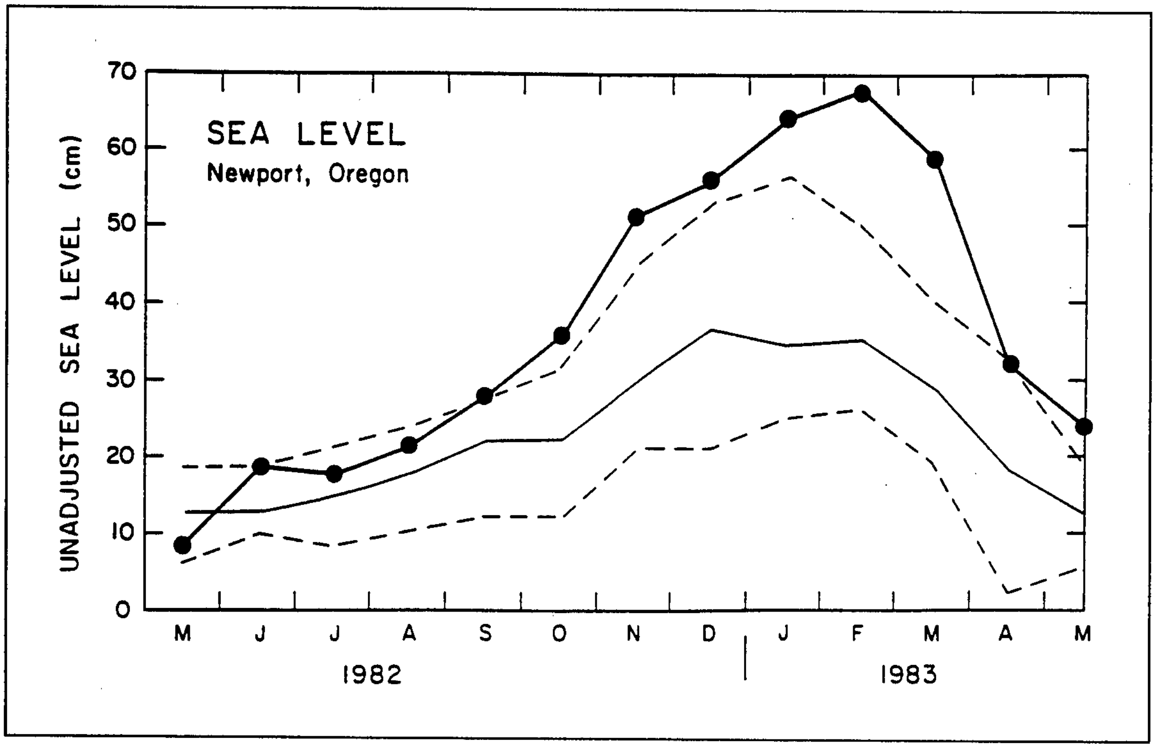

Figure 20. Monthly average sea levels measured at Newport, OR. Bold line indicates the 1982/83 El Niño values, which generally exceed the previous 10-year means (solid line). The two dashed lines indicate minimum and maximum ranges of the previous 10 years (from Komar (1986))

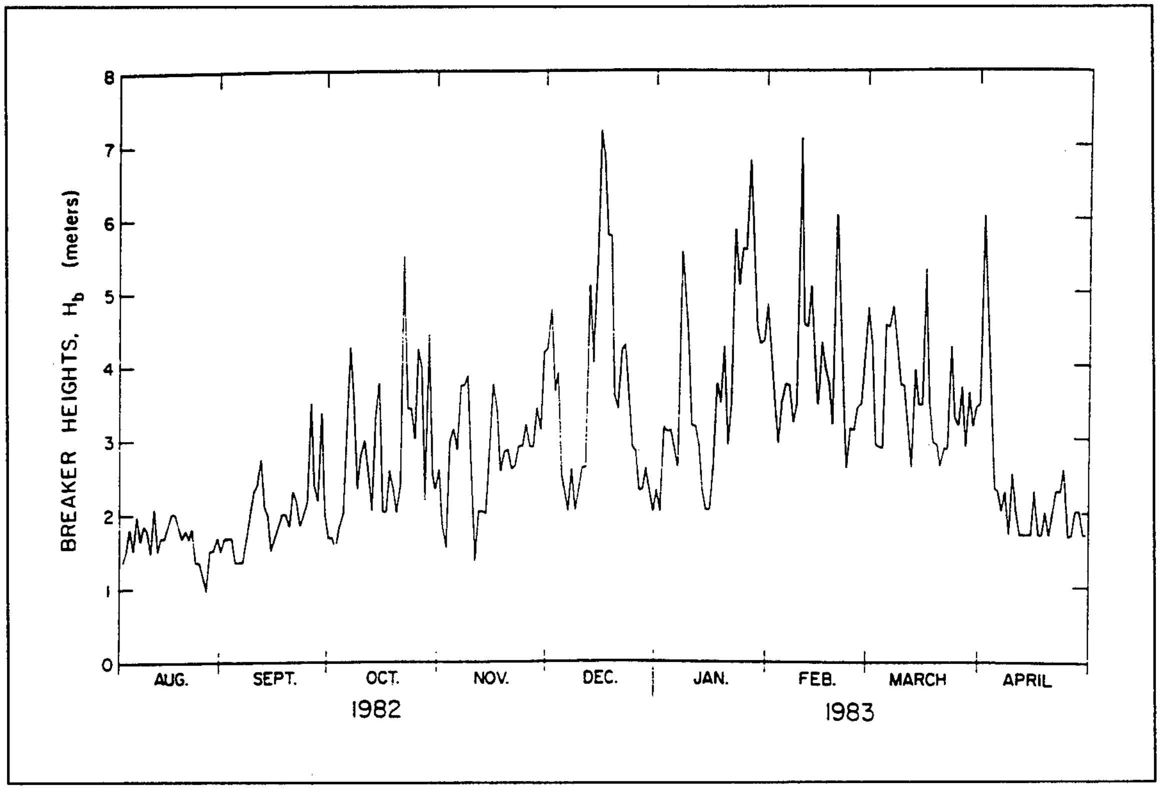

Figure 21. Significant wave heights (high-intensity waves) from Newport, OR, during the 1982/83 El Niño (from Peterson et al. (1990))

3 Current Patterns Adjacent to Spur Jetties

Background

Engineers and planners are often faced with a lack of knowledge of currents in the nearshore region. Quantitative information about currents is very important for the planning, design, construction, and evaluation of coastal structures. One objective of this MCCP study was to evaluate the effectiveness of spur jetties in deflecting current-transported sediment away from the entrance channel. A task of this objective was to establish whether the spur jetties did in fact induce a current circulation pattern off the spur tips and/or a current pattern that extended seaward of the jetty tips as was observed in physical model tests of the structures. Both current patterns have the potential to reduce shoaling in the entrance channel. In support of this task, prototype near-bottom localized current circulation patterns induced by the spur jetty configuration were verified and qualitatively compared with physical model testing conducted by Bottin (1981, 1983). The second technical report of this series (Pollock 1995) describes in detail these efforts and is summarized in this chapter.

Prototype Data Collection and Analysis

The Airborne Coastal Current Measurement system was developed in support of this study and proved to be an effective method for obtaining qualitative spatial understanding of bottom currents in hostile environments where boat operation is dangerous or where quick mobility is necessary. The system utilizes a helicopter as the support platform. A meter assembly including an electromagnetic current meter, an anchor, and a subsurface buoy is suspended by cable from the helicopter for data sampling approximately 1 m (3.28 ft) above the seabed (Figures 22, 23, and 24). Current information is collected at several locations within a short period of time. Data collected are reduced to resultant current vectors and are presented as a sequence of vectors discrete in time and location.

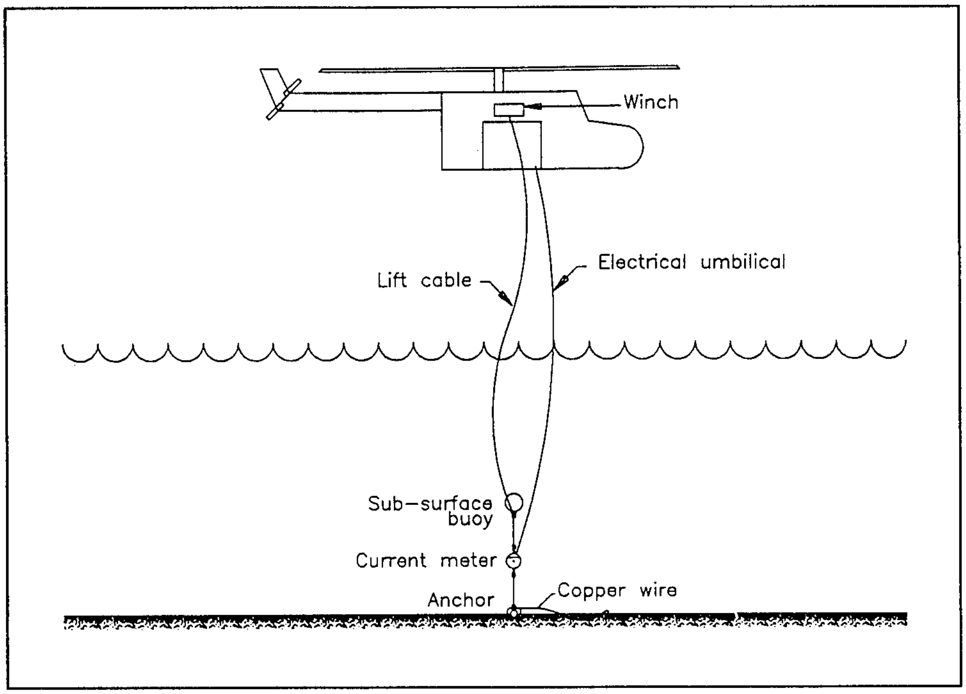

Figure 22. Meter assembly attached to the helicopter as it would appear in use at the seafloor

Figure 23. Airborne Coastal Current Measurement System in operation

These vectors are plotted to create a mosaic from which local current patterns can be inferred (Figure 25).

The system was used at Siuslaw River, to document currents near the entrance channel spur jetties. The system performed very well and met all of the study's requirements, sampling data at approximately 18 locations within an hour, operating in depths up to 7 m (23 ft), surviving in waves as high as 4 m (13.1 ft), and measuring currents over 1.6 m/s (5.2 ft/s). Capabilities of the system would have allowed it to measure currents as strong as 3 m/s (9.8 ft/s), and wave height and depth limitations were only constrained by the length of the cable used for

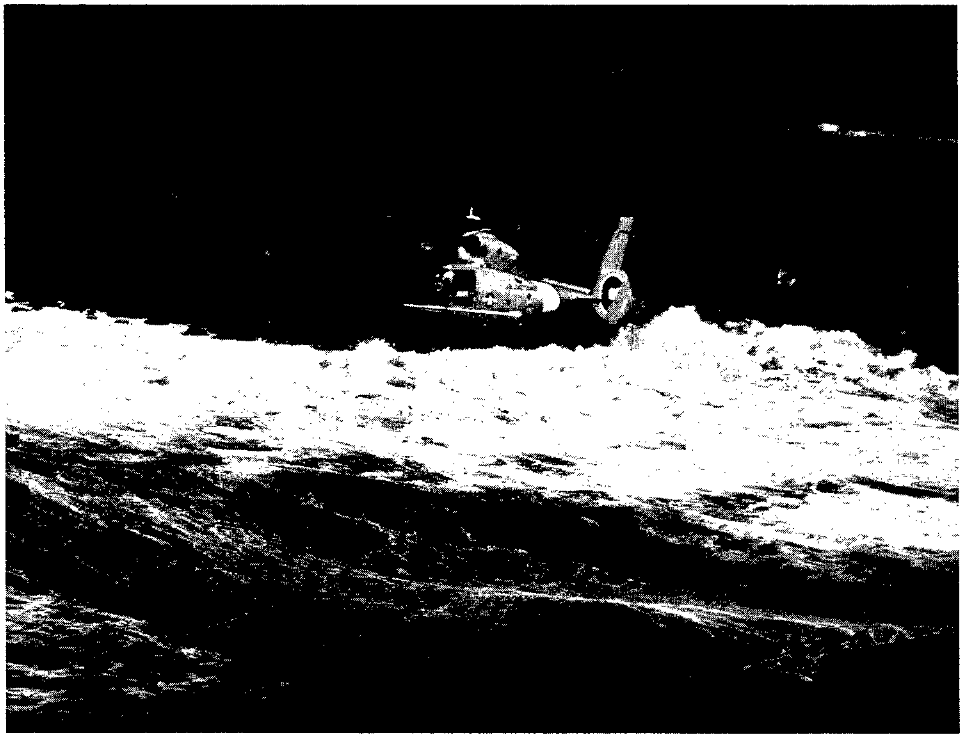

Figure 24. Airborne Coastal Current Measurement System operating in large waves

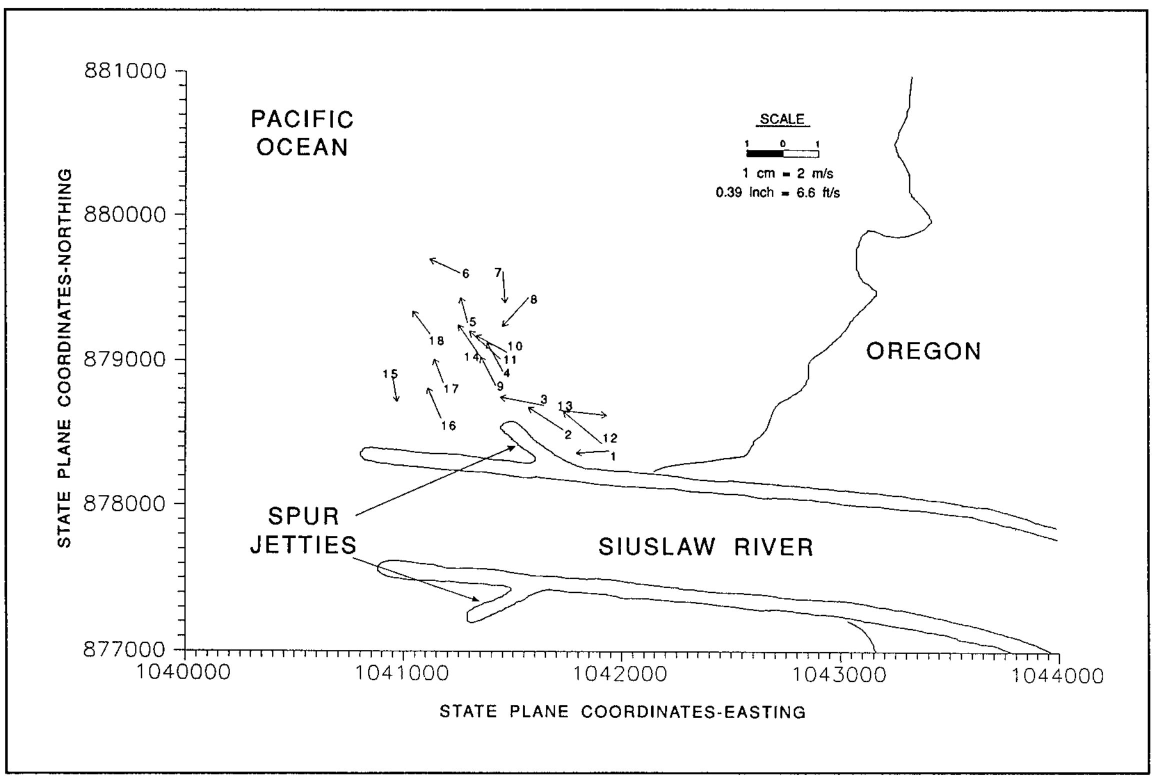

Figure 25. Current vector mosaic for sampling Interval III on 9 September 1992

the particular study. Data collected during the prototype field study were used to develop current vector mosaics and create visual interpretations of localized currents around spur jetties. Dye studies, aerial photos, and visual observations were used in support of the current information to develop the interpretations of the current patterns. For this site, on a qualitative level, it was determined that the bottom currents bear close resemblance to the surface currents. Interpretations of the prototype current patterns were qualitatively compared with current-induced sediment tracer patterns documented in physical model testing completed prior to construction modifications to the existing entrance channel structures.

The first use of the system was at Siuslaw River, in July 1990. Wind conditions during the study were very strong, directly out of the north. Current patterns during this period reflected a wind-dominated regime rather than a wave-dominated regime. From the vector mosaics of this study, no circulation patterns around the jetty spur were apparent. Although this prototype study did document conditions that occur at the Siuslaw River, results were not compared with the physical model study due to differences in the forcing climates.

An additional study was conducted at the same site during a 2-week period in September 1992, and included ground truthing with a stationary current meter located near the study site to substantiate airborne current measurements. Measurements taken by both meters compared closely. Averaged velocities for each of the meters differed by only 2 cm/s (0.79 in./s) in magnitude and 1 deg (0.02 rad) in direction. The variance is within the combined accuracy of the two instruments.

Four sampling intervals were conducted during the 2-week period. Two sampling intervals covered the high and low slack tidal periods and another two intervals were conducted during the ebb tide. Deepwater wave heights ranged from 0.8 to 2.2 m (2.6 to 7.2 ft) with breaker heights at the site of up to 3 m (9.8 ft), and peak wave periods during the sampling intervals were 7 to 9 sec. The vector mosaics of these intervals captured circulation patterns induced by the alongshore current flowing by the spur jetties. Sampling Interval I was conducted during the slack/low tide, and the current pattern interpretation displayed a split in the current at the end of the spur with a portion of the current turning toward shore and a portion of the current turning offshore (Figure 26). Sampling Interval II was conducted during the slack/high tide and showed an eddy forming past the spur that turned toward the shore (Figure 27). Sampling Intervals III and IV were conducted during the ebb tide. Both current pattern interpretations indicated the flow turned offshore past the jetty tip, then flowed parallel to the coast, and passed offshore of the jetty tips (Figures 28 and 29).

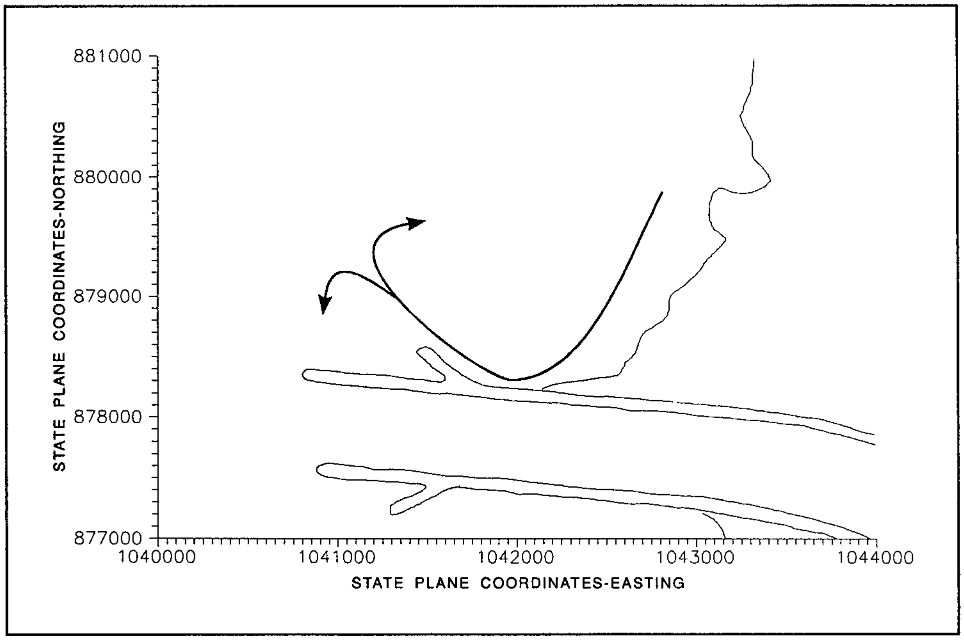

Figure 26. Interpretation of current flow patterns for sampling Interval I, 3 September 1992

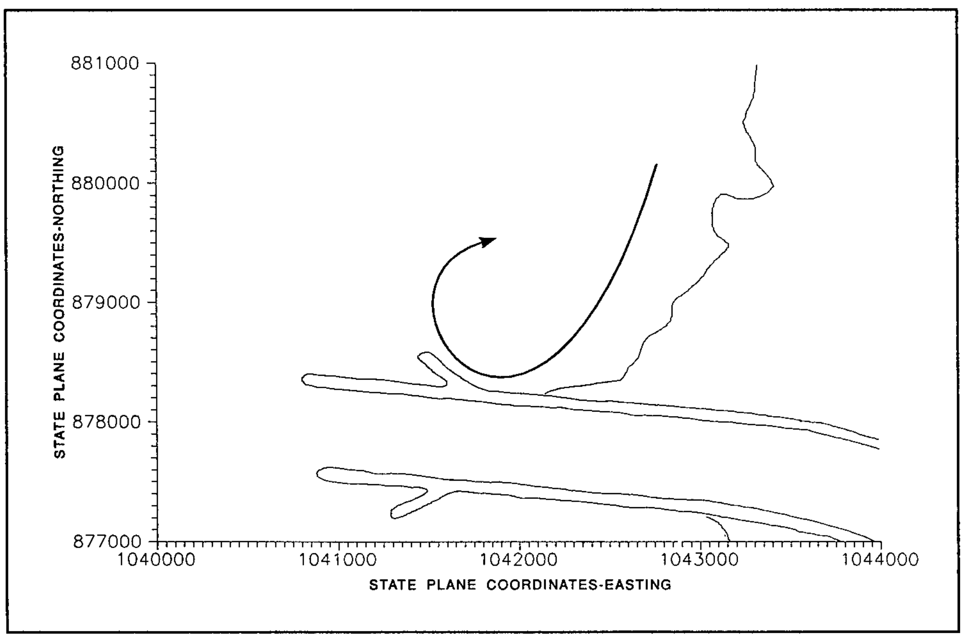

Figure 27. Interpretation of current flow patterns for sampling Interval II, 9 September 1992

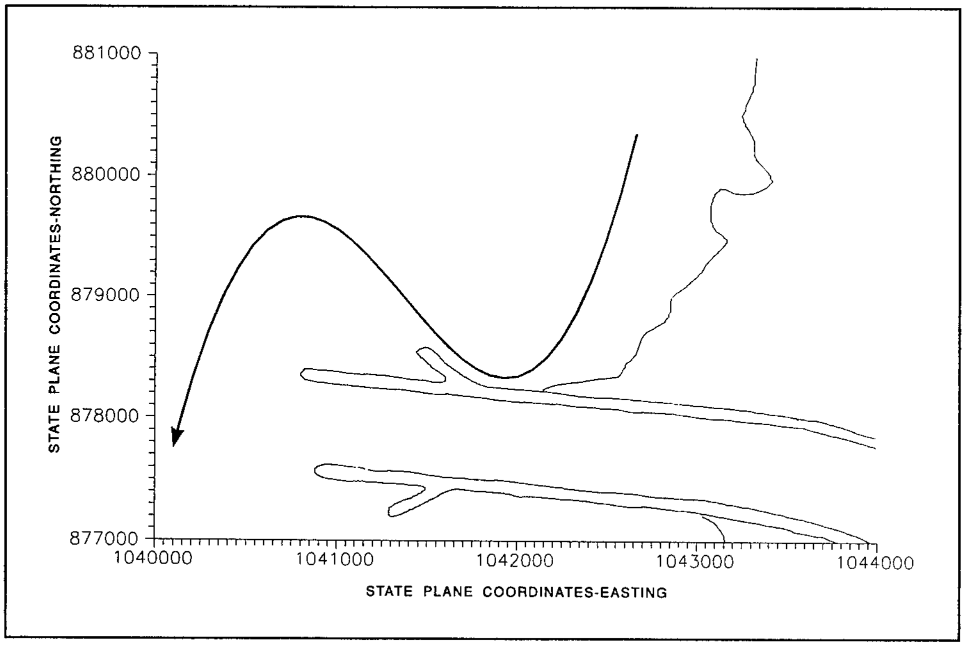

Figure 28. Interpretation of current flow patterns for sampling Interval III, 9 September 1992

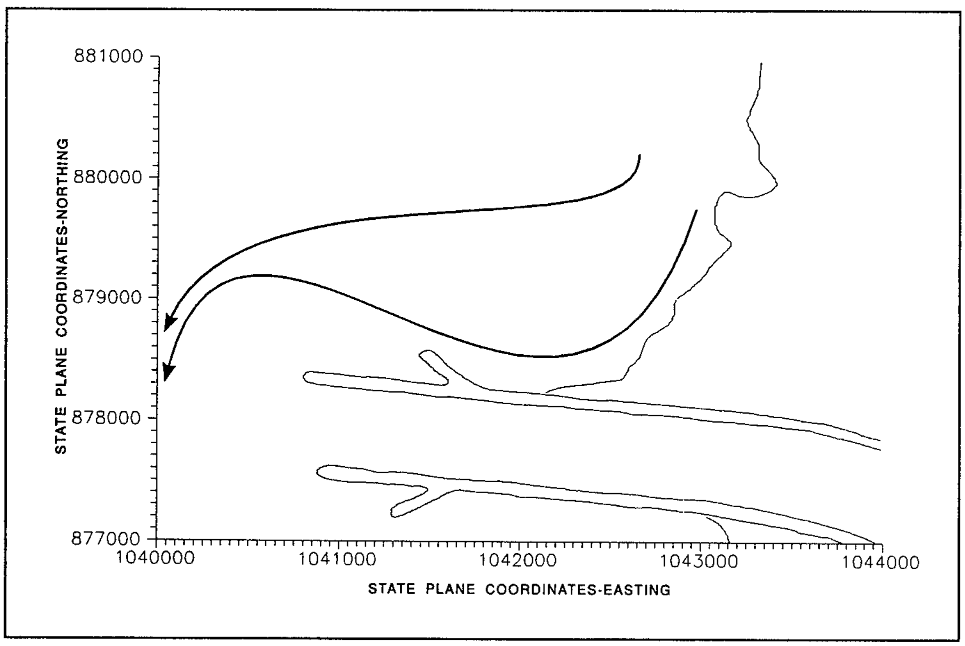

Figure 29. Interpretation of current flow patterns for sampling Interval IV, 9 September 1992

Prototype and Physical Model Comparison

Comparisons revealed that under certain conditions, the prototype structures deflected material away from the entrance channel as had been predicted by the physical model tests. Comparable prototype current and model sediment depositional patterns emerged. For all prototype conditions at the jetties, a rip current hugged very closely to the jetty trunk and spur. At the tip of the spur, different flow patterns occurred. These patterns can generally be described as circular eddies or "S"-shaped. The same patterns occurred in the models when the water depths were deep enough to allow a rip current to occur along the jetty. Prototype testing indicates that the current patterns take different forms for different strength alongshore currents and stages of the tide. For the model test, the different forms were also associated with the strength of the alongshore current and were altered by changing water levels and wave conditions. Similarities exist between model and prototype current patterns for relative water levels and alongshore current strengths.

It is hypothesized for the prototype that the tidal flows combine with the longshore currents, depending upon flow direction, to either increase or decrease the longshore current for the ebbing and flooding tides, respectively.

Additionally, the different water levels due to the tides, in effect, change the length of the jetty trunk and the depth of water near the jetty spur. This may also influence the strength of the current and alter the current patterns near the jetties.

These field tests were conducted during high wave energy periods. During lower energy periods, different current patterns and less sediment movement are likely. Prototype dye studies conducted previously during very calm conditions indicated that, during an incoming tide, the current wraps around the jetty tip and flows directly into the channel. The physical model study indicated similar occurrences for the lower wave conditions.

Based on the model tests and field studies, a simplistic interpretation of the evolution process that the current patterns experience was developed (Figure 30). The interpretation assumes that a rip current exists along the jetty trunk and spur, and relates the changes in the current pattern past the spur tip to the current strength. The evolution process begins with the current forming a circular eddy that is deflected back to shore. As the current increases in strength, the circular eddy uncoils and the flow resembles an "S" shape with larger radius curves and a longer mid-section for stronger currents.

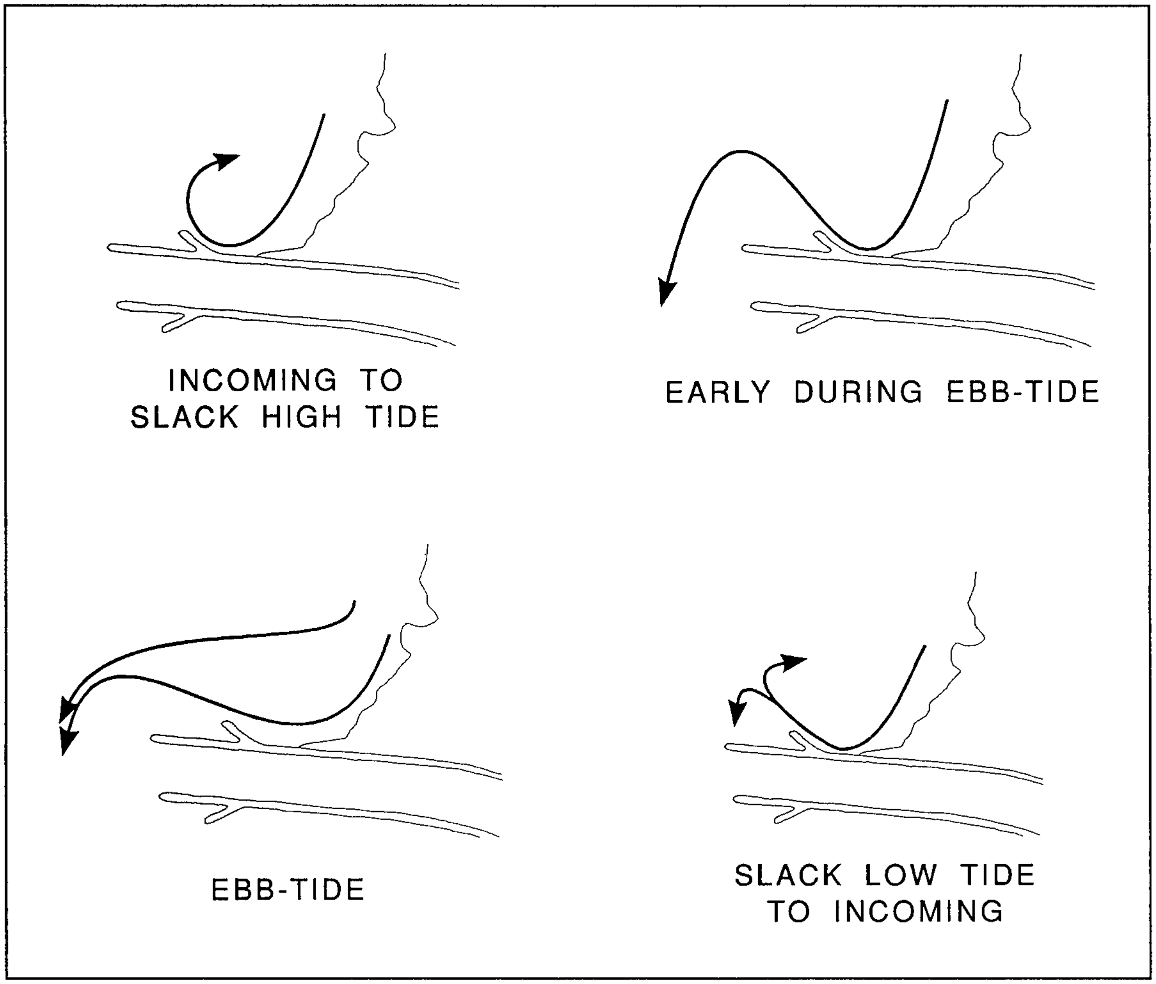

Figure 30. Sequential interpretation of current patterns through a tidal cycle

Conclusion

Results of this study indicate that the physical model study appropriately demonstrated the potential prototype current patterns. The prototype study verified the predicted currents and sedimentation patterns, indicating sediment is deflected away from the channel entrance under certain wave and current conditions.

4 Helicopter-Borne Nearshore Survey System Verifications

Introduction

Bathymetric surveying can be difficult and hazardous near coastal structures, or in regions of high seas and surf, or drastically varying topography. Using the Helicopter-Borne Nearshore Survey System (HBNSS), safe and reliable measurements can be made of coastal seabeds and structure relief. This system was employed for data collection at Siuslaw River and tested for accuracy under this MCCP project.

In 1960, the Portland District developed the HBNSS (Craig and Team 1985). The purpose of the system is to measure bathymetry (seabed elevations) to depths of -12 m (-39 ft) and relief of rubble-mound structures along the Pacific coast. The survey helicopter is fitted with a 26-m (85-ft) weighted cable, graduated like a surveyor's rod. A shore-based surveyor's level is used to read elevations, and horizontal positioning is obtained using a shore-based electronic total distance station (TDS) aimed at a cluster of prisms mounted on the helicopter. Because of the maneuverability of the helicopter, this survey system can operate safely and accurately in most hazardous regions during severe wave events and in most weather conditions, although heavy fog or winds in excess of 50 km/hr (31 mph) will prevent operation of the helicopter. Bathymetric and structure relief data gathered via HBNSS have been used to compare shoreline and nearshore bathymetric change and to aid in design and documentation of structure placement and stability. A video prepared by the Portland District and Craig and Team (1985) gives a detailed discussion of the system and its equipment. In the summer of 1990, the HBNSS was compared for accuracy and repeatability to the USACE Coastal Research Amphibious Buggy (CRAB) at CERC's Field Research Facility in Duck, NC (Figure 31).

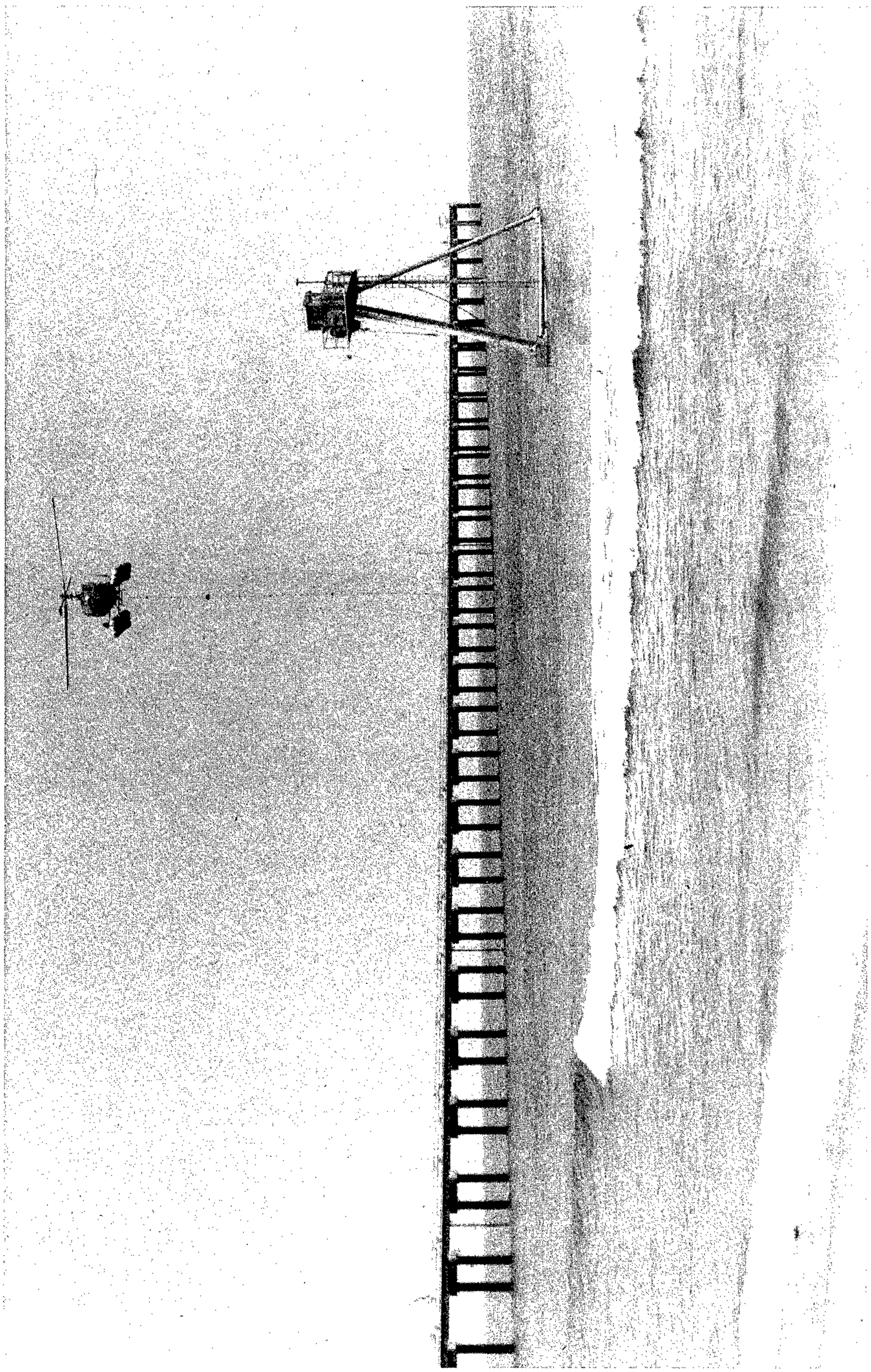

Figure 31. The CRAB and HBNSS survey systems operating side by side

Description of Study

Instrumentation and procedures

The HBNSS requires a helicopter crew, a helicopter equipped with an undercarriage-pulley system tailored for travel of the survey cable, a prism cluster (Figure 32), the survey cable, a land crew, a TDS, a surveyor's level, and range poles. The land crew is composed of four members: TDS operator, level reader, data recorder, and a person to assist and evaluate the angle of the cable. The survey cable consists of three parts: a weak link leader cable with a 27-kg (60-lb) main weight, the graduated cable, and the travel cable with an 18-kg (40-lb) counterweight (Figure 32).

Range poles and the TDS are set up on the beach along the profile line. The helicopter supporting the cable system moves offshore to the end of the profile line (Figure 33). Line of sight on the range poles and radio communication with the TDS operator help the pilot to position the helicopter at the

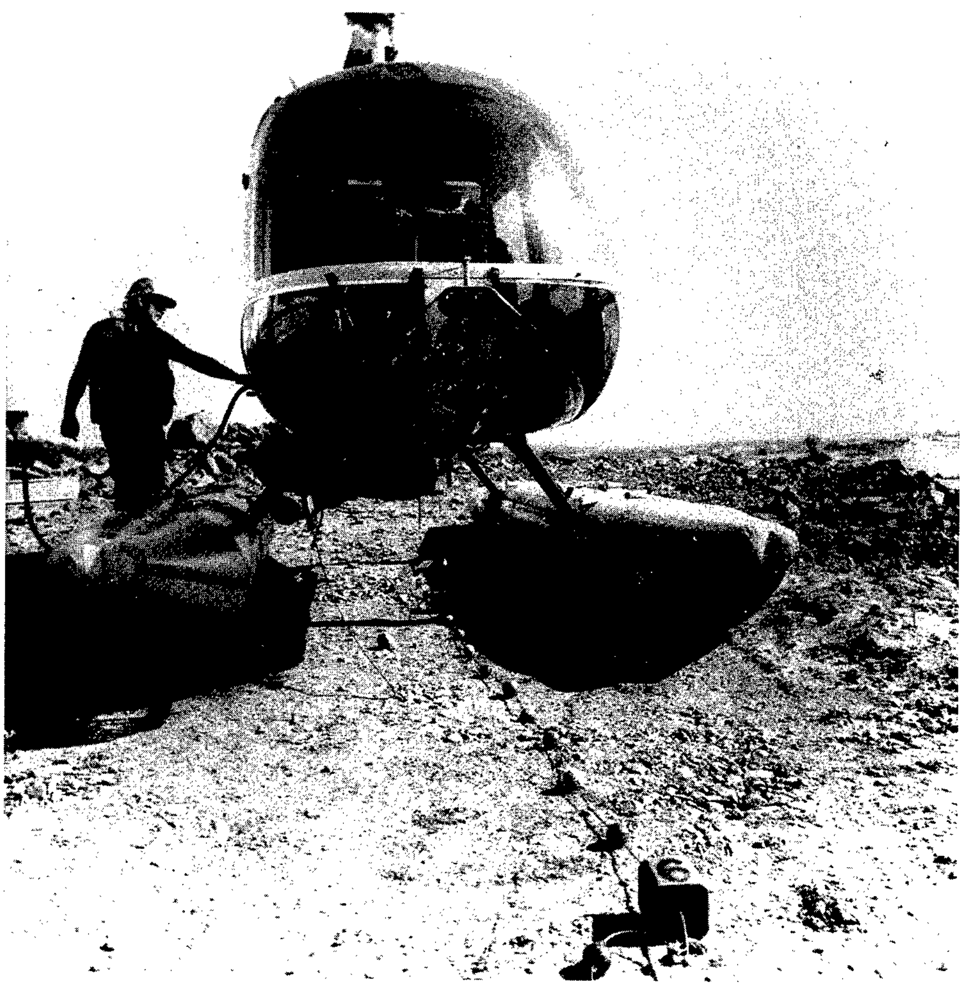

Figure 32. Helicopter, undercarriage, and survey cable

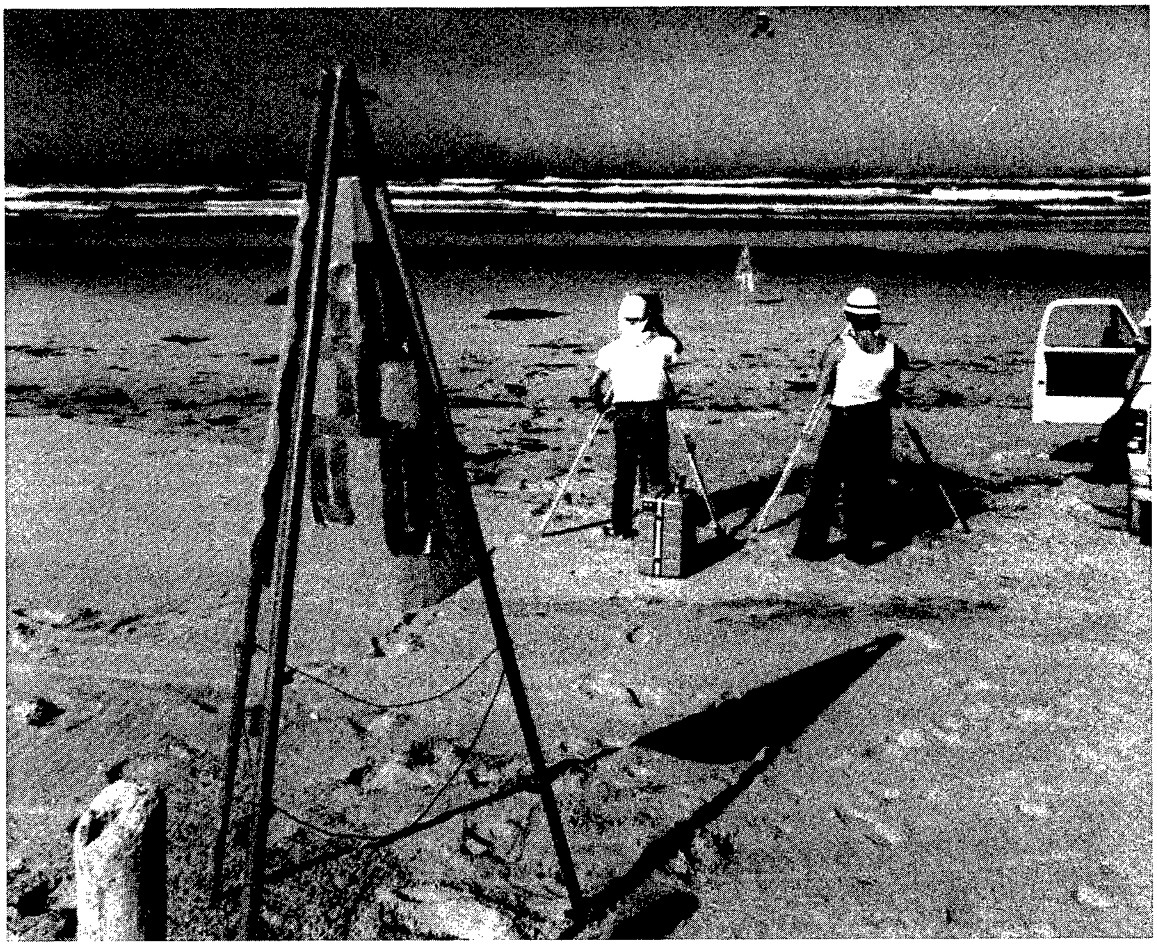

Figure 33. Helicopter, range poles, and total station on profile line

appropriate distance offshore while remaining on-line. The pilot lowers the helicopter until the main weight reaches the seabed and the cable tension goes slack. The level operator continuously views the graduated portion of cable through the level as the cable is lowered. At the instant the cable goes slack, the level operator reads the elevation to the nearest tenth of a foot and relays this information to the data recorder. At the same time, the TDS operator has the TDS aimed at the prism cluster mounted on the helicopter and takes a reading of the horizontal location of the helicopter, also providing the information to the data recorder. After the position and depth have been hand recorded, the pilot, notified by radio, raises the helicopter so that the weight clears the water surface and moves forward on the range line toward the beach to the next point, where the process is repeated.

Time efficiency

The distance between points is determined by density requirements of the survey. Each point requires 5 to 10 sec to read instruments and record data. The greater portion of the time is spent maneuvering the helicopter between points. Approximately 60 points can be surveyed along a 900- to 1,600-m- (2,955- to 5,250-ft-) long profile line in 20 min. Time required between lines ranges from the few minutes necessary to reposition the helicopter to the time required to move the TDS and level to a new position, if needed. In comparison, the CRAB which travels at 5 km/hr (8 mph) requires approximately 45 min for each profile line. Time required between lines is again a function of CRAB travel time and distance between lines and/or time required to reposition the TDS.[1]

Accuracy and repeatability

In July 1990, a field study evaluated the HBNSS for accuracy and repeatability, under the MCCP Program's Siuslaw River work unit. The CRAB survey system was used as a control. A detailed account is presented in Birkemeier and Mason (1984). Additionally, Clausner, Birkemeier, and Clark (1986) present a similar field comparison of the CRAB with other nearshore survey systems. In the previous comparison study, a Zeiss Elta-2 TDS provided the horizontal and vertical position of the CRAB. During the July 1990 study, a Geodimeter 140T self-tracking TDS replaced the Zeiss. The Geodimeter 140T increases the number of points that can be reasonably collected along a line, yielding an almost continuous profile. This increased the quality of the CRAB survey and the likelihood that positions of soundings taken using the HBNSS would closely coincide with those of the CRAB.

The July 1990 field test was designed to evaluate the HBNSS's ability to survey a known profile, stay on-line, and produce repeatable results. Test-day conditions were characterized by small, long-period waves and moderate to low longshore currents. Repeatability tests included five repetitive surveys on two profiles of diverse topography. For these tests, the reference profile shape was determined by two repetitive surveys by the CRAB. Therefore, accuracies are relative to the accuracy of the CRAB. Figures 34 and 35 show the envelope of four HBNSS surveys superimposed over one CRAB survey for test profile lines 100 and 200, respectively. The upper portion of the figures present the envelope of maximum vertical deviation and standard deviation along the profile between all four HBNSS measured profiles and the CRAB measured profile. These figures indicate that the HBNSS provides accurate and repeatable measurements of the true profile shape. For profiles 100 and 200, respectively, the absolute maximum vertical deviation is 0.6 m and 1.0 m (2 ft and 3.3 ft), the mean vertical deviation is 0.1 m and 0.07 m (0.3 ft and 0.22 ft), and the mean standard deviations are 0.06 m and 0.05 m (0.2 ft and 0.16 ft). The larger deviations occur where points were missed over the bars and can be eliminated by increasing the density of sampling. Tests of vertical

[1] Personal Communication, July 1991, William Birkemeier, Chief, Field Research Facility, Coastal Engineering Research Center, U.S. Army Engineer Waterways Experiment Station, Vicksburg, MS.

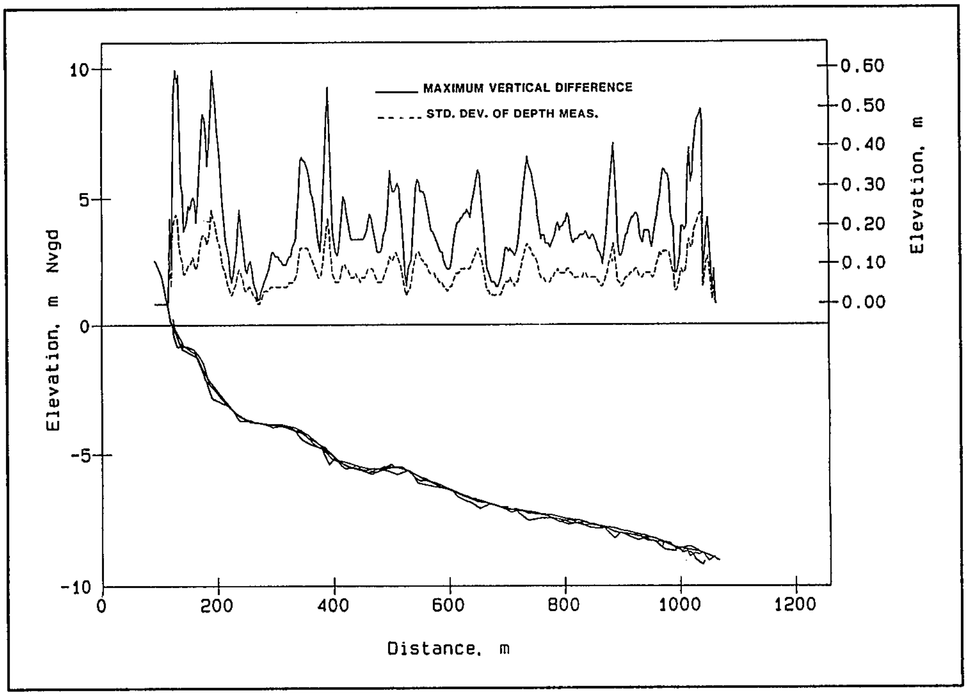

Figure 34. CRAB survey and four HBNSS surveys of line 100

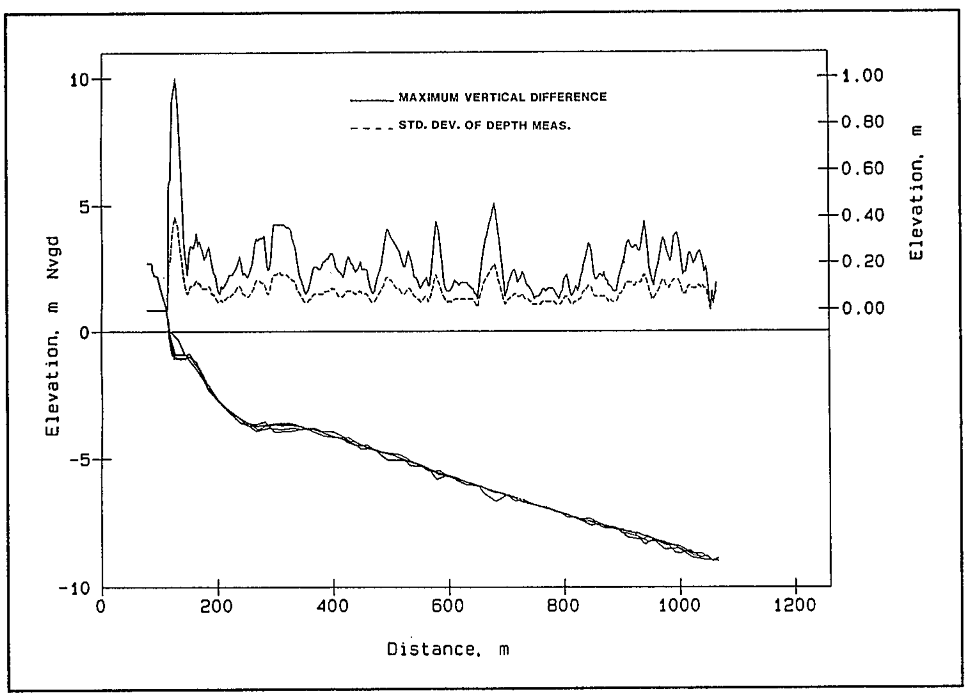

Figure 35. CRAB survey and four HBNSS surveys of line 200

accuracy differences between a fathometer survey and a CRAB survey conducted by Clausner, Birkemeier, and Clark (1986), indicate maximum deviations of the fathometer to be 0.67 m (2.2 ft) and mean vertical deviation to be 0.27 m (0.9 ft) in regions greater than 300 m (984 ft) offshore.

Figure 36 shows the positions of the CRAB, four helicopter surveys, and profile line 100. For the most part, the helicopter remained within 6 m (19.7 ft) of the profile line and the CRAB within 3 m (9.8 ft) of the line. Greater deviation from the line for both the CRAB and the helicopter occurred farther offshore. Large deviation in one of the helicopter surveys reflects communication problems between the pilot and land crew. Accuracy increases with crew experience.

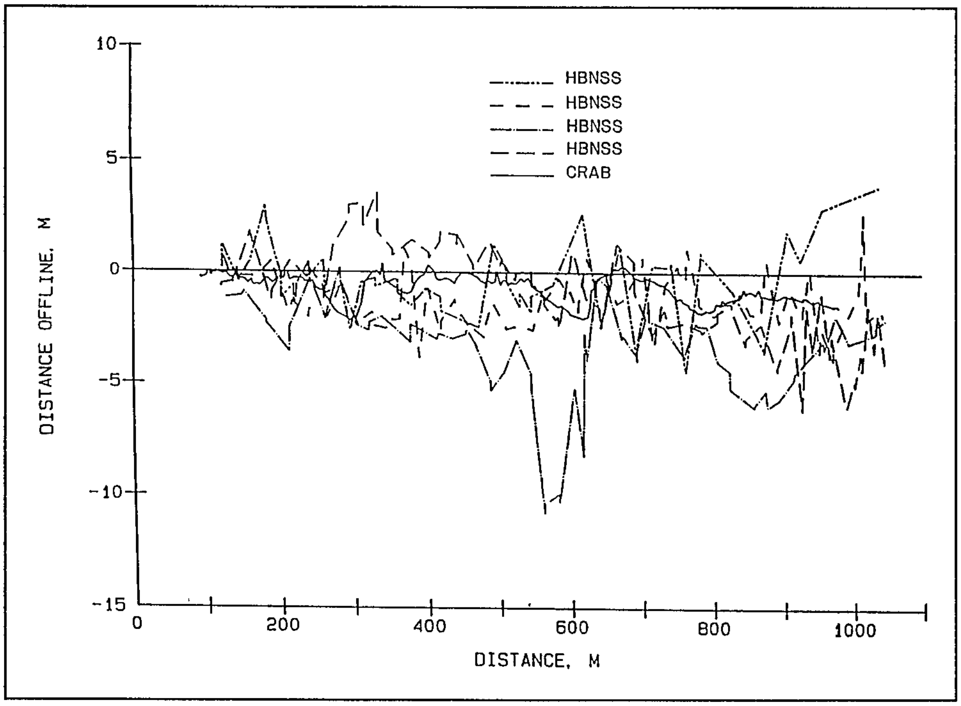

Figure 36. Distance off line of CRAB and four HBNSS surveys

Automation Improvements

Coupling the TDS with a data-logging computer would allow the horizontal positions to be recorded automatically. The level would still be used to read elevations, but these values could be directly entered into the computer as they are taken.

A further step in automating HBNSS would be to attach a ring of prisms on the cable and use a tracking TDS such as the Geodimeter 140T linked to a data logger. At the instant the cable weight reaches the seabed, the TDS operator marks the data point. Horizontal positioning and depths would automatically be entered into the data file. Marked data points would compose the profile. This process could reduce the land crew to one member. As a side effort, this process was briefly examined during the experiment. Because the TDS was capable of tracking the prism ring, the TDS operator did not view the helicopter through the TDS scope, but with the naked eye. Marked points indicate when the helicopter terminated its descent opposed to when the lead line became slack. Therefore, marked points lagged the actual event, reflecting a deeper than actual profile. Figure 37 shows a profile collected using the tracking TDS. Refinement of this method would certainly improve accuracy and reduce time and cost requirements during actual operation and in data reduction.

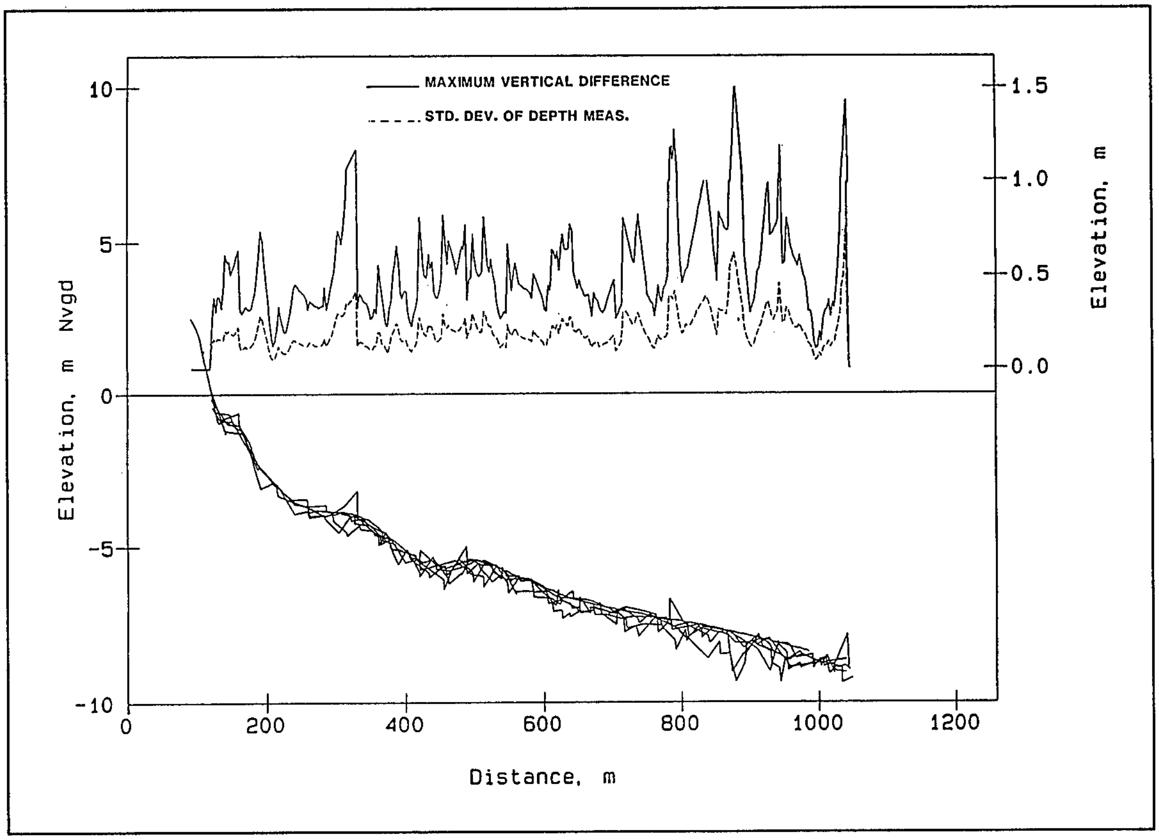

Figure 37. Profile comparison of TDS automatic tracking method and CRAB profiles

For both automation methods, a complete digital record (ASCII file) would be available at the end of each profile. This would circumvent the need to digitize hand-recorded field data, thereby reducing potential for error. Additionally, the TDS and level would not need to be moved from the start of one profile line to the next if the lines are within instrument ranges.

Summary and Conclusions

The Helicopter-Borne Nearshore Survey System can be used to measure seabed and structure topography in hazardous regions where other survey vessels cannot operate safely. Soundings can be taken quickly and are accurate and repeatable. Developed in 1960 by the Portland District, the system has been in use along the Pacific Coast since that time. In 1990, the HBNSS was tested at the USACE Coastal Engineering Research Center, Field Research Facility for speed and accuracy. Using the CRAB as the standard, mean vertical error for the HBNSS is 0.08 m (0.26 ft) compared to that of a fathometer reported to be 0.27 m (0.89 ft).

5 Dredging

Particulars of Analyses

Hydrographic survey data were analyzed to determine shoaling, scouring, and sedimentation volume trends within the Siuslaw River entrance channel area from 1982 to 1990 and to evaluate how the trends changed from pre- to post-jetty extension/spur construction as well as determine changes in maintenance dredging requirements.

Hydrographic survey data for the Siuslaw River entrance were provided by NPP. Condition surveys were taken prior to the dredging season to determine need and post-dredging surveys were taken to evaluate dredging efficiency. In general, each year the surveys were initiated in May and ended in September, but may have begun as early as April and ended as late as October (Table 5).

For this investigation, the study period is divided into three time segments relating to the construction period of the 1985 jetty extensions. Preconstruction is the time period before the 1985 jetty construction, September 1982 to May 1984; the transitional time period includes actual construction years of the 1985 jetty and 2 years after, allowing for a recovery time, October 1984 to July 1987; and post-construction begins 3 years after the 1985 jetty construction, June 1988 to May 1990.

As stated earlier, the jetties which were refurbished in 1960 are referred to as the 1960 jetties and the jetty extensions and the addition of spurs in 1985 are referred to as the 1985 jetties. The most seaward ends of these jetties are referred to as terminal points.

The study area encompasses a 152-m (500-ft) by 122-m (400-ft) channel located at the river entrance between the jetties, and extends approximately 305 m (1,000 ft) shoreward into the mouth of the 1960 jetty terminal points. Several polygons were employed to divide the study area to define and locate regions of volume change, shoaling, and scouring (Figure 38).

The polygon which delineates the minimum data boundaries or comparable regions for all surveys is labelled the MIN polygon (Figure 38). The MIN

Table 5
Siuslaw River Entrance 1982-1990 Dredging and Survey Data

Fiscal Year	Dredge	Date	Days	Total	Amount Dredged Fiscal Year Total		Graph Labels	Survey Dates
					cu yd	cu m		
1982	Yaquina	Jun 18-21	4		343,417	262,577		Apr 27
		Jun 20-25	2					Jun 3
		Jul 18-21	4					Jul 13
		Jul 26-28	3					Aug 5
		Jul 29-31	3				A	Sep 21
		Aug 1-10	10	26				
	Sandsucker	Jun 27-30	4					
		Jul 1-11	11	15				
1983	Yaquina	Jun 17	1		213,325	163,108	B	Apr 18
		Jun 19-22	4					Jul 26
		Jun 25-30	6				C	Sep 25
		Jul 2-7	6					
		Aug 26-31	4					
		Sep 1-4	4					
		Sep 8	1	20				
1984	Yaquina	Jun 3-4	2		276,159	211,151	D	May 30
		Jun 8-17	10					Jul 26
		Jun 21	1					Aug 21
		Jul 27-31	6					Sep 25
		Aug 1-16	16	29			E	Oct 23
	Westport	Sep 27-30	4		311,822	238,419		
		Oct 1-3	3	7				
1985	Yaquina	Jun 13-16	3		271,250	207,398	F	May 19
		Jun 17-30	14					Jul 27
		Jul 1-4	4				G	Oct 1
		Sep 16-18	3					
		Sep 20-22	3					
		Sep 30	1	22				

(Continued)

polygon is further divided into three polygons, 1 MIN, 2 MIN, and 3 MIN, with the 2 and 3 MIN polygons being of similar area and the 1 MIN being almost double the area of the 2 MIN. Since October of 1985, additional survey data were available for the area seaward of the MIN polygon. This region

Table 5 (Concluded)								
Fiscal Year	Dredge	Date	Days	Total	Amount Dredged Fiscal Year Total		Graph Labels	Survey Dates
					cu yd	cu m		
1986	Yaquina	May 22-25	4		218,836	167,322	H	May 21
		Jun 20-25	6					Jul 15
		Jul 4-10	7				I	Sep 30
		Jul 22-23	2					
		Aug 29-31	3					
		Sep 1	1					
		Sep 8-10	3	25				
1987	Yaquina	Jun 4-11	8		215,958	165,121	J	Jun 3
		Jun 28-30	2				K	Jul 28
		Jul 1	1					Oct 2
		Jul 21-29	9	20				
1988	Yaquina	Jun 30	1		114,485	87,535	L	Jun 22
		Jul 1-5	5				M	Aug 16
		Jul 24	1					
		Aug 11-14	4	11				
1989	Yaquina	Jul 6-11	6		116,604	89,155	N	May 2
		Aug 14-17	4					Jul 11
				10			O	Aug 1
1990	Padre Is	Jul 2-5	4		99,120	75,787	P	May 16
								Jun 26
				4			Q	Aug 6

is labelled the TIP polygon. The WHOLE polygon includes the MIN polygon plus the TIP polygon.

Examination of individual hydrographic survey bathymetric maps (Appendix A); comparison of difference maps, which were generated by subtracting one topographic surface from another; and analyses of cross-sectional profiles (Figure 39) from the hydrographic surveys aid in the determination of changes and trends in sediment movement throughout the study period.

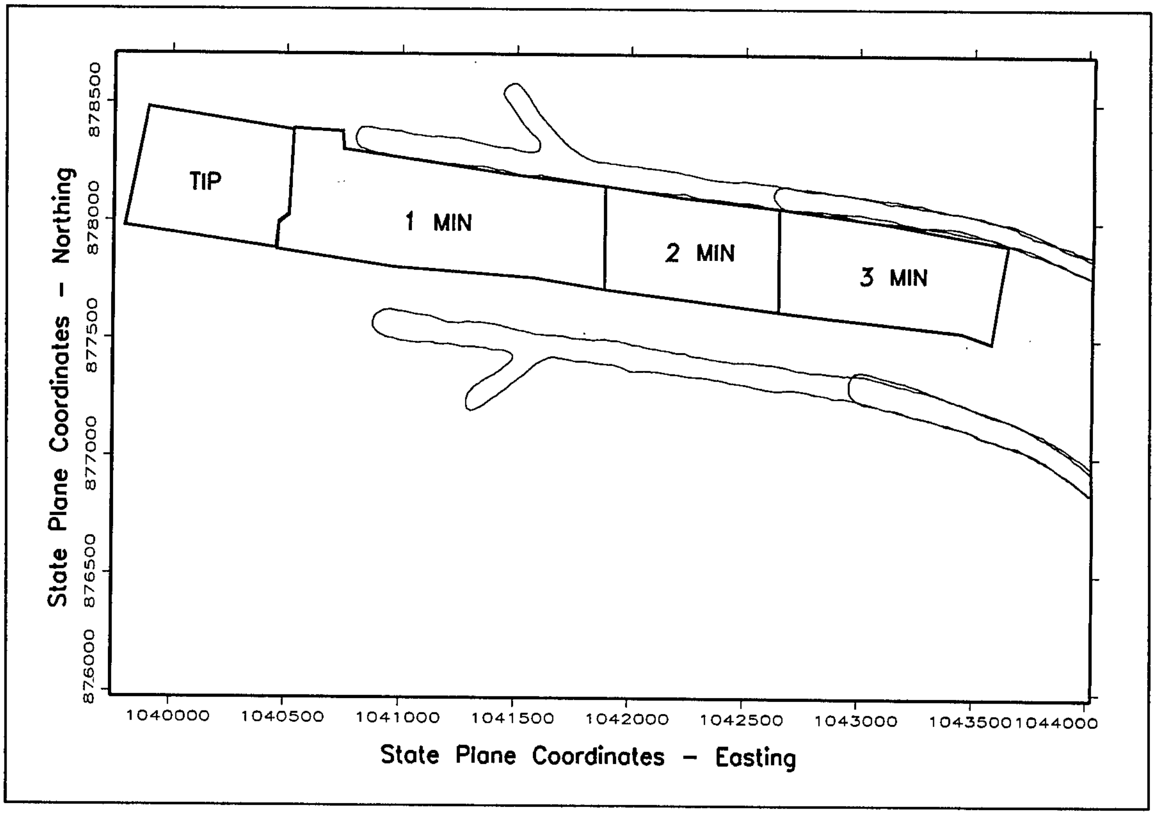

Figure 38. Polygons used to divide in-channel study area

Shoaling/Scouring

Interpretations of shoaling and scouring regions for the study area throughout the 1982-1990 study period were assessed (Figure 40). For this application, shoals are defined as areas of elevation -4.9 m (-16 ft) and shallower, and scoured areas are identified as -7.3-m (-24-ft) elevations or deeper.

Shoaling trends

Beginning south of the 1960 jetty terminal points, extensive shoaling extended from the south side of the channel north into the center of the channel. This shoaling area existed throughout the pre-jetty time period, diminished during the transition, and remained small throughout the post-jetty study period (Figure 40a). Examination of cross-sectional profiles illustrates that this same shoal is removed by the dredge and returns every year after the dredging season.

The region just landward of the shoal described in the previous paragraph is depicted as stable (no change in elevation between post-dredging survey and immediate pre-dredging survey) by comparing one hydrographic survey to the one immediately previous. Throughout the entire 1982-1990 study period, this

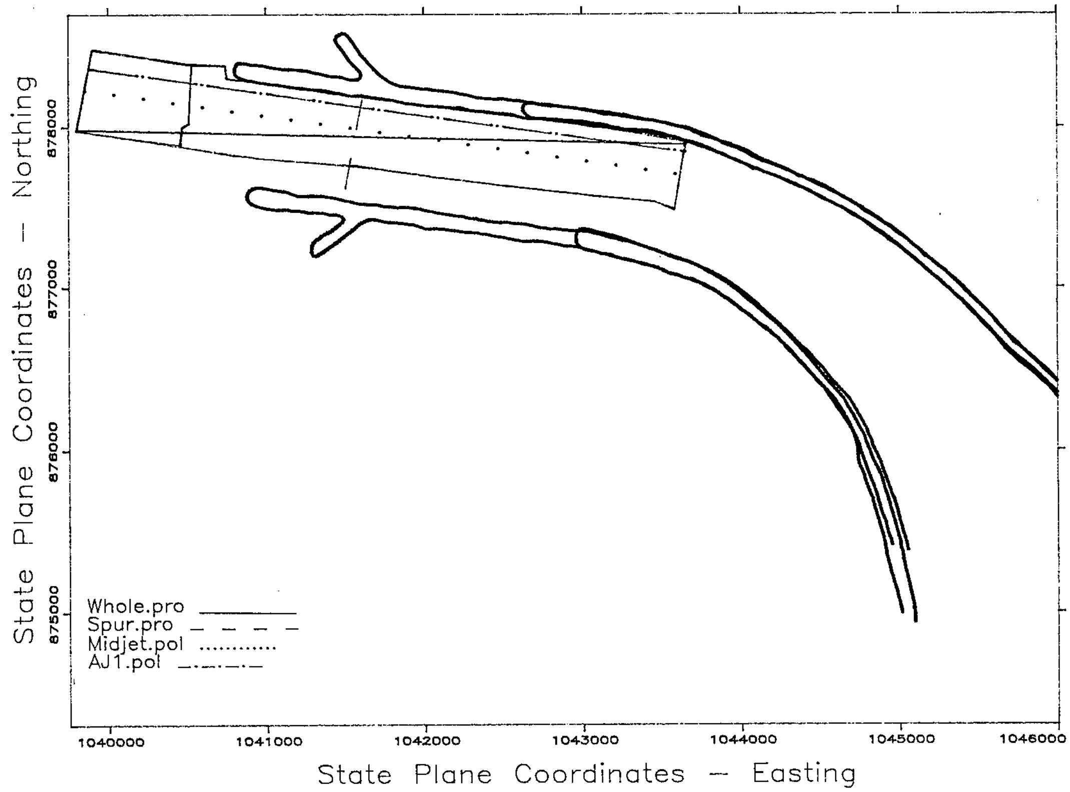

a. Locations of cross-sectional profiles

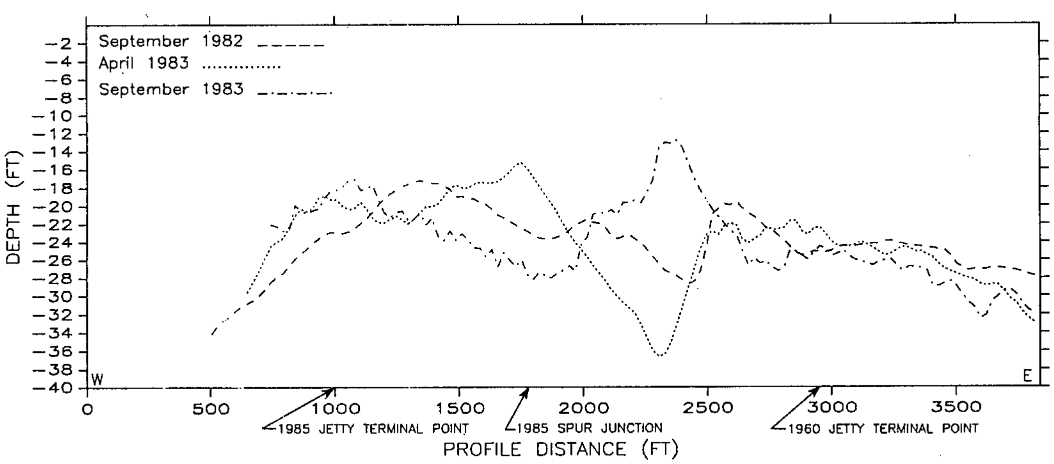

b. Cross-sectional profile, April 1983 "WHOLE" profile, depicting the formation of a shoal only 17 days after the summer dredging season

Figure 39. Cross-sectional profiles

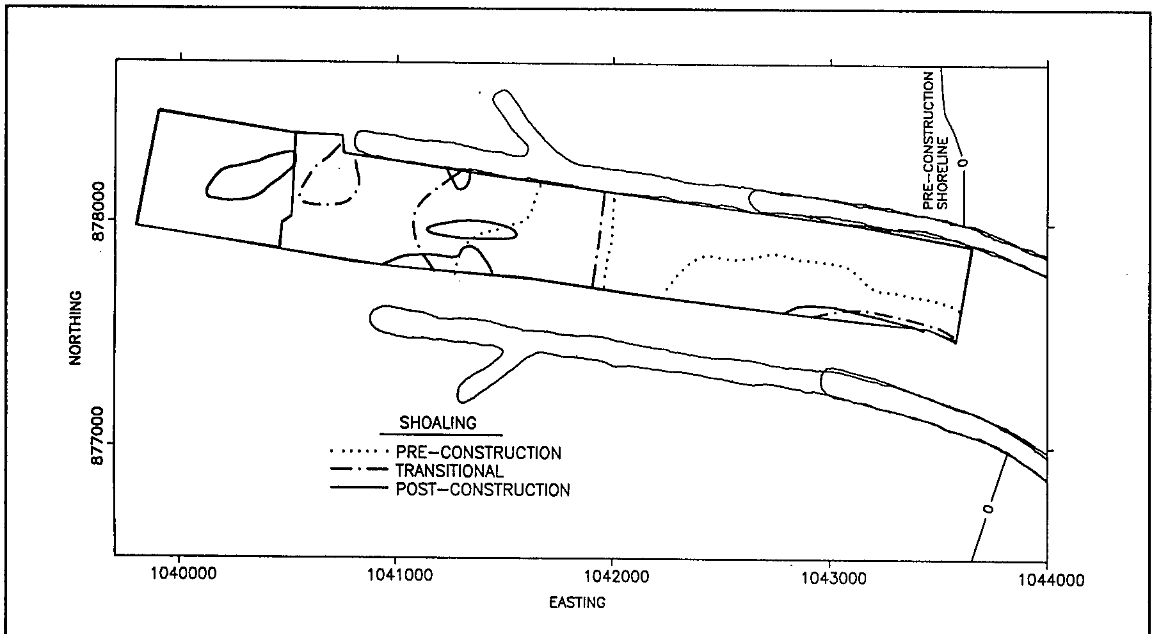

a. Interpretation of general shoaling trends

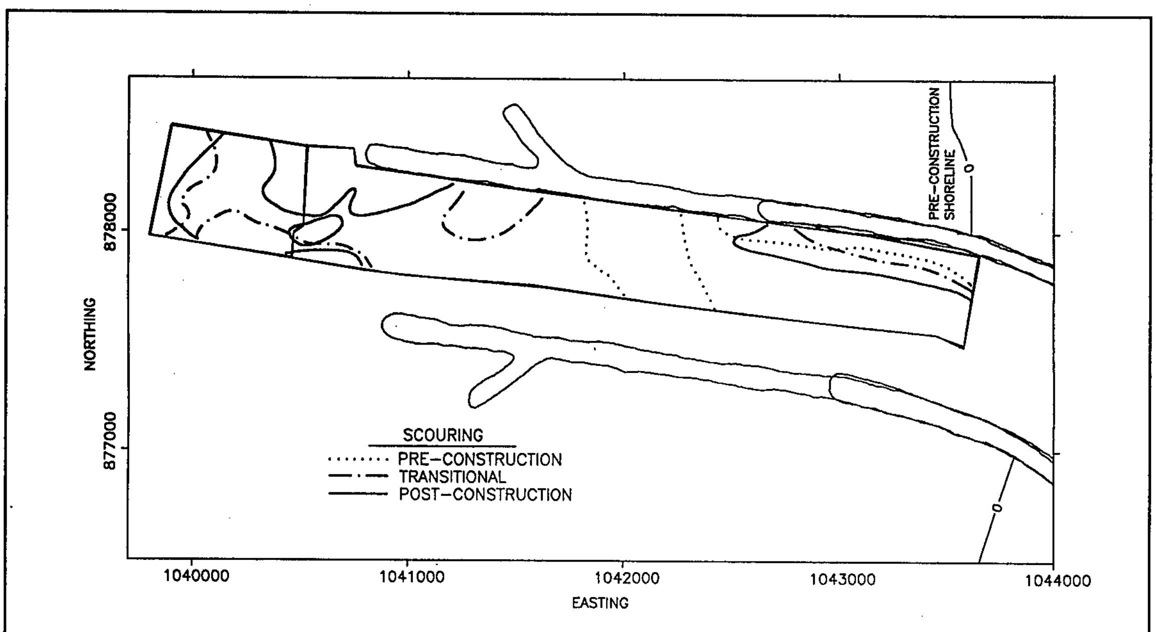

b. Interpretation of scouring trends

Figure 40. Interpretation of general shoaling/scouring trends

stable region varies in size and orientation slightly, but generally covers a common area, and enlarges significantly during the post-jetty years. Part of the shallow stable region may be a persistent shoal that is not removed by dredging activities and is therefore in equilibrium and present in all surveys to some degree.

During the post-construction period, a near stable (less than 2-ft change in elevation) area migrates from a region landward of the 1960 termination points, June 1988, to include the area landward of the 1985 spur junction location, May 1990. Analysis of the cross-section profiles, located from spur junction to spur junction, supports the near stable (approaching equilibrium) condition of this area. If the post-dredging survey of August 1988 is ignored, a small variation of about 1 m (3 ft) or less elevation in the channel center is observed for the post-construction years beginning in June 1988. The areas of near stabilization do not include a 396-m- (1,300-ft-) long 30-m- (100-ft-) wide trench located against the base of the 1960 north jetty.

During the pre-construction years, an offshore bar shoal is present that crosses the entire width of the channel between about 183 m (600 ft) and 335 m (1,100 ft) seaward of the 1960 north jetty terminal point, which is located between the spurs (Figure 40; Appendix B). The shoal shallowed toward the south side of the channel. During the transition years, this same shoaling area extended slightly offshore, to encompass a position from about 183 m (600 ft) to 457 m (1,500 ft) seaward of the 1960 north jetty terminal point, and became more equally distributed across the channel (Figure 40). During the post-jetty construction time period, the shoaling area diminished in size (Figure 40) with the southern portion of the shoal slightly shallower than the northern.

Located just south of the north 1985 jetty terminal point, a shoal is apparent in the transitional surveys (Figure 40). Hydrographic survey data were not available for this area until October 1985. The centroid of the shoal moved offshore about 122 m (400 ft) and increased in size during the post-construction years (Figure 40). This shoal may actually be part of the alongshore contours adjusting to the lengthening of the jetties; lack of survey data outside the channel prevents viewing of the continuous bar.

A shoal can develop very soon after the last dredge of a dredging season and may be illustrated on a post-dredging survey. One such instance is readily visible on the September 1983 hydrographic survey cross section (Figure 39), located about 107 m (350 ft) seaward of the north 1960 jetty terminal point. Therefore, interpretations of shoaling/scouring between surveys must be made with caution and must consider the possibility of early response of sedimentation processes being recorded on a post-dredging survey.

Scouring

Along the base of the north jetty, from the terminal point of the 1960 jetty to approximately 213 m (700 ft) landward, a persistent 30.5-m- (100-ft-) wide trench has existed for the entire 1982-1990 study period (Figure 40; Appendix A). A slight southward expansion of the trench is illustrated by comparing the pre-construction surveys to the post-construction surveys. Interpretation of cross-sectional profiles of the area, located about 23 m (75 ft) south and parallel to the north jetty, substantiates the interpretation of the near equilibrium state of the southern boundary of the trench for the 1982-1990 study period as well as illustrating the persistent depth of at least -7.3 m (-24 ft) extending from the terminal point of the north 1960 jetty landward since June 1987.

Located about 122 m (400 ft) seaward of the 1960 north jetty terminal point, a well-developed scour area existed prior to jetty construction (Figure 40; Appendix A). This scour hole dissipated and another appeared, located about 366 m (1,200 ft) seaward of the 1960 north jetty terminal point, during the early transitional years. Examination of cross-sectional profiles of this area shows that these two scour areas are not apparent during the remainder of the transitional surveys. It is unclear from the data sets whether these two scoured areas are actually the same scour hole migrating offshore or two entirely different phenomena occurring because the new jetty was constructed during the formation of the two scour holes. The more landward of the two scour areas is in the position to be influenced by the longshore bar/trough, which extends north and south of the jetties, but is excessively deeper (-10.4 m (-34 ft)) than the trough (-5.5 m (-18 ft)) (Appendices A and B). Again, this may be a portion of the alongshore contours but lack of data adjacent to the channel prevents confirmation. The more seaward of the two scour holes is likely associated with the in-progress north jetty construction.

Located about 183 m (600 ft) seaward of the terminal points of the south 1985 jetty, a scour hole developed during the middle of the transitional period, May 1986 (Appendix A). Approximately 1 year later at the end of the transitional period, June 1987, the hole migrated landward about 91 m (300 ft) and remained about the same depth and size. This scoured area became smaller during the post-construction time period while extensive scouring developed, enlarged, and migrated slightly seaward off the terminal point of the north 1985 jetty at the same time.

Conclusions of shoaling/scouring

Beginning about 335 m (1,100 ft) landward of the 1985 jetty terminal points and continuing landward, the southern portion of the channel experienced a decrease in shoaling and an increased region of stability associated with the 1985 jetty improvements. Other stable areas are in the central part of the channel beginning about 549 m (1,800 ft) landward of the 1985 jetty terminal points and continuing landward.

In-channel shoaling, between the jetties near the spurs, may be related to oceanographic sedimentation processes and not a result of the 1985 jetty alterations. The shoal was present prior to new jetty construction and is apparent as a longshore bar in overall coastal surveys of the area (Appendices A and B). Since the 1985 jetty extension, shoaling inside the jetties has diminished in area and elevation, thus improving navigability of the channel throughout the year, not just after dredging (Figure 40; Appendix A).

Scouring along the interior base of the north jetty, beginning about 488 m (1,600 ft) landward of the 1985 jetty terminal points, has remained evident throughout the 1982-1990 study period (Figure 40). The trench has deepened and encroached slightly more into the center of the channel from pre-construction through post-construction years and has maintained a depth of at least -7.3 m (-24 ft) since June 1987 (Appendix A). This pattern aids in natural channel maintenance.

Associated with the terminal points of the north and south 1985 jetties are scour areas occurring during the post-jetty time period (Figure 40; Appendices A and B). The northern scoured area is more pronounced, deeper and wider, than the southern scoured area. The southern scoured area appears to come and go, in presence and size, throughout the post-construction years, without preference to season, while the northern scoured area stays prevalent from March 1989 on to the end of the study period (Appendix B). The scouring may result in future foundation problems for the terminal points of the jetties.

Also associated with the terminal points of the 1985 jetty is a shoal which formed during the transitional survey period, then located adjacent to the north 1985 jetty terminal point, and progressively migrated seaward throughout the post-construction years (Appendices A and B). The migrated shoal is located seaward of the scour hole mentioned in the above paragraph associated with the north 1985 jetty terminal point. This may be part of the alongshore contour's adjustment to lengthening the jetties. Lack of data adjacent to the channel prevents confirmation of this issue.

Volumes

Sediment volume calculations

Sediment volume computations for both pre-dredging and post-dredging surveys were examined using a control depth of -16.8 m (-55 ft). These overall volume values show sediment accumulation trends in the channel. Sediment volumes above the -5.5-m (-18-ft) contour were also calculated, and are considered to represent annual maintenance dredging requirements. Volume changes from 1982 through 1990 aid in tracking sediment movement, identifying trends due to the construction of the new jetty system, and confirming changes in annual maintenance dredging volumes. Pre-dredging surveys indicate the volume of material accumulating over the winter season and are used to indicate differences in volume accumulation for pre- and post-construction years. The post-dredging surveys aid in accounting for sediment removed from the system.

Analysis considerations

Several obstacles were encountered when evaluating the data sets. Most of the obstacles were confined to the pre-construction time period, but not all.

The volcanic eruption of Mount St. Helen in late 1980 caused clean-up demands from dredges in and about the area for 1981 and possibly 1982. Due to these demands on dredges, normally scheduled dredging activities for the Siuslaw River and other areas were severely reduced in 1981. This diverting of regular dredging for the Siuslaw River in 1981 and 1982 resulted in the accumulation of larger sediment volumes than usual in the study area.

The 1982/83 El Niño caused greater erosion of beaches and introduction of more sediment in the littoral system than usual for the Siuslaw River area. Due to the El Niño phenomenon, shoaling, scouring, and sediment volumes reacted in an unusual manner. An unusually large amount of sediment from the south was transported to the north during the 1982/83 El Niño. Afterwards, typical sediment transport resumed, moving the large amount of sediment to the south. This transportation of sediment southward most likely resulted in large amounts of sediment in the Siuslaw River channel in the next few years following El Niño.

Jetty construction operations altered typical shoaling, scouring, and sediment transportation patterns in the channel near the jetty extension area. Jetty construction began in 1984 and was officially accepted as complete on 1 February 1986. After construction was completed, coastal processes appeared to seek an equilibrium, requiring a recovery period. Additionally, new work dredging may have been required to initially deepen the river channel in the area between 1985 jetty extensions. Therefore, the new work may possibly result in higher than usual dredging volumes for the time period 1 and 2 years after construction.

The decrease in volumes dredged from 1987 through the end of the study period may reflect new management scheduling policies. In 1986, the dredge was scheduled to work based on channel history. In 1987, reduced maintenance dredging requirements resulting from the 1985 jetty improvements prompted a reevaluation of dredge work scheduling to better meet need as opposed to history.

The previously listed factors definitely affect specific fluctuations of pre-dredging and post-dredging volumes and shoaling/scouring patterns, but in general, trends are apparent when comparing averages of the pre-construction and post-construction surveys.

Volume trends

As expected, during the approximate 9-month fall to spring time period (pre-dredging), all polygon areas located landward from a position beginning about 91 m (300 ft) seaward of the 1985 jetty terminal points (Figure 38) generally experienced greater volumes than for the post-dredging 3-month time period (Figure 41), except for one instance, April 1983 (Figure 41b) in the 2 MIN polygon. The pre-dredging survey of April 1983 was recorded as having much less sand volume than the earlier and later post-dredging surveys for polygon 2 MIN only. This phenomenon may be a result of El Niño altering coastal sedimentation processes during 1982 and 1983.

The studied area seaward of the position located 91 m (300 ft) seaward of the 1985 jetty terminal points (TIP polygon) experienced no such seasonal trend in survey volumes until the post-construction time period, May 1989 (Figure 42). The volume of the TIP polygon is influenced by a scour hole diminishing in size and migrating east out of the area and by the formation and growth of a shoal that migrates from northeast to southwest traveling through the polygon. Only the outer regions of the scour hole are included in the polygon before it migrates out of the study area. The unique trend of volume accumulation is shown as a general increase, then decrease, spanning seven surveys through the transition and early post-construction years, October 1985 through August 1988. Scouring diminished and the area flattened out with the beginning of shoal formation (Appendix B). The largest volume shoal in the TIP polygon, May 1989, happened to be located in the middle of the polygon (Figures 42 and 43; Appendix B). By calculating the volume of sediment exceeding -5.5 m (-18 ft), only the shoaling areas which require dredging to maintain the channel are apparent (Figure 43).

The volume analysis indicates, as the shoaling analysis had, that the accumulation of sediment has physically shifted seaward into deeper water in conjunction with the seaward extension of the jetties. The shift of the accumulation of sediment to deeper water results in less shoal relief and reduced maintenance dredging requirements.

The study area located from the 1960 jetty terminal points landward, polygon 3 MIN (Figure 38), experienced high pre-dredging volumes during the pre-construction and beginning transitional surveys (Figure 41c). This area experienced persistently lower pre-dredging volumes beginning in the middle of the transitional time period (May 1986) and throughout the post-construction period.

The area located seaward of the 1960 jetty terminal ends to the region between the junction of the spurs, polygon 2 MIN (Figure 38), experienced high pre-dredging volumes during the end of the pre-jetty through the end of the transitional time period (Figure 41b). Persistently lower pre-dredging volumes began in June 1988 and continued through the post-construction years.

The study region located from the junction of the spurs to about 76 m (250 ft) seaward of the 1985 jetty terminal ends, polygon 1 MIN (Figure 38), experienced high pre-dredging volumes during just the transitional period (Figure 41a). Lower pre-dredging volumes began at the same

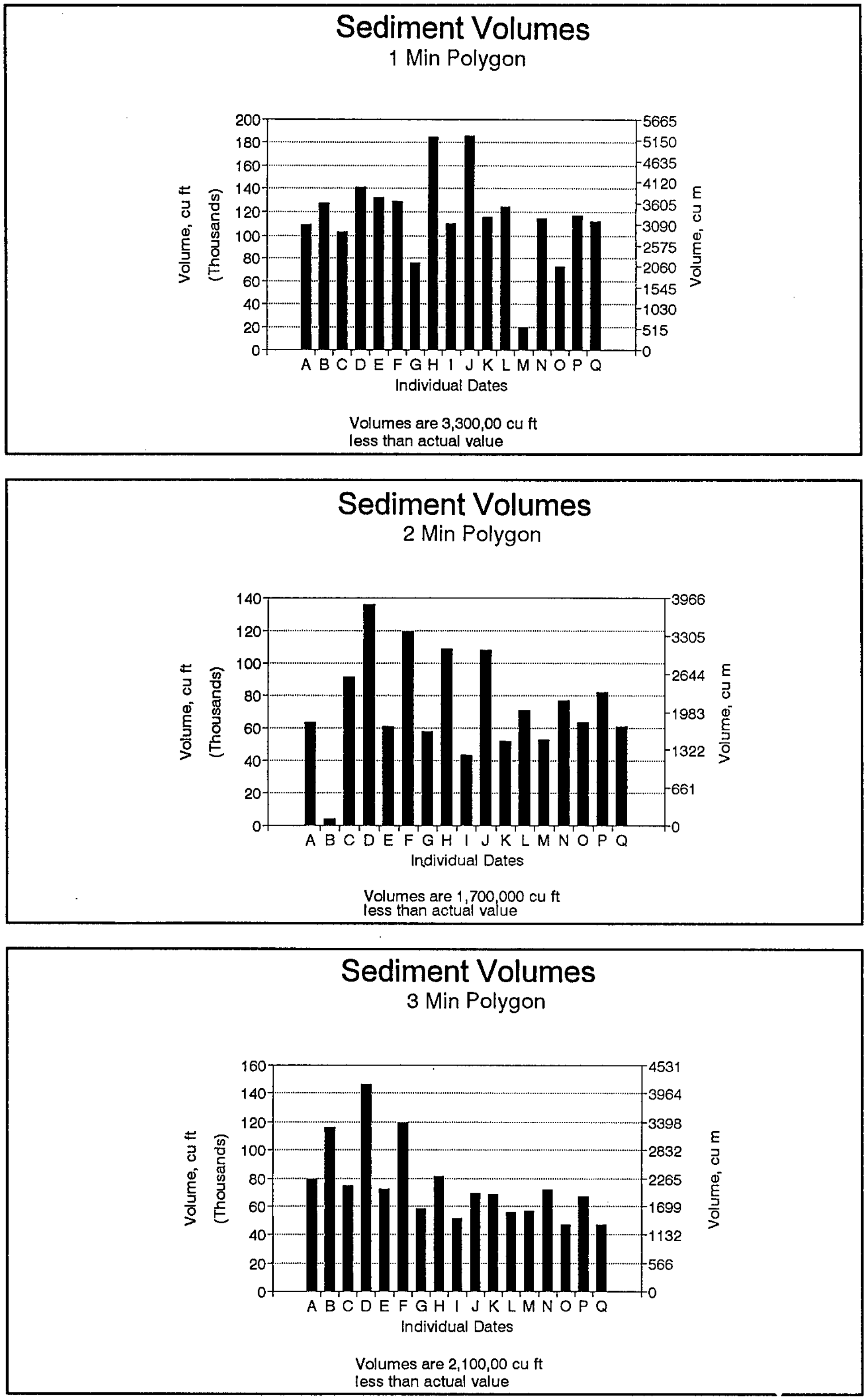

Figure 41. Sediment accumulation volumes of selected polygons for individual dates

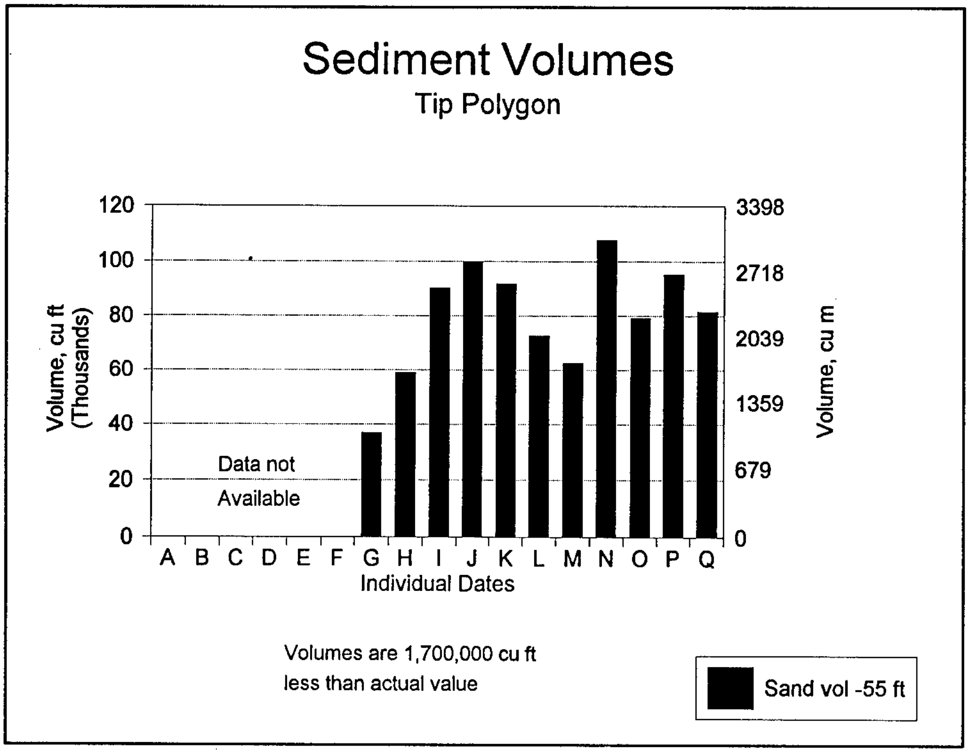

Figure 42. TIP polygon sediment accumulation volumes for individual dates

post-construction date as for polygon 2 MIN, June 1988, and continued through the end of the post-construction years.

It is again obvious that the region of sediment volume accumulation for the three polygons shifts seaward from the pre-construction to the post-construction time period (Figure 41). As a result, the annual accumulation of sediment inside the channel, based on volumetric calculations of all polygons (1 MIN, 2 MIN, 3 MIN, and TIP polygon), has decreased from the pre-construction to the post-construction years and maintenance dredging requirements are also reduced.

The annual maintenance dredging requirements for the overall study area are easily detected when volumes are calculated above the -5.5-m (-18-ft) elevation (Figures 43b and 43c). The MIN polygon is the only polygon that has data for the entire study time period and is used for this analysis. This polygon does not extend the entire channel length; therefore, relative differences are conservative and only reflect trends. Additionally, over-dredging is often accomplished to a depth of -6.7 m (-22 ft), 1.2 m (4 ft) greater than the depths used for this analysis. The decreasing trend in annual maintenance dredging requirements for the MIN polygons is in agreement with the reduced post-construction volumes dredged, estimated by the NPP to be on the order of 76,460 m^3 (100,000 yd^3) annually, as compared to pre-construction (Figure 44).

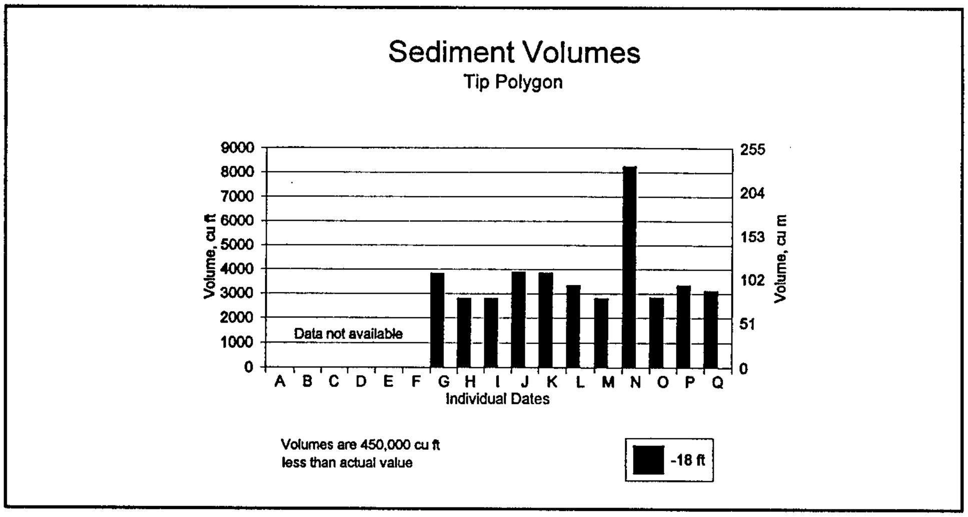

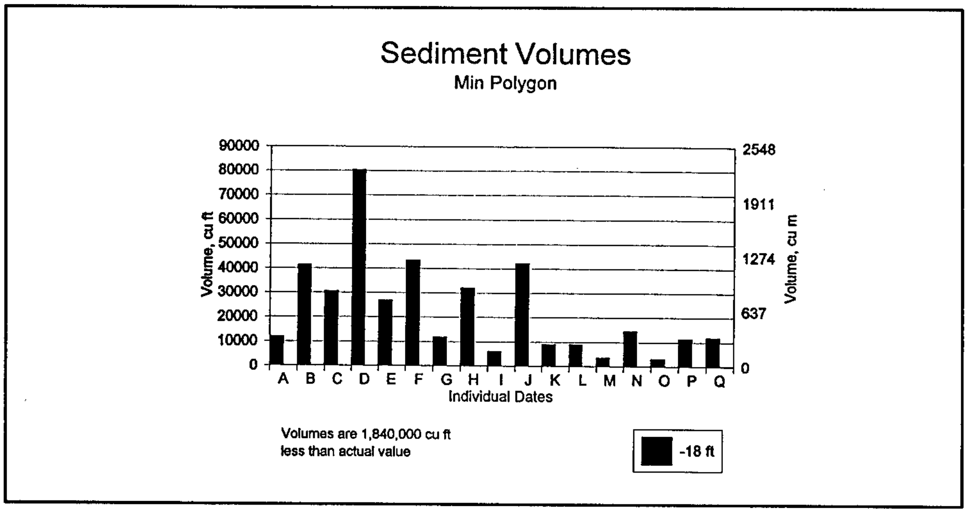

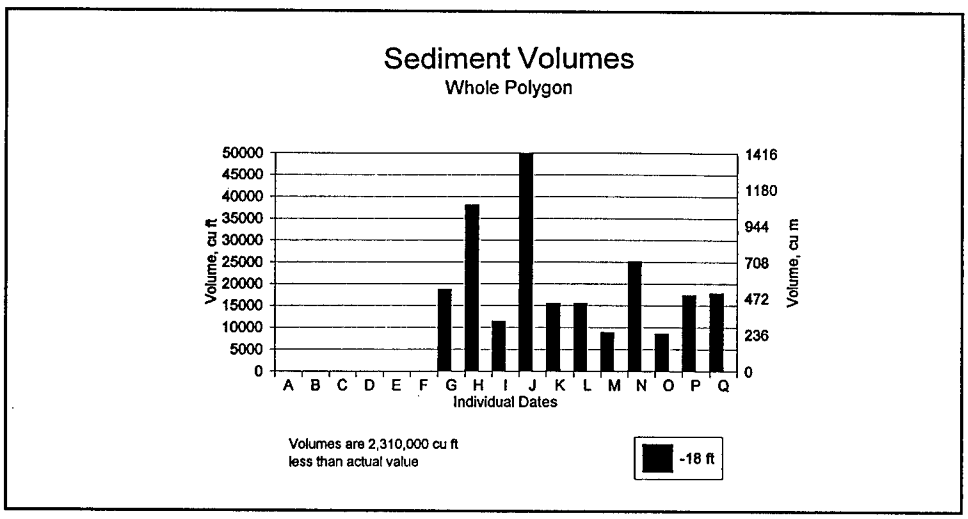

Figure 43. Annual maintenance dredging requirements for selected polygons for individual dates

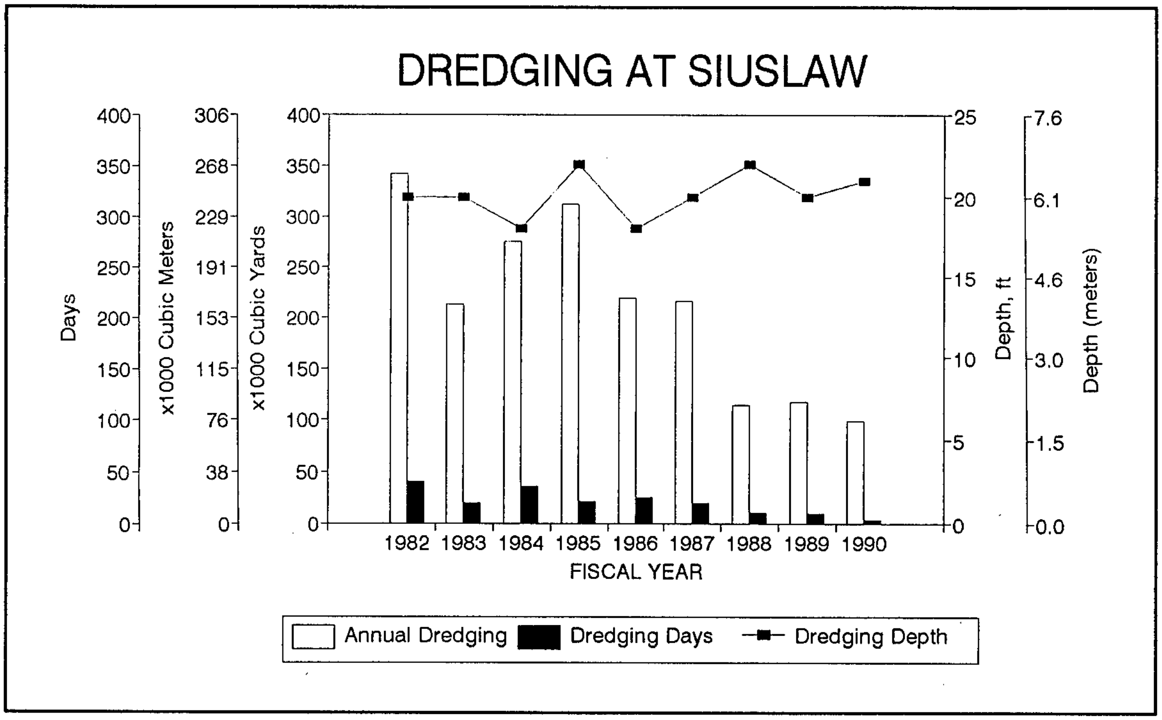

Figure 44. Actual dredging volumes and corresponding days and depths of dredging

Conclusions of volumes

All studied areas, except for the area seaward of the 1985 jetty terminal ends (TIP polygon), generally experienced greater volumes in the pre-dredging than the post-dredging surveys, as was expected. The most likely explanation for the TIP polygon's unique volume trend was the migration of a scour and then shoal through the polygon. The expected trends, similar to those exhibited in polygons 1 MIN, 2 MIN, and 3 MIN, began in the TIP polygon in May 1989.

Volume and shoaling analysis show the accumulation of sediment has shifted seaward in conjunction with the seaward extension of the jetties. By June 1988, all areas landward of the 1985 jetty terminal points (polygons 1 MIN, 2 MIN, and 3 MIN) were experiencing lower volumes of sediment accumulation. The area seaward of the 1985 terminal points (TIP polygon) did not experience significantly lower volumes in the post-construction years due to the incursion of a substantial shoal into the area. Since the shoal was migrating east-southeast out of the polygon, lower volumes may occur later, but this would be beyond the study period.

In agreement with actual volumes dredged and reported by NPP, volumetric analysis of annual maintenance dredging requirements for the channel have decreased from the pre-construction to the post-construction time period.

Conclusion of Shoaling/Scouring and Volumes

Shoaling inside the jetties has diminished in size and elevation since the 1985 jetty extension. Shoaling patterns shift offshore into deeper water in correlation with 1985 jetty extensions. Annual maintenance dredging requirements, along with wave shoaling and breaking in the channel, are reduced and navigation improved as a result of the 1985 jetty improvements.

6 Beach and Nearshore Response

Introduction

The introduction of any structure into a littoral system may alter the local coastal processes, changing wave, current and sedimentation depositional patterns. This investigation of beach and nearshore response to the 1985 jetty improvements is divided into two study elements. Both elements address concerns of seasonal and long-term changes in shoreline, volumetrics, scour and shoaling associated with the jetty extensions and the spurs as a system. Because the two improvements, the extensions, and the spurs were constructed in unison, it is difficult to attribute responses singularly to either improvement. The first study element investigates 18 km (11 miles) of shoreline adjacent to the entrance channel extending 8 km (5 miles) to the north and 10 km (6 miles) to the south. Changes are looked at in a global perspective relating to climatic events as well as the jetty construction. Results of the first element are viewed as a control data set of regional coastal sediment processes for evaluation of the localized sedimentation response to the jetties.

The second element focuses in on the area immediately adjacent to the entrance channel extending approximately 1,219 m (4,000 ft) to the north and to the south. This closeup evaluation more readily identifies localized volumetric changes and shoaling/scour patterns that may be associated with sedimentation processes induced by the jetty extensions and spurs as opposed to coastal processes responding primarily to climatic events. For the basis of this analysis, the surveys were grouped as follows: Pre-construction, May 1981 - March 1985; Construction, September 1985 - September 1987; Post-construction, March 1988 - September 1990.

Data Collection

Data for this study were collected by NPP under the Shoreline Surveillance Program (SSP) (Chesser 1992) beginning in 1981 and entailing semiannual surveys in early spring (April-May) and early fall (September-October) over a

2- to 3-week period through 1990. Thirty-two profiles were established on the north beach and thirty-eight on the south beach. Five additional profiles were added to each side of the jetties in 1987 and more detailed surveys were taken at the jetties for the MCCP study between 1987 and 1990. The profiles are surveyed along established profile lines extending from a baseline behind the foredune and out to about a -5.5-m (-18-ft) to -7.3-m (-24-ft) depth. The profile lines are more closely spaced for approximately the first 914 m (3,000 ft) from the entrance, and then spaced at about 305-m (1,000-ft) intervals. Table 6 lists the numbering system for the profile lines on the north and south beaches. Station numbers indicate distance in feet from the jetties, i.e., Station 1+84 is 56 m (184 ft), Station 83+46 is 2,544 m (8,346 ft), etc. Figure 1 of this report shows the approximate physical location of the profiles. The portion of each profile line above mllw was surveyed using standard survey techniques. The submerged portion below mllw was surveyed using a helicopter technique developed by the Portland District (Craig and Team 1985) and tested for accuracy under this MCCP project. The helicopter system and the accuracy test are documented in Chapter 4 of this report. Twice yearly for 10 years, 70-80 profile lines were surveyed. Each profile line consisted of approximately 100 individual survey points. This resulted in about 7,000 survey points twice yearly for 10 years, or 140,000 data points. Figure 45 is a map of all the fall 1988 data collected. This is the optimum survey pattern for data collection. All other surveys lacked coverage mostly near the end of the jetties.

18 Km (11 Miles) of Shoreline

Original survey data have been processed using two different software systems. The first is ISRP (Interactive Survey Reduction Program). This Corps-developed program allows two-dimensional comparisons of single profile lines for multiple years showing volume changes and shoreline movement between years. Changes in volume above and below mllw were computed for each profile between consecutive surveys and for selected time intervals. All ISRP computations were conducted by the NPP under the SSP. The second software program used is the Contour Plotting System (CPS-3). This software uses all profiles to develop three-dimensional surface sets from which bathymetric maps can be created and volumes calculated. Volume changes generated by each system were then entered into spreadsheets for further graphical comparisons. ISRP data analysis is based on spring (May 1981) to spring (March 1990) surveys, while the CPS-3 data analysis relates fall (September 1981) to fall (September 1990) data. Major climatic events considered are El Niño, from 1982-83, the recovery period of 1-2 years afterward, and slightly above normal wave activity in the winters of 1988 and 1990.

Shoreline surveillance study profile analysis

The first level of analysis is to compare consecutive surveys throughout the 10-year period for both beach and offshore volume changes. The cumulative

Table 6
Numbering System for Profiles

Station No.	North Profile No.	Station No.	South Profile No.
1+84	1	-3+35	3[1]
3+50	3[1]	0+00	0
5+00	5	2+50	2[1]
7+70	7[1]	5+00	5
10+37	10	7+50	7[1]
12+50	12[1]	9+95	9
14+65	14	11+35	11
17+50	17[1]	12+50	12[1]
20+00	20	15+00	15
22+50	22[1]	17+50	17[1]
25+00	25	20+00	20
29+93	29	22+50	22[1]
35+54	35	25+00	25
47+15	47	30+19	30
52+86	52	38+75	38
65+33[2]	65	50+00	50
70+08	70	60+25	60
76+98	76	70+25	70
83+46	83	77+45	77
97+30[2]	97	84+00	84
100+78[2]	100	90+00	90
109+70	109	99+75	99
126+31	126	110+00	110
131+18	131	120+50	120
136+01	136	130+00	130
146+00	146	139+75	139
156+00	156	150+00	150
166+00	166	160+12	160
176+00	176	170+00	170
185+66	185	180+00	180
193+85	193	190+30	190
204+42	204	199+75	199
214+90	214	210+00	210
226+48	226	220+00	220
239+44	239	230+40	230
249+51	249	240+00	240
259+79	259	250+80	250
270+61	270	259+85	259
		270+00	270
		280+00	280
		290+10	290
		299+90	299
		309+10	309
		319+43	319

[1] Added 1987.
[2] Riprap present.

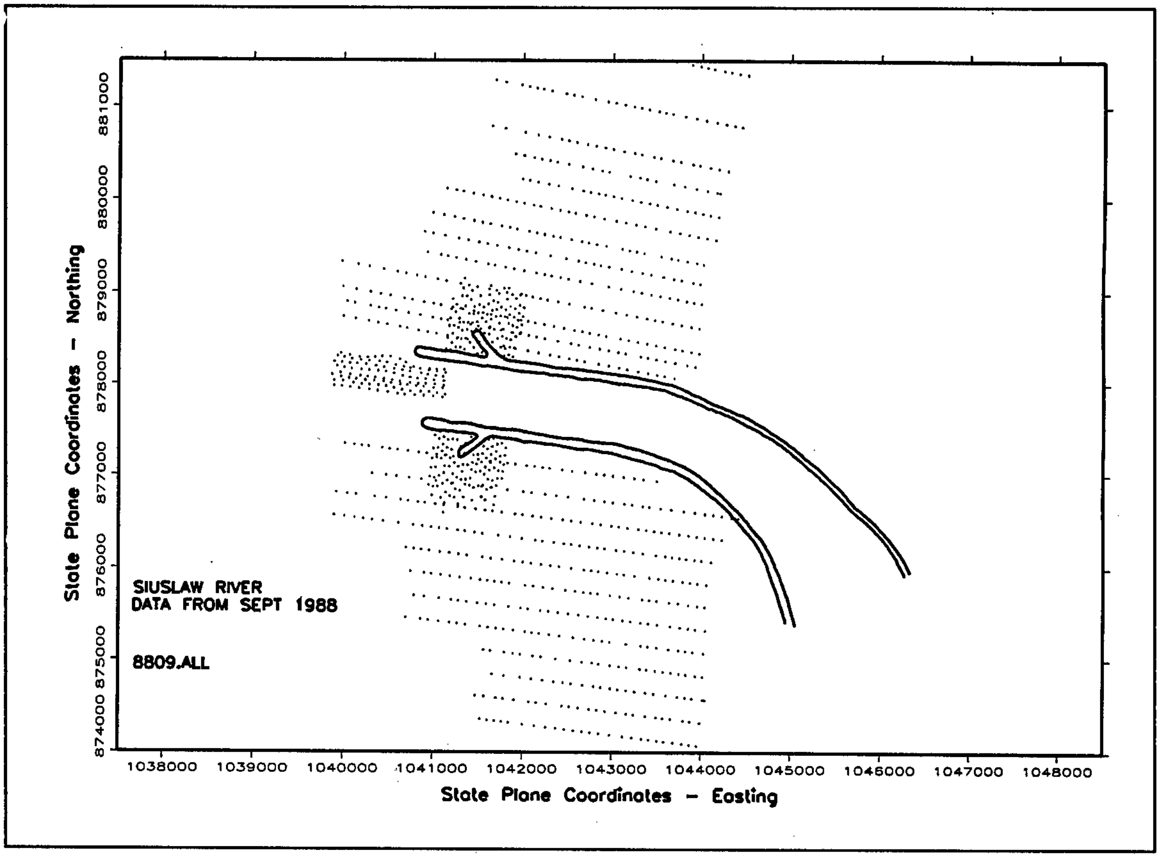

Figure 45. Map of the most complete data coverage, fall 1988

volume change over the entire 10-year period was calculated for each profile. The volume change above mllw between consecutive surveys represents beach changes. The volume change below mllw represents offshore changes. Although changes in beach volume are the most observable changes, volume changes below mllw are important. Material eroded off the beach is carried offshore. If it stays within the depths surveyed, there should be a gain offshore. However, the depth of offshore transport in winter exceeds the survey depths and the volume offshore greatly exceeds the beach volume. This can lead to net loss in both beach volume and offshore volume. Changes were summed over the entire 10-year period. If there are more positive values the result is an overall gain (accretion) and vice versa. Figure 46 was plotted using these sums for all the profiles north of the jetties. The cumulative beach volume change shows that there was much more accretion than erosion, and that most of this accretion took place near the jetties. The offshore pattern is clear, with net accretion to profile 65 followed by net erosion from profile 70 to 270 except for profiles 214 and 226. Figure 47 shows the area south of the jetties. Here the pattern is less consistent, with both the beach and offshore showing significant accretion. Significant offshore erosion occurs between profiles 20 and 50 and beyond profile 199. The cumulative beach volume

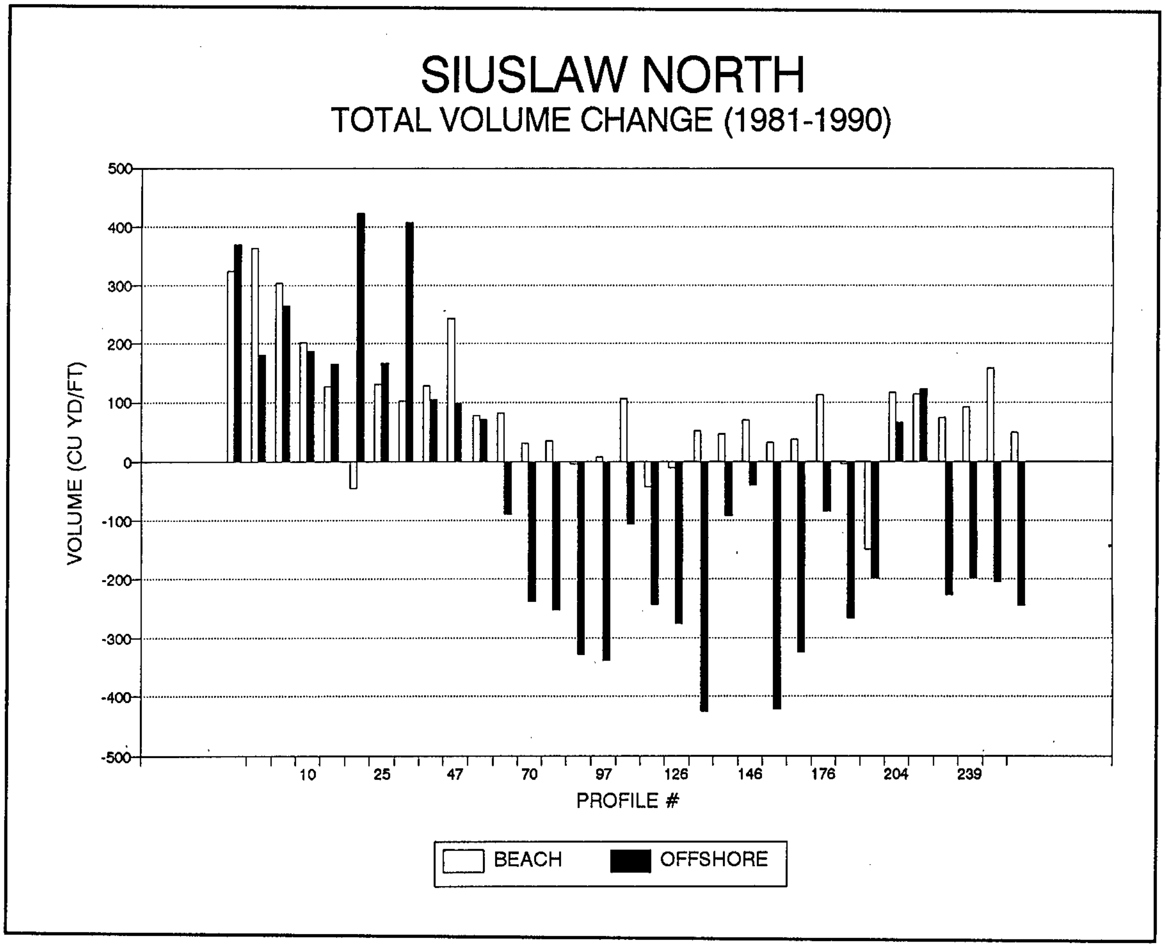

Figure 46. Cumulative volume changes for all profiles, beach and offshore, north of jetties

change south of the jetties is overwhelmingly positive, with only one or two minimal instances of erosion.

To complete the analysis of beach and offshore changes, Figure 48 shows the total cumulative change. This combines the volumes for both above mllw and below mllw between consecutive survey dates. On the north there was both a large net gain in volume and a large loss. The area of gain extends 2,134 m (7,000 ft) north while the next 4,267 m (14,000 ft) shows a net loss. On the south there is an area of gain for 610 m (2,000 ft) north from the jetty followed by a loss of 1,219 m (4,000 ft). Between 1,829 m and 6,400 m (6,000 and 21,000 ft) is the area of largest net gain to the south. Beyond 6,400 m (21,000 ft) on both the north and south, the patterns of loss and gain are less pronounced.

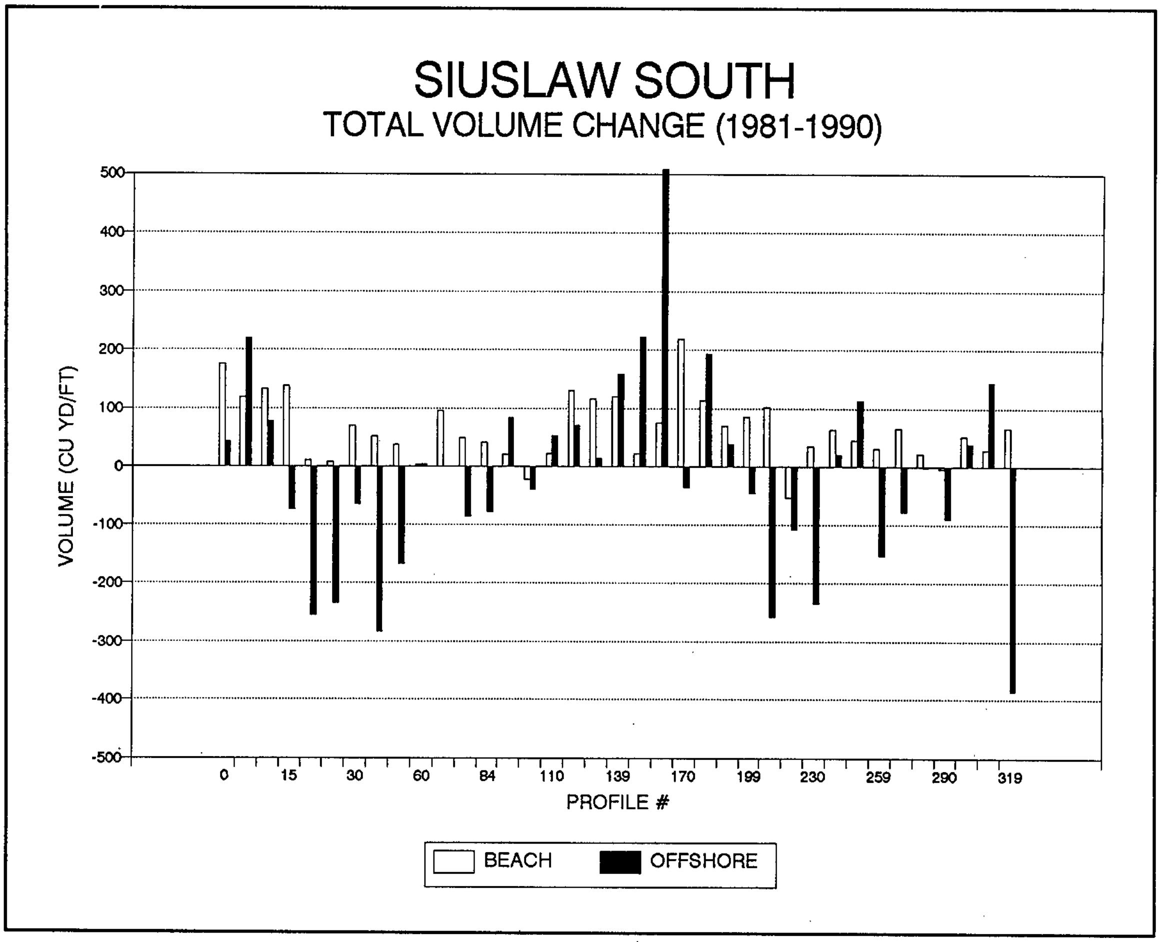

Figure 47. Cumulative volume changes for all profiles, beach and offshore, south of jetties

Beach changes for selected periods

The initial purpose of this study was to account for changes after jetty extension. However, in the third year of monitoring prior to construction, an oceanographic event of global significance occurred. This was the El Niño-Southern Oscillation (El Niño) event of 1982-1983 which resulted in catastrophic storms along the entire west coast with widespread beach erosion (Komar 1986). Jetty construction began 1 year after this event in spring 1984 and was completed over 1 year later in February 1986. Since completion of the jetty extensions, there have been no other events as significant as El Niño.

In order to account for El Niño, the spring 1981 survey was compared to the spring 1983 survey to determine the magnitude of the effect. Then the spring 1983 survey was compared to the spring 1985 survey to evaluate the post-El Niño period. Finally, the spring 1986 survey was compared to the spring 1990 survey to relate how the beach responded after jetty extension was complete.

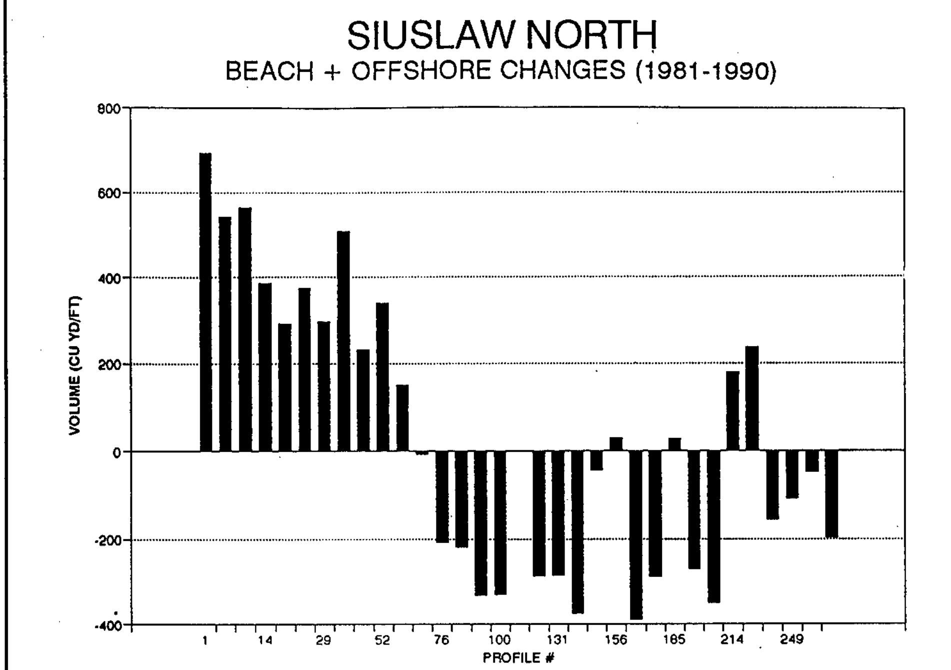

a. North cumulative changes

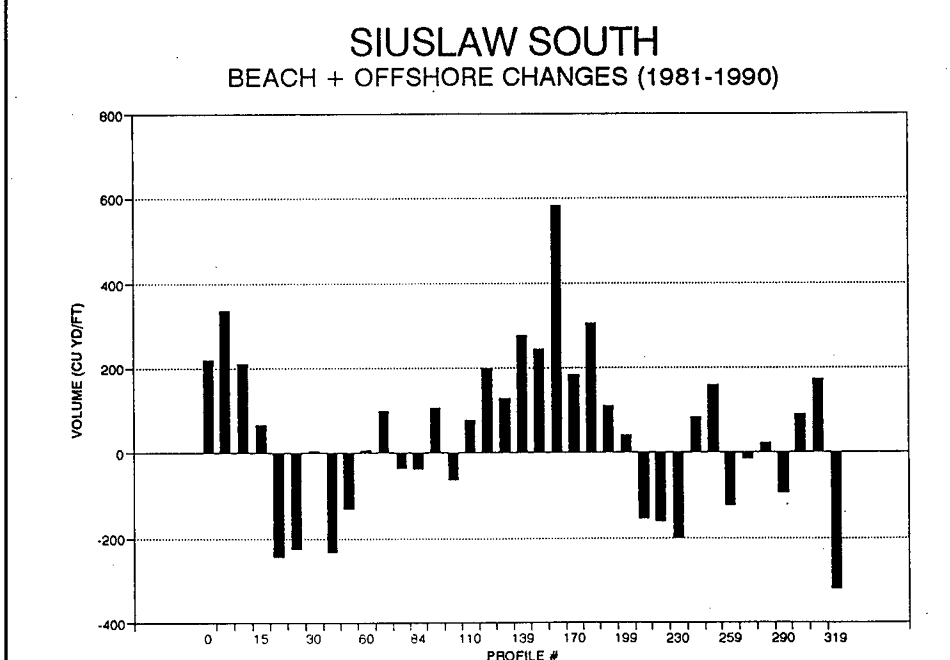

b. South cumulative changes

Figure 48. Total cumulative change combining beach and offshore

Figure 49 illustrates this detailed analysis for the selected time periods. The 1981-1983 period for the north beach shows the erosive effects of the El Niño storms with erosion throughout the area. The period 1983-1985 was a recovery period of mostly accretion. The post-construction period of 1986-1990 shows substantial accretion within about 2,134 m (7,000 ft) of the jetties with one area of severe erosion about 3,840 m (12,600 ft) north of the jetties. The second series for the south beach is similar to the north beach, showing erosion for 1981-1983, recovery for 1983-1985, and both substantial accretion near the jetties and overall accretion for 1986-1990. This confirms the influence of the large-scale erosion event (El Niño) and the subsequent recovery.

Seasonal beach changes

The previous analysis shows the magnitude of an extraordinary erosion event and normal recovery. However, on the Oregon Coast there is a normal cycle of winter beach erosion followed by summer beach accretion. In the previous figures, the spring surveys were compared for periods 2 or more years apart. In order to explore seasonal beach changes, the following figures compare volume changes between consecutive surveys for individual profile lines 2,134 m (7,000 ft) to either side of the jetties.

In Figure 50 for the north beach, the seasonal pattern seems to begin normally with accretion following erosion until initial jetty construction the summer of 1984. The following winter shows mostly accretion. Normal erosion occurs the winter of 1985-86, but subsequent winters show minor erosion until 1989-1990. By summer 1989, the normal cycle seems to be present again. There is more overall accretion from 1986-1989. Also, the magnitude of change is larger for the north beach than for the south. There appears to be a clear effect of jetty extension on the seasonal cycle within 2,134 m (7,000 ft) north of the jetties for several years following extension and then seasonal equilibrium returns in 1989.

In Figure 51 for the south beach, there is overall accretion from spring 1981 to fall 1981 (summer) followed by overall erosion from fall 1981 to spring 1982 (winter), as expected. This pattern repeats with only minor perturbations throughout the 10-year record. The south beach clearly illustrates the normal erosion/accretion cycle with minor exceptions from the summer of 1981 to the summer of 1990. There is little apparent effect of the El Niño event; however, the magnitude of seasonal changes appears to increase following jetty extension for several years.

Jetty effects

Komar (1975) analyzed the historic shoreline changes following initial jetty construction and predicted future changes resulting from jetty extension. His predictive model used a very simple wave energy littoral transport equation

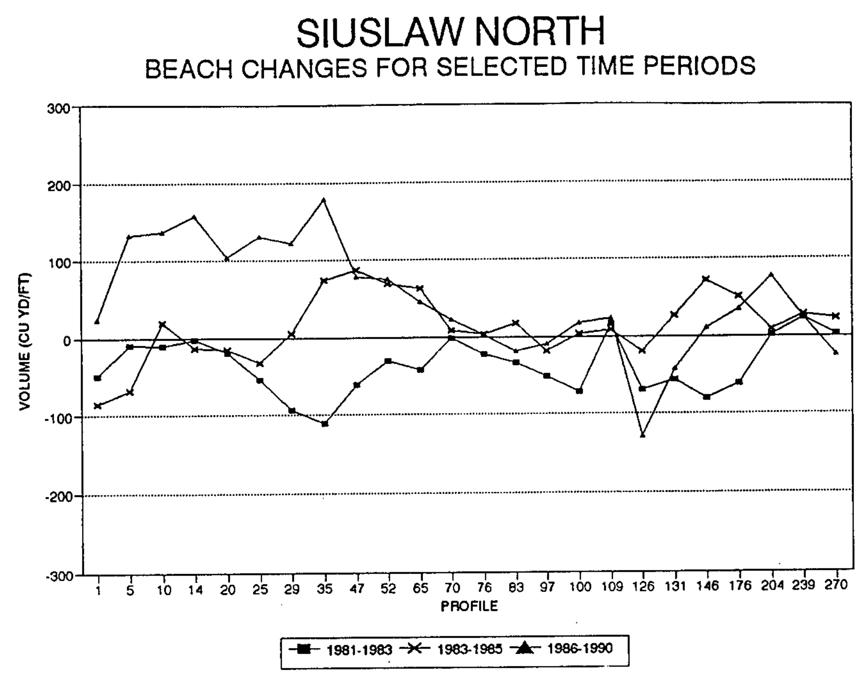

a. Beach volume change north

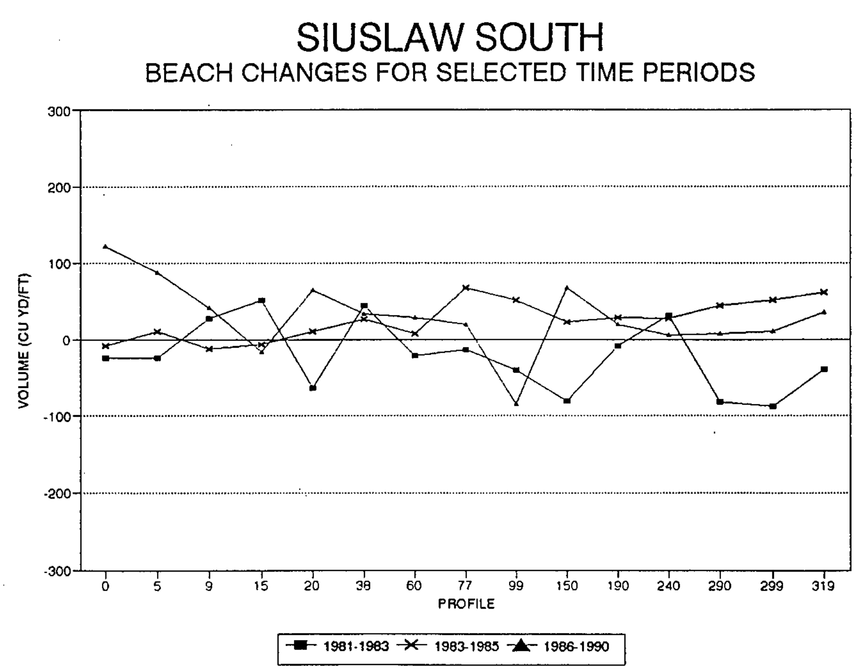

b. Beach volume change south

Figure 49. Beach volume change for selected time periods

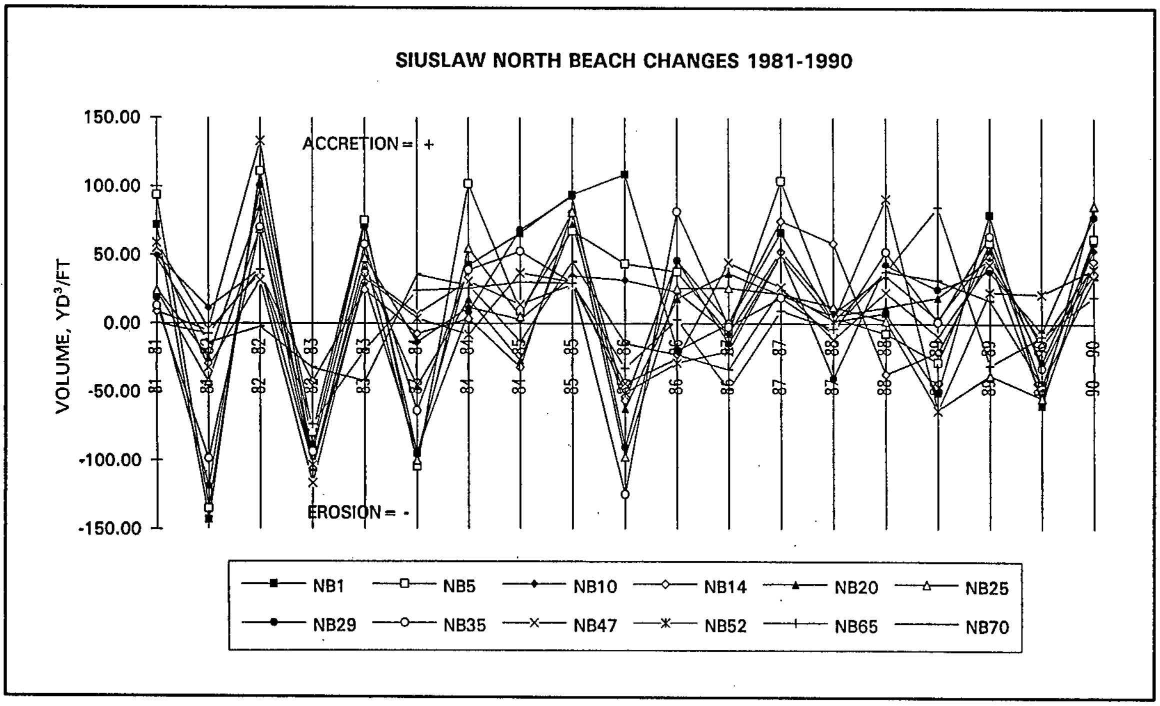

Figure 50. Seasonal beach volume fluctuations for the north

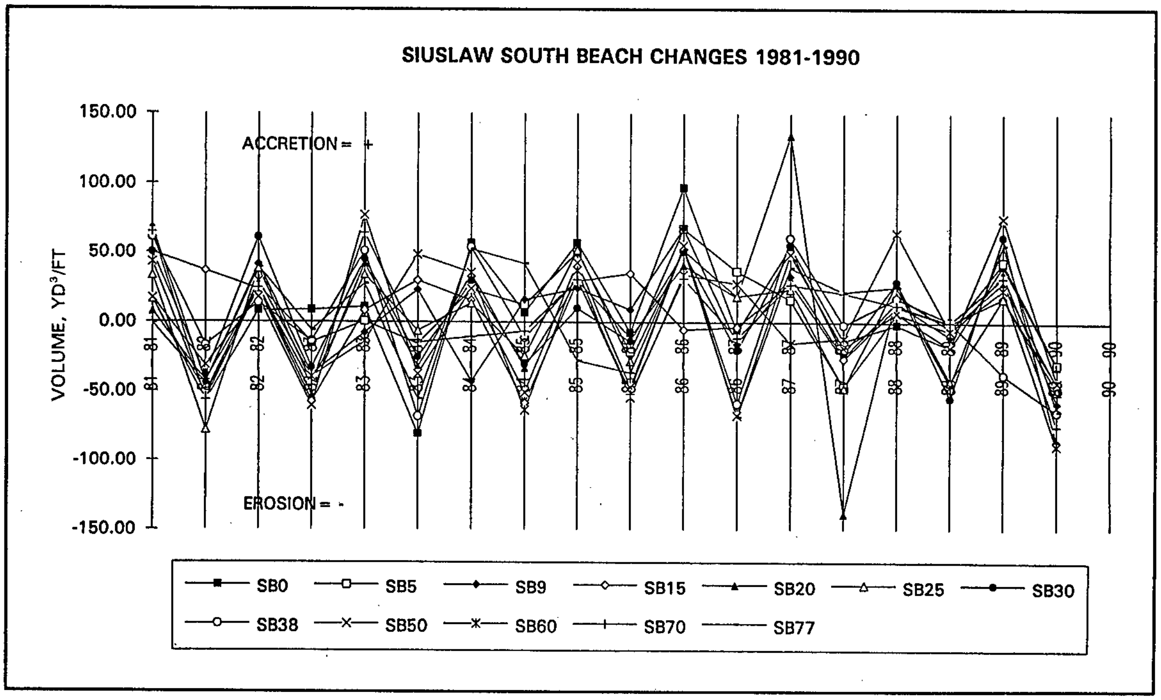

Figure 51. Seasonal beach volume fluctuations for the south

and an equilibrium shoreline concept. This model agreed reasonably well with historic shoreline changes following initial jetty construction, showing erosion distant from the jetties supplying sand for the shoreline advance near the jetties. For future changes from jetty extension, he analyzed the changes in alongshore waves due to sheltering effects of the jetties. Figure 52 shows this wave height variation with the magnitude decreasing to zero some distance from the jetty. This distance is a function of both wave height and jetty length. The area beyond the zero or null point may erode to supply the material which accretes near the jetty. One effect of the extension would be generation of an alongshore current flowing towards the jetty, then turning seaward as a rip current. This was seen in the physical model study (Bottin 1981) and in the current studies conducted for this MCCP study (Pollock 1995).

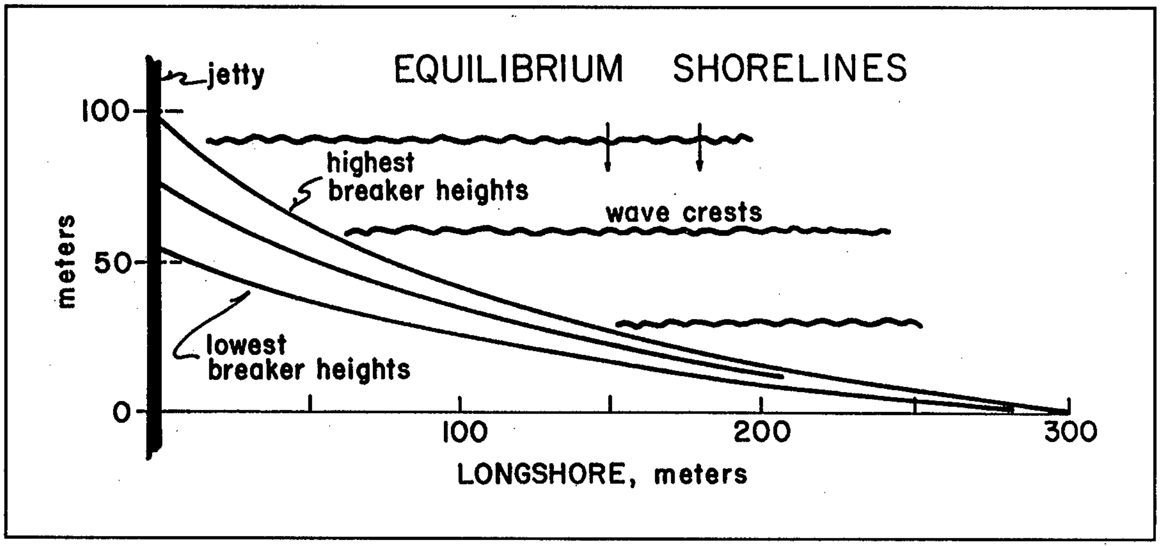

Figure 52. Wave height variation relative to distance from jetties

The shoreline survey analyses seem to fit well with predicted shoreline adjustment. The seasonal analysis, in particular, seems to show the effect of the jetties especially within the first 2,134 m (7,000 ft) north and south. It appears that these effects were minimal after 1988. The fact that the adjustment is more apparent on the north probably reflects a predominance of winter waves from the southwest. In that case the jetties would provide more sheltering effect to the north, minimizing erosion. In addition, if the net littoral sediment transport is to the south there would be more accretion north of the jetties as they impound sediment.

CPS-3

Polygons are used in CPS to delineate the data borders and divide areas for regional comparisons for volume calculations. Figure 53 illustrates the

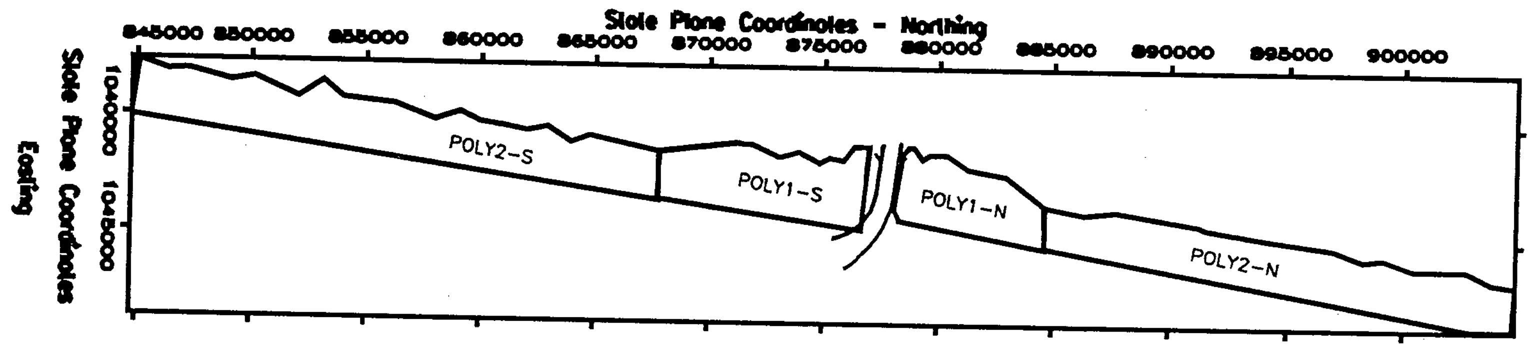

Figure 53. Polygons used in CPS-3 volume calculations

polygons that were used. Beach volumes were calculated between mllw and +2.7 m (+9 ft) in all polygons. These beach volumes for south of the jetties corroborate the seasonal pattern identified under the SSP. The north volumes, also in agreement with SSP results, vary from seasonal equilibriums due to El Niño and jetty construction. Poly2-N appears to recover from the jetty construction in the winter of 1987-88, while poly1-N does not recover until the winter of 1988-89.

Offshore volumes were calculated below mllw. Figure 54 displays offshore volumes for each survey. The first notable event is the occurrence of El Niño in 1982-83. Offshore volumes for the north and the south both experienced a large amount of erosion at this time. This time frame was to be the data control set for jetty construction but has been tainted by the El Niño event. Also evident from the figure is the influence of the jetty construction and subsequent recovery from March of 1985 to March of 1987. The seasonal pattern is interrupted at this time and offshore volumes experience their most substantial erosion. After the recovery from this great loss, seasonal patterns begin to resume. The extreme loss in south poly1-S in 1990 may be attributed to increased wave activity at that time and a dominant winter southern swell. The combination of the offshore and beach surveys deviates from the seasonal erosion/accretion pattern due to the fact that the magnitude of the offshore volumes is much greater than that of the beach and therefore the combination will parallel offshore responses. It must also be considered that the 10 km (6 miles) south of the jetties is only a fraction of the entire 42-km (26-mile) littoral cell responsible for sediment movement. The northern 8 km (5 miles) comprise a complete littoral cell. Additionally, the surveys do not extend to a depth of closure for the area, and the winter bar/trough system moves on and offshore across the seaward survey boundary.

Conclusion

Shoreline changes can be divided into three distinct time periods. The 1981-1983 surveys depict the most significant erosion, and can be related to the El Niño winter storms of 1982-1983. The period 1983-1985 was a time of recovery with a net accretion for the area. The post-construction surveys, 1986-1990, show substantial accretion, most occurring near the jetties. For the entire study period, there was overall accretion in the area, most developing north of the jetties. The most significant area of beach accretion was within the first 2,134 m (7,000 ft) north of the jetties and for 457 m (1500 ft) south. Although there appear to have been beach changes due to jetty extension, the long-term effects were harmless.

Offshore volumes can also be grouped into distinct time periods. There was significant offshore erosion as a result of El Niño (1982-1983) and jetty construction (1985-1986). The recovery period following each event is responsible for most of the accretion that occurred. Seasonal equilibrium seems to have stabilized and returned by 1990 throughout the study area. The entire

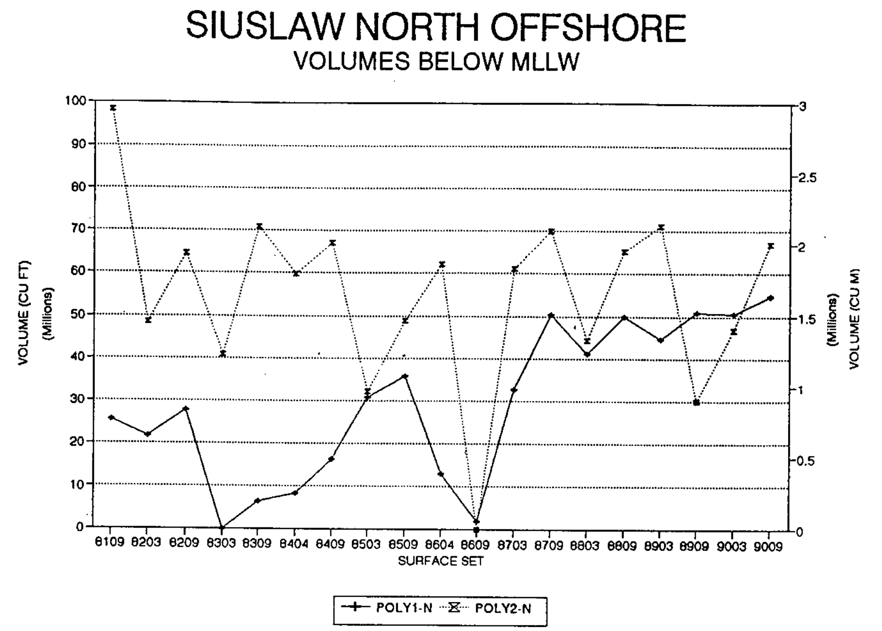

a. Offshore volumes for the north

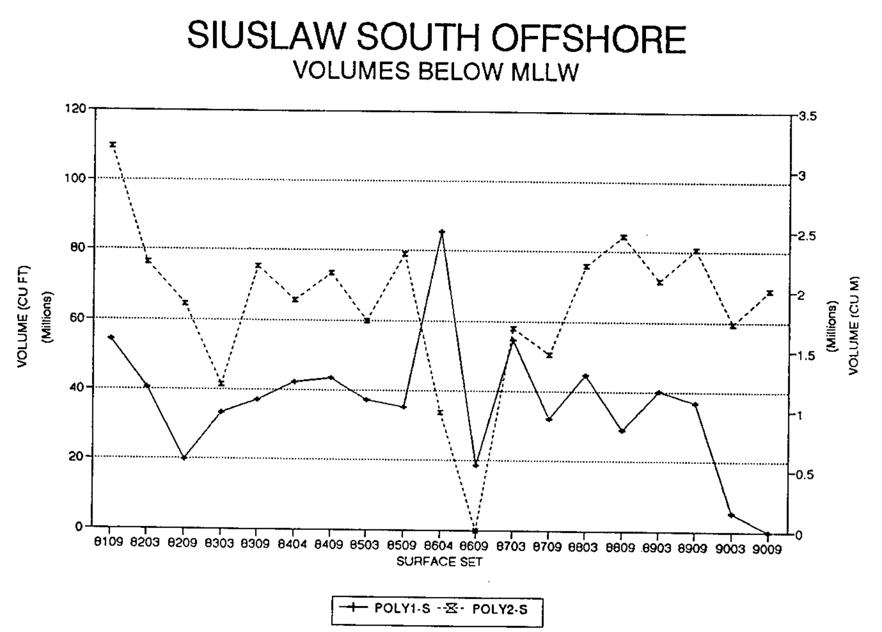

b. Offshore volumes for the south

Figure 54. Offshore volumes for each survey

system appears to have readjusted to a new balance relative to the extended jetties; however, continued accretion may occur immediately adjacent to the jetties.

Localized Region Surrounding the Entrance Channel

The following interpretations are based on CPS-3 generated contour and difference maps for the localized region within 1,219 m (4,000 ft) north and south of the jetties. These maps were created using the most complete data coverage possible. This includes all data shown in Figure 45. The contour maps used in this analysis may be found in Appendix B.

Contour adjustment to jetty extension (3D)

The presence of a longshore bar system at the end of the 1960 jetties was one of the reasons for the 1985 extensions. This bar caused navigation problems; therefore, the channel needed to be repeatedly dredged. The bar usually occurred at depths between -2.7 m and -3.7 m(-9 and -12 ft). After the jetty extensions were completed, the bar system was interrupted, and navigation in the channel improved immensely. Inspection of Appendices A and B shows the presence of this bar in the channel prior to jetty extension and the response by the bar and offshore contours as they adjusted to the jetty extensions. The jetty extensions impaired development of the longshore bar system in the channel, shifting its crest offshore and reducing its crest relief. On successive surveys it is also apparent that the deeper water contours are curving offshore similar to a delta or headland in response to the jetty extension. This contour metamorphosis is most likely a result of the new current and wave patterns induced by the jetty extensions and spurs. The contour lines for these maps likely connect north to south, with some fluctuation at the channel, but due to deficiencies in data coverage, the computer-generated contours shown on the map often do not.

Shoreline change

Seasonal beach changes are also apparent on these maps. The pattern of erosion in the winter and accretion in the summer is most easily recognized by the position of the shoreline on the maps and the volumetric evaluation of the above mllw region. Figure 55 represents the shoreline position for pre-construction, construction, and post-construction for all surveys. From the figure it is seen that the jetty extensions allowed the shoreline to advance seaward immediately adjacent to the jetty as fillets are being built. Further from the jetties, the shoreline position did not undergo a large migration. This process is more pronounced on the north than on the south. These observations closely parallel predictions made by Komar (1975) and in the physical

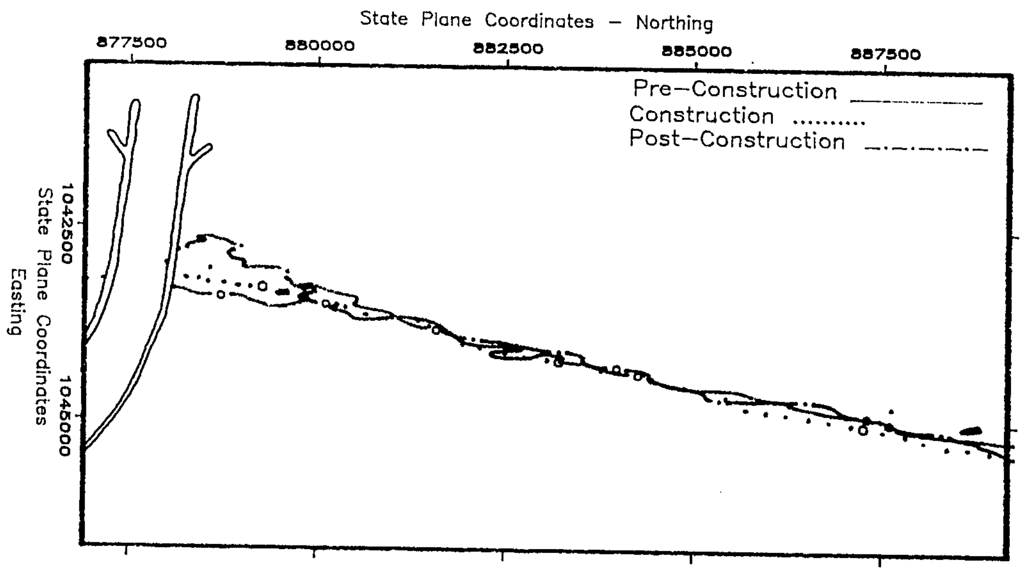

a. North shoreline positions

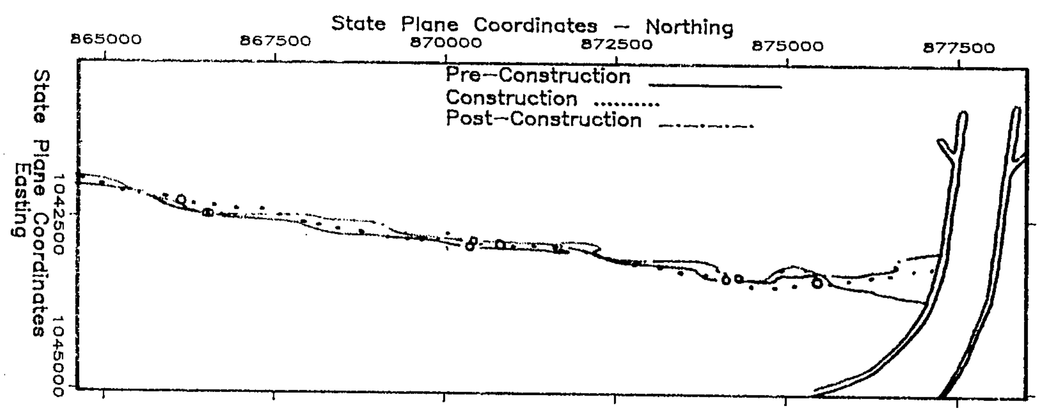

b. South shoreline positions

Figure 55. Typical shoreline position for each time period

model studies (Bottin 1981, 1983). Pollock (1995) suggests that an equilibrium distance between shoreline and spur location may fluctuate relative to the magnitude of the longshore current and may eventually control fillet building.

Scouring and shoaling

Consistent throughout the pre-construction (September 1981 - April 1984) spring surveys is a scour associated with the north jetty. This scour usually occurs off the jetty terminal point and sometimes extends into the channel. The depth to which this scour typically extends is -10 m (-33 ft). The pre-construction fall surveys are devoid of scours except for the fall of 1983 when the scour apparently persisted throughout the year. This scour reached an approximate depth of -9.1 m (-30 ft). The only consistent shoaling during the pre-construction period is associated with the longshore bar or the entrance channel mouth. Shoaling in the channel was addressed in Chapter 5.

The same pattern of scours during spring surveys also exists for the construction period (September 1984 - April 1986). Scouring in 1984-85 is invariably associated with the north jetty while scouring in 1986 takes place off the south jetty. As the spurs and jetty extensions were introduced into the system, troughs began to form along the seaward side of the spurs, especially on the north side. The trough is often undistinguishable in the bathymetric maps due to lack of dense data inshore of the spurs. The trough still remains, but the profile spacing is too large for the contouring program to identify it. These troughs parallel the current patterns around the spurs identified in Chapter 3, and rip currents predicted by Komar (1975) and Bottin (1981, 1983) are well-defined and usually can be seen when standing on the jetties. Figures 56 and 57 illustrate the generalized location of the scour, shoal, and trough, and superimposed current patterns as a result of the jetty/spur configuration.

No well-defined scour trend off the jetty terminal points is obvious for the post-construction (September 1986 - September 1990) surveys. The largest scour occurs in September 1986 offshore of the south jetty terminal point. It appears large enough to cause foundation problems, and in fact, slumping of the head stones on the south jetty has occurred. Data for this survey were checked to ensure that the scour was not just a function of interpolation by the contouring program and several data points do define this scour hole. Also apparent during this time is the continued evolution of the trough adjacent to the seaward side of the jetty trunk and spur. Additionally a shoal develops as a result of the current and depositional patterns created by the spurs. The headland also continues to form but is somewhat hidden by the data limitations mentioned previously. Sediment being trapped in the spur "v" is also inferred by the data, although weak data coverage does not allow for definite confirmation.

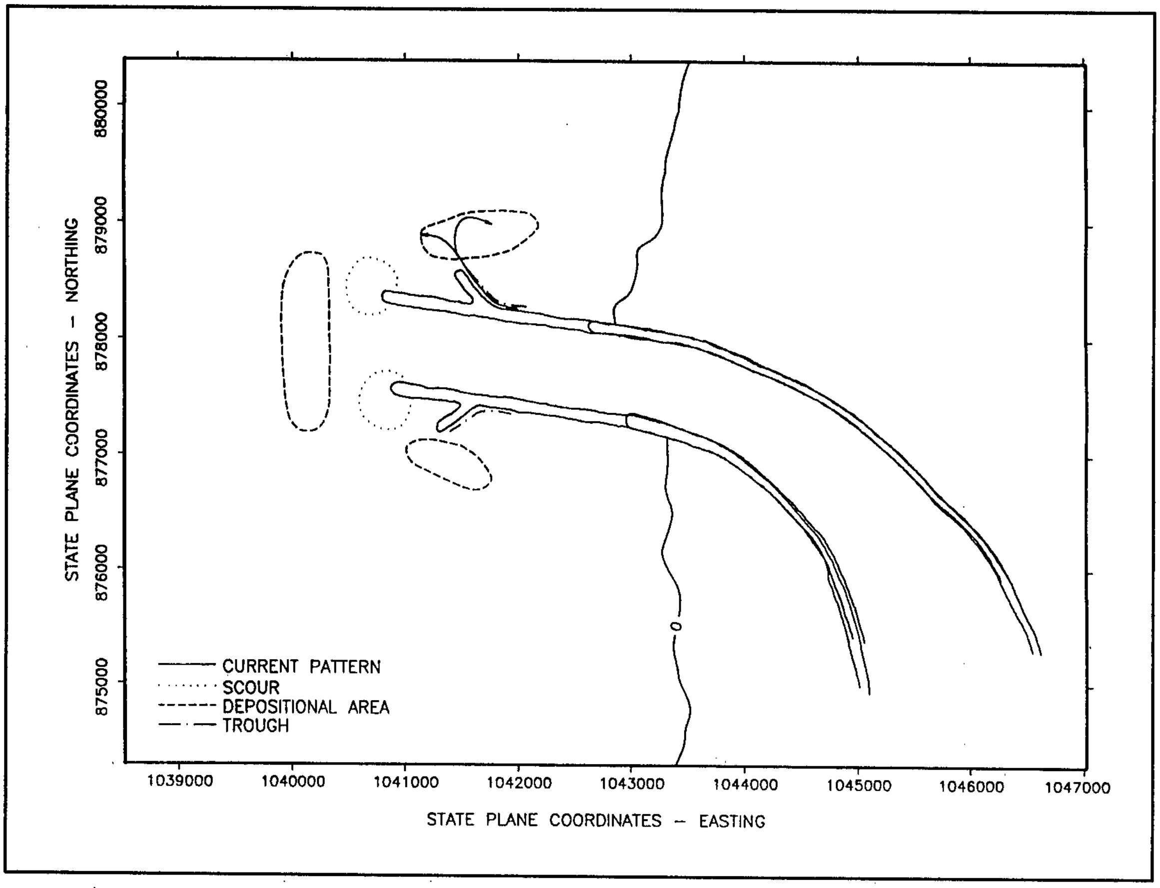

Figure 56. Splitting current pattern superimposed over shoal, scour, and trough general locations

Correlation of current and sediment depositional patterns

As the current pattern follows the spurs, it carries sediment and once the current leaves the confined flow of the spur, the velocity decreases and the sediment is deposited. The sediment may also be deflected back toward shore where it is reintroduced into the littoral zone by wave action or is deposited in a depositional region adjacent to the spur tips. The currents may also carry the sediment in a straight, parallel path away from the spur where it meets the longshore current and is turned to flow down the coast and around the jetty tips. These current patterns are associated with intensity of the longshore current. Figures 56 and 57 illustrated these current patterns superimposed over general depositional and scouring patterns for the post-construction period. These illustrations are for a north to south longshore current. The mirror image occurs for the reverse, though less pronounced, possibly due to the dominant longshore flow direction from the north or the slightly more acute angular orientation of the jetties toward the north. Figure 56 shows the current patterns for the lesser magnitude currents and a somewhat oval-shaped depositional area likely resulting from the splitting current reduction in velocity and

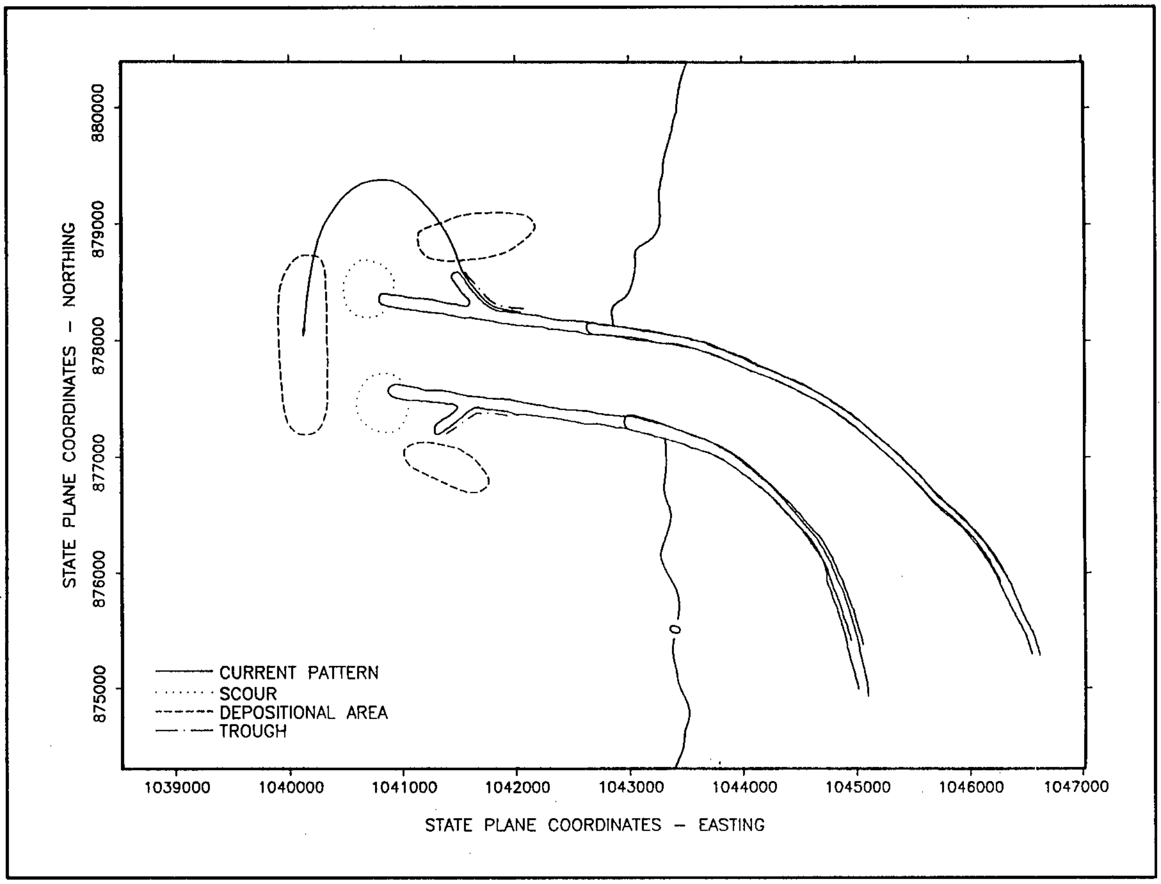

Figure 57. Stronger magnitude current pattern superimposed over shoal, scour, and trough general locations

depositing sediment. This depositional area is also apparent when observing wave breaking patterns in this locality. Figure 57 shows the current pattern for the stronger magnitude current superimposed over the contours that develop seaward of the jetty extensions. Bathymetric contour patterns closely parallel interpreted current patterns. Additionally, Chapter 5 of this report identified a trough or scour area immediately seaward of the jetty tips and slightly more seaward, a bar or shoal region. In the currents portion of this MCCP study (Pollock 1995), aerial photos associated with this current pattern show clear water flowing past the ends of the jetty terminal points and the path of the sediment plume located as the current interpretation path indicated directly over the greater elevation contours or bar.

Volumetric analysis

Figure 58 depicts the polygons that were used to calculate volumes in CPS-3. These volumes were calculated as beach (above mllw to +9) and offshore (below mllw). Figure 59a illustrates the seasonal beach fluctuations that occur near the jetties. Figure 59b is the offshore volumes. The pattern

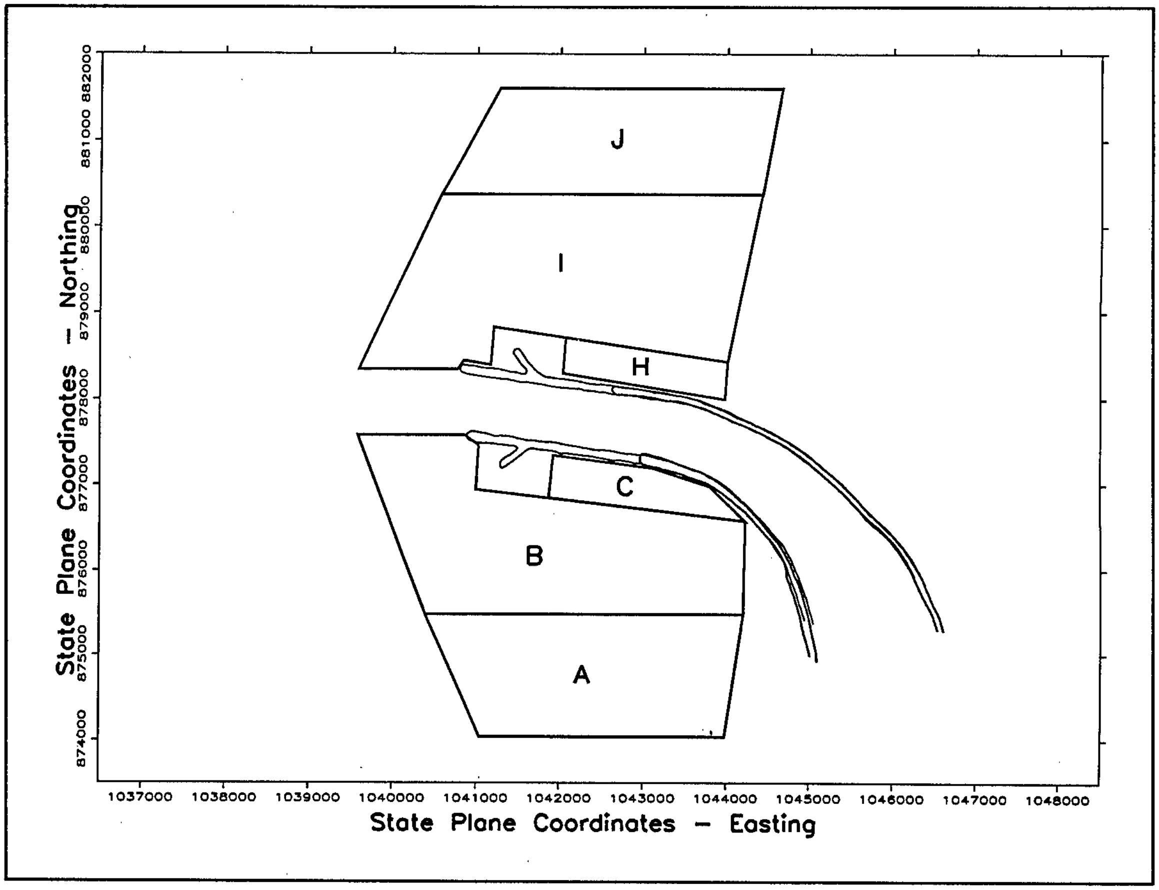

Figure 58. Polygons used to calculate volumes in CPS-3

for this figure is very inconsistent and therefore, no conclusions were made based on this analysis.

Conclusion

The navigation problem caused by the longshore bar in the channel seems to have been corrected by the 1985 jetty extension. The bar formation is interrupted and develops to a lesser elevation in deeper water. Also apparent is the offshore migration of the shoreline immediately adjacent to the jetty trunks as sand fillets are built. This process has advanced more rapidly on the north side of the jetties than on the south. Although there appear to have been beach changes due to jetty extensions, the long-term effects were harmless. Scour holes occur predominantly during the spring surveys (following winter storms and other erosional events) and are routinely positioned just offshore of the jetty terminal points. The scour holes associated with the terminal points are much more evident in the pre-construction period than in the post-construction. The jetty extension has also altered the longshore contours to more closely resemble a delta or headland.

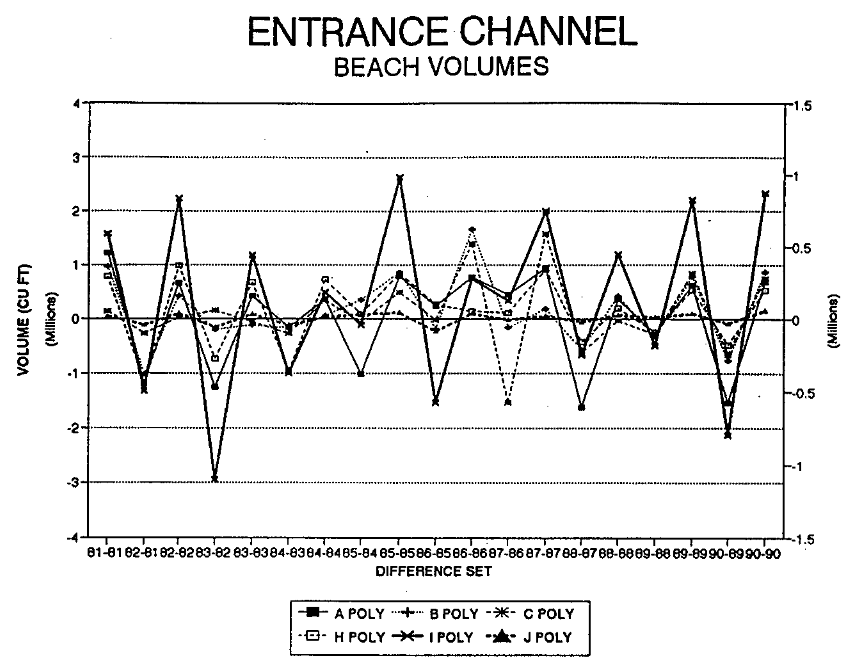

a. North seasonal fluctuations

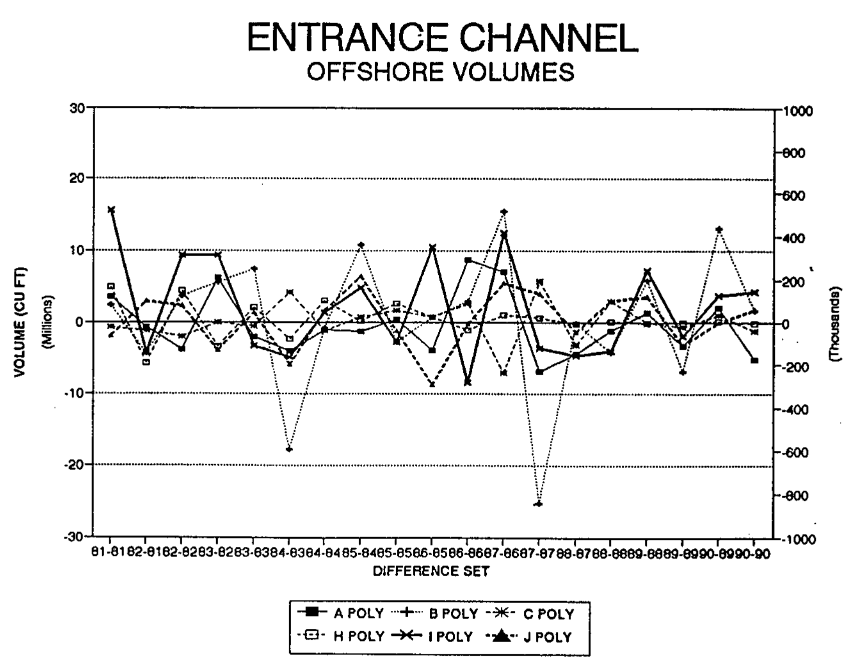

b. South seasonal fluctuations

Figure 59. Seasonal volume fluctuations for beach and offshore

Correlations are made between the spur-induced current circulation patterns identified in Pollock (1995) and sediment shoaling patterns evolving in the post-construction period. The jetty trunk and spur define a rip current that results in a trough adjacent to their seaward side. Once the current passes the tip of the spur, the intensity of the flow defines the path the current takes and the resulting depositional pattern of the sediment it carries. The deflection of sediment caused by the spurs has introduced new shoaling patterns directly off the spur tips and may be responsible for the contour shape evolution seaward of the channel entrance. Building of the shoreline fillet adjacent to the jetty trunks may reach equilibrium, fluctuating relative to longshore current magnitude.

7 Summary and Conclusions

Summary

Siuslaw River, OR, 1985 Jetty Improvements

To improve navigability of the entrance channel to Siuslaw River, OR, design plans originally called for lengthy extension of the twin parallel jetties to a depth of -9.1 m (-30 ft) mllw, requiring extensions of 609.9 m, (2,000 ft) and 762 m (2,500 ft) for the north and south jetties, respectively. As a cost-reducing alternative, shorter extension to a depth of -8 m (-25 ft) and the addition of spur jetties on the seaward side were investigated (Bottin 1981, 1983) and construction between 1984 and January of 1986. Actual construction depth of the terminal end of the jetties was approximately -7 m (-22 ft).

The innovative concept of the spur jetties arose as a result of physical model studies conducted at CERC for the Rogue River project on the southern Oregon coast (Bottin 1983). Model results with spur jetties indicated that sediment in the nearshore zone moved toward the jetties and into an eddy which tended to deflect material away from the structure. Sediment would flow back toward shore where it is either reintroduced into the littoral transport system or carried by a jet of water away from the jetty parallel to the spur. Under certain conditions, some material was carried around the end of the spurs and into the "V" formed by the spurs and the jetty trunk, and some material continued around the jetty head and into the entrance. Qualitative evaluations of the Siuslaw River jetty extensions were made using the Rogue River physical model (Bottin 1983). Overall, the model study indicated the spurs would alter the circulation pattern and potentially cause significant reduction of sediment shoaling in the navigation channel.

Monitoring completed coastal projects (MCCP) study

The jetty system was monitored and evaluated through the MCCP Program by CERC in coordination with NPP, which already had underway a shoreline surveillance program to evaluate impacts of the jetty extensions on the adjacent shoreline. Data collected during field monitoring of the area are related to incident wave conditions and analyzed to evaluate structure performance. The favorable results of this MCCP study substantiate physical model test findings and indicate potential application of spur jetties at other sites.

MCCP study objectives. Objectives of the study were to determine if the spurs effectively deflect sediment; to identify shoaling patterns near the jetties; to compare existing prototype conditions to those predicted by the physical model study; to evaluate the effectiveness of the system in reducing the requirements for maintenance dredging; and to evaluate the impact of the jetties on the surrounding beaches. The last objective is chiefly addressed in a companion study, "Siuslaw Shoreline Surveillance 1981-1990" conducted by NPP (Chesser 1992). Because the two improvements were constructed in unison, it is difficult to attribute responses singularly to either the spurs or the extension. Therefore, changes are generally viewed as response to the jetty improvements.

Prototype monitoring. Monitoring has included waves, currents, and bathymetric changes. In general, data collected prior to 1984 (start of 1985 jetty improvement construction) are considered a control set used for relative comparison of post-construction changes and coastal process response to the 1985 jetty improvements. Data collected between 1984 and varying from 1986 to 1987 are considered to be a transitional/recovery or construction period where responses are treated as transitional. The final years of the study (1987-1990), post-construction, are evaluated and related to pre-construction conditions. Major factors affecting the pre-, transitional, and post-construction data sets were:

1982-83	El Niño climatic event resulting in major coastal erosion
1984-85	1985 jetty construction completed February 1, 1986
1986-87	Recovery from construction and coastal process adjustment to new jetty configuration
1988 and 1990	Winter storm waves slightly higher than normal

Beginning in 1981 and ending in 1990 on a biyearly basis, NPP has collected beach profiles adjacent to the jetties using a helicopter-supported lead line system that allowed collection of a continuous transect across the beach through the surf zone and into deep water. In addition, bathymetry soundings have been taken in the navigation channel. After the construction of the jetty extensions, since September 1986, bathymetry measurements in a close grid have been taken around the spurs. These data are investigated to estimate annual dredging requirements and to identify shoaling patterns within the channel and exterior to the channel, as well as to evaluate the impacts of the jetty system improvements on the surrounding beaches (Chapter 5). An accuracy test of the helicopter bathymetry measurement technique, in use since 1960 along the north Pacific coast, was conducted as part of this MCCP study (Chapter 4).

To evaluate incident wave activity at Siuslaw River, a wave gauge was deployed offshore of the entrance for approximately 1 year, and the measurements correlated with other longer-term sources of data. Under the Coastal Field Data Collection Program, wave information was collected from a Wave Rider buoy located offshore of the Coquille River approximately 97 km (60.3 miles) south of the Siuslaw River in 10 m (32.8 ft) of water. This document compares wave elevation and period at the Coquille buoy to those at the buoy located directly offshore of the Siuslaw River entrance. Measured differences were found to be within the uncertainty of the individual measurements, and therefore wave climatology at both locations can be considered equivalent (Chapter 2). Data from the Coquille buoy are related to current and shoaling patterns near the Siuslaw River jetties to evaluate system response.

Bottom trailing drogues, dye studies, and aerial photographs were conducted to define current patterns in the area, but these efforts were not adequate to delineate bottom currents. The drogues only provided release and recovery locations and were relatively inconclusive for identifying any circulation patterns except direction of littoral transport. The dye studies and aerial photos exhibited the circulation patterns of the surface currents but did not establish that the bottom currents were similar to the surface currents in this dynamic area, which included the breaker zone and regions seaward of the breaker zone. To address this short-coming, a helicopter current measurement system was developed and employed on two separate occasions to measure bottom currents and to establish bottom current patterns in the area. Localized current patterns induced by the spur jetties were identified and related to longshore current strengths and correlated with physical model studies instrumental in the design of the jetty structures (Chapter 3).

Study contributions to coastal engineering

In addition to meeting the objectives of this study to evaluate the Siuslaw River spur jetties, four significant contributions were made by this study to aid in coastal engineering investigations.

Chapter 2 provides evidence that adjacent wave gauges, located in similar environments, can be correlated, thus allowing the long-term wave records from one location to be applicable to the adjacent site.

Chapter 4 documents field study tests at Duck, NC, verifying the accuracy and efficiency of a helicopter-borne bathymetric sampling system developed and used by NPP to not only survey hazardous offshore, surf zone, and dry beach topography in one transect, but also to survey profiles over rubble-mound structures.

Report 2 (Pollock (1995)) of this MCCP series (summarized in Chapter 3 of this report) documents the development and use of the Airborne Coastal Current Measurement system. The system proved to be an effective method for obtaining qualitative spatial understanding of bottom currents in hostile environments where boat operation is dangerous or where quick mobility is necessary.

The equilibrium shoreline response predicted by Komar (1975) and discussed by Pollock (1995) was verified by observation. This provides a valuable predictive tool for future jetty design.

Conclusions

Overall, the 1985 jetty improvements are a success, both in terms of the MCCP objectives and the NPP navigation program. Navigability has been improved, construction cost of the spur system was estimated to be approximately $5 million less than the original design cost estimate for jetty extension (Chapter 1), and annual maintenance dredging requirements have been reduced to approximately 100,000 cu yd (Chapter 5).

The results of this MCCP study provide strong support for the effectiveness of the spur jetties at this site and their potential use at futures sites. Design guidance for spur jetties is being investigated under the Coastal Engineering Research and Development Program.

Navigational improvements are supported by survey analysis of shoaling and sediment volume accumulation in the channel and by inspection of bathymetric data indicating that the jetty extensions interrupt longshore bar formation in the channel. Accumulation of material has shifted offshore into deeper water, resulting in lower elevations of bar crests and straight parallel contours across the channel, thus reducing wave shoaling, diffraction and refraction occurring within the channel, which may impair vessel navigation. Conversations with the local U.S. Coast Guard indicate that previous to the 1985 jetty improvements, the channel could only be passed in the summer months at high tide and fishing operations had to be moved to other harbors in the winter months. After the 1985 jetty improvements, vessels are able to pass the entrance year round, barring storm events, and are not confined solely to periods of high tide.

The jetty spurs were found to effectively deflect sediment away from the structure. Sediment either circulates back toward shore where it is reintroduced into the littoral transport system or is carried by a jet of water offshore away from the jetty parallel to the spur, rejoining the longshore transport and bypassing the jetty tips. Evidence of these spur-induced circulation patterns was seen in the current evaluation portion of this study (Chapter 3 and Pollock (1995)) as well as in the sediment depositional patterns identified through inspection of bathymetric contour maps of the local region immediately adjacent to and surrounding the jetties (Chapter 6). From the current study, circulation patterns can be related to the intensity and direction of the longshore currents. These findings parallel predictions of current flow and sediment depositional patterns (Bottin 1981, 1983; Komar 1975; Chapter 3; Pollock (in preparation)) and verify physical model evaluation for spur jetties

(Bottin 1981, 1983). These current patterns are correlated with sediment depositional patterns evolving in the post-construction years. The deflection of sediment initiated by the spurs has introduced a new shoaling pattern directly off the spur tips and may contribute to the contour shape evolution seaward of the channel entrance.

Seasonal winter erosion and summer accretion are fairly consistent for the beach (above mllw) throughout the study years except for some reversal during the transitional/construction period with recovery lasting until 1987. The subaqueous survey region (below mllw) fluctuates less consistently and may be a result of the bar system moving onshore and offshore across the study's deep-water boundary. Shoreline change north and south of the jetties seems to be most prevalent immediately adjacent to the jetties where fillets have been built. This process is more pronounced to the north. These fillets were predicted by both Komar (1975) and Bottin (1981, 1983). Pollock (in preparation) hypothesized that there may be an optimum distance from shore to spur location fluctuating relative to the strength of the longshore current. It is further hypothesized here that the rip current that develops adjacent to the seaward side of the jetty may seek an equilibrium fillet size and location, thus controlling fillet building in the future. Further study of this issue is necessary. Overall, after equilibrium adjustments to the new jetty configurations have occurred, long-term effects to the shoreline appear to be benign.

Recommendations

Further study of the spur jetties should investigate relationships among wave period and height, water level, and tidal flows, and the distance between shoreline and spur location, length of spur, and distance to jetty tip. The investigation should also evaluate whether tidal flows outside of the jetties affect alongshore current velocities. Also to be considered is whether the direction the current pattern travels past the spur jetty tip is related to the rip current located along the spur ending within or outside the surf zone.

This study verifies the effectiveness of physical models for evaluating spur jetty designs and supports their use in future studies. Incident waves, resultant wave patterns, incident longshore currents, spur-induced current patterns and sediment depositional patterns should all be documented for complete study evaluation. For prototype investigations, data sets need to provide better coverage of the region seaward of the jetties and adjacent to the jetties. Lack of data prevented confirmation of trough development, fillet building, and deep-water contour and volume changes.

References

Birkemeier, W. A., and Mason, C. (1984). "The CRAB: A unique nearshore surveying vehicle," *Journal of Surveying Engineering* 110, 1-7.

Bottin, R. R., Jr. (1981). "Siuslaw River Jetty extension study, Oregon," Letter Report, September 1981, Hydraulics Laboratory, U.S. Army Engineer Waterways Experiment Station, Vicksburg, MS.

__________. (1983). "Design for flood control, wave protection, and prevention of shoaling, Rogue River, Oregon: Hydraulic model investigation," Technical Report HL-82-18, U.S. Army Engineer Waterways Experiment Station, Vicksburg, MS.

Brooks, R. M., and Brandon, W. A. (1995). "Hindcast wave information for the U.S. Atlantic Coast: Update 1976-1993 with hurricanes, WIS Report 33, U.S. Army Engineer Waterways Experiment Station, Vicksburg, MS.

Chesser, S. A. (1992). "Siuslaw River and Bar, Oregon Shoreline Surveillance Program, 1981-1990, final report," U.S. Army Engineer District, Portland, OR.

Clausner, J. E., Birkemeier, W. A., and Clark, G. E. (1986). "Field comparison of four nearshore survey systems," Miscellaneous Paper CERC-86-6, U.S. Army Engineer Waterways Experiment Station, Vicksburg, MS.

Craig, R., and Team, W. (1985). "Surf zone and nearshore surveying with helicopter and a total station." *Proceedings of US Army Corps of Engineers Surveying Conference.* U.S. Army Engineer Waterways Experiment Station, Vicksburg, MS.

Fox, W., and Davis, R. (1974). "Beach processes on the Oregon coast, July 1973," Tech Rep 12, Williams College, Williamstown, MA.

Hicks, L., and Babcock, S. (1988). "Currents and sediment transport at the Siuslaw Ocean dredged material disposal site—dye and seabed drifter studies," U.S. Army Engineer District, Portland.

Huyer, A., Gilbert, W. E., and Pittock, H. L. (1983). "Anomalous sea levels at Newport, Oregon, during the 1982-83 El Niño," *Coastal Oceanography and Climatology News* 5, 37-39.

Jensen, R. E., Hubertz, J. M., and Payne, J. B. (1989). "Wave information studies of U.S. coastlines; Pacific coast hindcast phase III north wave information," WIS Report 17, U.S. Army Engineer Waterways Experiment Station, Vicksburg, MS.

Komar, P. D. (1975). "A study of the effects of a proposed extension of the Siuslaw River jetties," Oregon State University Publication 75-9, School of Oceanography, Corvallis, OR.

__________. (1986). "The 1982-83 El Niño and erosion on the coast of Oregon," *Shore & Beach* 54(2), 3-12.

Komar, P. D., and Good, J. W. (1989). "Long-term erosion impacts of the 1982-83 El Niño on the Oregon Coast," *Coastal Zone '89* 4, 3785-3794.

Komar, P. D., Lizarraga-Arciniega, J. R., and Terich, T. A. (1976). "Oregon coast shoreline changes due to jetties," *Journal of the Waterways, Harbors, and Coastal Engineering Division*, American Society of Civil Engineers 102, 13-30.

Kraus, N. C. (1990). "Prediction of eroded versus accreted beaches," Coastal Engineering Technical Note (CETN) II-2, U.S. Army Engineer Waterways Experiment Station, Vicksburg, MS.

Larson, M., and Kraus, N. C. (1989). "SBEACH: Numerical model for simulation storm-induced beach change; Report 1, Empirical foundation and model development," Technical Report CERC-89-9, U.S. Army Engineer Waterways Experiment Station, Vicksburg, MS.

Lizarraga-Arciniega, J. R., and Komar, P. D. (1975). "Shoreline changes due to jetty construction on the Oregon coast," Sea Grant Publication No. ORESU-T-75-004, Oregon State University, Corvallis, OR.

McLellan, T. N., Kraus, N. C., and Burke, C. E. (1990). "Interim design guidance for nearshore berm construction," Dredging Research Technical Notes DRP-5-02, U.S. Army Engineer Waterways Experiment Station, Vicksburg, MS.

Peterson, C. D., et al. (1990). "Littoral cell response to interannual climatic forcing 1983-1987 on the central Oregon coast, USA," *Journal of Coastal Research* 6(1), 1, 87-110.

Pollock, C. E. (1995). "Effectiveness of Spur Jetties at Siuslaw River, Oregon; Report 2, Localized current flow patterns induced by Spur Jetties airborne current measurement system and prototype/physical model correlation," Technical Report CERC-95-14, U.S. Army Engineer Waterways Experiment Station, Vicksburg, MS.

Quinn, W. H., Zopf, D. O., Short, K. S., and Kuo Yang, R. T. W. (1987). "Historical trends and statistics of the southern oscillation, El Niño, and Indonesian droughts," *Fishery Bulletin* 76, 663-678.

Scripps Institution of Oceanography. (1990). "Coastal Data Information Program; monthly report, December 1989, "Monthly summary Report No. 167, SIO REF. 89-28, U.S. Army Corps of Engineers and State of California Department of Boating and Waterways.

Seymour, R. J., Castel, D., Thomas, J. O., and McGehee, D. D. (1992). "Coastal Data Information Program, Multi-Year Report, Volume 1, 1975 through 1991," SIO REFERENCE NO. 91-32, Scripps Institution of Oceanography, Coastal Engineering Research Center, U.S. Army Engineer Waterways Experiment Station, and California Department of Boating and Waterways.

Appendix A
Hydrographic Survey Bathymetric Contours, from 1982 to 1990, for the In-Channel Study Area

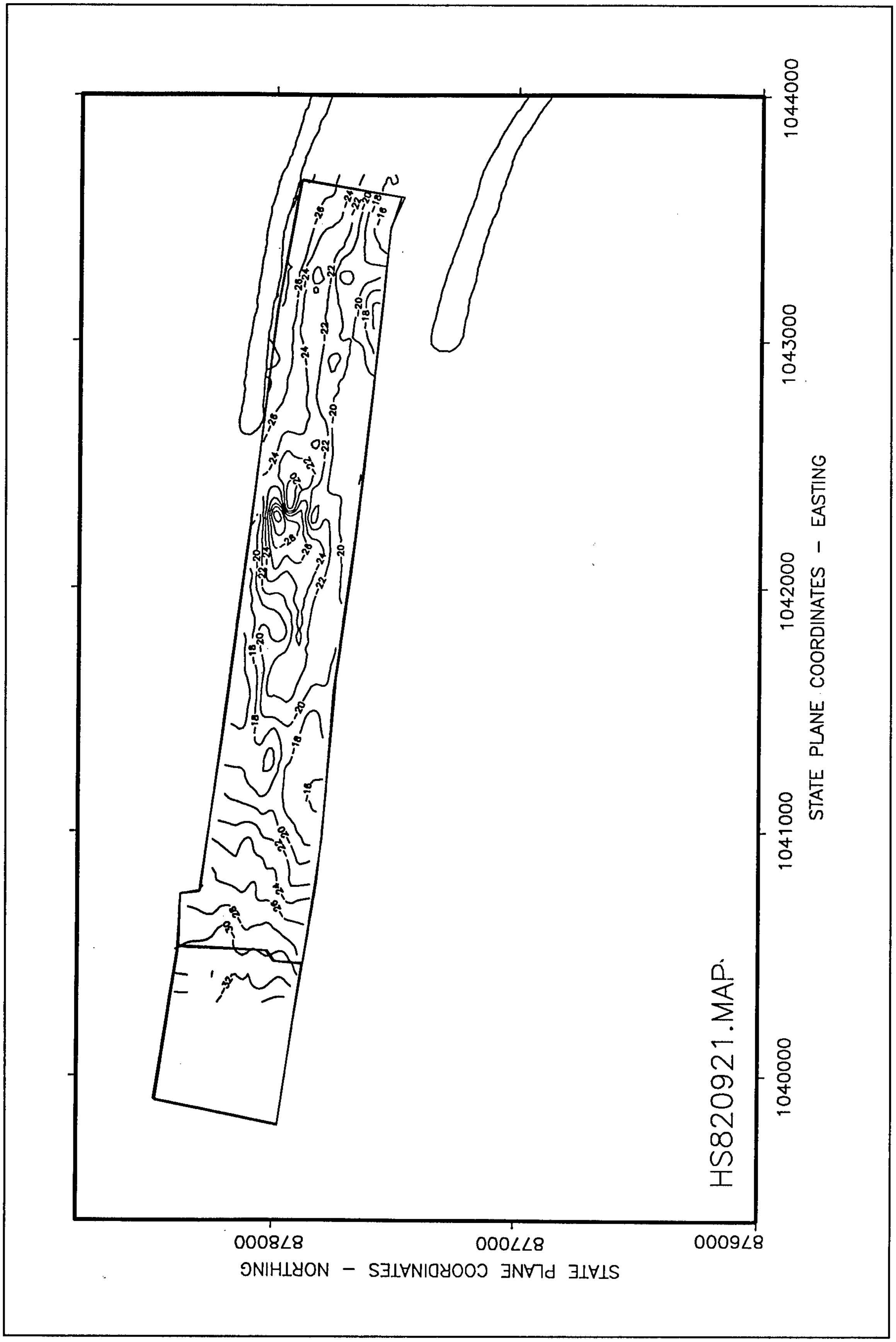
HS820921.MAP
STATE PLANE COORDINATES - EASTING
1040000
1041000
1042000
1043000
1044000
STATE PLANE COORDINATES - NORTHING
876000
877000
878000

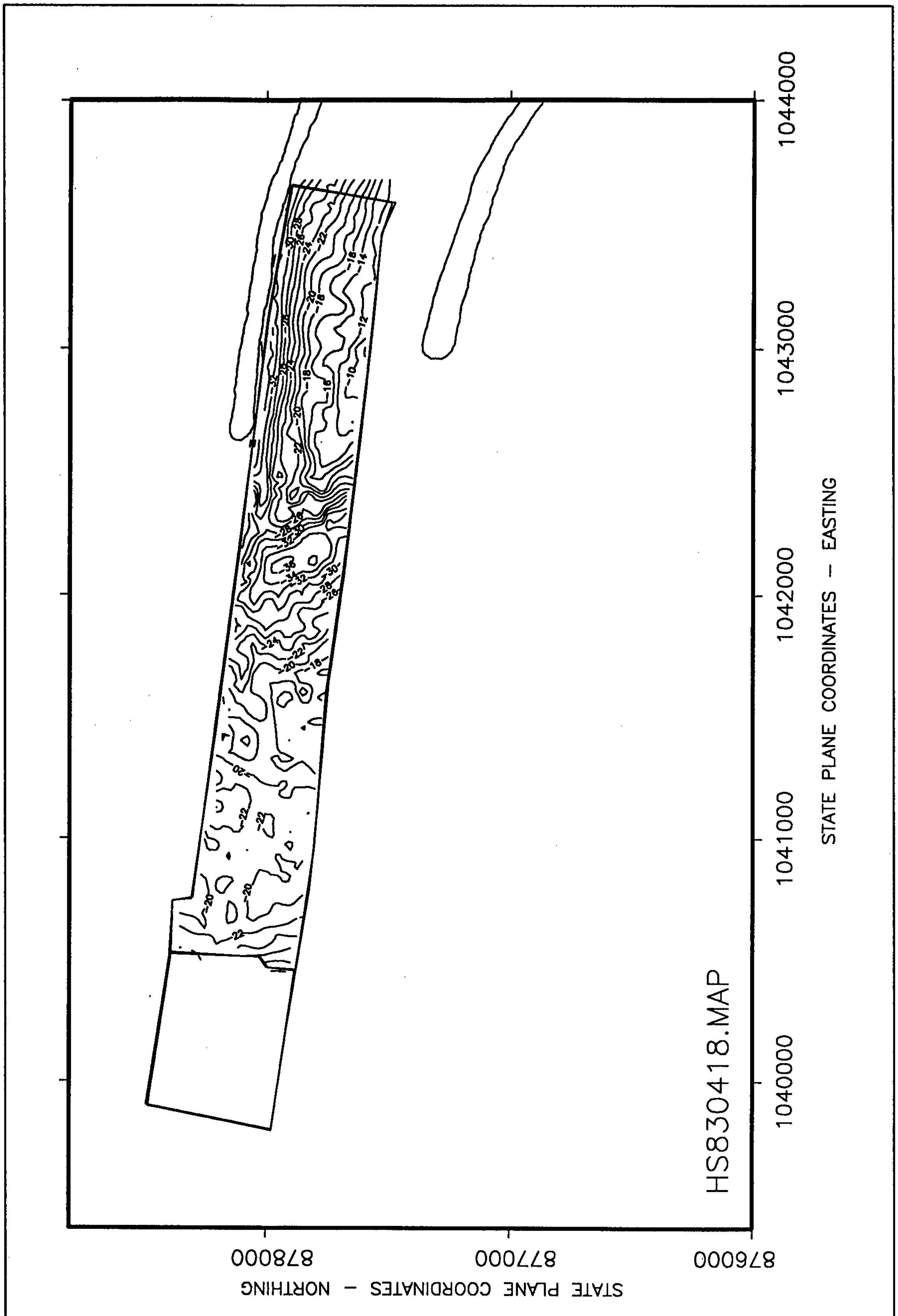
1044000
1043000
1042000
1041000
1040000
STATE PLANE COORDINATES — EASTING
878000
877000
876000
STATE PLANE COORDINATES — NORTHING
HS830418.MAP

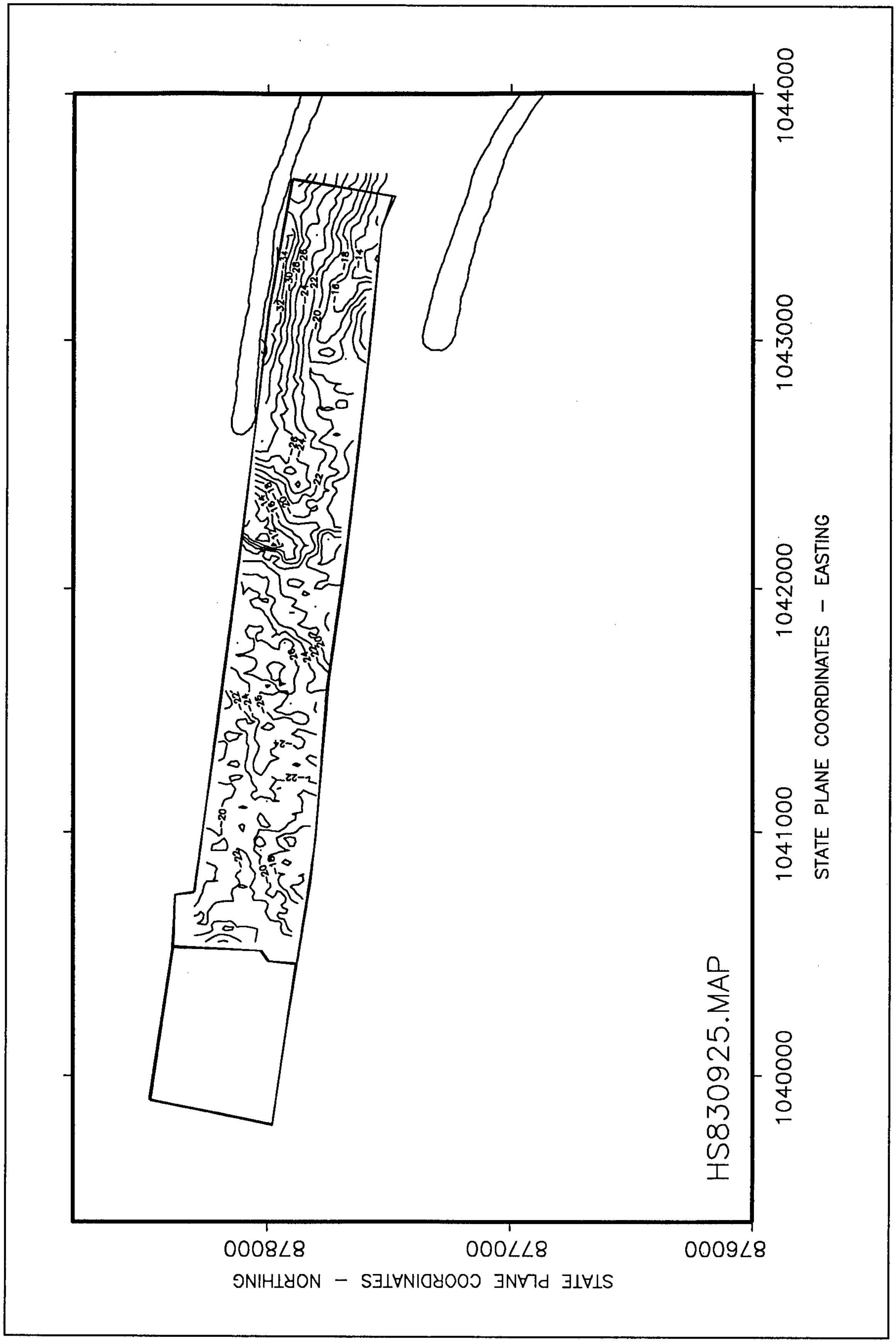

HS830925.MAP
1040000
1041000
1042000
1043000
1044000
STATE PLANE COORDINATES - EASTING
876000
877000
878000
STATE PLANE COORDINATES - NORTHING

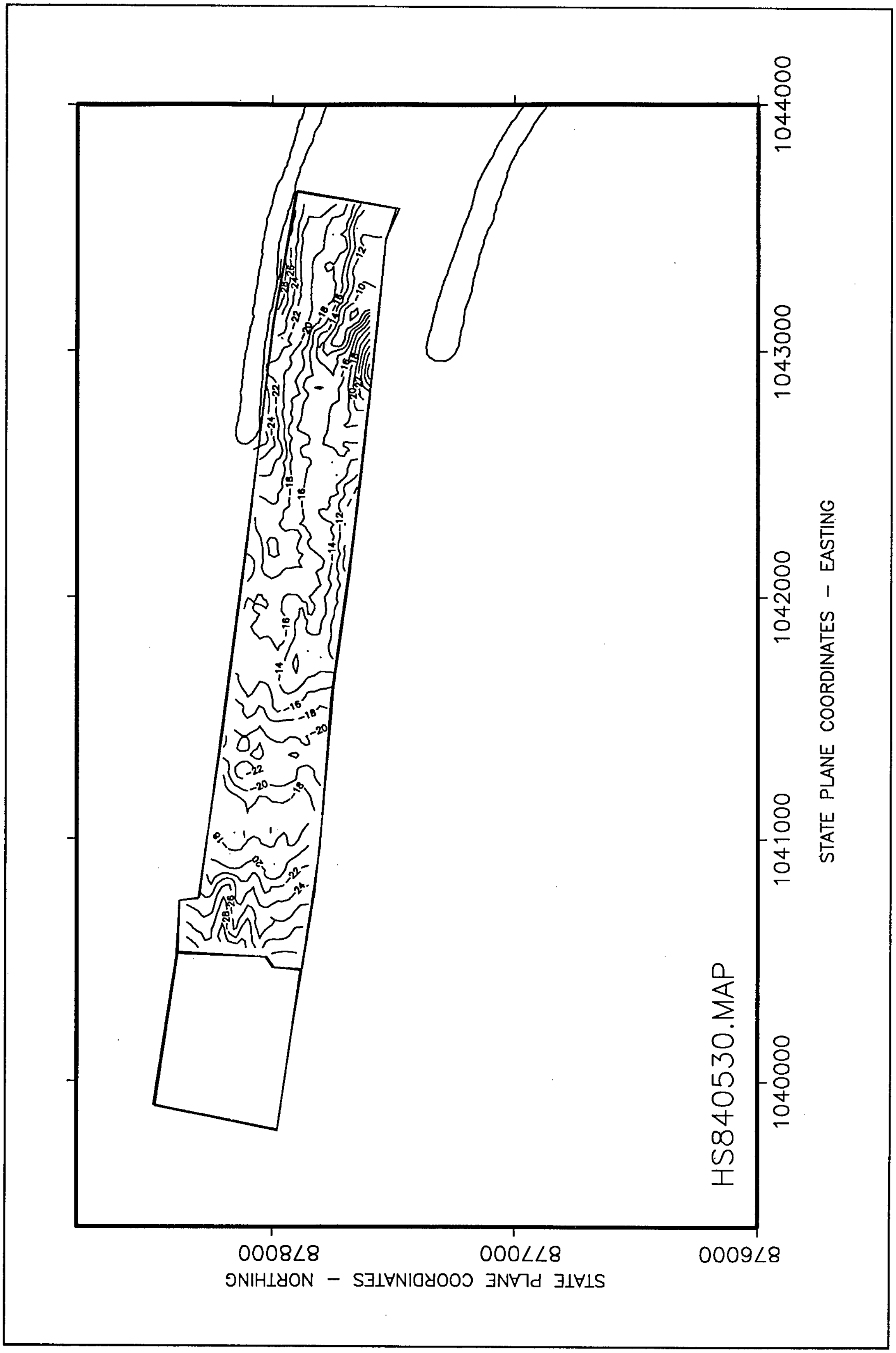
HS840530.MAP
STATE PLANE COORDINATES - EASTING
1040000
1041000
1042000
1043000
1044000
STATE PLANE COORDINATES - NORTHING
876000
877000
878000

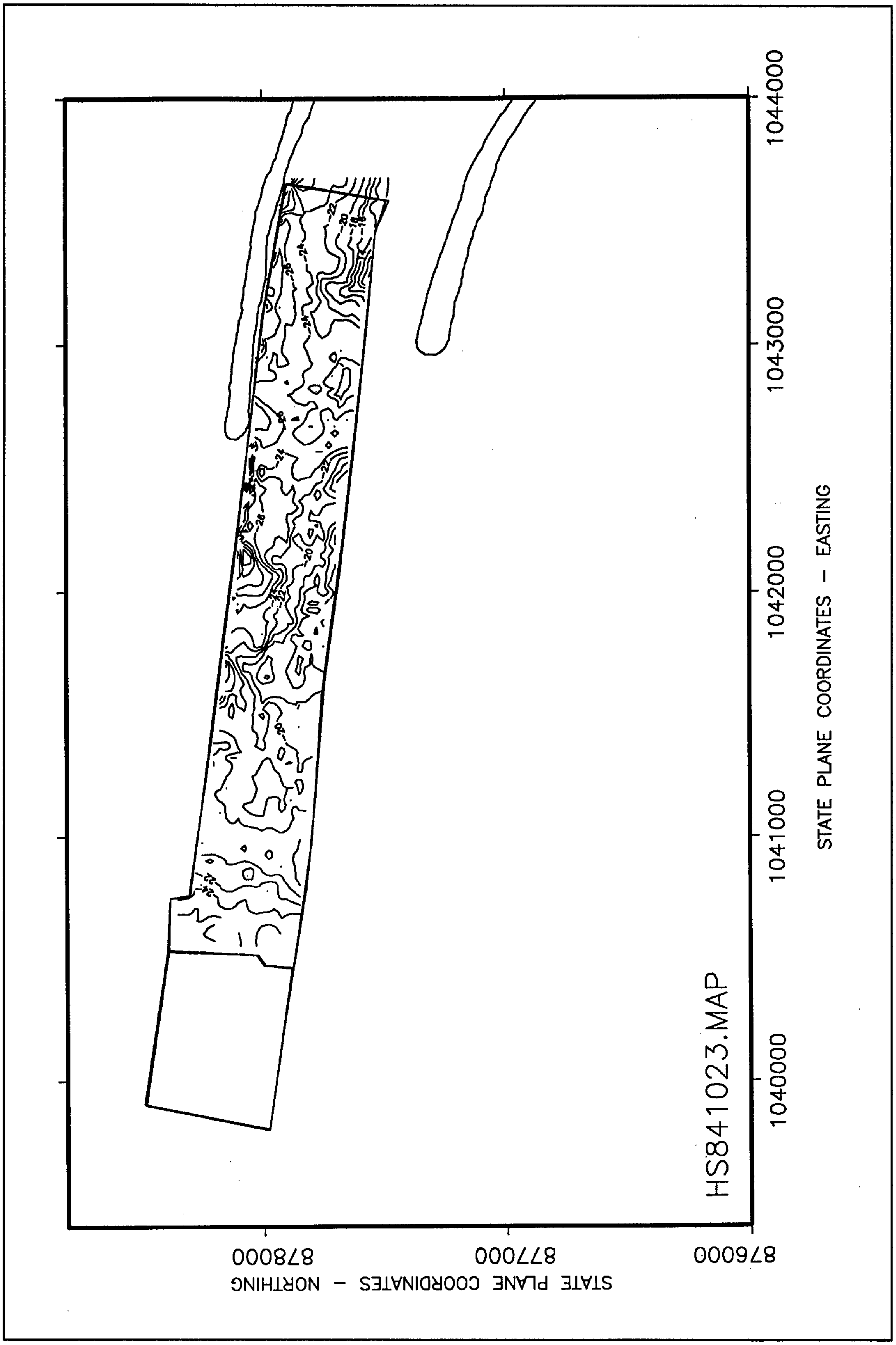
HS841023.MAP
1040000
1041000
1042000
1043000
1044000
STATE PLANE COORDINATES - EASTING
876000
877000
878000
STATE PLANE COORDINATES - NORTHING

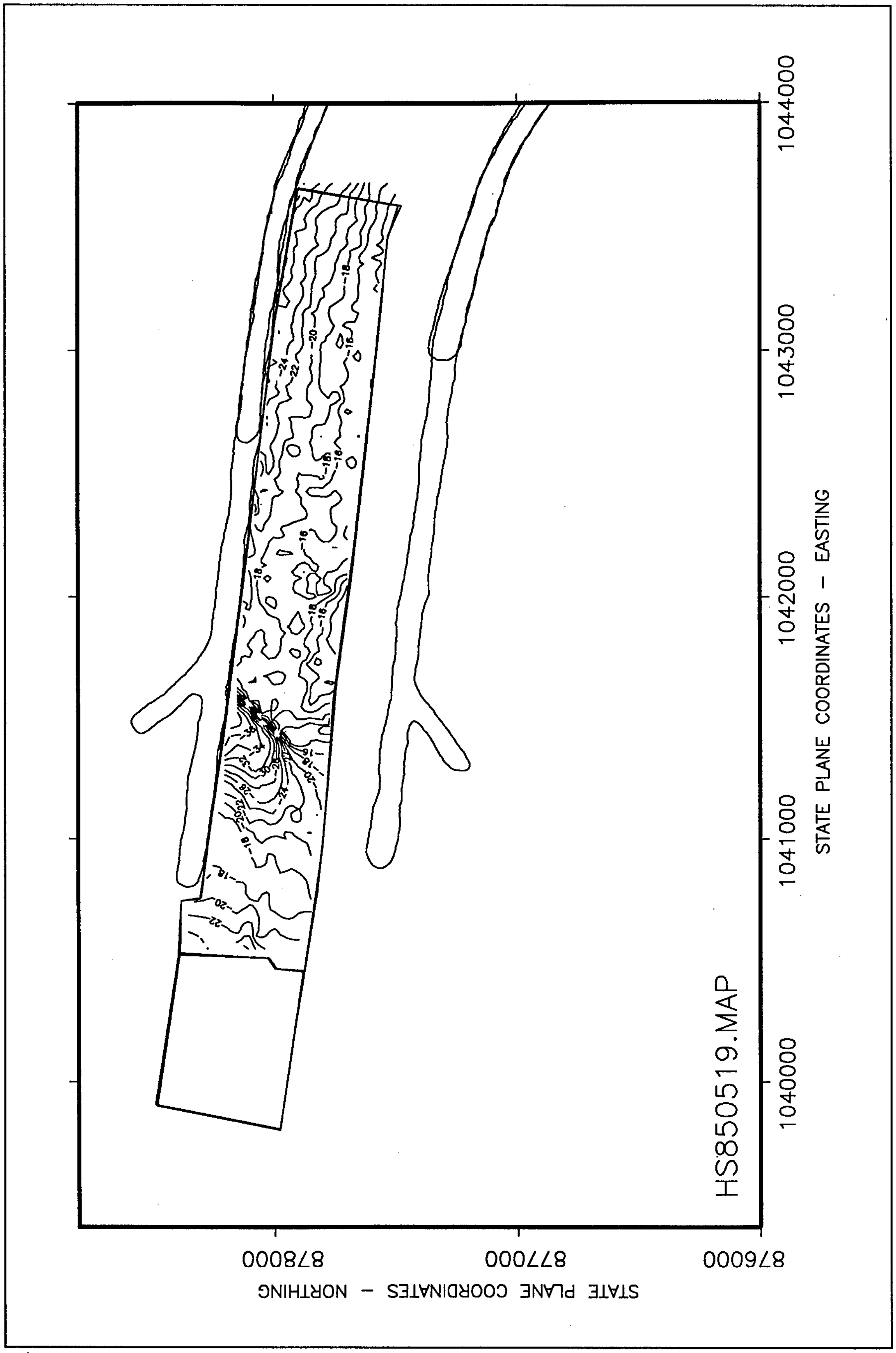
HS850519.MAP
1040000
1041000
1042000
1043000
1044000
STATE PLANE COORDINATES - EASTING
878000
877000
876000
STATE PLANE COORDINATES - NORTHING

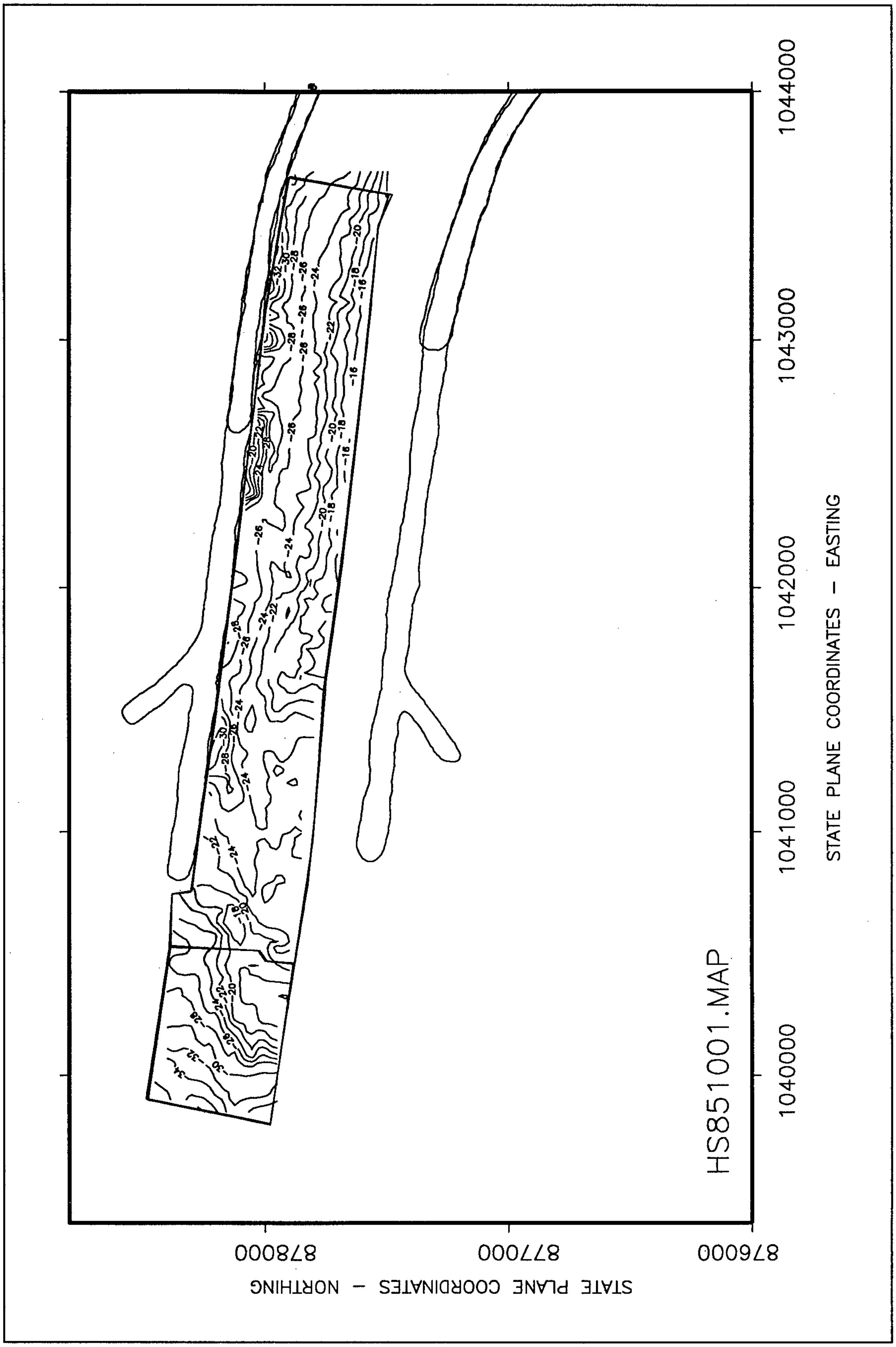
HS851001.MAP
1040000
1041000
1042000
1043000
1044000
STATE PLANE COORDINATES – EASTING
876000
877000
878000
STATE PLANE COORDINATES – NORTHING

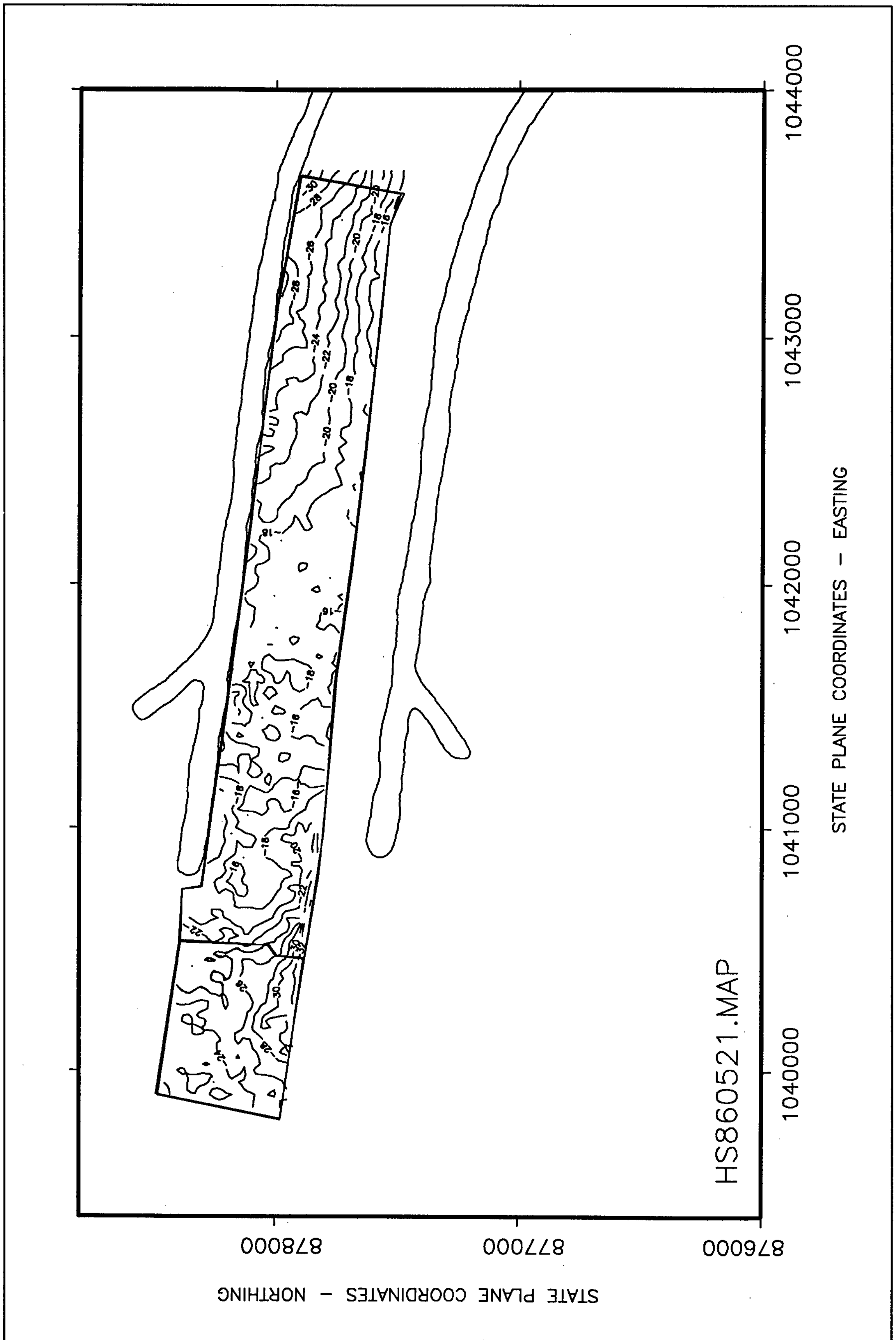
HS860521.MAP
1040000
1041000
1042000
1043000
1044000
STATE PLANE COORDINATES – EASTING
876000
877000
878000
STATE PLANE COORDINATES – NORTHING

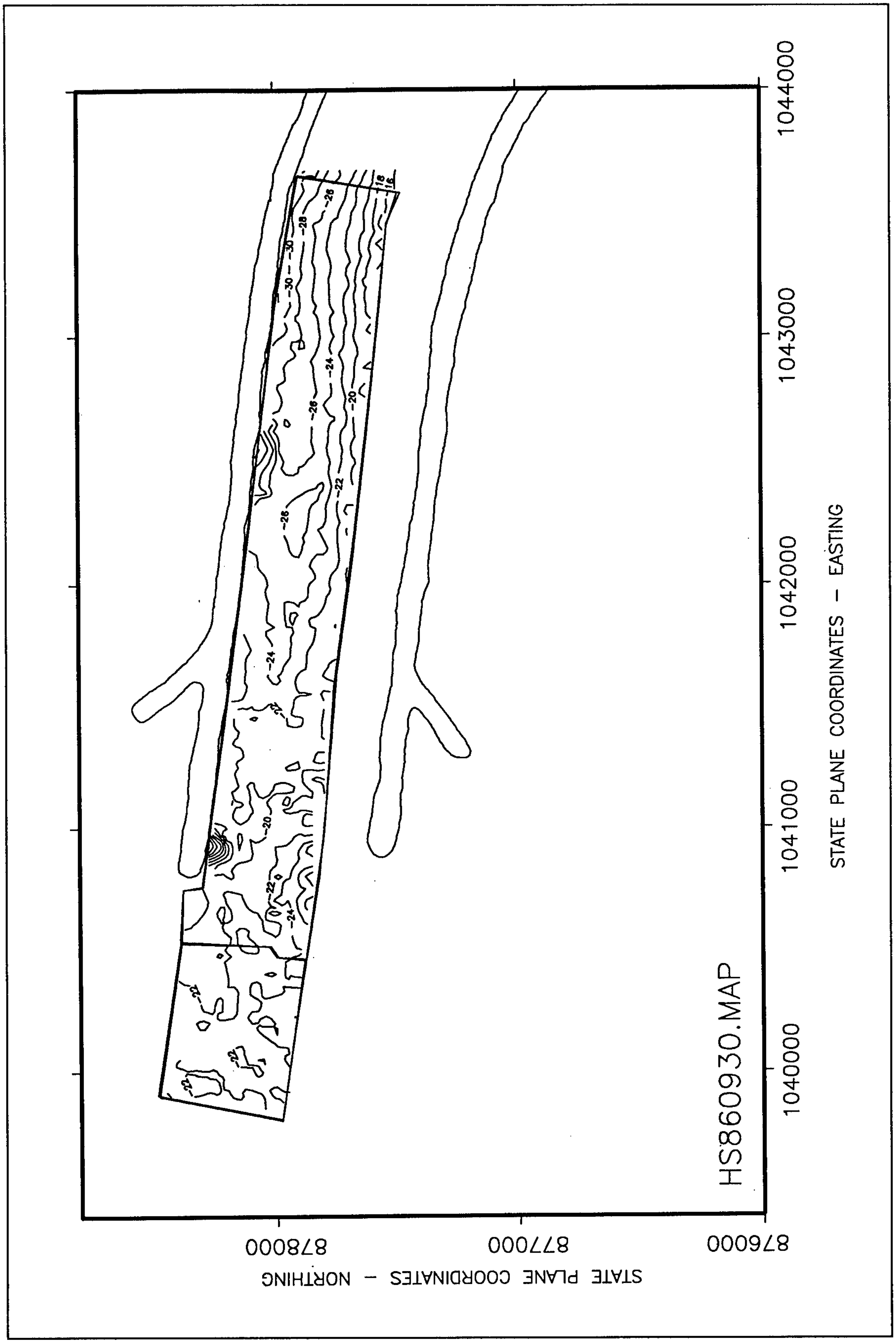

HS860930.MAP
1040000
1041000
1042000
1043000
1044000
STATE PLANE COORDINATES - EASTING
876000
877000
878000
STATE PLANE COORDINATES - NORTHING

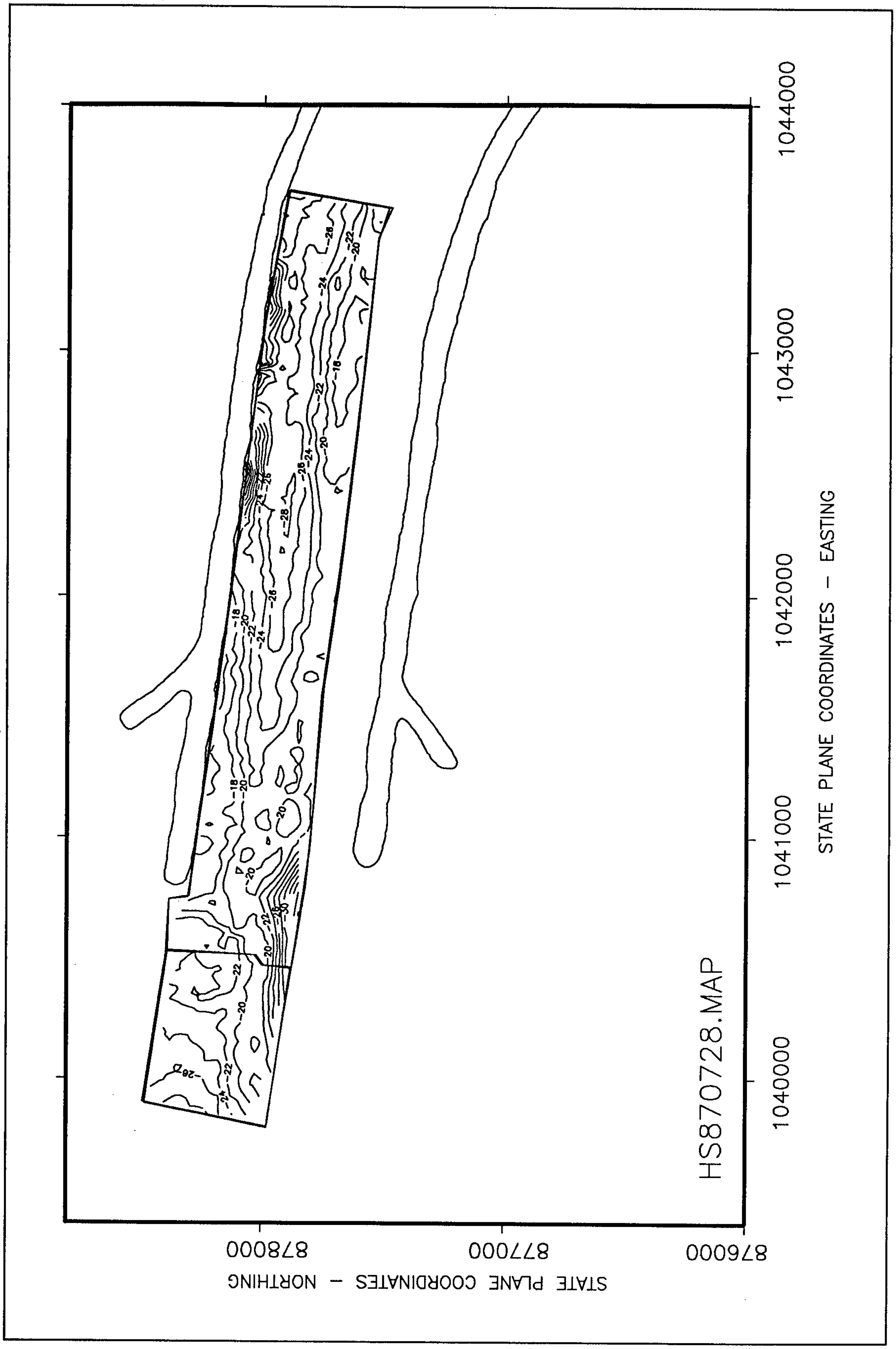

HS870728.MAP
STATE PLANE COORDINATES - EASTING
1040000
1041000
1042000
1043000
1044000
STATE PLANE COORDINATES - NORTHING
876000
877000
878000

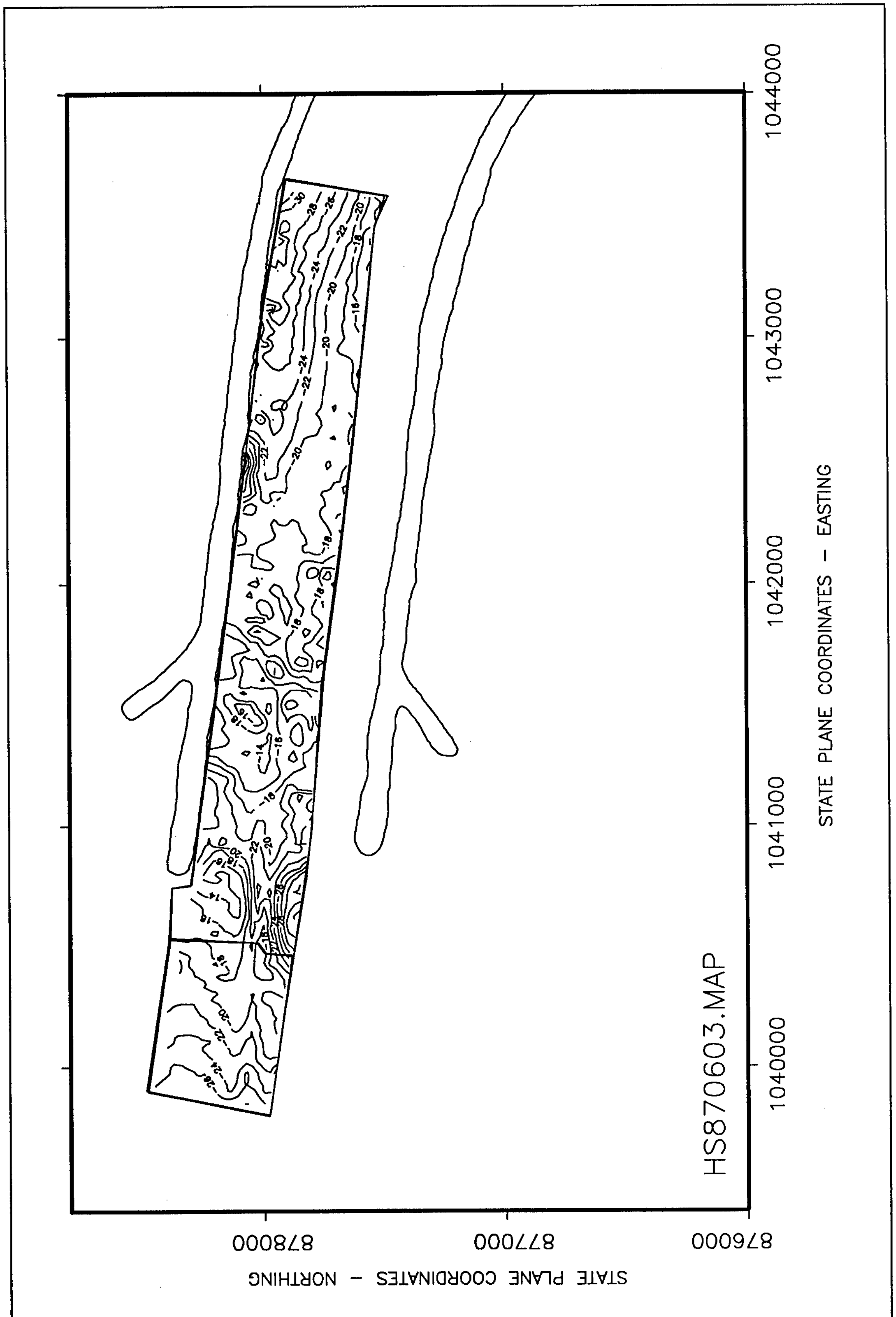
HS870603.MAP
1040000
1041000
1042000
1043000
1044000
STATE PLANE COORDINATES - EASTING
876000
877000
878000
STATE PLANE COORDINATES - NORTHING

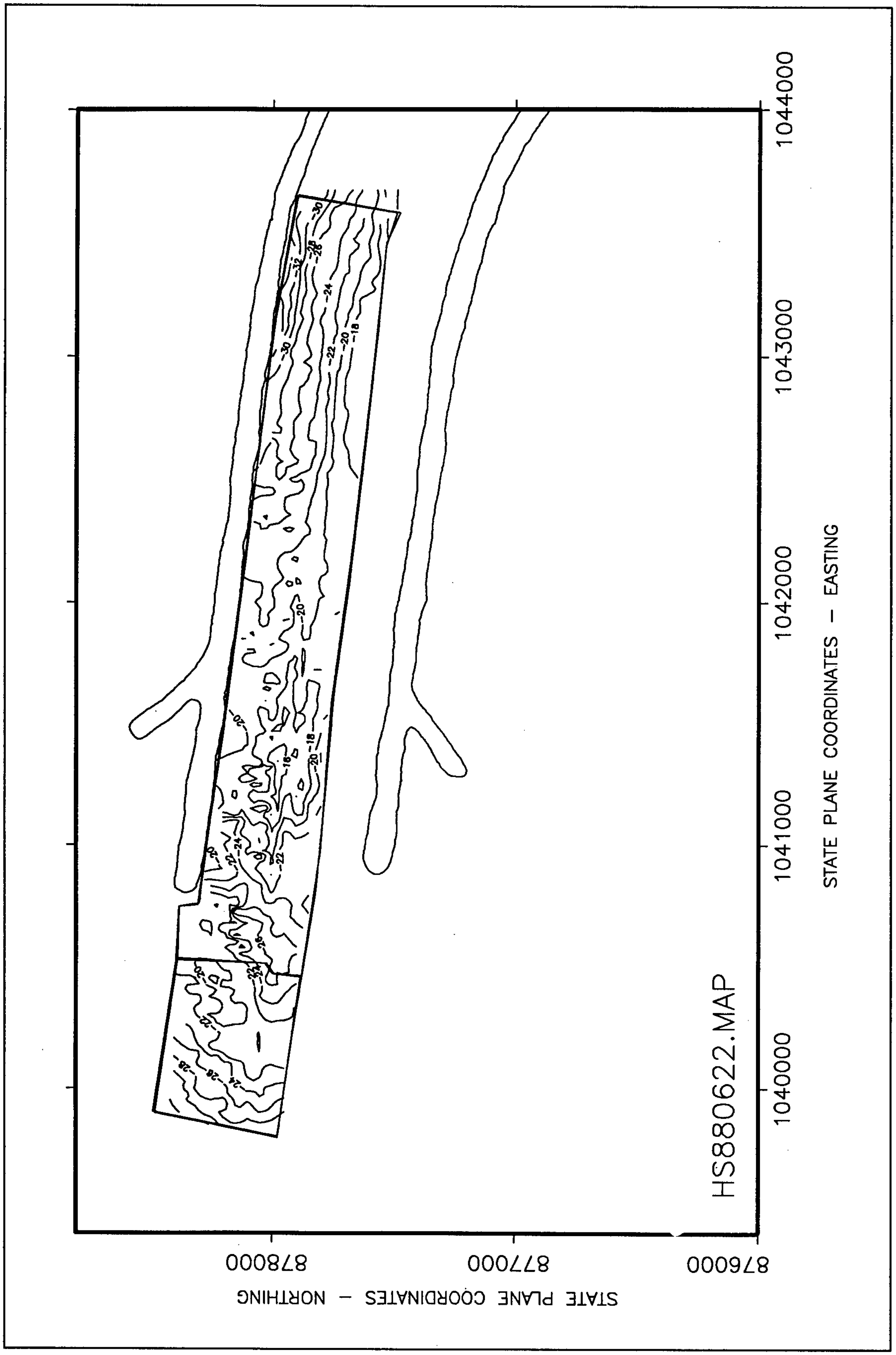
HS880622.MAP
1040000
1041000
1042000
1043000
1044000
STATE PLANE COORDINATES - EASTING
876000
877000
878000
STATE PLANE COORDINATES - NORTHING

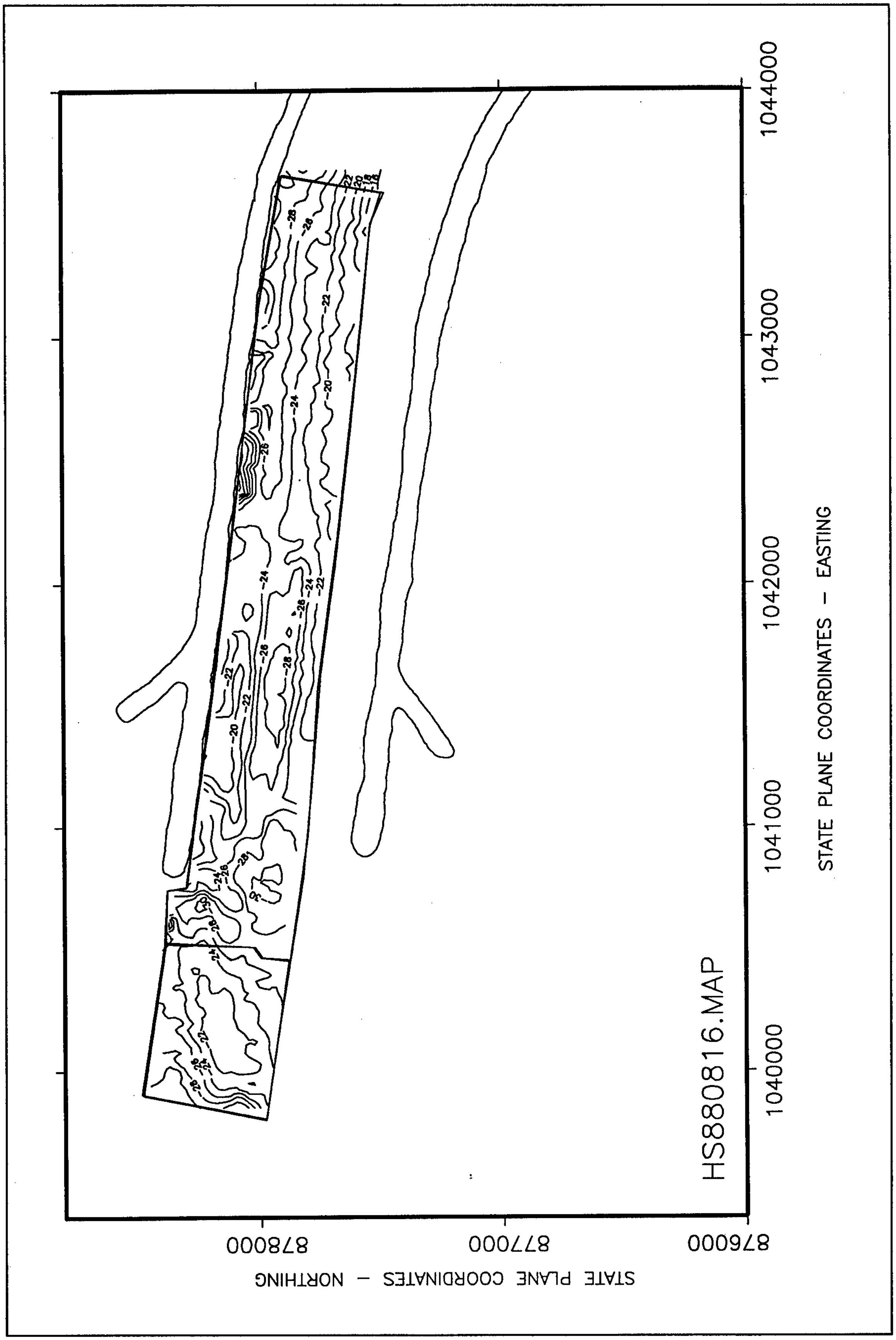
HS880816.MAP
STATE PLANE COORDINATES – EASTING
1040000
1041000
1042000
1043000
1044000
STATE PLANE COORDINATES – NORTHING
876000
877000
878000

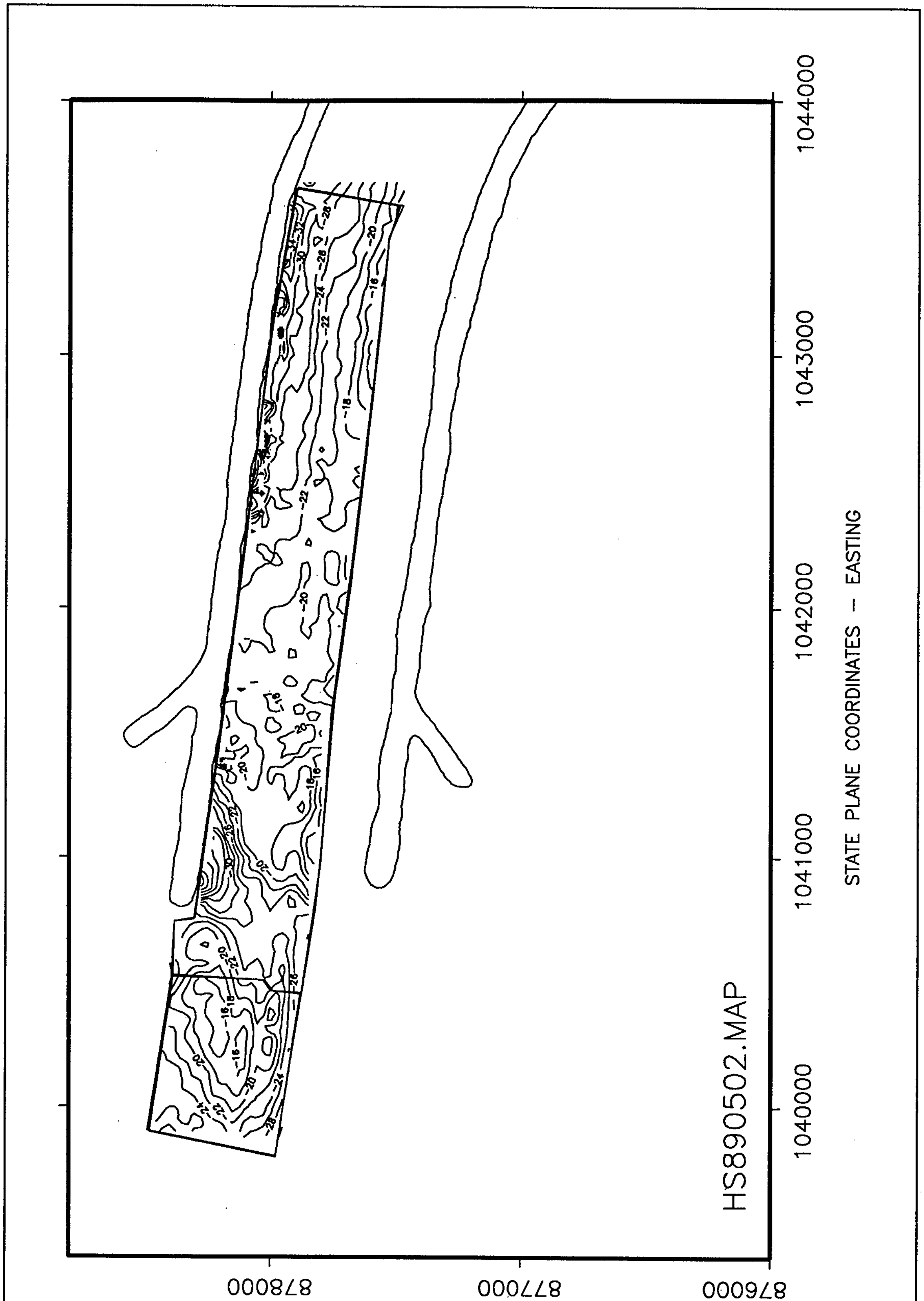

HS890502.MAP
1040000
1041000
1042000
1043000
1044000
STATE PLANE COORDINATES - EASTING
876000
877000
878000
STATE PLANE COORDINATES - NORTHING

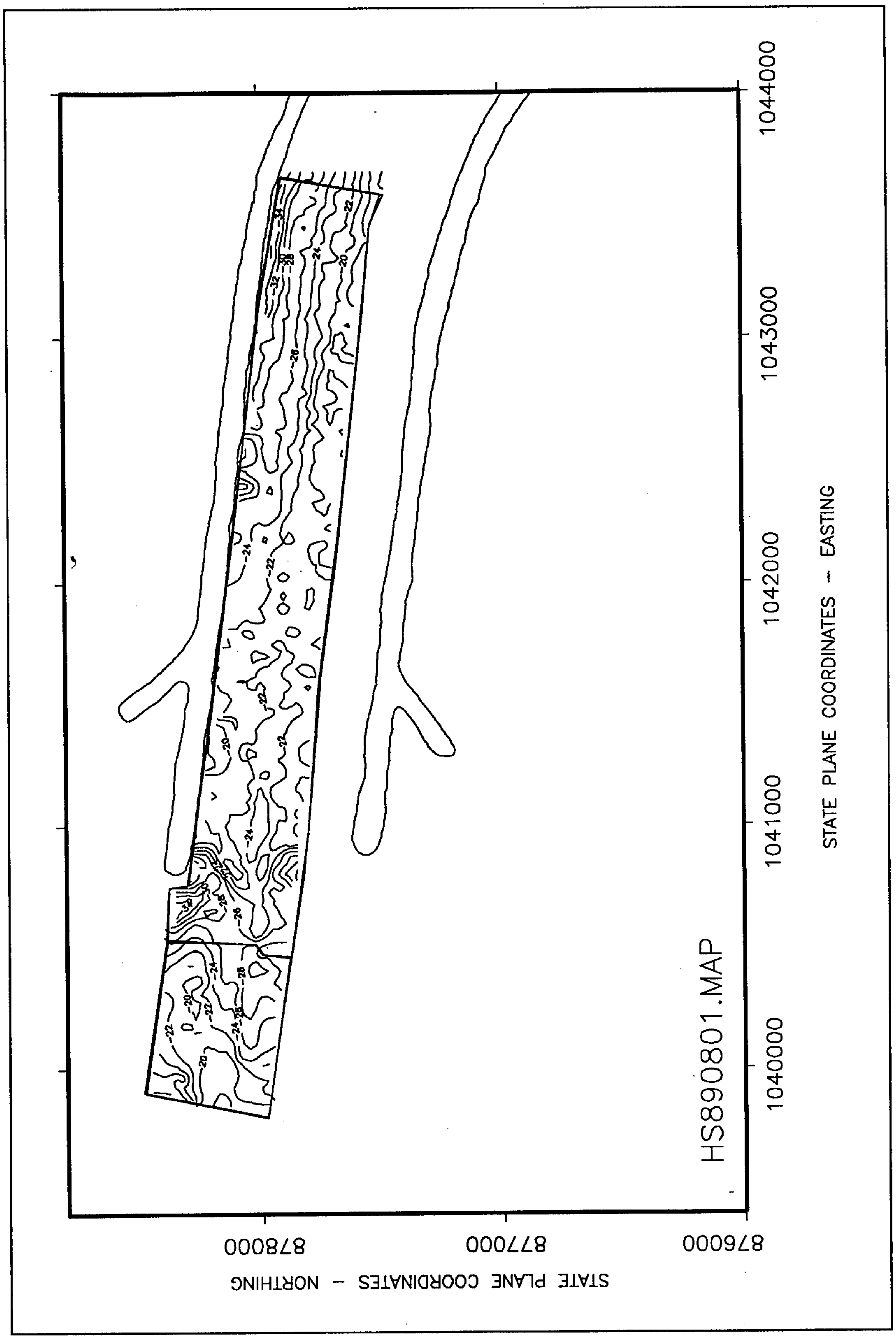
HS890801.MAP
STATE PLANE COORDINATES – EASTING
1040000
1041000
1042000
1043000
1044000
STATE PLANE COORDINATES – NORTHING
876000
877000
878000

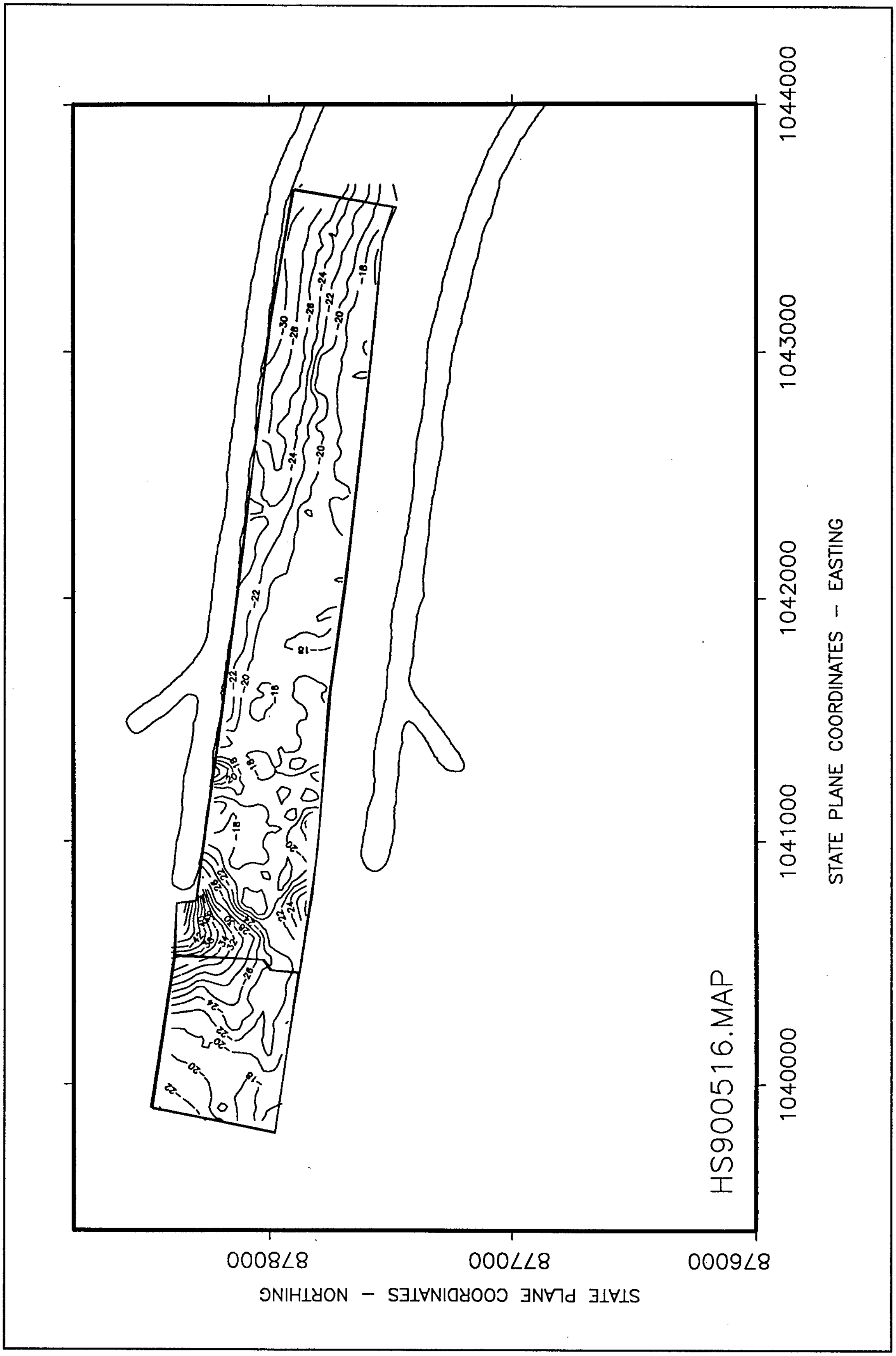
HS900516.MAP
STATE PLANE COORDINATES – EASTING
STATE PLANE COORDINATES – NORTHING
1040000
1041000
1042000
1043000
1044000
876000
877000
878000

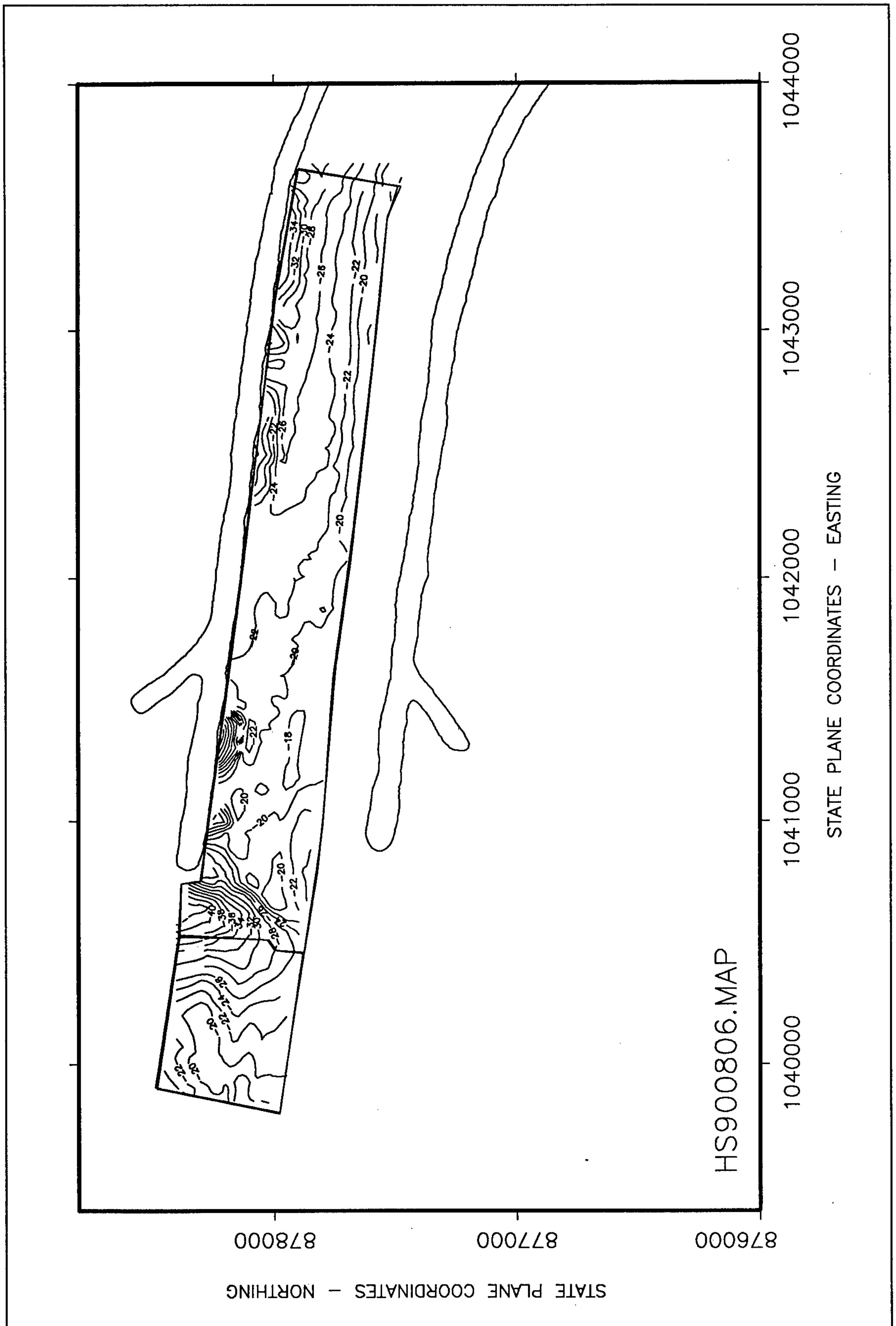
HS900806.MAP
STATE PLANE COORDINATES – EASTING
1040000
1041000
1042000
1043000
1044000
STATE PLANE COORDINATES – NORTHING
876000
877000
878000

Appendix B
Bathymetric Contours, from 1981 to 1990, for the Localized Region Surrounding the Entrance Channel

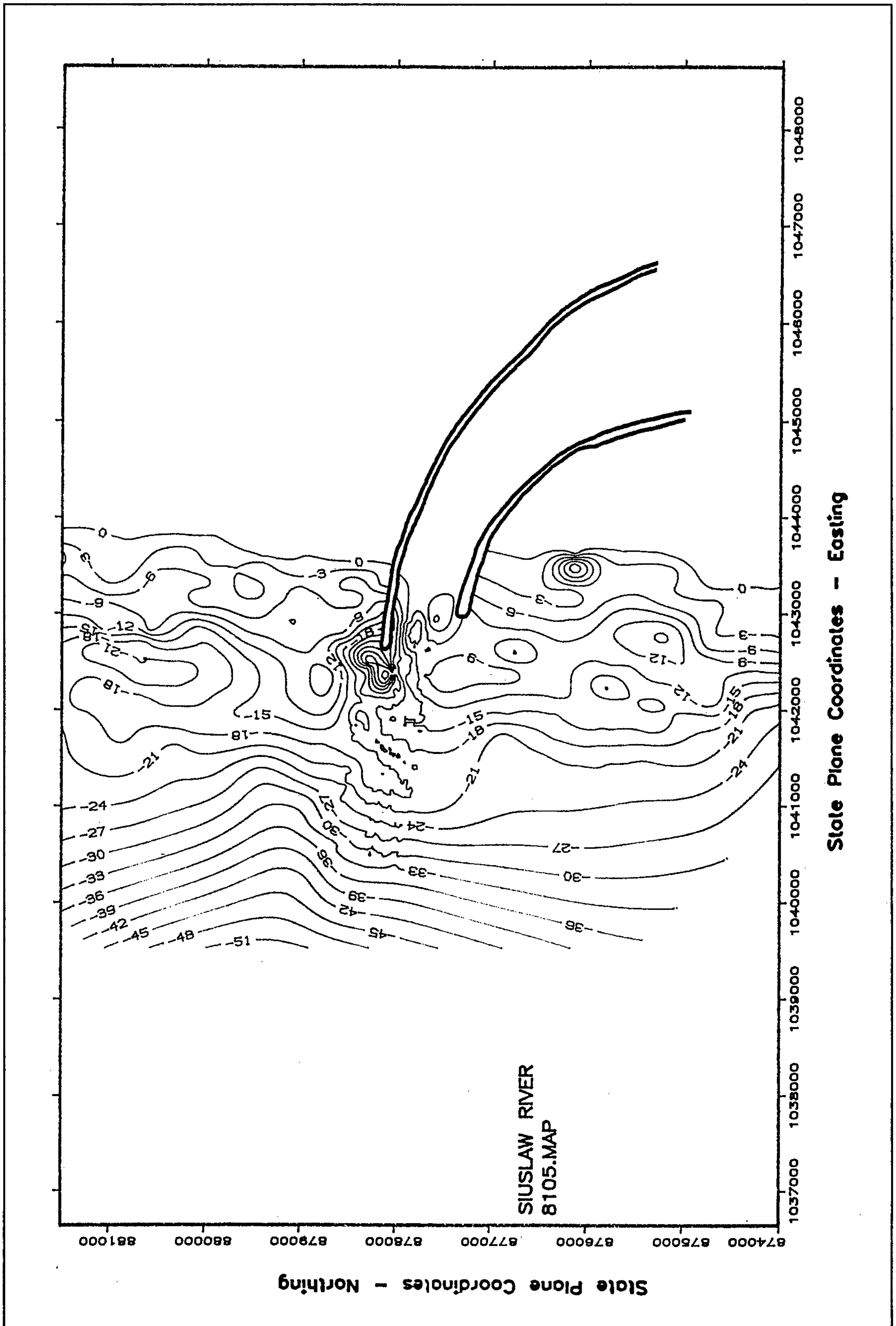
SIUSLAW RIVER
8105.MAP
State Plane Coordinates - Easting
State Plane Coordinates - Northing

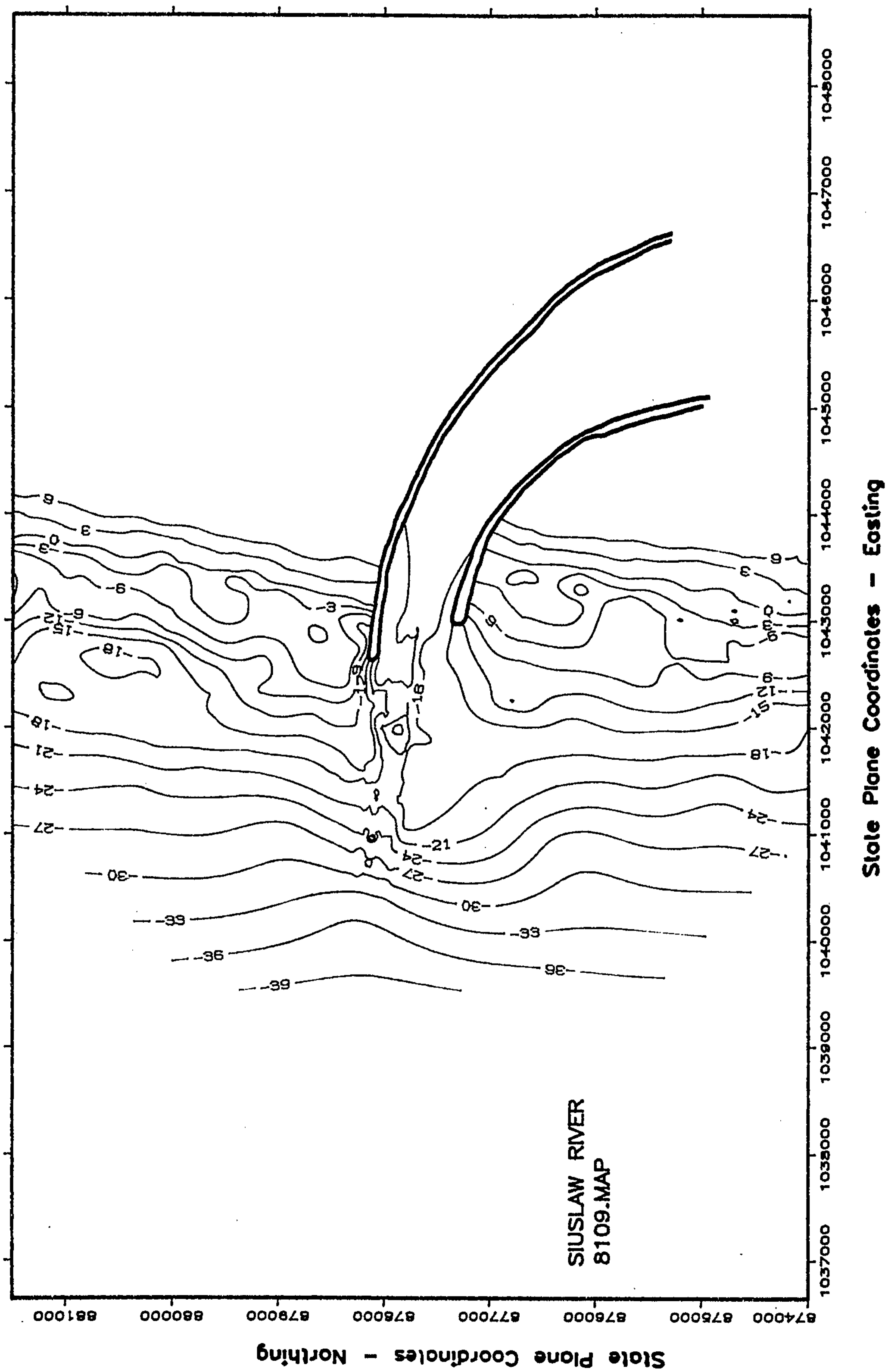
SIUSLAW RIVER
8109.MAP
State Plane Coordinates - Easting
State Plane Coordinates - Northing

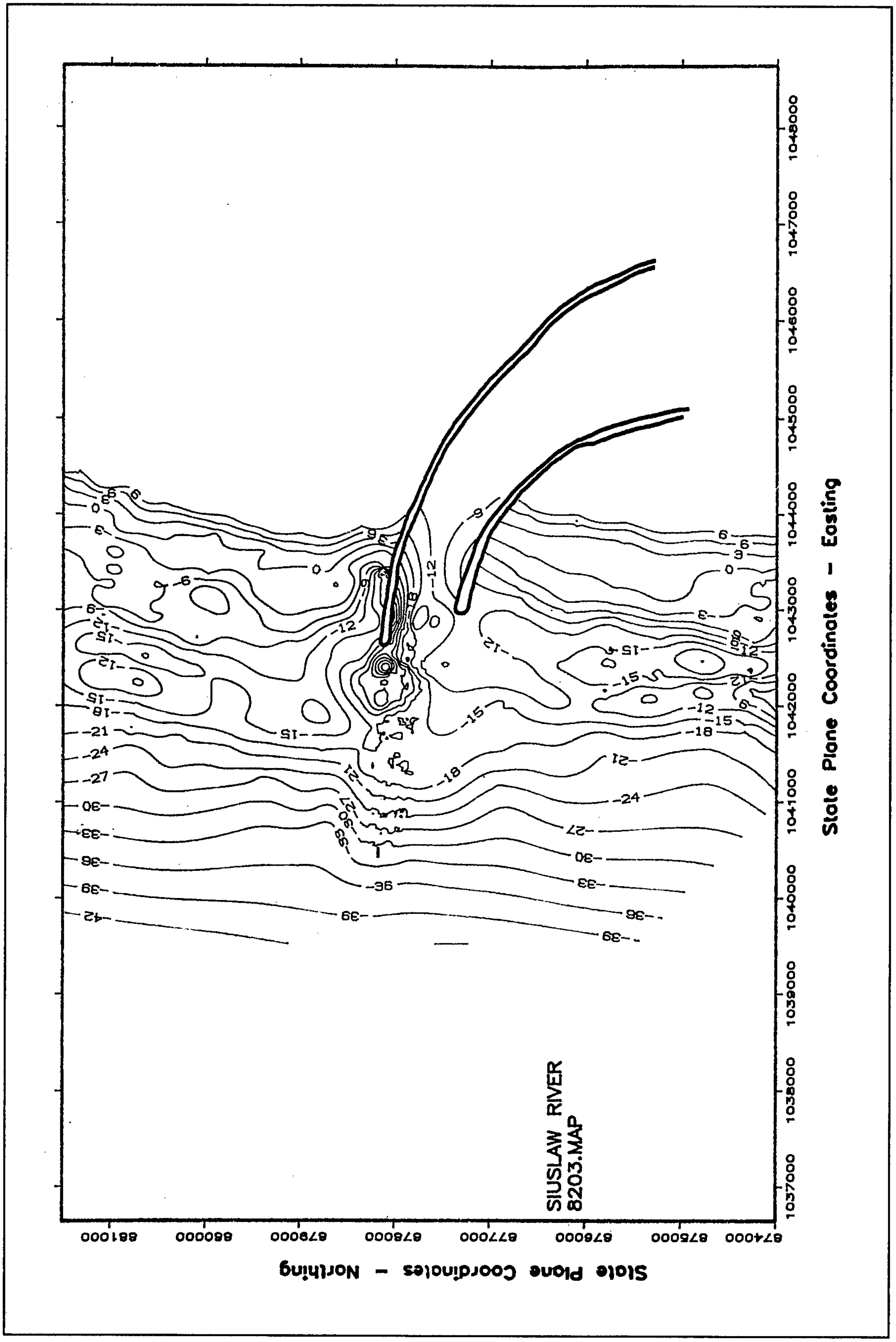
SIUSLAW RIVER
8203.MAP
State Plane Coordinates - Easting
State Plane Coordinates - Northing
1037000
1038000
1039000
1040000
1041000
1042000
1043000
1044000
1045000
1046000
1047000
1048000
874000
875000
876000
877000
878000
879000
880000
881000

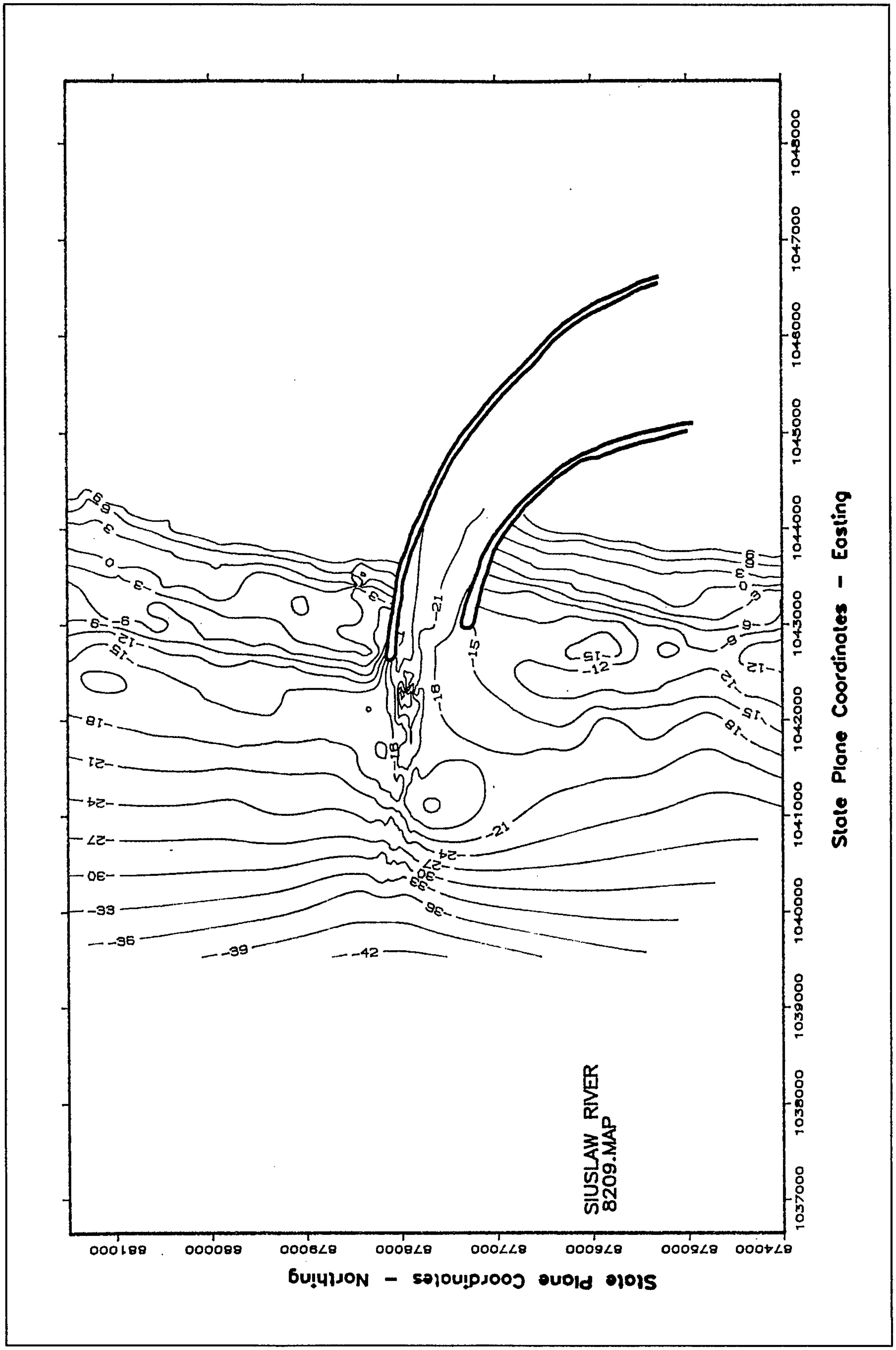
SIUSLAW RIVER
8209.MAP
State Plane Coordinates - Easting
State Plane Coordinates - Northing

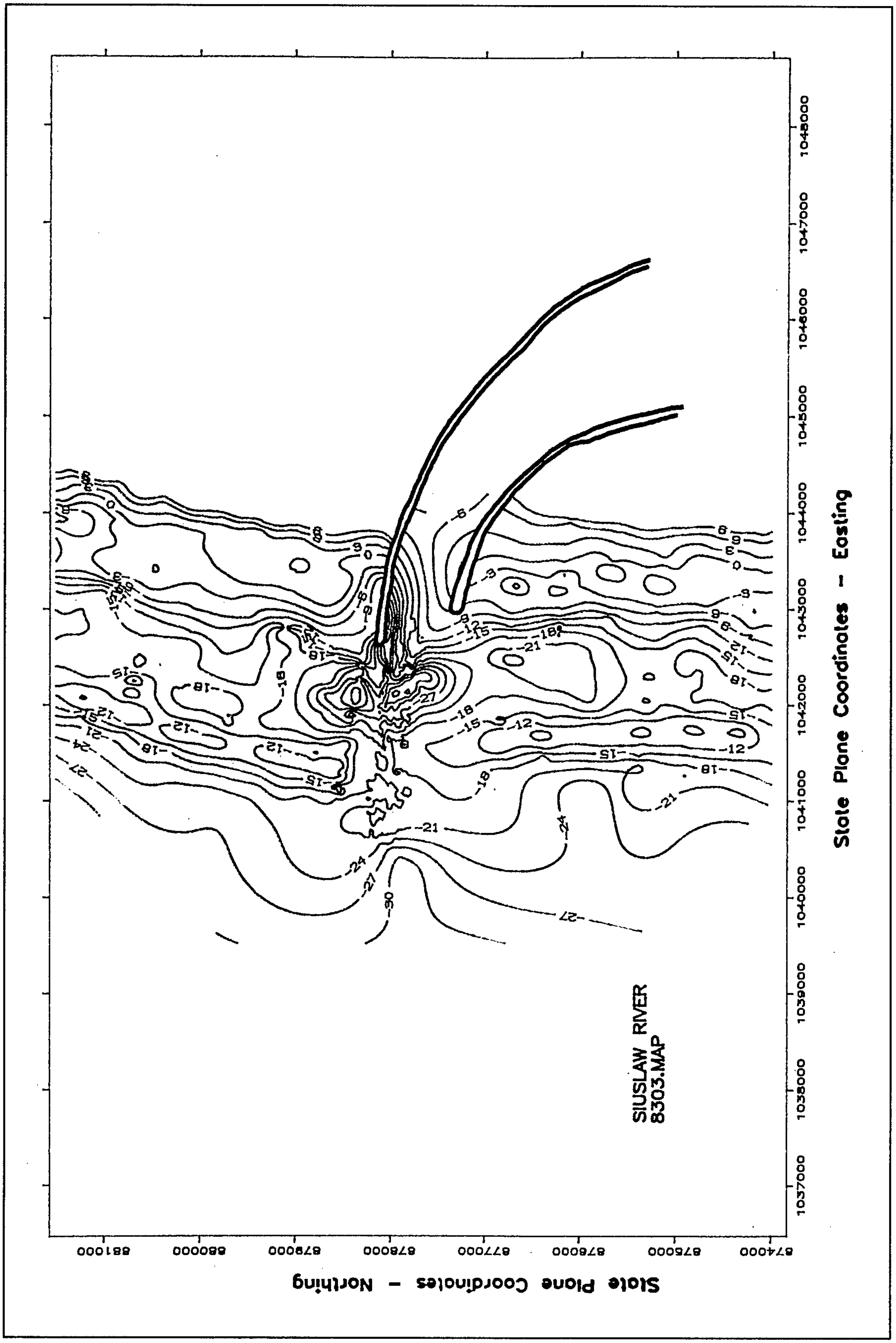
SIUSLAW RIVER
8303.MAP
State Plane Coordinates - Easting
State Plane Coordinates - Northing

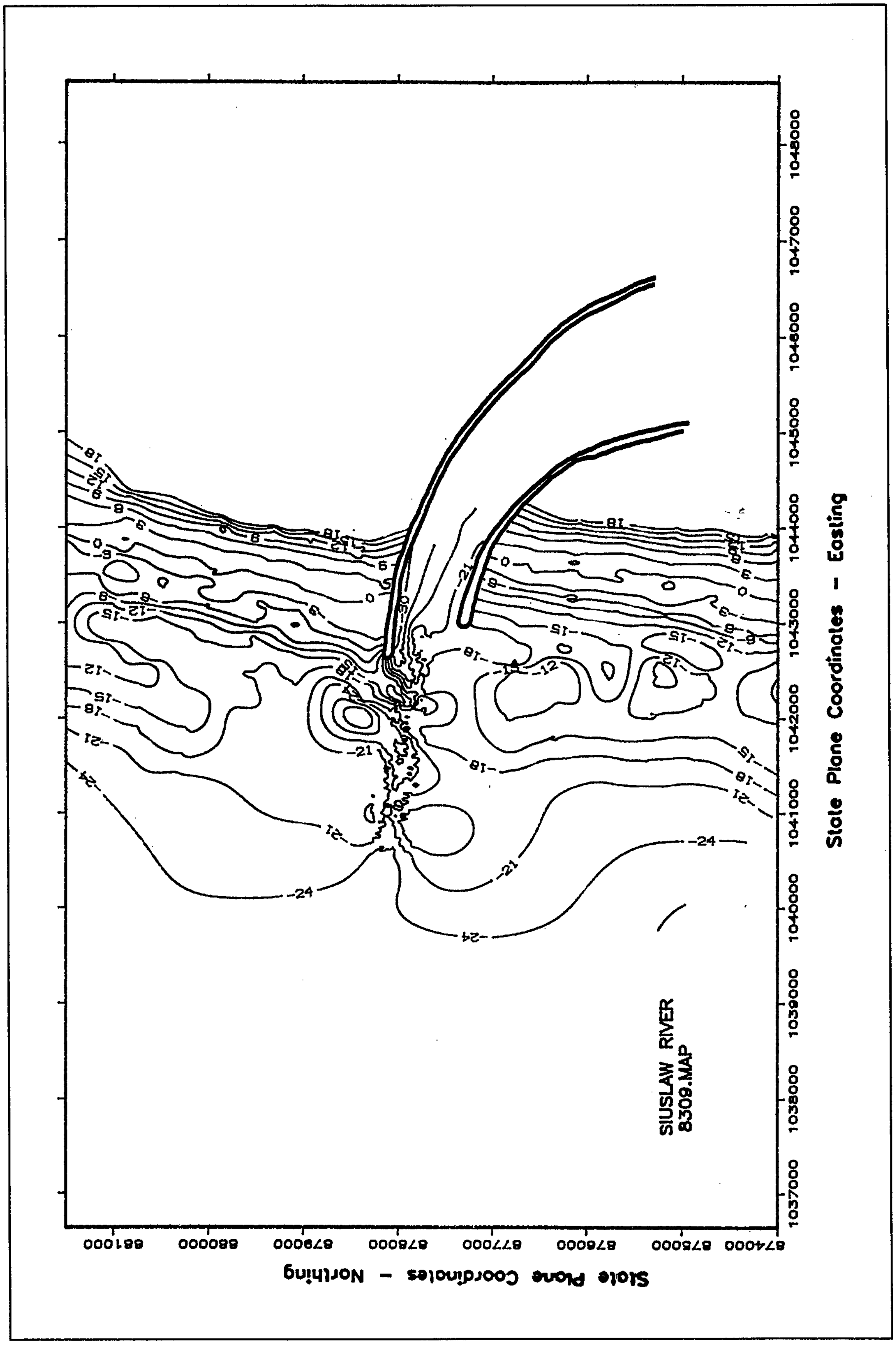
SIUSLAW RIVER
8309.MAP
State Plane Coordinates - Easting
State Plane Coordinates - Northing
1037000
1038000
1039000
1040000
1041000
1042000
1043000
1044000
1045000
1046000
1047000
1048000
874000
875000
876000
877000
878000
879000
880000
881000

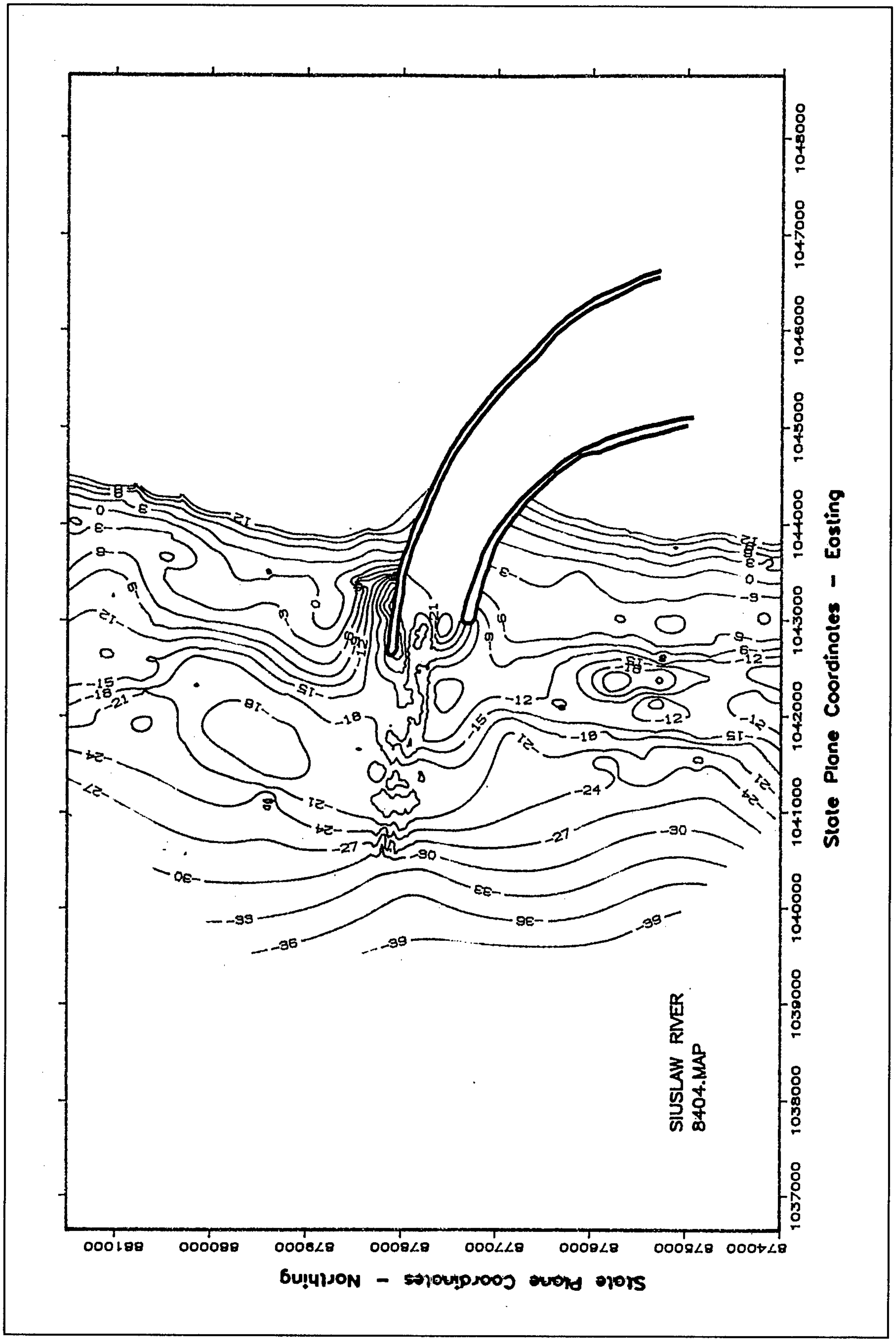
SIUSLAW RIVER
8404.MAP
State Plane Coordinates - Easting
State Plane Coordinates - Northing

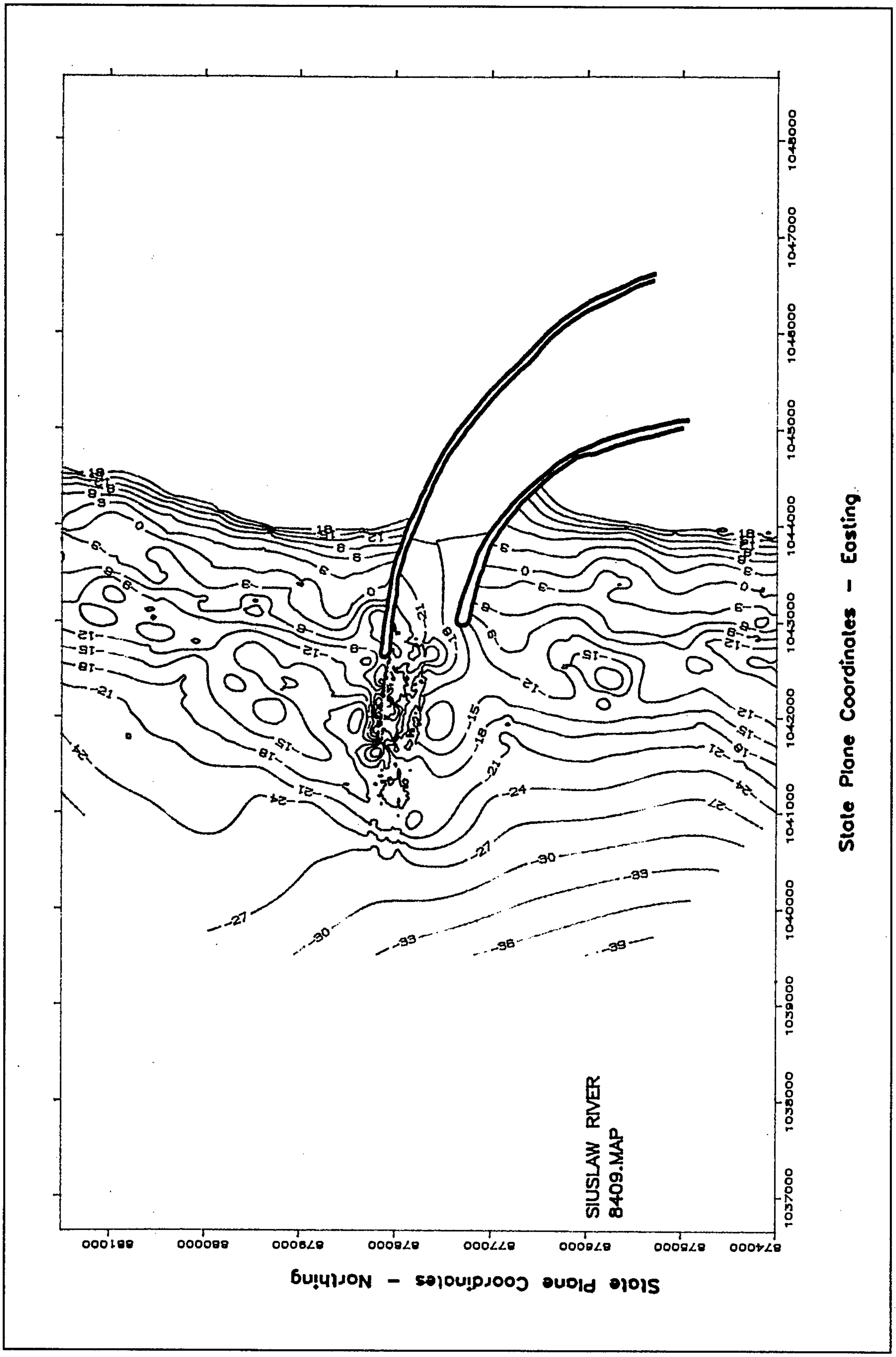
SIUSLAW RIVER
8409.MAP
State Plane Coordinates - Easting
State Plane Coordinates - Northing
1037000
1038000
1039000
1040000
1041000
1042000
1043000
1044000
1045000
1046000
1047000
1048000
874000
875000
876000
877000
878000
879000
880000
881000

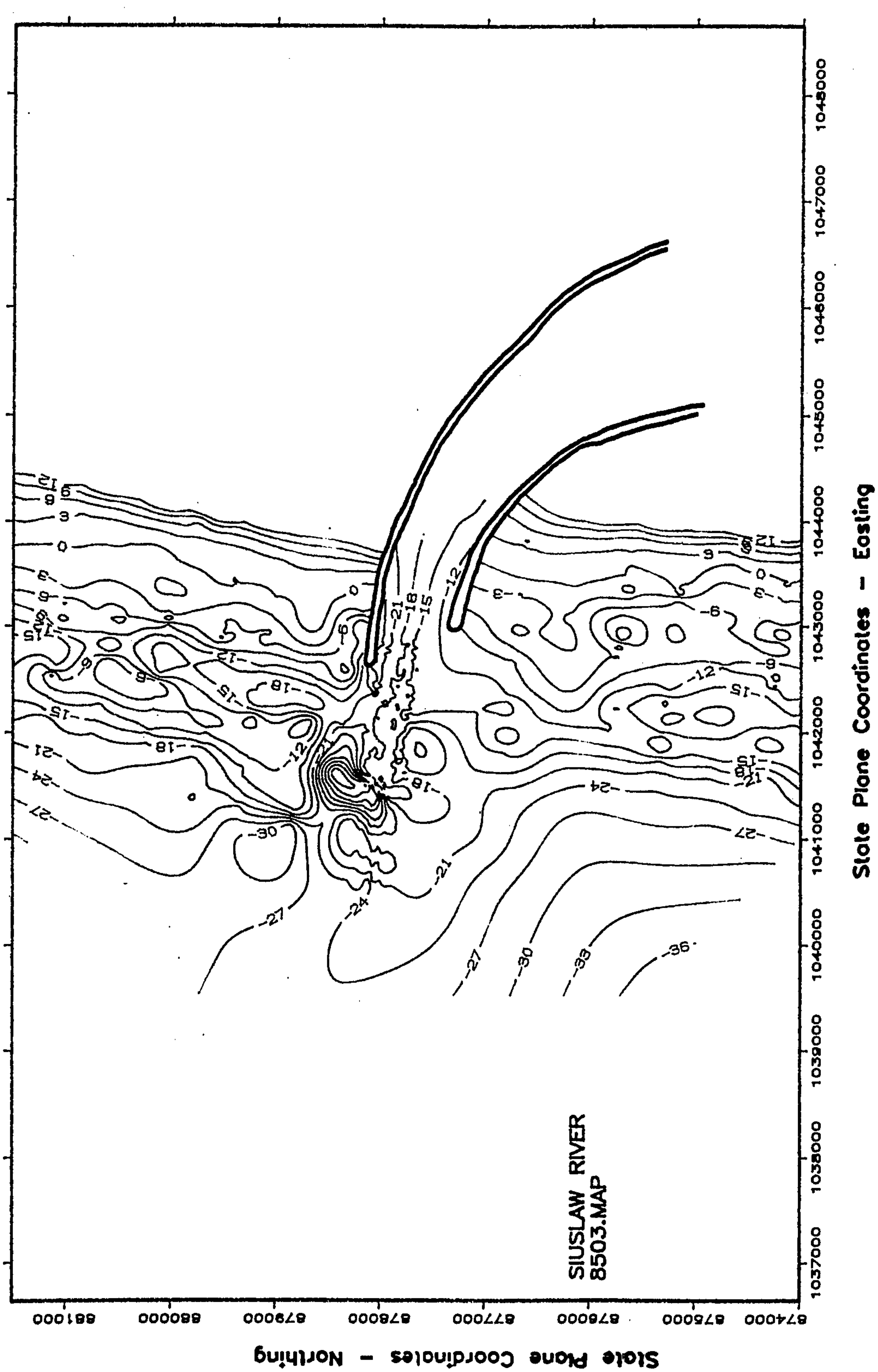
SIUSLAW RIVER
8503.MAP
State Plane Coordinates - Easting
State Plane Coordinates - Northing
1037000
1038000
1039000
1040000
1041000
1042000
1043000
1044000
1045000
1046000
1047000
1048000
874000
875000
876000
877000
878000
879000
880000
881000

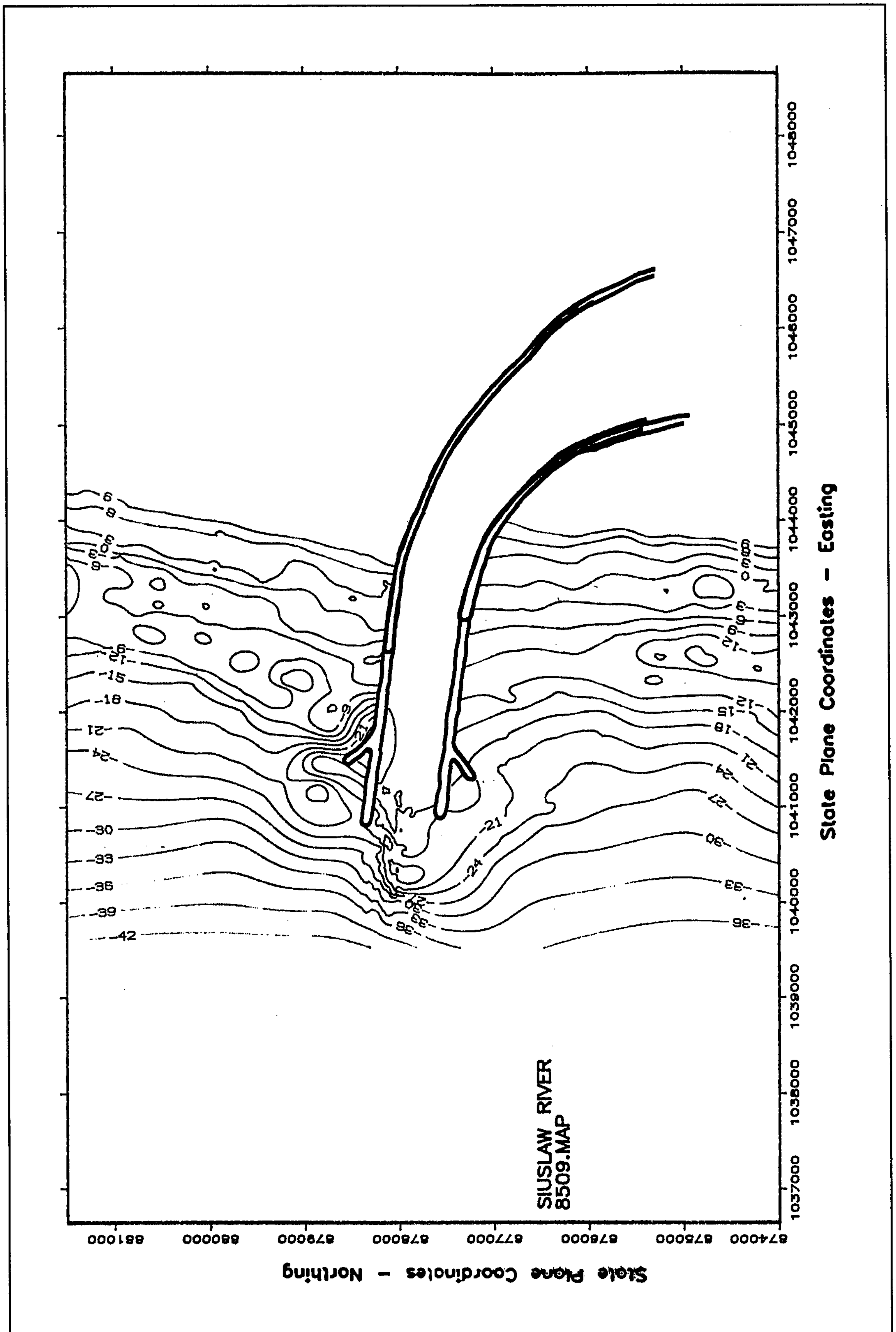
SIUSLAW RIVER
8509.MAP
State Plane Coordinates - Easting
State Plane Coordinates - Northing

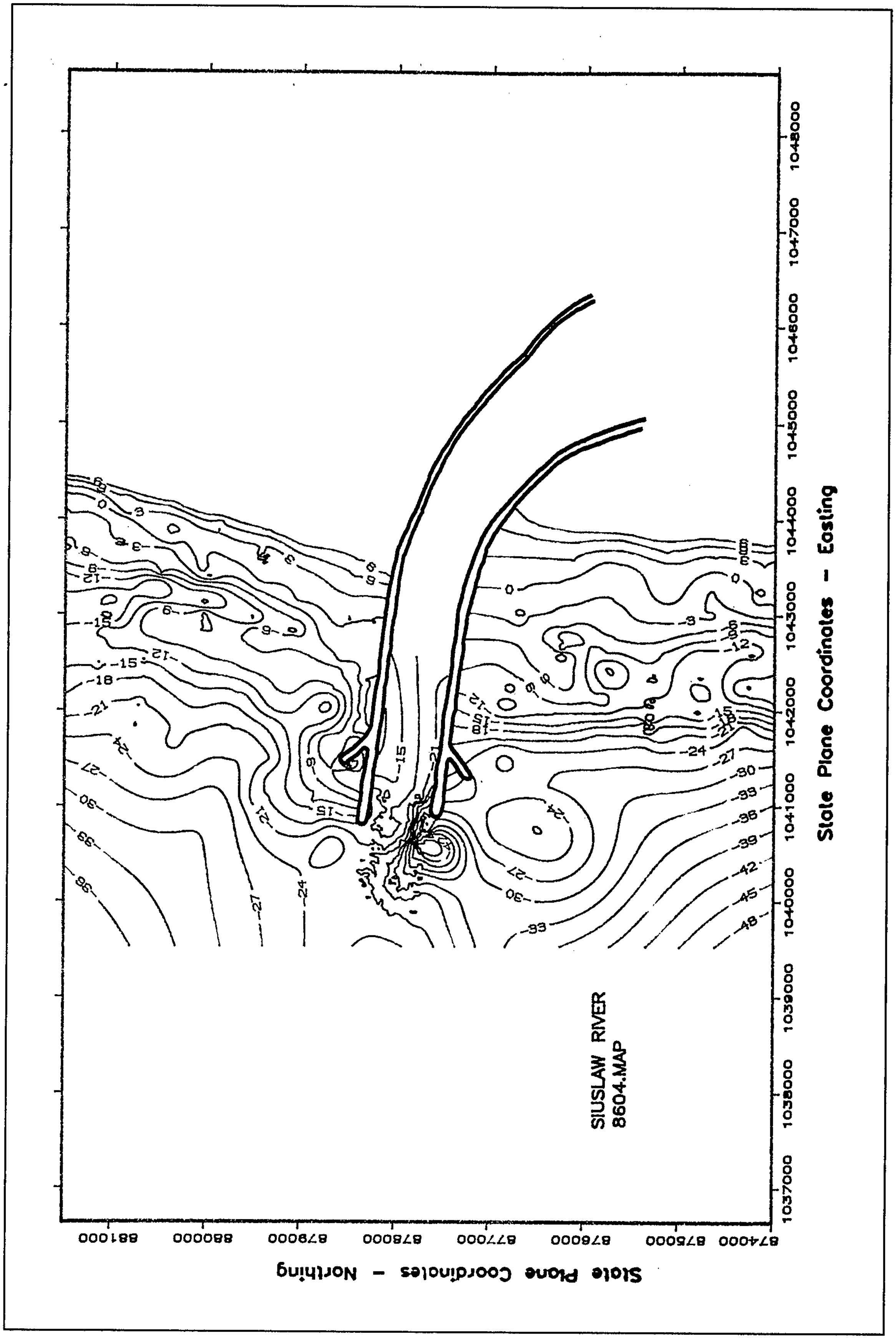
SIUSLAW RIVER
8604.MAP
State Plane Coordinates - Easting
State Plane Coordinates - Northing

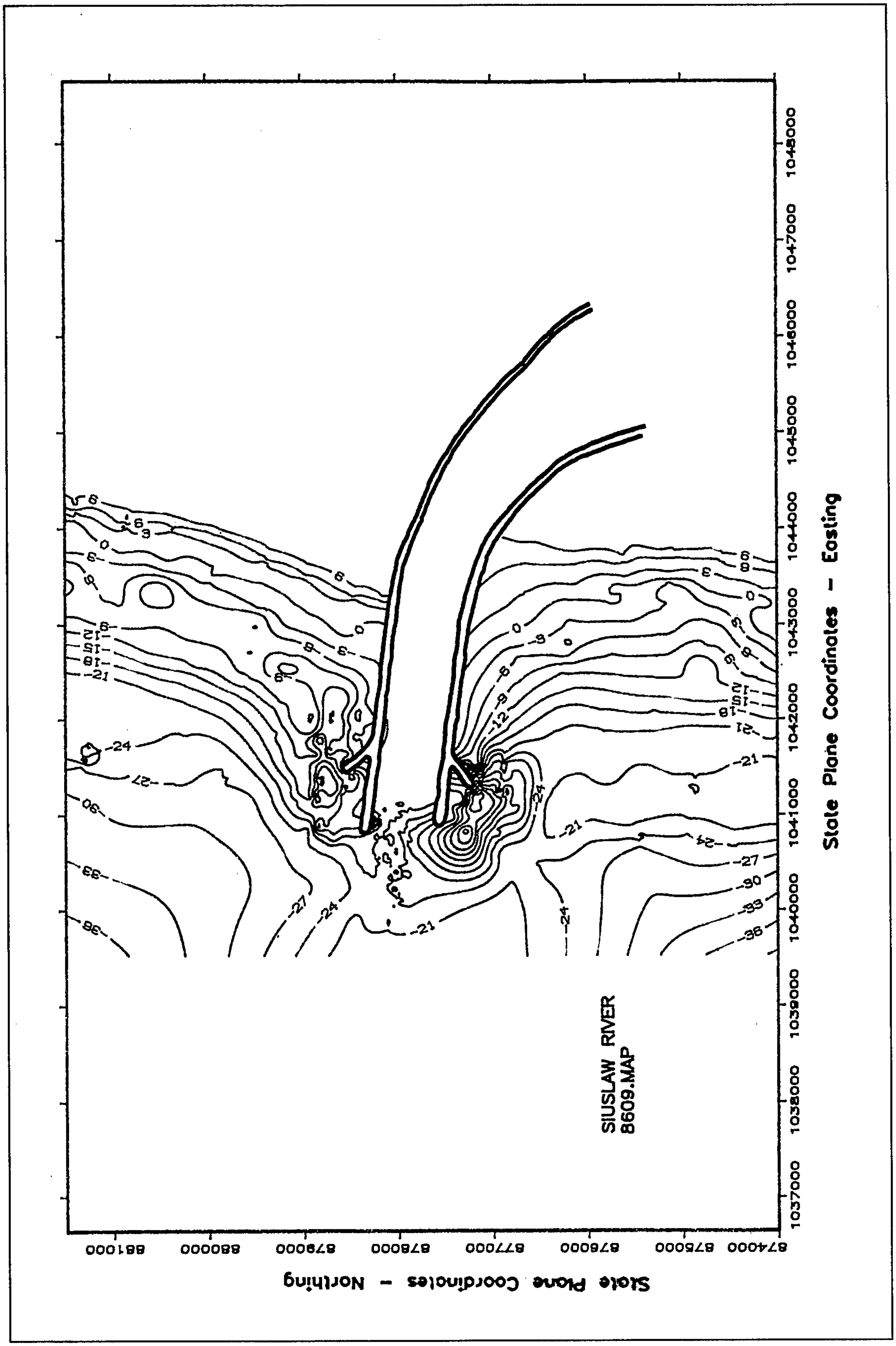
SIUSLAW RIVER
8609.MAP
State Plane Coordinates – Easting
1037000
1038000
1039000
1040000
1041000
1042000
1043000
1044000
1045000
1046000
1047000
1048000
State Plane Coordinates – Northing
874000
875000
876000
877000
878000
879000
880000
881000

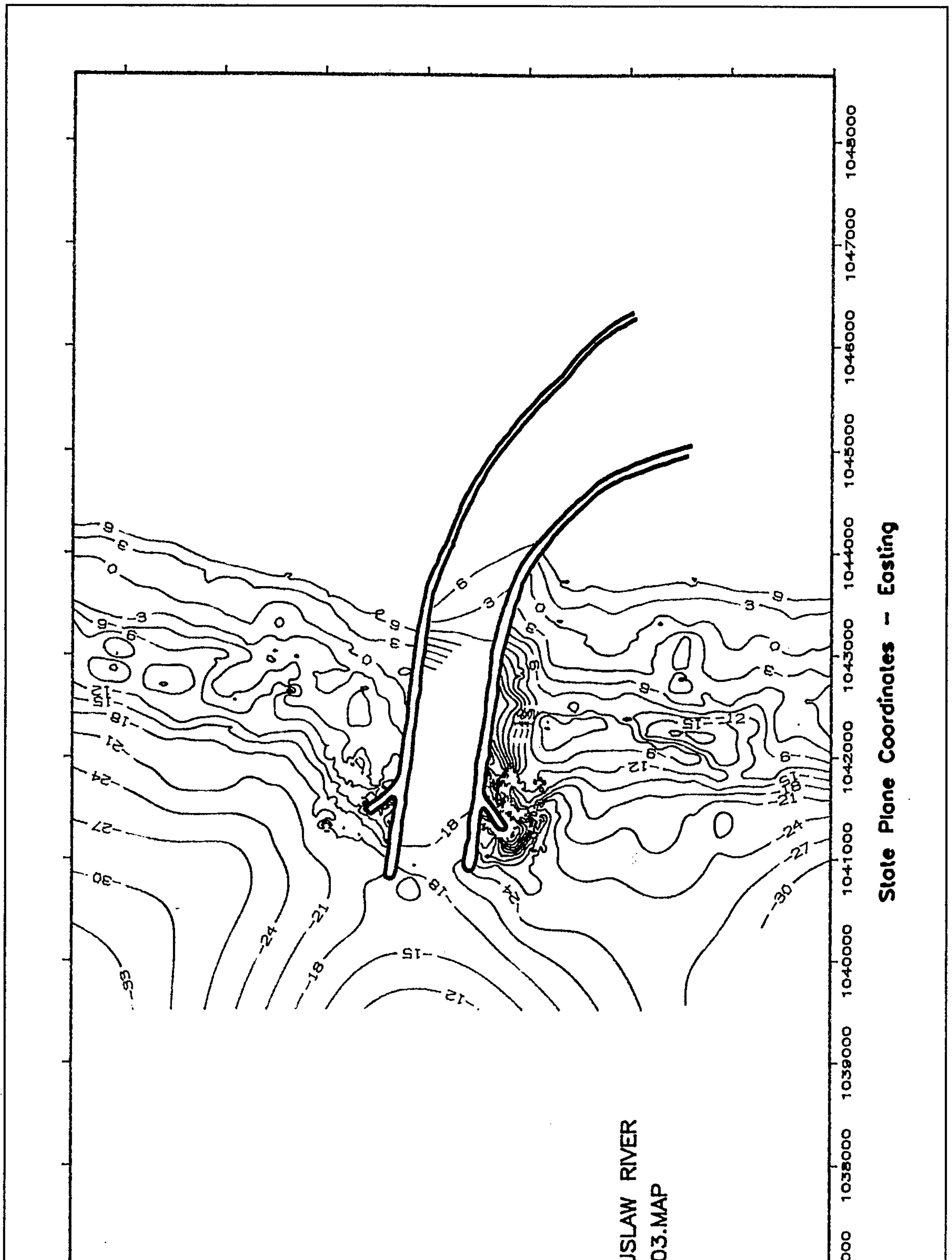
SIUSLAW RIVER
8703.MAP
State Plane Coordinates - Easting
State Plane Coordinates - Northing
1037000
1038000
1039000
1040000
1041000
1042000
1043000
1044000
1045000
1046000
1047000
1048000
874000
875000
876000
877000
878000
879000
880000
881000

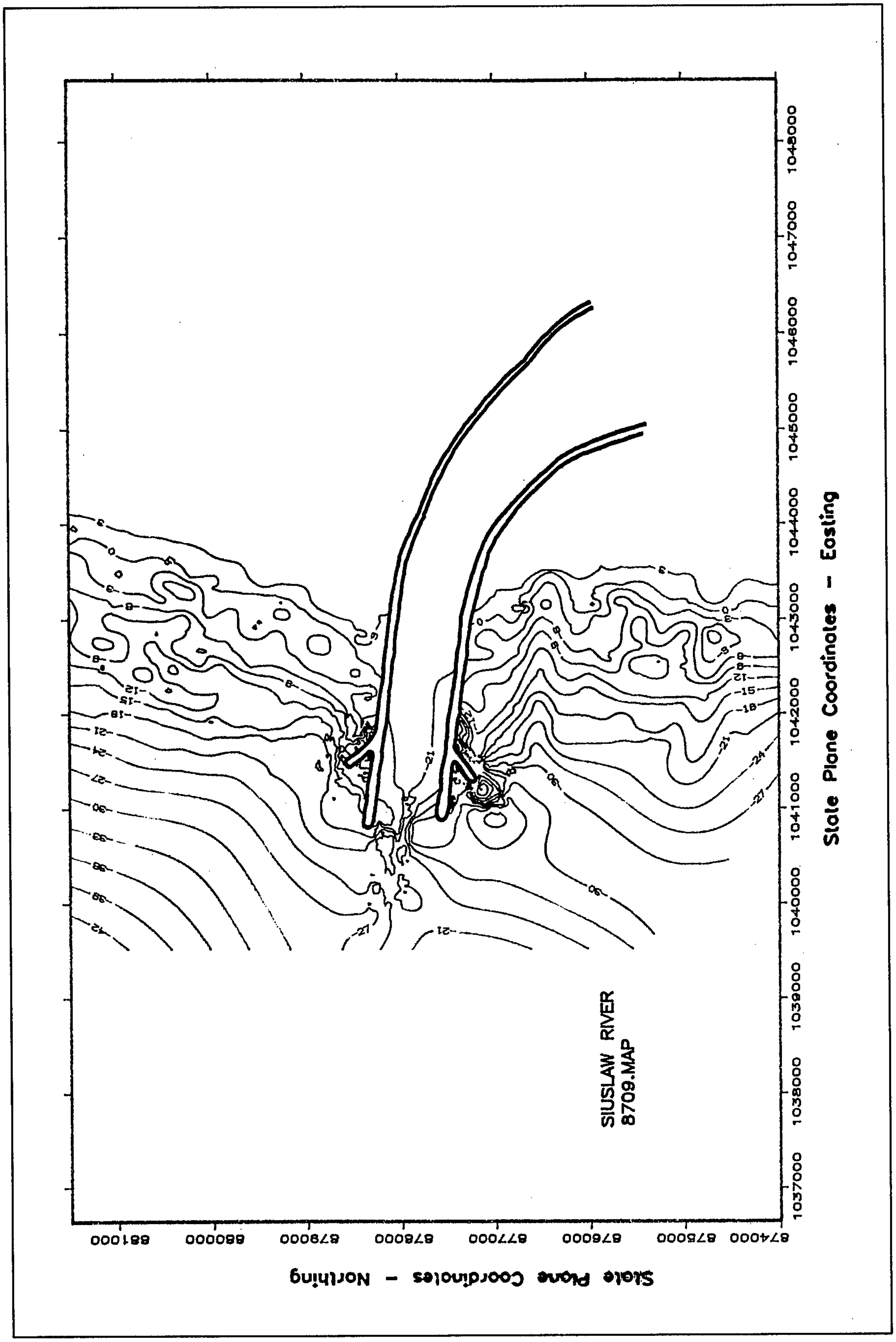
SIUSLAW RIVER
8709.MAP
State Plane Coordinates - Easting
State Plane Coordinates - Northing
1037000
1038000
1039000
1040000
1041000
1042000
1043000
1044000
1045000
1046000
1047000
1048000
874000
875000
876000
877000
878000
879000
880000
881000

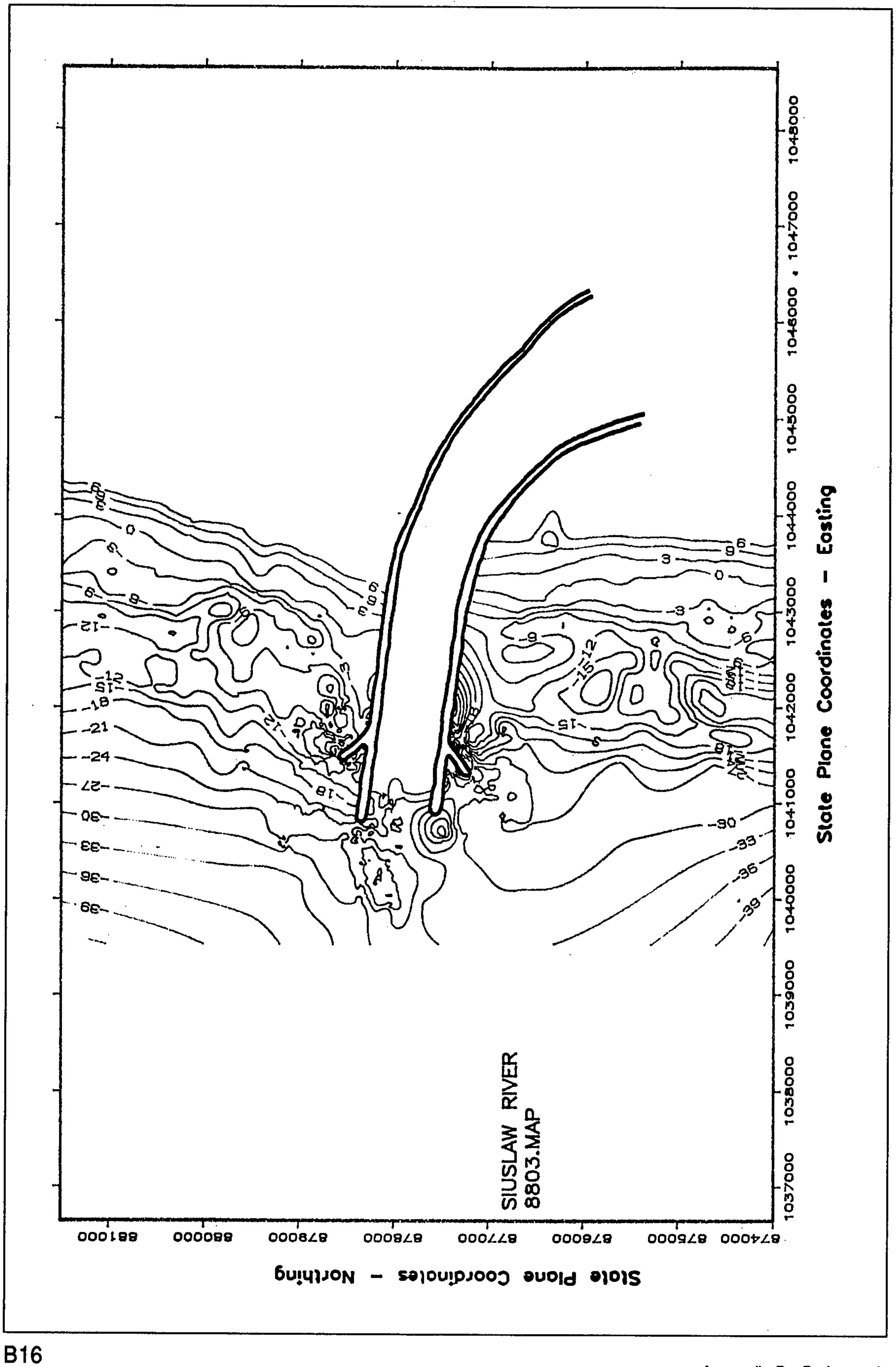
SIUSLAW RIVER
8803.MAP
State Plane Coordinates - Easting
State Plane Coordinates - Northing

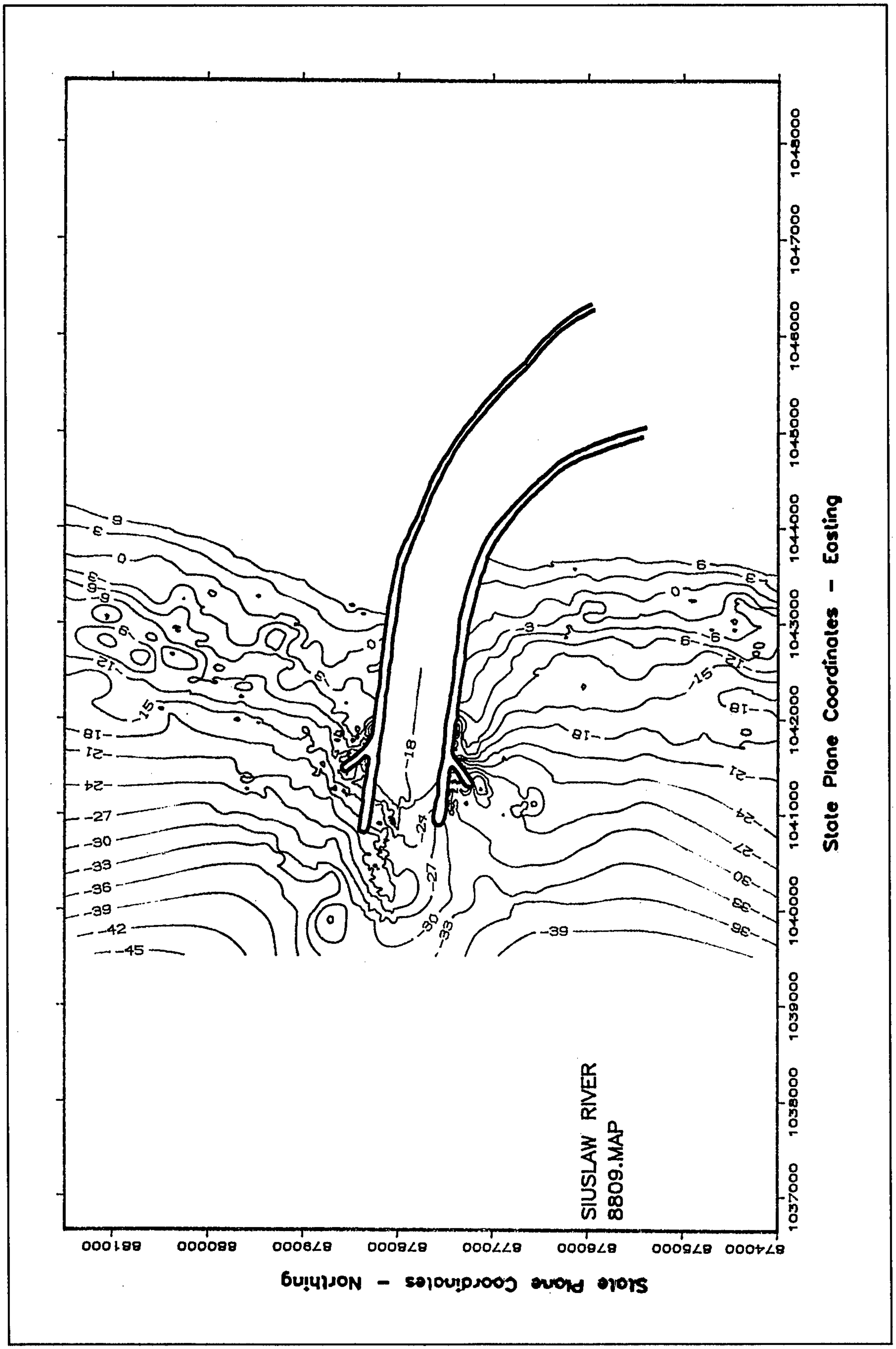
SIUSLAW RIVER
8809.MAP
State Plane Coordinates - Easting
State Plane Coordinates - Northing

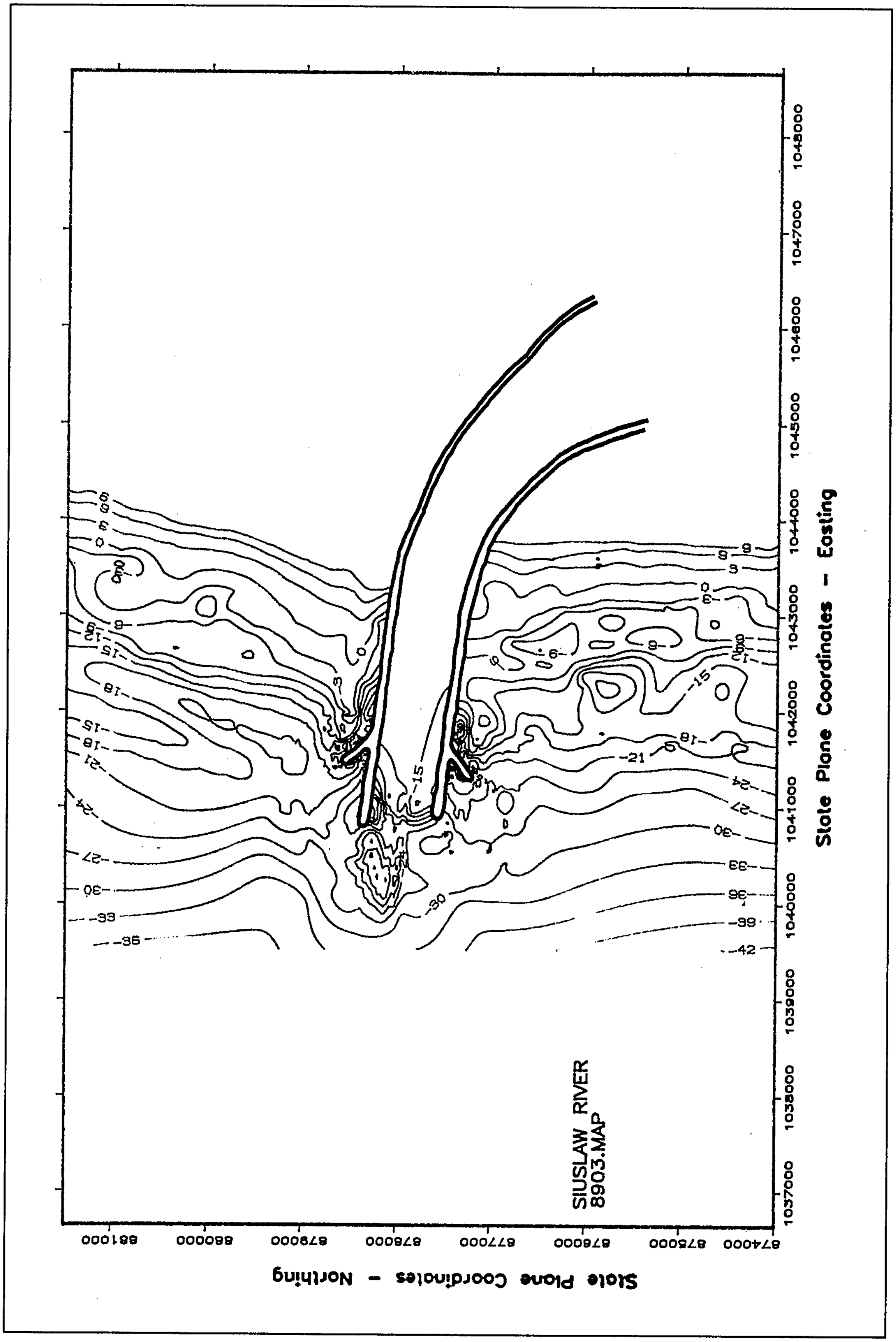
SIUSLAW RIVER
8903.MAP
State Plane Coordinates - Easting
State Plane Coordinates - Northing

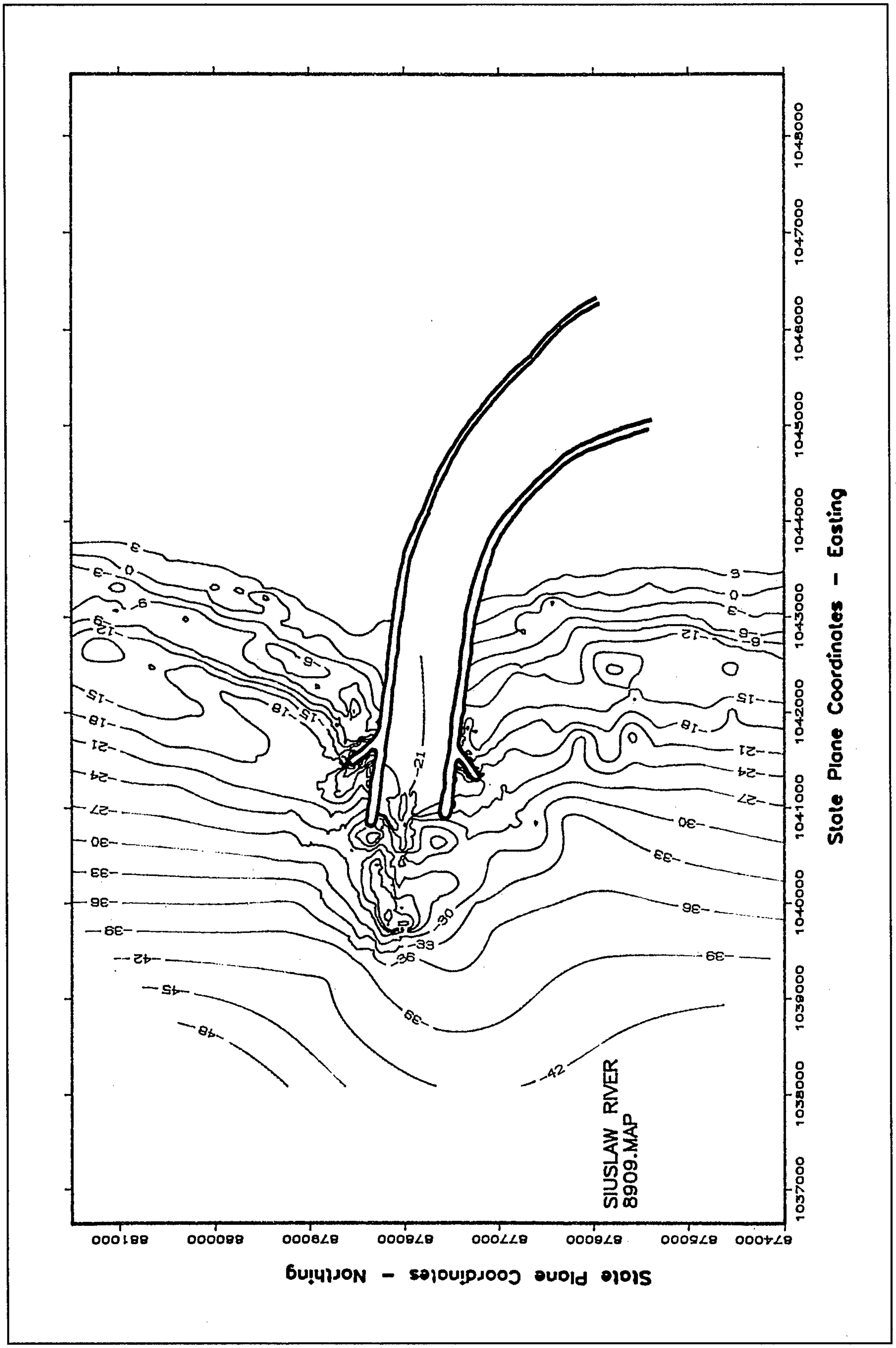
SIUSLAW RIVER
8909.MAP
State Plane Coordinates - Easting
State Plane Coordinates - Northing
1037000
1038000
1039000
1040000
1041000
1042000
1043000
1044000
1045000
1046000
1047000
1048000
874000
875000
876000
877000
878000
879000
880000
881000

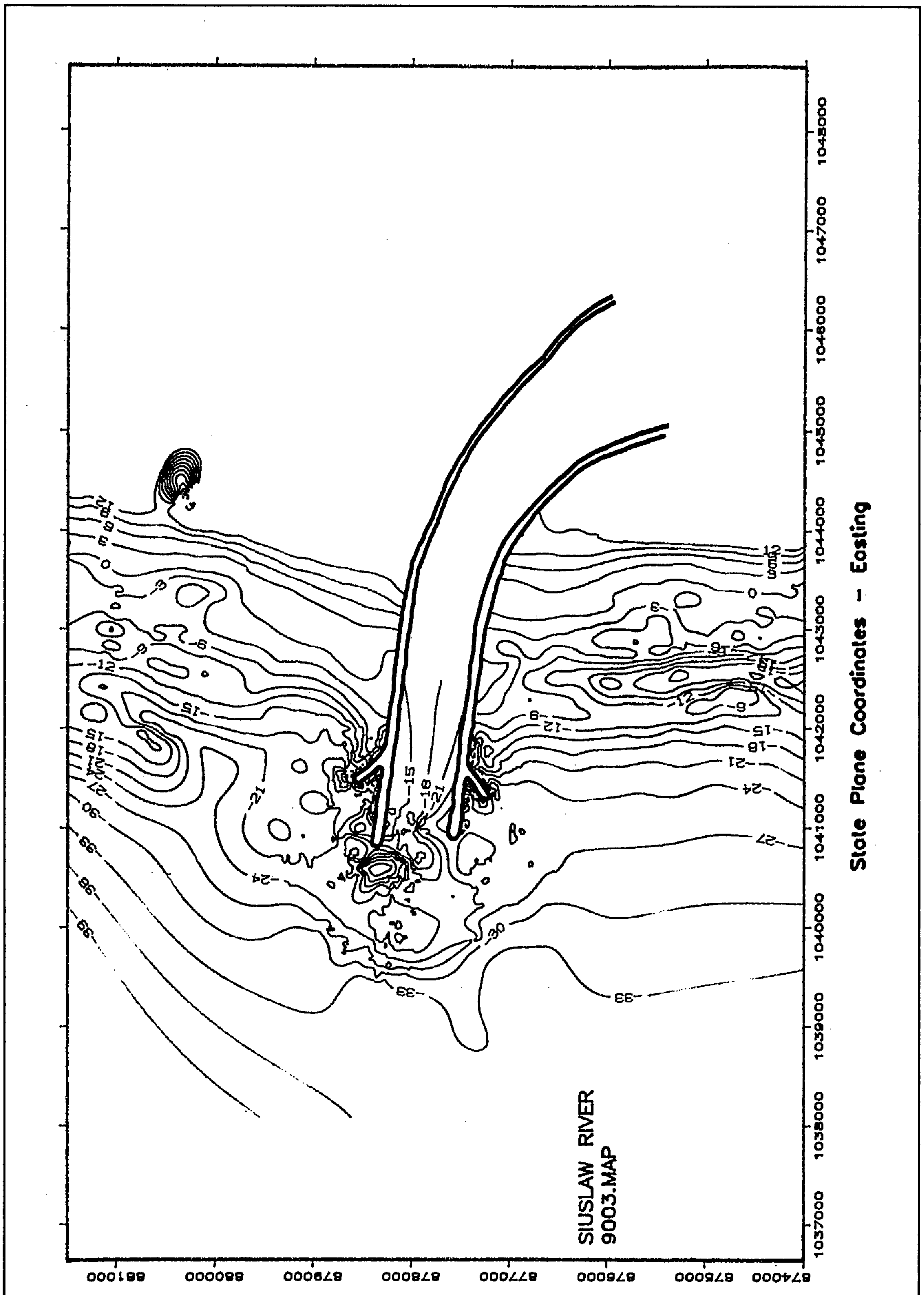
SIUSLAW RIVER
9003.MAP
State Plane Coordinates - Easting
State Plane Coordinates - Northing

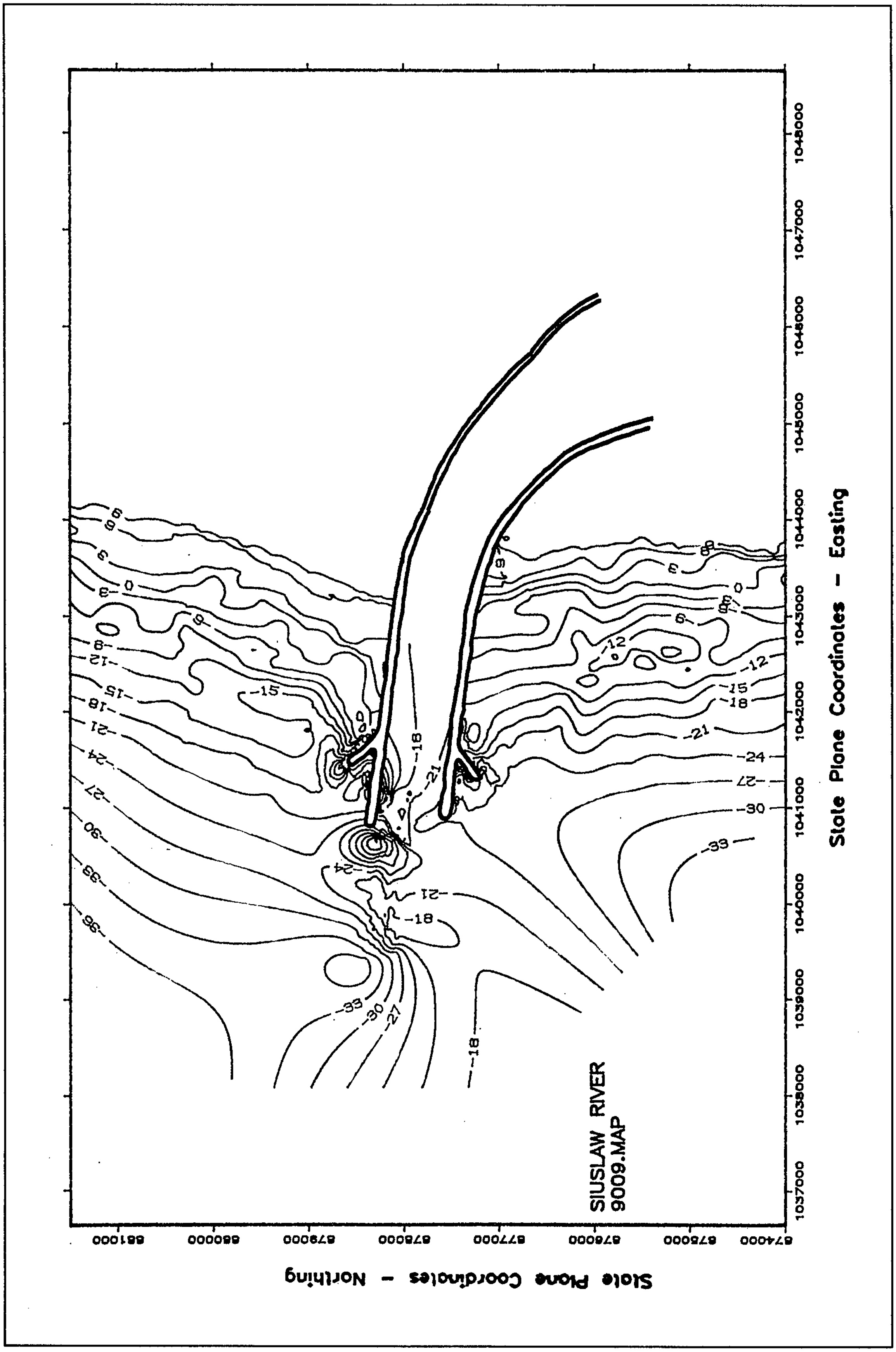
SIUSLAW RIVER
9009.MAP
State Plane Coordinates - Easting
State Plane Coordinates - Northing
1037000
1038000
1039000
1040000
1041000
1042000
1043000
1044000
1045000
1046000
1047000
1048000
674000
675000
676000
677000
678000
679000
680000
681000

REPORT DOCUMENTATION PAGE

Form Approved
OMB No. 0704-0188

1. AGENCY USE ONLY *(Leave blank)*

2. REPORT DATE
November 1995

3. REPORT TYPE AND DATES COVERED
Report 1 of a series

4. TITLE AND SUBTITLE
Effectiveness of Spur Jetties at Siuslaw River, Oregon;
Report 1, Prototype Monitoring Study

5. FUNDING NUMBERS

6. AUTHOR(S)
Cheryl E. Pollock, Stephan A. Chesser, David McGehee,
Claire Livingston, Ronald W. Neihaus, Jr.

7. PERFORMING ORGANIZATION NAME(S) AND ADDRESS(ES)
U.S. Army Engineer Waterways Experiment Station, 3909 Halls Ferry Road,
Vicksburg, MS 39180-6199; U.S. Army Engineer District, Portland,
333 SW First Avenue, Tenth Floor, Portland, OR 97208-2946;
DynTel, 3530 Manor Dr., Suite No. 4, Vicksburg, MS 39180

8. PERFORMING ORGANIZATION REPORT NUMBER
Technical Report CERC-95-14

9. SPONSORING/MONITORING AGENCY NAME(S) AND ADDRESS(ES)
U.S. Army Corps of Engineers
Washington, DC 20314-1000

10. SPONSORING/MONITORING AGENCY REPORT NUMBER

11. SUPPLEMENTARY NOTES
Available from National Technical Information Service, 5285 Port Royal Road, Springfield, VA 22161.

12a. DISTRIBUTION/AVAILABILITY STATEMENT
Approved for public release; distribution is unlimited.

12b. DISTRIBUTION CODE

13. ABSTRACT *(Maximum 200 words)*

In 1985, the rubble-mound jetties at the entrance to the Suislaw River, Florence, OR, were extended offshore. In addition, on the ocen side of each jetty, one long spur oriented 45 deg to the main structure was constructed shoreward of the seaward end of each of the twin jetties. The spur system was investigated as a cost-reducing alternative to significant linear jetty length extension which would reduce sediment shoaling and dredging requirements in the channel and improve navigability. Cost reductions were expected in reduced maintenance dredging and in actual construction and material cost.

Monitoring and evaluation of the jetty system were conducted through the U.S. Army Corps of Engineers, Monitoring of Completed Coastal Projects (MCCP) Program by the Coastal Engineering Research Center (CERC) in coordination with the U.S. Army Engineer District, Portland (NPP). Data collected during field monitoring of the area are related to incident wave conditions. Spur-induced current patterns and sediment deposition patterns, along with annual dredging records are analyzed to evaluate structure performance. The favorable results of this MCCP study substantiate physical model test findings and indicate potential application of spur jetties at other sites.

14. SUBJECT TERMS

Coastal engineering	Dredging	Shoaling
Current measurements	Florence, OR	Siuslaw River
Currents	Oregon	Spur jetties
Current/structure interaction	Scour	

15. NUMBER OF PAGES
157

16. PRICE CODE

17. SECURITY CLASSIFICATION OF REPORT	18. SECURITY CLASSIFICATION OF THIS PAGE	19. SECURITY CLASSIFICATION OF ABSTRACT	20. LIMITATION OF ABSTRACT
UNCLASSIFIED	UNCLASSIFIED		

NSN 7540-01-280-5500

Standard Form 298 (Rev. 2-89)
Prescribed by ANSI Std. Z39-18
298-102

*U.S. GOVERNMENT PRINTING OFFICE: 1996-733-144/40018